New Routes to Fluorine-18 Radiolabelled Prosthetic Groups for use in the Medical Imaging Technique – Positron Emission Tomography

Michael Charlton

Submitted in fulfilment of the requirements for the degree of Doctor of Philosophy.

Sir Bobby Robson Foundation PET Tracer Production Unit,

Bedson Building, School of Chemistry,

Faculty of Science, Agriculture and Engineering,

University of Newcastle upon Tyne

September 2014

For my family.

Abstract

The use of biomacromolecules, e.g. peptides and antibodies, as therapeutics, so-called 'biologics', is experiencing an increase in interest as more and more small molecule therapeutics fail to meet the regulatory requirements for human use.

To expedite the examination of such biologics as useful therapeutics, positron-emission tomography (PET) is being used as an early stage non-invasive *in vivo* imaging modality to rule in, or to rule out, candidates from the drug discovery pipeline. To realise this goal, small, reactive radiolabelled compounds, termed prosthetic groups, are often used to label the biologic of interest. Furthermore, prosthetic groups may also be incorporated into small molecule therapeutics, thus enabling rapid elucidation of candidates in a pre-clinical environment from a single appropriate prosthetic group precursor/apparatus set up.

Diaryliodonium salts have been considered as useful precursors to prosthetic groups, as this class of compound may facilitate the one-step introduction of a nucleophilic radiolabel, e.g. [18F]fluoride ion, onto any position of a given arene. However, direction of the radiolabel onto the target arene is generally dictated by stereoelectronics, where the nucleophile is substituted upon the least electron-rich arene. To achieve this effect, electron-rich arenes, such as 2-thienyl, are employed. However, a potentiated product where the second arene is also electron-rich is the poorly characterised 2-[18F]fluorothiophene. To ensure that the products of radiofluorination processes reported herein are correctly assigned, an authentic sample of 2-[19F]fluorothiophene has been prepared on a 750 mmol scale (Scheme A).
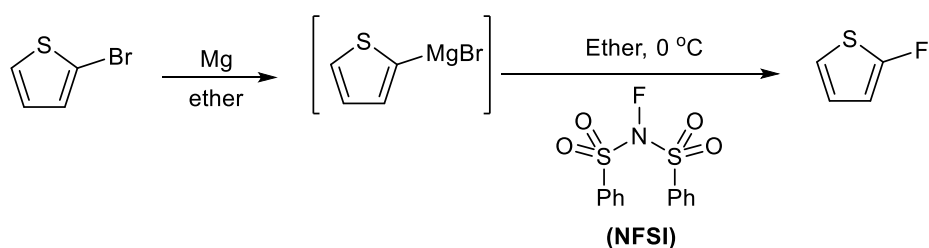
Scheme A: Synthesis of 2-[19F]fluorothiophene.

Unambiguous verification of the detection of 2-[18F]fluorothiophene has herein been achieved for the first time by radiofluorination of the highly electrophilic electron-rich dithienyliodonium trifluoroacetate, using a microfluidic apparatus.

Microfluidic apparatus is a technology which is experiencing an emergence as a useful means of probing the conditions advantageous to the production of radiolabeled material. We investigated the use of such apparatus in the optimised preparation of regioisomers of a key prosthetic group, [^{18}F]fluorobenzaldehyde ([^{18}F]FBA). The successful optimisation of the radiolabeling process has delivered 4-[^{18}F]FBA in excellent radiochemical yields (>95%), as well delivering the associated regioisomer, 3-[^{18}F]FBA, which is unavailable by convention means, by use of diaryliodonium salt precursors (Scheme B).
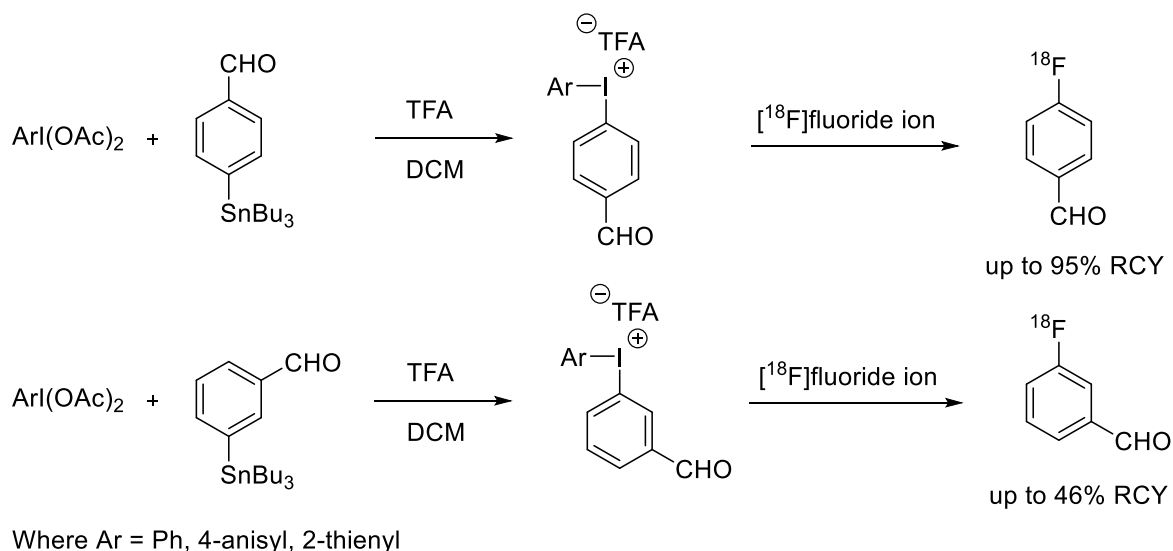
Scheme B: Radiosynthesis of 4-[^{18}F]FBA and 3-[^{18}F]FBA from diaryliodonium salt precursors.

Another prosthetic group considered bears the thiol reactive maleimide. An appropriate synthesis of a suitable diaryliodonium salt precursor (Scheme C) is reported herein.
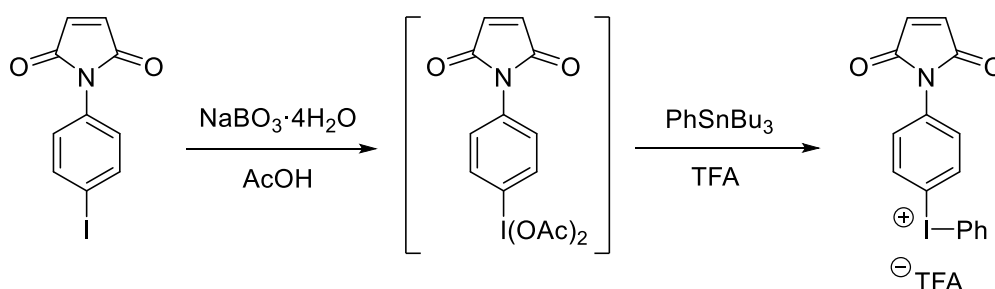
Scheme C: Synthesis of the precursor to the prosthetic group *N*-(4-[^{18}F]fluorophenyl)maleimide.

Acknowledgements

Contents

List of Abbreviations

AcOH	Acetic acid
Bq	Becquerel
^{13}C NMR	Carbon-13 NMR
°C	Degrees Celsius
Ci	Curie
d_7-DMF	Deuterated Dimethylformamide
DMF	Dimethylformamide
d	Doublet
DCM	Dichloromethane
dd	Double doublet
EIMS	Electron ionisation mass spectrometry
eV	Electronvolt
Eq	Equivalents
Et	Ethyl
FTIR	Fourier Transform Infra-Red
g	Grams
GCMS	Gas chromatography mass spectrometry
Hz	Hertz
h	Hour
IR	Infra-Red
J	Coupling constant measured in Hz
K_{222}	K·4,7,13,16,21,24-hexaoxa-1,10-diazabicyclo[8.8.8]hexacosane
M	Molar
M^+	Molecular ion peak
$[M+H^+]$	Molecular ion peak plus mass of proton
m	Multiplet
Me	Methyl
MeCN	Acetonitrile
min	Minute(s)
mL	Millilitre
mmol	Millimole

mp	Melting Point
m/z	Mass/Charge ratio
NMR	Nuclear Magnetic Resonance
p	Pentet
Ph	Phenyl
ppm	Parts per million
q	Quartet
RCY	Radiochemical yield
R_f	Retention factor
RT	Room temperature
s	Singlet
S_NAr	Nucleophilic aromatic substitution
t	Triplet
TLC	Thin Layer Chromatography

List of Figures

List of Schemes

xvii

xviii

List of Tables

1   Chapter One: Introduction

Imaging agents, which have been labelled with positron (β^+) emitters, are playing an increasingly important role in drug discovery/development and in the diagnosis of disease, for example in the early stage detection of biological abnormalities, such as tumours, both malignant and benign.[1-5] Information regarding biochemical mechanisms, metabolic processes, and receptor function cannot typically be obtained by medical imaging techniques such as X-ray and magnetic resonance imaging (MRI). These techniques generally yield information about a subject's anatomy and therefore provide little detail of molecular or metabolic events. The nuclear medicine imaging techniques Positron Emission Tomography (PET) and Single Photon Emission Computed Tomography (SPECT), provide a means of obtaining this information.

1.1   Positron Emission Tomography

PET is a non-invasive *in vivo* medical imaging technique which is used to detect compounds which have been labelled with a positron emitting radioisotope. There are many advantages to this procedure, such as the ability to quantitatively determine the biodistribution of a given imaging agent, and therefore determine the pharmacokinetic profile of that imaging agent.[6] A picture and a representation of what occurs inside a PET scanner (Figure 1) are provided below.
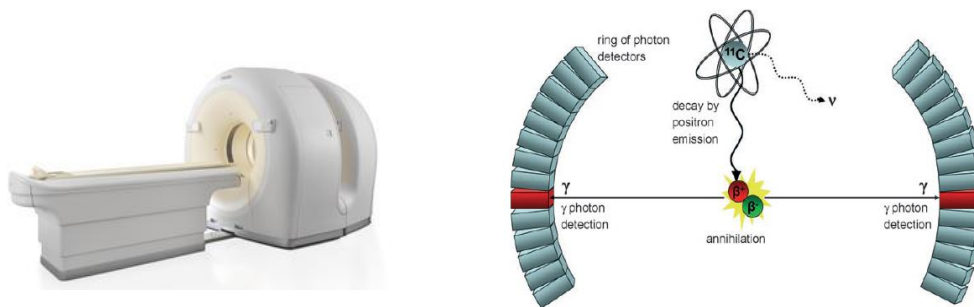
Figure 1: A PET scanner (left), and a schematic representation of what occurs inside the scanner when a positron emitting isotope decays (right).[3] The line-of-coincidence (LoC) is represented where both gamma photons are emitted in opposing directions.

The subject is injected with the imaging agent of choice, e.g. an imaging agent labelled with fluorine-18, and after a period of rest, around 30 to 40 minutes in case of [^{18}F]FDG (see section 1.4) then moved into the PET scanner. Fluorine-18 decays in the body largely by positron emission (97% - remainder via electron capture) forming oxygen-18, a positron and a neutrino (ν) (Scheme 1).

$$^{18}F \longrightarrow {}^{18}O + \beta^+ + \nu$$

Scheme 1: Radioactive decay of the radioisotope fluorine-18.

γ Photons are emitted as a consequence of an annihilation event which occurs between antimatter, (the positron emitted by decay of the radioisotope) and matter (a nearby electron).[7] Very large numbers of these annihilation events need to occur in order to produce a PET image of sufficient quality. The energy at which a positron is emitted from a decaying isotope is a critical parameter regarding the resolution of the PET image, as, ideally, the annihilation event should occur as close as possible to the imaging agent. A high energy positron will travel further in matter, and therefore the annihilation event will occur further away from the site of interest, leading to a PET image of lower resolution. Signal to noise ratio (SNR) will also impact upon the resolution and therefore the quality of a PET image, though methods to take this into account, such as the noise equivalent count rate aim to mitigate this effect.[7] The PET scanner is essentially a ring of photon detectors, or cameras, which detect the two gamma (γ) photons emitted at approximately 180° to each other as a result of the positron annihilation event. Many γ photons leave the body along a line of

coincidence (LoC) (Figure 1). By exploiting the LoC, i.e. using software algorithms to construct an image, it is possible to detect, with an acceptable degree of accuracy, where the annihilation event took place and hence the *in vivo* location for the fluorine-18 radiolabeled imaging agent.

The quality of an image obtained by PET scanning can also be affected by an phenomenon known as Compton Scattering,[8] whereby a γ photon emitted from the annihilation event interacts with an electron in the outer shell of a nearby atom. The γ photon's path is changed, causing a slight loss in energy. In the majority of cases, the γ photon's path is altered to such an extent that it is scattered out of the field of a detector and is therefore not counted; this is process is known as attenuation. When the effect of Compton Scattering is applied to subjects under study, it follows that an increase in subject size increases the relative amount of attenuation, consequently the number of lines of coincidence are decreased resulting in the diagnostic benefit of the scan being compromised (Figure 2).[9]
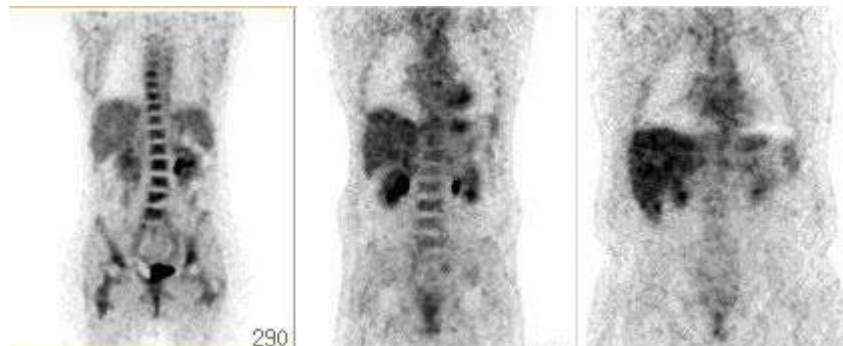
Figure 2:[9] The effect of Compton Scattering on the quality of PET images obtained from slim (left), average (middle) and heavy (right) patients.

As the two γ photons produced in an annihilation event travel independently, it is possible that one γ photon may be attenuated, leaving the other γ photon without a partner in its LoC. If a γ photon is scattered and remains in the field of view, a scattered LoC can be observed (Figure 3). Scattered photons can be detected by measuring the energy deposited onto the crystal, as scattered photons will have a lower energy than non-scattered photons. The energy differences can be measured to ±5% which removes most of the scattered events and improves the accuracy of the image produced.[10] Another detection problem arises due to accidental coincidences,

which may occur when two non-partnered γ photons reach the detectors within the coincidence timing window (τ), simulating an authentic LoC (Figure 3). The number of accidental coincidences can be reduced by reducing τ.[10]
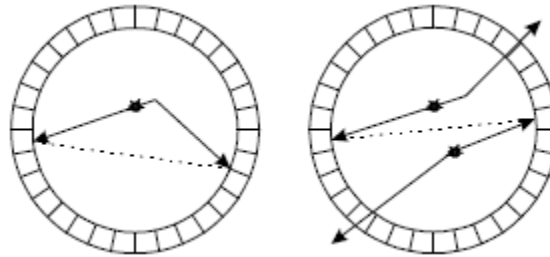
Figure 3:[10] Non-collinear LoC (dotted line) observed due to scattering (left) and accidental coincidences (right).

The first medical applications, utilising a positron emitting radioisotope for medical applications, were carried out in 1951 by Sweet[11] and Wren and co-workers,[12] with the first human studies carried out in 1974.[13, 14] The first scanner for human use was termed PETT III, for Positron Emission Transaxial Tomography III, however, the name was reduced to PET once it became apparent images could be obtained other than those only in the transaxial plane (Figure 4).
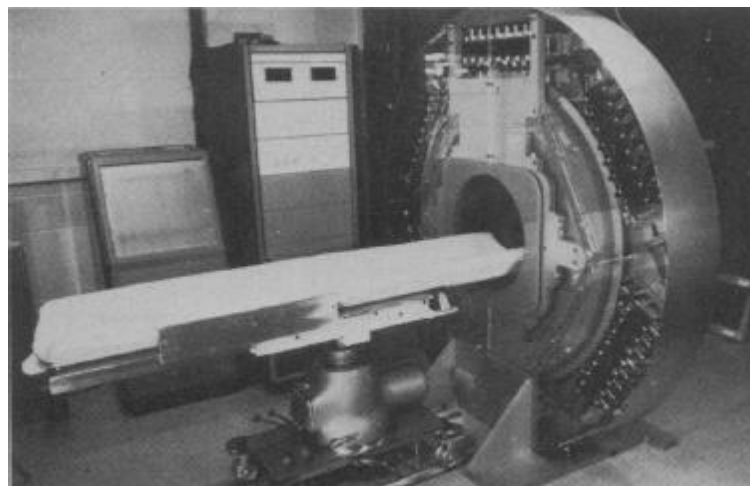
Figure 4: The first PET machine for human use, termed PETT III.[14]

Since 2000, PET has been integrated with a technique termed X-ray computed tomography (CT).[15] CT provides detailed anatomical information about the subject, the data obtained can then be combined with the data obtained from a PET scan, the combined technique is known as PET-CT.[2]

PET has been used extensively as an imaging modality in the fields of oncology,[2] neurology,[16] including the characterisation of Alzheimer's and Parkinson's disease, and cardiology.[17] It is widely anticipated that PET will be widely used as an *in vivo* pharmacological imaging modality, and therefore play a major role in drug development.[18] Data obtained from a PET image will allow drug developers to better understand the mode of action of lead compounds, their biodistribution, in addition to guiding the correct dosages for that compound.

1.2 Positron Emitting Isotopes used in PET

Commonly used positron emitters in PET include, ^{11}C, ^{13}N, ^{15}O, ^{18}F, ^{64}Cu and ^{68}Ga (Table 1). The radioactive isotopes (interchangeably termed radionuclides) of carbon, nitrogen, and oxygen are an attractive choice to the radiochemist, as these elements are already present in many biologically active molecules and, as a result, the incorporation of their radionuclide equivalents does not compromise the *in vivo* activity.[3]

Some of the radionuclides presented in Table 1 can be produced in a cyclotron. A cyclotron is a small particle accelerator that is capable of producing high energy beams of charged species, such as protons, which when directed at a particular target source, afford the corresponding radionuclide. Other radionuclides, such as gallium-68, may be produced in a generator.

Radionuclide	Half-life ($t_{1/2}$)	Decay Product	% (β^+ decay)	E_{MAX} (β^+) (KeV)
^{11}C	20.3 min	^{11}B	100	961
^{13}N	9.97 min	^{13}C	100	1190
^{15}O	2.04 min	^{15}N	100	1732
^{18}F	109.7 min	^{18}O	97	634
^{64}Cu	12.8 h	^{64}Ni	19	656
^{68}Ga	67.6 min	^{68}Zn	89	1899
^{81}Rb	4.57 h	^{81}Kr	96	335
^{89}Zr	71.4 h	^{89}Y	22	897
^{124}I	4.17 days	^{124}Te	23	603

Table 1: Radionuclides used in PET and their properties.[19]

Careful consideration of the choice of the radioisotope to be used for the PET study is required for several reasons. Firstly, the half-life of the radioisotope determines its effectiveness at studying certain biological processes. For instance, using oxygen-15 to measure a slow biological process, such as protein synthesis, would not be very useful as the half-life of oxygen-15 is too low at only 2.04 minutes. Consequently, most of the oxygen-15 radiolabeled imaging agent would have decayed before any useful data could be obtained. In this instance, it would be more appropriate to use a radionuclide with a longer half-life such as fluorine-18 ($t_{1/2}$ = 109.7 min). Secondly,

the positron emitted from different decaying radionuclides does so at several different energies (Table 1). The energy at which a positron is emitted from a decaying radioisotope is a critical parameter regarding the resolution of the PET image, as, ideally, the annihilation event should occur as close as possible to the origin of the positron. A high energy positron will travel further, and therefore the annihilation event will also occur further away from the site of the radiopharmaceutcial leading to greater uncertainty in its location and hence a lower resolution PET image.

Cyclotrons, of which a number are available, enable the production of positron emitting radionuclides by bombarding a particular target with accelerated charged particles (Figure 5). Cyclotron technology is an extremely complex topic and is beyond the scope of this chapter, however, an explanation of the essential features is provided. For an in-depth discussion of cyclotron technology, the reader is directed elsewhere.[20]
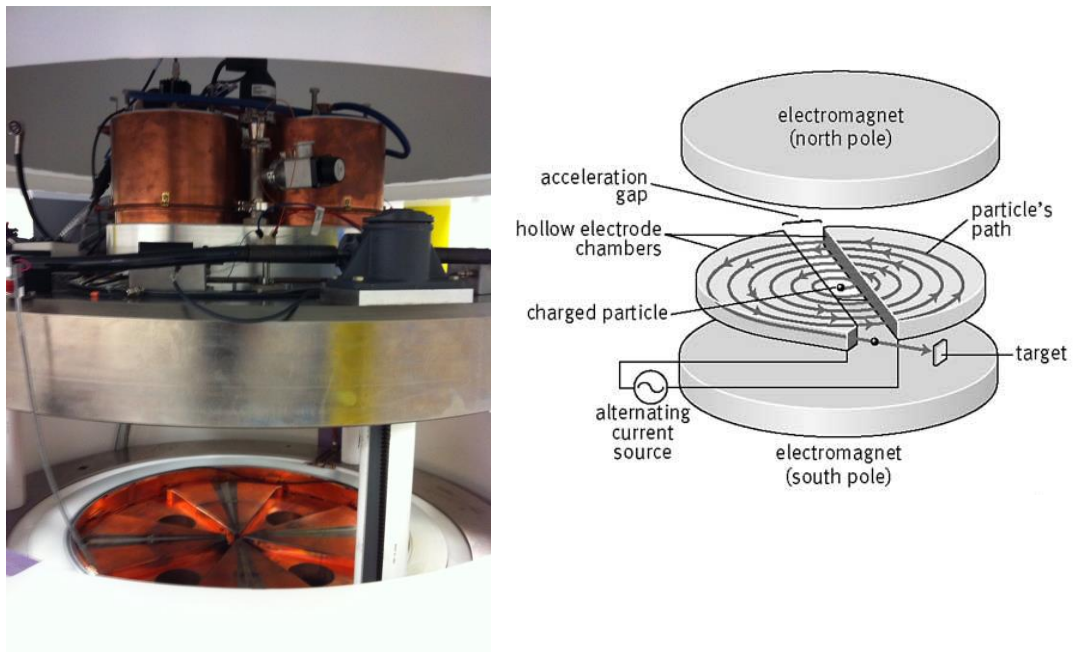
Figure 5: ABT mini-cyclotron in the raised position (left) showing the vacuum chamber and a simplified schematic representation of what occurs when the cyclotron is in operation.

The first cyclotron was developed in 1934 by E. O. Lawrence and M. S. Livingston,[21] both of whom subsequently developed the first medical cyclotron in 1938 (Figure 6).[22]
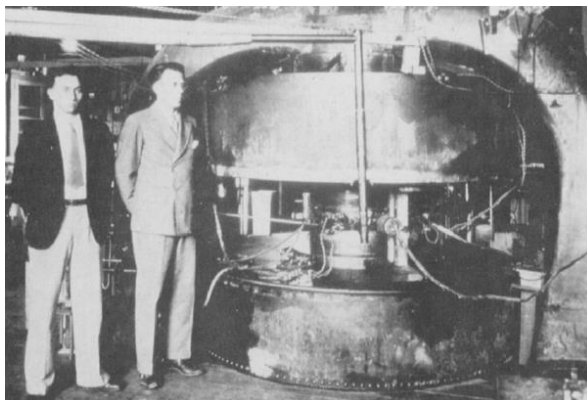
Figure 6:[22] M. S. Livingston (left) and E. O. Lawrence (right) next to the first medical cyclotron, manufactured in 1938.

Some of the most important radionuclides for PET, and their corresponding targets, which are produced in cyclotrons are presented in Table 2.

Radionuclide	$t_{1/2}$ (min)	Nuclear Reaction	Target	Product	Decay Product
^{11}C	20.3	$^{14}N(p,\square)^{11}C$	$N_2(+O_2)$	$[^{11}C]CO_2$	^{11}B
			$N_2(+H_2)$	$[^{11}C]CH_4$	
^{13}N	9.97	$^{16}O(p,\square)^{13}N$	H_2O	$[^{13}N]NO_x$	^{13}C
			$H_2O+EtOH$	$[^{13}N]NH_3$	
^{15}O	2.04	$^{15}N(d,n)^{15}O$	$N_2(+O_2)$	$[^{15}O]O_2$	^{15}N
^{18}F	109.7	$^{20}Ne(d,\square)^{18}F$	$Ne(+F_2)$	$[^{18}F]F_2$	^{18}O
		$^{18}O(p,n)^{18}F$	$[^{18}O]H_2O$	$^{18}F^-$	

Table 2: PET radionuclides and their corresponding targets.

1.3   Pharmaceuticals Containing Fluorine

Only since 1957 have pharmaceuticals been synthesised which contain fluorine,[23] since then, over 150 fluorinated pharmaceutical compounds have been developed, covering around 20% of today's market.[23-26] Many of the world's top pharmaceuticals also contain fluorine,[25] such as fluoxetine, atorvastatin and ciprofloxacin (Figure 7).

Fluoxetine   **Atorvastatin**   **Ciprofloxacin**
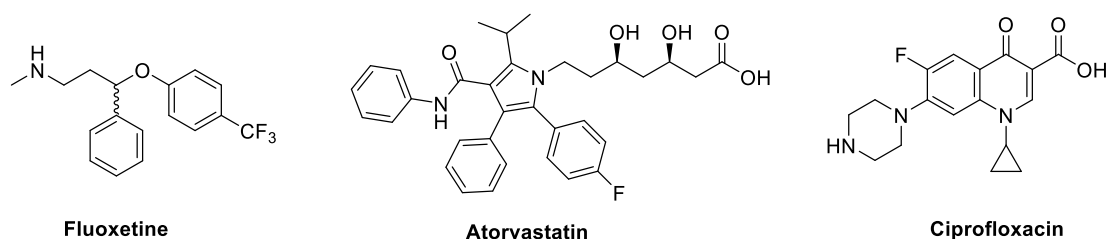
Figure 7: Examples of drugs containing fluorine.

The chart below shows how the incorporation of fluorine into drugs has developed between 1957 and 2006 (Figure 8).[27]
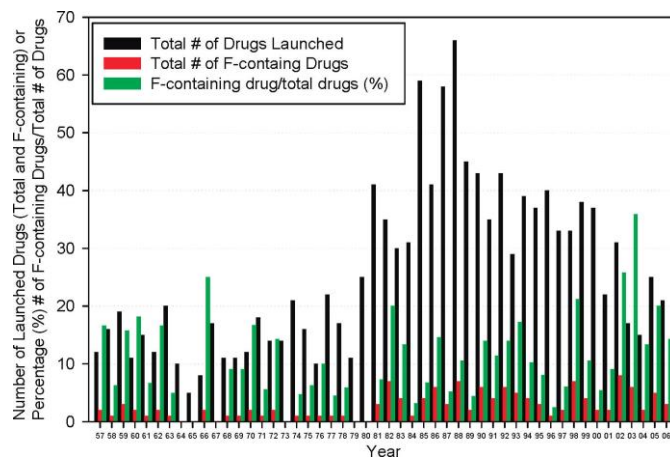
Figure 8: Number of drugs released, and those which contain fluorine, 1957-2006.[27]

Fluorine has many physical and pharmacokinetic properties which may be exploited to the medicinal chemists' advantage.[28] For instance, fluorine can in many cases enhance metabolic stability of nearby functionalities to oxidation by cytochrome P450 enzymes.[29] Often, fluorine is used to replace hydrogen atoms in drug

compounds suffering from undesired metabolism, even though the size and electronic nature of the two atoms are very different. Furthermore, there is a difference in bond length between C-H (1.09 Å) and C-F (1.41 Å), with the C-F bond being more akin to a C-O bond (1.43 Å).[29] Even though, successful H to F substitutions are known,[30] such as Ezetimib (also with fluorine substitution of one of the methoxy groups) (Scheme 2)[31] and fluoroquinolines (Scheme 3).[32]

SCH 48461
ED$_{50}$ (hamster) = 2.2 mg/kg

Ezetimib (SCH 58235)
ED$_{50}$ (hamster) = 0.04 mg/kg
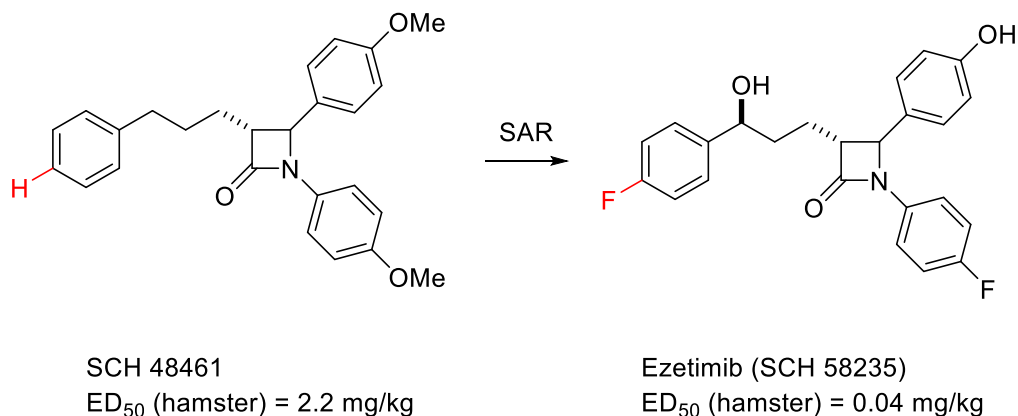
Scheme 2: H to F substitution, shown in red, which was found to block metabolic processes at the site of substitution as a result of structure activity relationship (SAR) studies.

Nalidixic acid
Lacks substantial Gram-positve
activity, blood levels below min
-imum inhibitory concentrations
(MIC)

Enoxacin
Wide range of Gram-positive
activity, low MIC
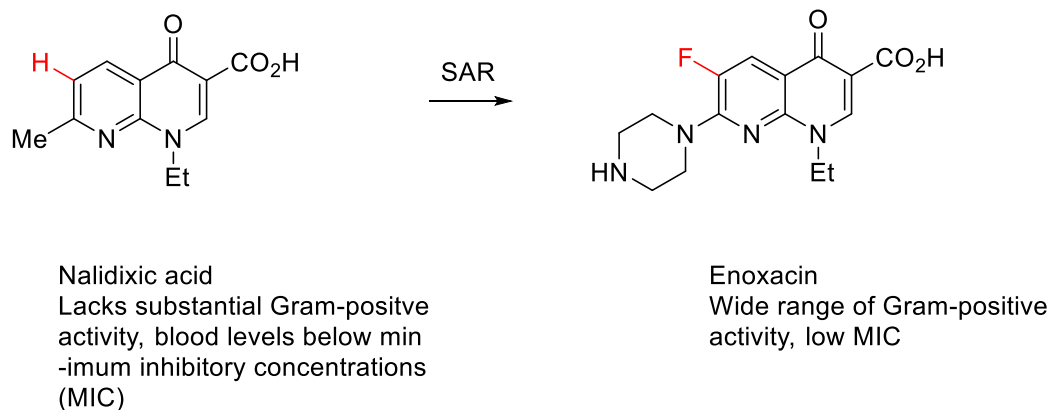
Scheme 3: H to F substitution, shown in red and determined as a result of structure activity relationship (SAR) studies, aided in facilitating activity *vs* a wide range of Gram-positive bacteria as well as increasing oral efficacy.

A measure of lipophilicity can be achieved by using the logarithmic coefficient for distribution (logD) of a compound between octanol and water, at pH 7.4. As logD increases, the lipophilicity of the compound in question increases.[33] A general trend discovered across a series of 300 pharmaceutical compounds was that the logD of the

drug is raised upon switching an atom of hydrogen with fluorine,[30] thus making the drug more lipophilic. It should be noted that this is a general trend, but that logD values may decrease when fluorine is substituted near an oxygen,[34] or nitrogen[35] atom.

Addition of fluorine to a compound often affects the pK_a of the functional groups in that compound. Rules have been developed which help predict the change in pK_a of a basic amine as a consequence of being near a fluorine atom.[36] If there are sufficient fluorine atoms present, the amine can remain sufficiently un-protonated at physiological pH, thus increasing the bioavailability of the compound. This increase in bioavailability was observed in a study using human 5-HT$_{1D}$ receptor inhibitors, as the incorporation of fluorine into a 5-HT$_{1D}$ receptor ligand was found to significantly reduce the pK_a of the compound, and this reduction of basicity was shown to have a dramatically beneficial influence on oral absorption, although the effect on a compound's oral bioavailability could not always be accurately predicted (Scheme 4).[37]
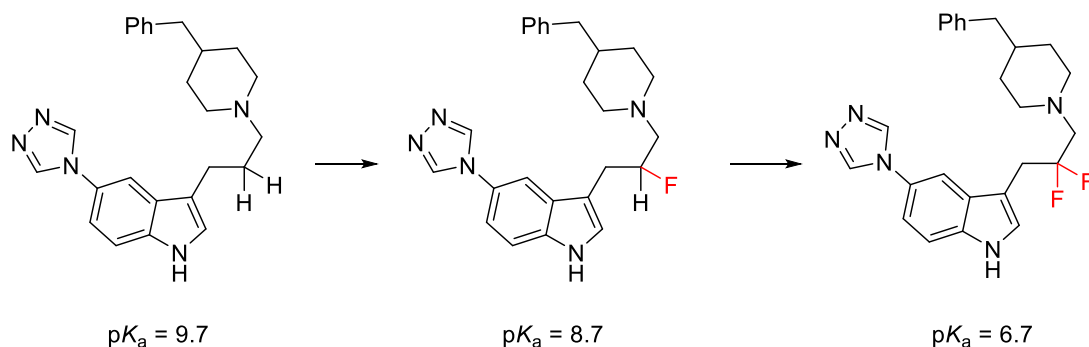
Scheme 4: A decrease in compound pK_a, found to be beneficial to the study, was observed across a range of human 5-HT$_{1D}$ receptors *via* sequential H to F substitutions (shown in red).

1.4   Fluorine-18 in Positron Emission Tomography

Of the several positron emitters available, fluorine-18 is termed the 'radionuclide of choice' and is also the most used radionuclide in PET. There are several reasons why fluorine-18 has many advantages over its β^+-emitting counterparts listed in Table 1. Fluorine-18 has a half-life ($t_{1/2}$) of 109.7 minutes, which is a convenient timescale to perform a multistep radiosynthesis, purification and radiopharmaceutical formulation. Additionally, the $t_{1/2}$ of fluorine-18 enables one to probe physiological processes which have appropriate kinetics, such as metabolic processes. A fluorine-18 imaging agent can be transported to an imaging centre several hours away and retain a level of activity required for a PET scan, in a process termed centralised distribution. For instance, a 5 GBq dose of a fluorine-18 imaging agent could be delivered to an imaging centre four hours away and still comprise a dose suitable for a PET scan (Figure 9). Carbon-11 based imaging agents suffer from the limitation that centralised distribution is not an option, due to its very short half-life; therefore, if feasible, patients may have to travel to a site where such an imaging agent is available.[38]
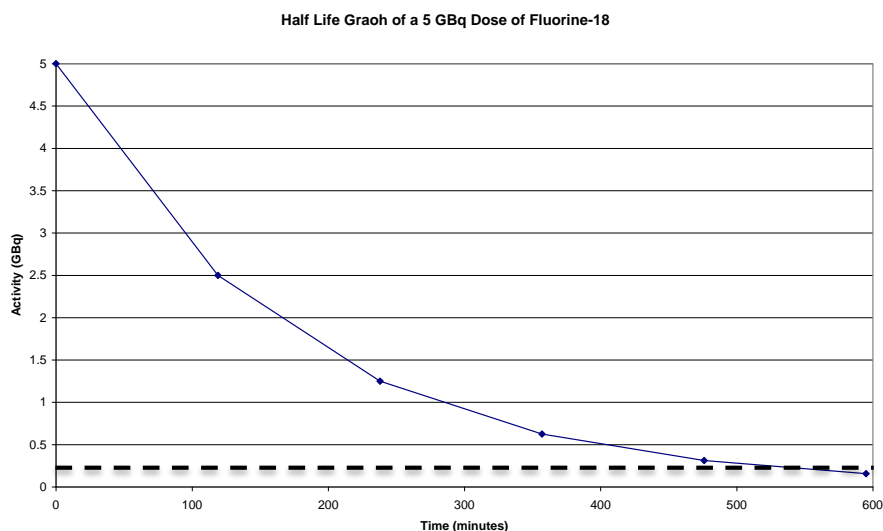
Figure 9: Half life graph showing the exponential decay of fluorine-18 (the dashed line indicate the approximate activity needed for a useful PET scan with [^{18}F]FDG).

Fluorine-18 emits a relatively low energy positron (0.635 MeV) which has a short range in tissue before annihilation with an electron (~2.3 mm), closely matching the spatial resolution of most modern PET cameras. Consequently, an image obtained

with a fluorine-18 imaging agent will provide an image of the highest resolution relative to other PET radionuclides.

The development of the radiopharmaceutical 2-deoxy-2-[^{18}F]fluoro-D-glucose (commonly known as [^{18}F]FDG), which was first synthesised (for further synthetic details see sections 1.6.2 and 1.7.3) by Ido and co-workers in 1978,[39] provided a means of measuring glucose metabolism *in vivo* and established fluorine-18 as a key isotope for use in PET studies. Glucose is transported around the body, where it is eventually phosphorylated by the enzyme hexokinase, to glucose-6-phosphate (Scheme 5, pathway A). In the case of [^{18}F]FDG, once phosphorylated, the resultant 2-fluoroglucose-6-phosphate is no longer able to participate further in the natural reaction cascade do to incorporation of fluorine-18 in place of the naturally occurring –OH moiety (Scheme 5, pathway B).
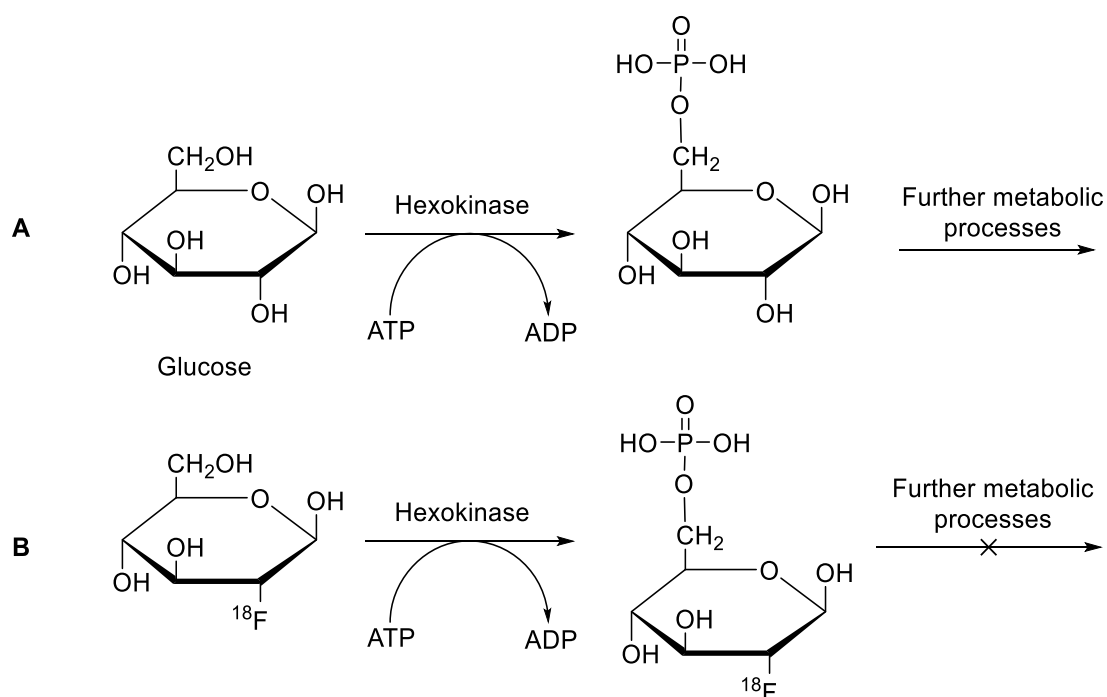
Scheme 5: Incorporation of the fluorine-18 atom blocks further metabolism of [^{18}F]FDG.

Accordingly, concentrations of the radiolabel build-up within a cell which is associated with, for instance, high hexokinase activity. The increased concentration is a marker for an area with high levels of energy metabolism, areas such as the brain, heart, or some tumour types. Clinical data has shown that [^{18}F]FDG uptake in some cancer cells correlates with tumour growth and the tumour degree of metastasis.[3]

13

Hence [^{18}F]FDG remains a universally popular choice for imaging certain tumour types, in addition to investigating cardiovascular and neurological issues.

1.4.1 A Further Comparison of Fluorine-18 Relative to Other Radionuclides used in Positron-Emission Tomography

Comparative imaging studies between carbon-11 and fluorine-18 imaging agents have been reported, whereby fluorine-18 has outperformed its carbon-11 counterpart, not only due to resolution, but also due to increased counting statistics; *i.e.* the greater $t_{1/2}$ of fluorine-18 enables greater image data acquisition.[40, 41] Image comparison by *in vivo* imaging of the non-human primate's 5-hydroxytyptamine (5-HT) system, a system responsible for anxiety and mood-related illnesses, by binding to the critical 5-HT$_{1A}$ receptor, responsible for playing a key role in the regulation of the 5-HT system, has revealed that the fluorine-18 imaging agent provides twelve times more image data and superior detection sensitivity in brain regions with lower 5-HT$_{1A}$ densities, relative to its carbon-11 counterpart (Figure 10).[41]
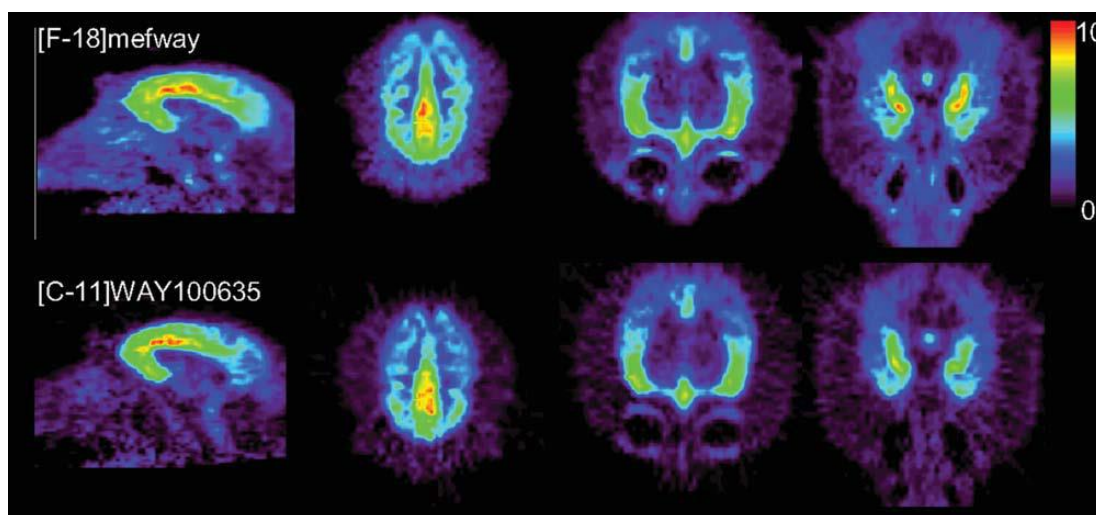
Figure 10:[41] Comparison between [^{18}F]Mefway and [^{11}C]WAY100635 in the rhesus monkey brain. Three transaxial slices highlight imaging agent binding.

1.5   Practical Aspects of Synthetic Radiochemistry

The synthesis of radiolabeled compounds which are applied in pre-clinical and clinical environments, places stringent requirements upon the operators of a radiopharmaceutical production facility (Figure 11).
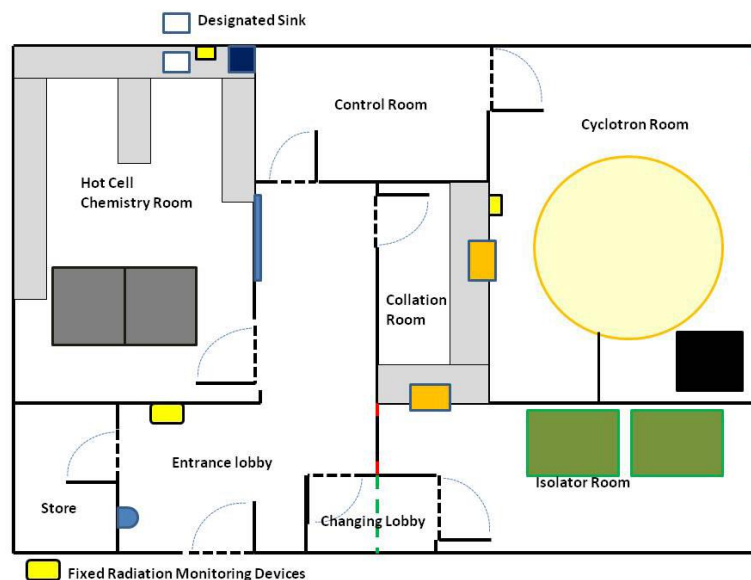
Figure 11: The Sir Bobby Robson Foundation PET Tracer Production Unit, Newcastle University.

Synthetic radiochemistry, for many reasons, needs to be treated differently to standard bench synthetic chemistry. The handling of radioactive material needs to be carried out in a safe and controlled fashion, in a laboratory which has appropriate facilities for this purpose. Furthermore, many radioactive materials, such as fluorine-18, have a half-life which is restrictive on the total time spent on synthesis and purification of a target compound. The reasons outlined above have resulted in a requirement for automated synthetic apparatus, which facilitates rapid incorporation of radionuclides into a target molecule. The apparatus needs to be placed behind an appropriate shield, often, a so-called hot cell is used (Figure 12). Due to the use of shielding, radiation levels in the laboratory are maintained at a safe level, enabling the automated equipment to be controlled by the radiochemist from within the radiopharmaceutical facility.

Figure 12: Hot-cells (Gravatom) within the Sir Bobby Robson Foundation PET Tracer Production Unit at Newcastle University.

1.5.1 Automated Apparatus used in Synthetic Radiochemistry

The time constraint introduced by a radionuclide's inherent half-life has resulted in the development and use of automated apparatus which enables the rapid production of radiolabeled targets; achievable even when using the appropriate precursor on the μmol scale. Development of automated systems for PET imaging agent synthesis began in the late 1970's and the early 1980's, and to this day many of the innovations from this period are used in modern radiochemistry facilities. For instance, the 1982 radiosynthesis of [^{11}C]glucose utilised automated equipment comprising: 19 Teflon coated solenoid valves, 2 reactors, 2 heaters, 4 reagent vials, a vacuum pump, a purification column including 2 Sep-pak cartridges and 4 photo-sensors.[42] A modern system, such as the modular Advion NanoTek microfluidic synthesis system used in Newcastle University, still requires significant assembly by the radiochemist and is made up of similar components (contains 4 modules which consist of 3 reagent pumps, 2 concentrator vials, reactors and a distribution hub).

1.5.1.1 Automated Microfluidic Radiosynthesis Platforms

An increasing number of microfluidic systems have been used in radiochemistry; some are commercial whilst others have been bespoke apparatus. For excellent reviews on this topic the reader is directed elsewhere,[43, 44] and a general overview is provided below. Microfluidic apparatus can be divided into three major sub-groups, namely, capillary-based systems, hybrid devices and lab-on-a-chip systems.

Capillary-based systems include the Advion NanoTek[45] and comprise of a simple hardware setup, using syringe pumps and automated switching valves in conjunction with well understood micro-bore tubing and connectors, resulting in laminar flow across the microfluidic flow apparatus (Figure 13). Microfluidic synthesis systems have provided many advantages in the research and development of radiotracers, such as low reaction times, minimal use of often very expensive precursors, high levels of isotope incorporation and the ability to perform multiple reactions using a single batch of isotope.

Figure 13: A commercially available microfluidic synthesis system (NanoTek®, Advion Biosciences, Inc., Ithaca, NY).

Hybrid devices occupy the middle-ground between capillary-based systems and lab-on-a-chip systems, and are often bespoke in design, utilising conventional hardware such as syringe pumps with monolithic chip devices. Elizarov and co-workers recently described such a system, used in the synthesis of the ubiquitous imaging agent [^{18}F]FDG in doses suitable for preclinical use (Figure 14).[46] Hybrid systems

are utilised to avoid the macro-scale to micro-scale change in technology which is needed to utilise capillary-based systems, *e.g.* during the sequestration of fluorine-18 from the target water obtained from the cyclotron. They also do not suffer from the use of volumes <5 μL like their continuous flow counterparts. However, none have been utilised for routine clinical production, with the design of the aforementioned hybrid device unsuitable for some human studies due to the properties of the material used in the novel reactor.[46]
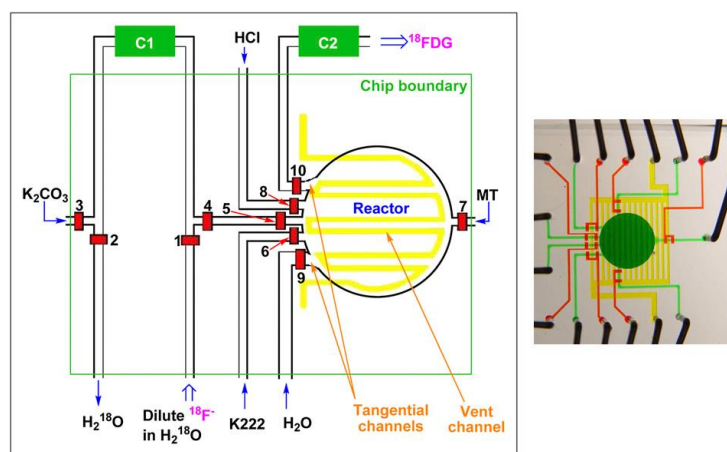
Figure 14:[46] A schematic of a hybrid microfluidic device (left) used in the synthesis of [^{18}F]FDG. The apparatus (right) is presented with dyes loaded into the capillaries for clarity; the fluid network is shown in green, valves in red and vent in yellow.

Finally, lab-on-a-chip devices possess a high level of functionality integrated around a central microfluidic core. An example of this apparatus has been demonstrated by van Dam and co-workers in the novel synthesis of [^{18}F]FDG using electrowetting-on-dielectric (EWOD) microfluidic apparatus (Figure 15).[47] EWOD devices are a 2D system which manipulate droplets using their inherent surface tension.[48] A standard setup comprises a pair of parallel plates, plate one consists of a plate patterned with electrodes and coated with dielectric and non-wetting layers. The dielectric layer is an electrical insulator which may be polarised by an applied electric field. Plate two acts a cover chip which is coated with a conductor (to act as a ground electrode), dielectric and non-wetting layers.[47] Droplets are sandwiched between the parallel plates, with subsequent manipulations such as droplet transport, splitting and merging achieved by applying an electrical potential to individual or multiple electrodes.[49] As liquid manipulations are performed electronically, the requirement

for moving parts such as pumps and valves is eliminated, thus simplifying the chip and the external control system. Additional electronically controlled functions can also be incorporated into the chip, such as sensors to monitor liquid volumes[50] and composition[51] as well as heating elements and temperature sensors for heating or evaporating solvent.[52]
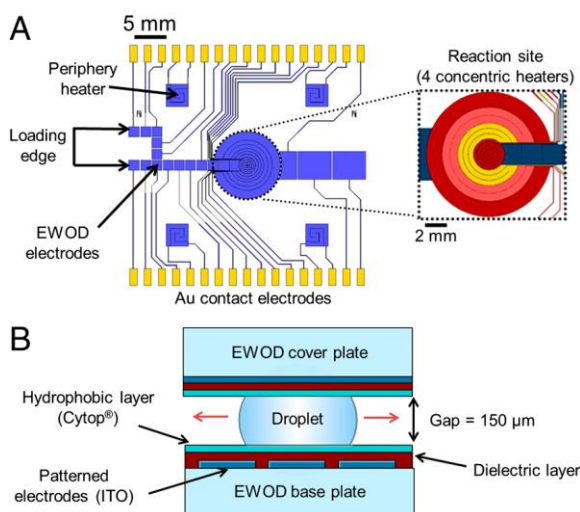
Figure 15:[47] (A) A schematic of an EWOD microchip with four concentric heaters (inset) with a maximum volume of 17 μL. Inset shows magnified area of the heater with four concentric individually controlled resistive heating rings. (B) Schematic side view of the EWOD chip sandwiching a reaction droplet between two plates coated with indium tin oxide (ITO) electrodes, a dielectric layer (silicon nitride) and a hydrophobic layer.

However, hybrid devices and lab-on-a-chip systems suffer from major drawbacks. Hybrid devices, to date, comprise a reactor medium constructed from poly(dimethylsiloxane) (PDMS), a material known to be incompatible with a range of organic solvents as well as being able to interact with and absorb reagents.[53] Lab-on-a-chip systems are currently in an early developmental stage, carrying associated developmental risks, as well as suffering from a lack of compatibility with GMP regulations which is critical to translate radiopharmaceutical production from a preclinical environment to the clinic.[44] Capillary-based devices, such as the Advion NanoTek, do not suffer from these limitations and have demonstrated clinical utility in the repeated synthesis of $[^{18}F]$fallypride,[54] which was administered to twelve patients as part of a clinical trial in the US.[55] Additionally, further imaging agents synthesised using capillary-based devices have been approved for human use, such as $[^{18}F]$FLT[56] and $[^{18}F]$HX4 (Figure 16).[57]
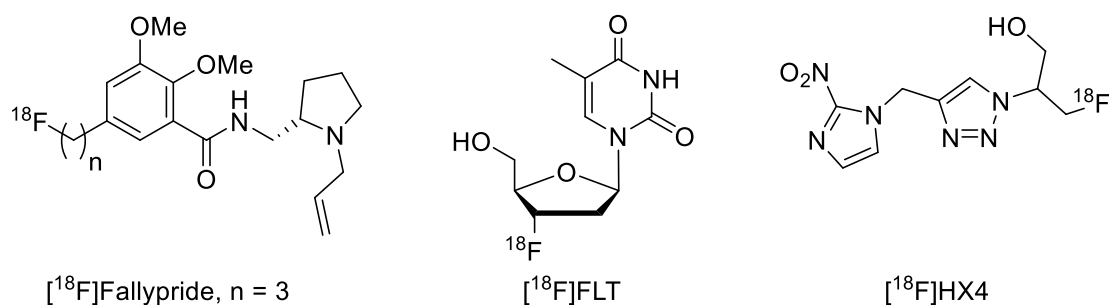
Figure 16: The structures of compounds approved for human use synthesised using microfluidic apparatus; [^{18}F]Fallypride is the only compound used so far in a clinical trial.[55]

[^{18}F]Fallypride, n = 3   [^{18}F]FLT   [^{18}F]HX4

1.5.1.2   Further Automated Radiosynthesis Platforms

Apart from the recent example of [^{18}F]fallypride, highlighted above, microfluidic systems have primarily been used for pre-clinical production. The majority of clinically used imaging agents are synthesised using batch reactors in association with cassette based devices *e.g.* FASTlab (GE Healthcare),[58] Elixys (Sofie Biosciences)[58] and Scintomics GRP cassette module (Scintomics GmbH)[58] amongst others. For clinical production a cassette based device (Figure 17) is particularly useful from a regulatory standpoint, as centralised and controlled manufacture of the requisite cassette is enabled, and subsequently the cassette can be distributed to PET centres in various regions. Additionally, as the cassettes are disposable and replaced after each imaging agent synthesis, fluid paths and validation of a cleaning process is not required. From a synthetic chemistry standpoint, the central manufacture of cassettes which also include all of the reagents required to produce a particular imaging agent reduces the work and error associated with a production run. The disadvantages of the batch based approach are apparent in a research and development scenario, as a limited number of reaction parameters can be investigated per dose of radioisotope. The greater quantity of precursor required to be used in a batch process may not always be feasible, e.g. due to availability and cost limitations, e.g. certain peptides may only be available in small amounts.

Figure 17: A FASTlab loaded with a disposable cassette (GE Healthcare), used for the clinical production of PET imaging agents.

1.6 Fluorine-18 Labelling Strategies

There are two major routes to incorporate fluorine-18 into a compound: direct and indirect labelling. Direct labelling incorporates fluorine-18 into the molecule of interest in a single step thereby minimising the degree of automation required to furnish the final product. Inclusion of fluorine-18, using either of these approaches, can be carried out using two different sources for the fluorine-18, the first is $[^{18}F]F_2$ (electrophilic) and the second $[^{18}F]$fluoride (nucleophilic). Indirect labelling involves the use of prosthetic groups and mitigates any tolerance issues between the molecule to be radiolabeled and the radiolabelling process, e.g. many large biomolecules can not tolerate the conditions required to label with fluorine-18 directly. Prosthetic groups are primarily small molecules, bound to a fluorine-18 label, which possess at least one further reactive functional group, *e.g.* an aldehyde. These groups then go on to react with appropriate pendant functionality on the target molecule, such as the primary amine moiety present at the N-terminus of a peptide. This sequence results in a minimum two-step process as part of the complete synthesis of the imaging agent.

1.6.1 Preparation of Electrophilic Fluorine-18

Electrophilic fluorinations involve, at some stage, the use of $[^{18}F]F_2$. The major drawback in using $[^{18}F]F_2$ is a consequence of its preparation in unavoidably low specific activity (SA), relative to $^{18}F^-$. $[^{18}F]F_2$ is prepared by bombardment of one of two targets, neon, or $[^{18}O]H_2O$ and then removal of the generated fluorine-18 from the target with carrier F_2. Both of these irradiation targets clearly have major limitations in that dilution with fluorine-19 occurs. Additionally, using a neon target results in the nuclear reaction $^{20}Ne(d,\square)^{18}F$, a process which intrinsically yields low specific activity $[^{18}F]F_2$. The aforementioned process was used historically, but is not widely used nowadays.

A technique which produces $[^{18}F]F_2$ in high specific activity (high, that is, relative to previous $[^{18}F]F_2$ production methods) is by use of an electric discharge with $[^{18}F]$fluoride and has been demonstrated to yield $[^{18}F]F_2$ in specific activities up to 100 GBq/μmol.[59]

If $[^{18}F]F_2$ is used as the fluorinating agent, a mixture of labelled products will generally be obtained. This is attributable to the fact that $[^{18}F]F_2$ lacks specificity due to its highly reactive nature. In an attempt to avoid the lack of specificity, more selective electrophilic reagents have been developed by reaction of an appropriate precursor with $[^{18}F]F_2$.

1.6.2 Electrophilic Fluorine-18 Reagents

One of the most important PET imaging agents, which is still the most commonly used imaging agent to this day, is $[^{18}F]$fluorodeoxyglucose ($[^{18}F]$FDG) **12** which was originally prepared by electrophilic fluorination of **11** using $[^{18}F]$acetyl hypofluorite (Scheme 6).[60]
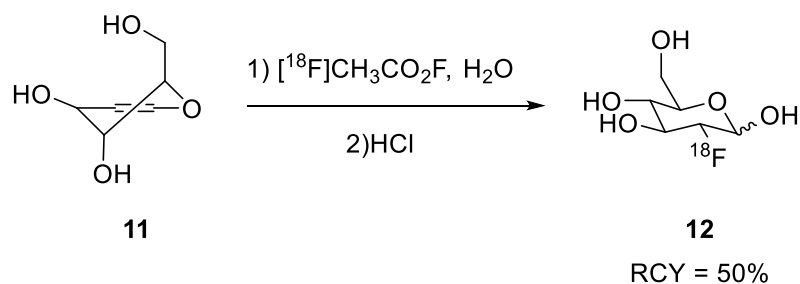
Scheme 6: Preparation of [18F]FDG using [18F]acetyl hypofluorite.

However, [18F]FDG is more commonly synthesised using nucleophilic fluorine-18, as doses of [18F]FDG in much higher specific activity (SA) can be obtained by a nucleophilic approach (see section 1.7.3).

The N-F reagent [18F]Selectfluor™ has been prepared (Scheme 7) as its bistriflate salt by reaction of compound **1**[61] with [18F]F$_2$ generated by an electrical discharge.[59]
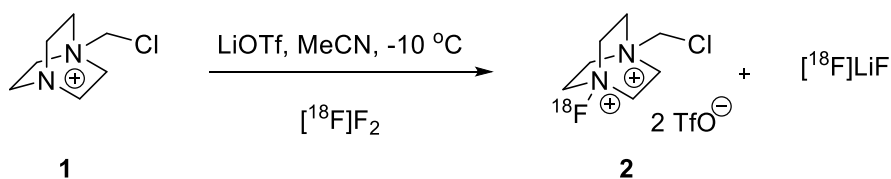
Scheme 7: Preparation of [18F]Selectfluor™ bistriflate.

[18F]Selectfluor™ has been synthesised as its bistriflate salt, as opposed to the bistetrafluoroborate salt, as this would introduce complications arising from isotopic exchange ([18F]fluoride will exchange with the fluorine atoms in the tetrafluoroborate counter-ion releasing [19F]fluoride into the reaction). Conveniently, the bistriflate salt reacts with similar substrates as its bistetrafluoroborate counterpart without the additional complications of diluting the sample with fluorine-19. [18F]Selectfluor™ has been used in electrophilic fluorodestannylation reactions with electron-rich aromatic compounds, such as **2**, mediated by silver triflate, yielding fluorine labelled electron-rich aromatics such as **[18F]3** (Scheme 8).[61]
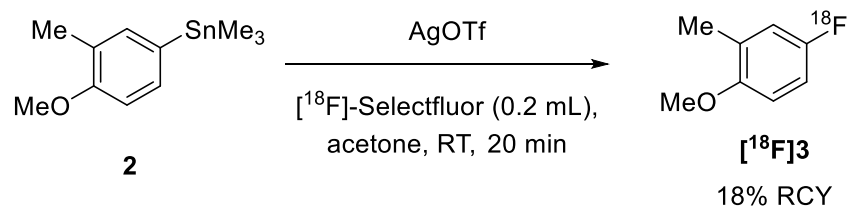
Scheme 8: Electrophilic fluorodestannylation of an electron-rich aryl stannane.

N-[¹⁸F]Fluorobenzenesulfonamide ([¹⁸F]NFSi), is another important electrophilic N-F fluorinating reagent, prepared by reaction of **4** with [¹⁸F]F$_2$ (Scheme 9).[62]
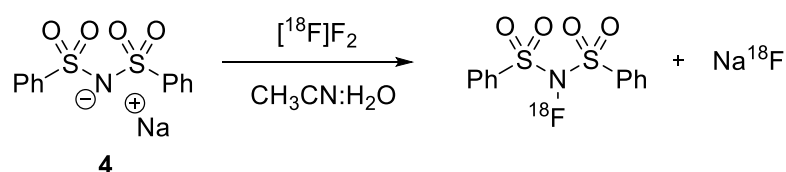
Scheme 9: Preparation of [¹⁸F]NFSi.

To demonstrate the scope of the reagent, [¹⁸F]NFSi has been used to successfully fluorinate silyl enol ether **5** generating fluorine-18 labelled ketone **[¹⁸F]6**, and to fluorinate allyl silane **7** affording allylic fluorine-18 labelled **[¹⁸F]8** (Scheme 10).[62]
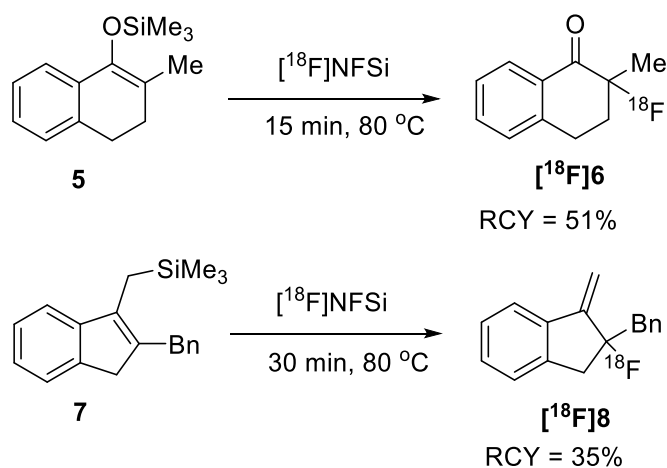
Scheme 10: Electrophilic fluorination reactions utilising [¹⁸F]NFSi.

1.7   Production of Nucleophilic Fluorine-18

Many of the most valuable PET imaging agents are routinely produced using nucleophilic fluorine-18 (abbreviated as $^{18}F^-$). As fluorine-19 carrier is not used in the preparation of $^{18}F^-$, high SA of 100-400 GBq/μmol of $^{18}F^-$ can be achieved. High SA may be a requirement of the imaging agent in question, e.g. where images are to be obtained from sites of low receptor concentration, such as certain neuronal receptors.[63] If a low SA imaging agent was used for this application, the resultant image would be of poor quality, as the non-radioactive fluorine-19 containing compound would compete with the imaging agent at the site of interest giving misleading information on the density of the receptor. For receptors that are only present at very low densities their presence may be missed completely.

The availability of high SA $^{18}F^-$ is clearly a major advantage of nucleophilic fluorination, as the maximum SA one can obtain using electrophilic fluorine is around 100 GBq/μmol.[59] The most common method of production of $^{18}F^-$, can be broken down into several stages.[64] $^{18}F^-$ is obtained by irradiation of $[^{18}O]H_2O$, where the nuclear reaction $^{18}O(p,n)^{18}F$ is particularly high yielding, even at low proton energies. $^{18}F^-$ is then sequestered onto an ion exchange resin, such as a QMA cartridge, enabling the recovery of the excess $[^{18}O]H_2O$. Elution of the trapped $^{18}F^-$ is achieved with a weak base, such as potassium carbonate in a water/acetonitrile solution. In this state, the $^{18}F^-$ is hydrated and therefore poorly nucleophilic so to facilitate the removal of water, and thus enhance the nucleophilic reactivity of the $^{18}F^-$, a phase transfer agent is employed. Kryptofix-222® (K_{222}) may be used in this role, as it forms a strong complex with the potassium cation, consequently exposing, and hence making reactive, the $^{18}F^-$ ($[^{18}F]KF.K_{222}$) (Figure 18).

13
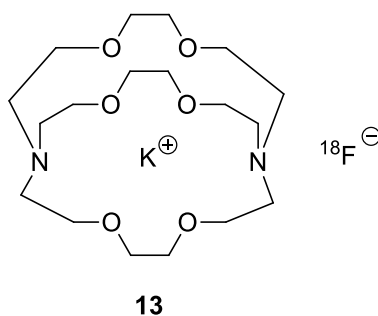
Figure 18: Exposed [^{18}F]fluoride due to complexation of the potassium with K$_{222}$.

An alternative phase transfer agent is tetrabutylammonium bicarbonate which generates [18F]tetrabutylammonium fluoride, [18F]TBAF as the reactive species.[65] [18F]F[-] is trapped onto an ion exchange resin, which is then eluted with tetrabutylammonium bicarbonate, which functions simultaneously as the source of a weak base and an organic soluble cation for the [18F]F[-]. Experiments conducted using [19F]fluoride have shown that for some reactions [19F]TBAF increases reaction yields compared to [19F]KF.K$_{222}$ over ten minute reaction times.[66]

A further, recently developed alternative exists: [18F]tetraethylammonium fluoride, [18F]TEAF.[67] [18F]TEAF has been shown to have equivalent fluorination properties relative to the phase transfer agents discussed above,[67, 68] and in particular benefits over [18F]KF.K$_{222}$ when used in conjunction with microfluidic apparatus due to reduced blockages of the apparatus' capillary tubing.[69, 70]

1.7.1 Reactions with Nucleophilic Fluorine-18: Balz-Schiemann and Wallach Reaction

The Balz-Schiemann and Wallach reactions are historically important reactions regarding the nucleophilic synthesis of fluoroarenes. The Balz-Schiemann reaction concerns the transformation of an aryl diazonium salt which thermally decomposes, in the presence of a source of fluoride, forming the corresponding fluoroarene (Scheme 11).[71]
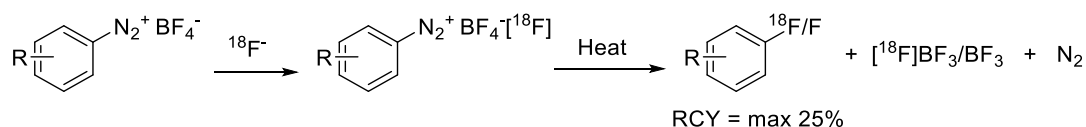
Scheme 11: A radiosynthesis using Balz-Schiemann reaction.

As highlighted earlier (see section 1.6.1) it must be noted that this reaction suffers from several severe limitations. If a fluoride labile anion is used, such as BF$_4^-$, the maximum theoretical radiochemical yield one could obtain is 25%, this is a consequence of the presence of isotopic dilution due to fluorine-19 carrier. BCl$_4^-$ has

been used in an attempt to avoid adding carrier, with little success, as this results in chloroarene formation which have subsequently proven to be difficult to separate from the target fluoroarenes under the time constraints of the fluorine-18 half-life.[72]

The Wallach reaction also involves decomposition of a reactive intermediate, in this instance, of diazene compound in the presence of acid (Scheme 12).[73]
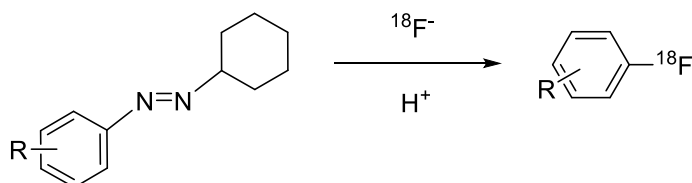
Scheme 12: The diazene intermediate formed during the Wallach reaction.

As above this reaction suffers from low RCYs, even though attempts have been made to optimise the reaction by modification of the reaction solvent, acid and reaction equivalents.[74] As both the Balz-Schiemann and Wallach reactions suffer serious flaws when applied to radiosynthesis, many new methodologies have been developed to incorporate [^{18}F]F$^-$ into an imaging agent.

1.7.2 Reactions with Nucleophilic Fluorine-18: Nucleophilic Aromatic Substitution Reactions

Nucleophilic aromatic substitution (S$_N$Ar) radiochemistry provides a direct one-step route to radiolabeled aromatic compounds, on the premise that the aromatic ring on which substitution is to occur is activated in the *ortho* or *para* position by an electron-withdrawing moiety.[64] Reactions conditions associated with this class of transformation are typically harsh, with temperatures in the range of 100–180 °C, DMSO as the solvent, a base and potentially a kryptand.[64] Commonly employed leaving groups in such reactions include trialkylamine, mesylate, tosylate, triflate, or halogens (Scheme 13).

R = I < Br < Cl < F < NO$_2$ ≈ Trialkylammonium
EWG = 3-NO$_2$ < 4-Ac < 4-CHO < 4-CN ≈ 4-CF$_3$ < 4-NO$_2$
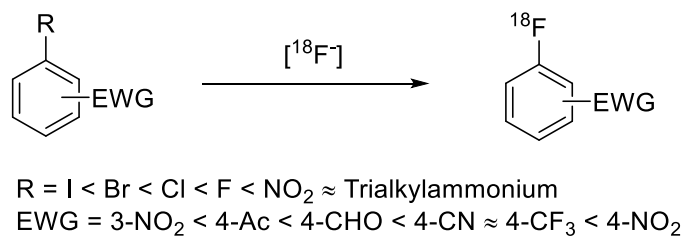
Scheme 13: Production of [^{18}F]fluoroarenes using S$_N$Ar chemistry.

The trialkylamine moiety is an excellent leaving group, but suffers from unwanted side reactions, and may, in the case of trimethylammonium derivatives form [^{18}F]fluoromethane, a radioactive gas, as a side product instead of the intended fluoroarene. The influence of aromatic versus aliphatic substitution has been evaluated by a detailed mechanistic study, which has found that *p*-substituted arenes, with a high Hammet σ constant, favour the formation of the fluorinated arene over [^{18}F]fluoromethane (Figure 19).[63]
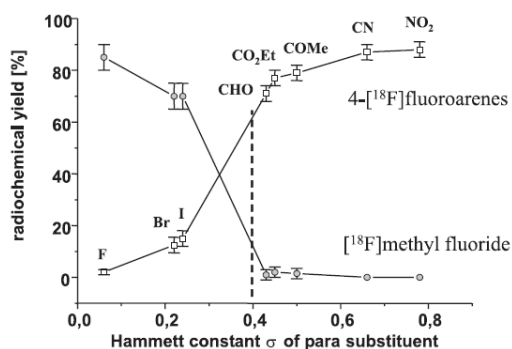
Figure 19:[63] The influence of *p*-substituents on the competitive formation of [^{18}F]fluoroarenes and [^{18}F]fluoromethane where trimethylamine is the leaving group.

An example of this procedure of direct S$_N$Ar chemistry has been applied in the synthesis of the imaging agent [^{18}F]Flumazenil, where the careful choice of precursor **9** demonstrates the success of the fluorination of a weakly activated arene (Scheme 14).[75]
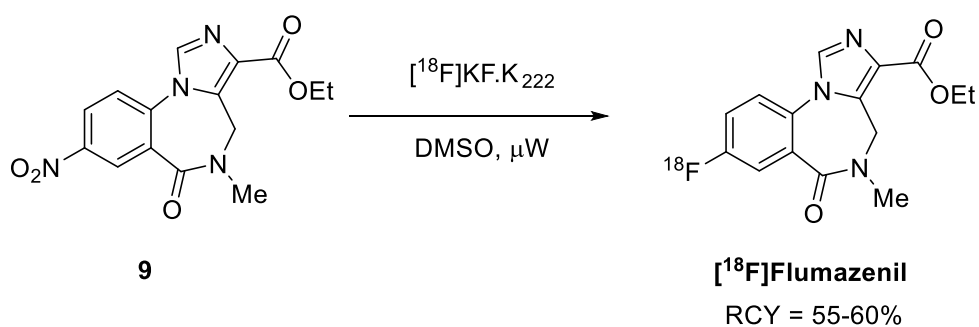
Scheme 14: Direct S_NAr radiosynthesis of [¹⁸F]Flumazenil.

The disadvantage of a direct nucleophilic approach is that any other sites, also susceptible to nucleophilic attack by [¹⁸F]fluoride ion, need to be protected, such as ROH, RCO₂H and RNH₂, due to the ability of fluoride to abstract labile protons from these functional groups. Consequently, additional synthetic steps to protect this functionality are required to prepare the precursor and once the fluorine label has been introduced then remove the protecting groups, and therefore the RCY of the radiosynthesis is likely to suffer.

1.7.3 Reactions with Nucleophilic Fluorine-18: Aliphatic Nucleophilic Substitution Reactions

Aliphatic nucleophilic substitution with ¹⁸F⁻ follows the reactivity of a typical S_N2 reaction, with higher yields obtained at a primary carbon, and the reactions are typically performed in polar aprotic solvents.

[¹⁸F]FDG, the aforementioned ubiquitous imaging agent, is widely used in PET studies. The synthetic route to [¹⁸F]FDG by nucleophilic means proceeds by an aliphatic nucleophilic substitution reaction (Scheme 15).[76] A synthetic process has now been fully automated for this reaction, and takes around 30 minutes for a complete radiosynthesis and purification. However, this synthesis of [¹⁸F]FDG does suffer from the same disadvantage that was highlighted by S_NAr chemistry, i.e. the requirement of additional steps (protection/deprotection of **10** and **11**, the latter being critical in the radiosyntheis) where sensitive functionalities are present in the imaging

agent. However, the excellent RCY and SA obtained more than outweigh the disadvantages.
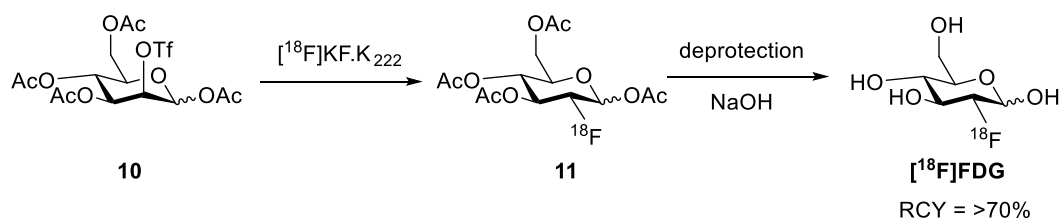
Scheme 15: Synthesis of [¹⁸F]FDG.

Not all nucleophilic aliphatic substitution reactions rely on multi-step syntheses. A synthesis of the selective dopamine transport ligand [18F]LBT-999 has been achieved in a one-step process from the aliphatic halide precursor **12** (Scheme 16).[77]
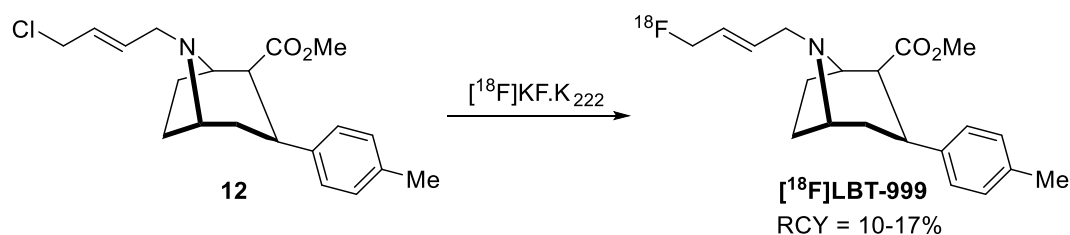
Scheme 16: One step radiosynthesis of [¹⁸F]LBT-999.

Nucleophilic ¹⁸F⁻ can also be used to open some cyclic systems, such as **13a** or **13b** to afford [18F]fluoro-3'-deoxy-3'-L-fluorothymidine, [18F]FLT (Scheme 17).[78] The nucleoside [18F]FLT is used as a cellular proliferation marker.[79]

R = H, **13a**
R = 4,4′-Dimethoxytrityl, **13b**

[¹⁸F]FLT
RCY = 5-14%
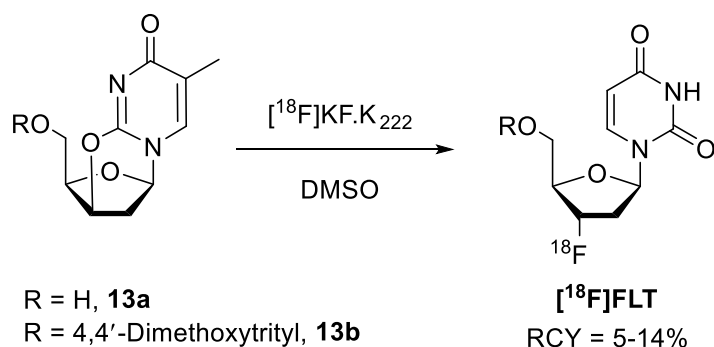
Scheme 17: Opening of cyclic systems 13a and 13b with ¹⁸F⁻.

Unfortunately, ring opening chemistry can't be routinely exploited in the case of epoxides, as an acid catalyst is typically required.[80] It is necessary to take specific precautions, as quantities of dilute hydrofluoric acid could be generated between a source of fluoride and a source of protons. Although hydrofluoric acid is a weak acid in a dilute solution,[81] it is highly corrosive, and will dissolve a wide range of materials.

1.7.4 Reactions with Nucleophilic Fluorine-18: Substituion Reactions upon Heteraromatics

The main class of heteroarenes for which the S_NAr chemistry with $^{18}F^-$ has been examined are pyridines.[82] A consequence of the occurrence of the pyridinyl moiety in many natural products such as compounds which bind to nicotinic receptors.[3] Compounds possessing these features could therefore be modified to incorporate a radiolabel, and function as PET imaging agents. The synthesis of several classes of fluoropyridines (Figure 20) using conventional fluorine-19 chemistry has been demonstrated, and could potentially be exploited to prepare fluorine-18 counterparts.
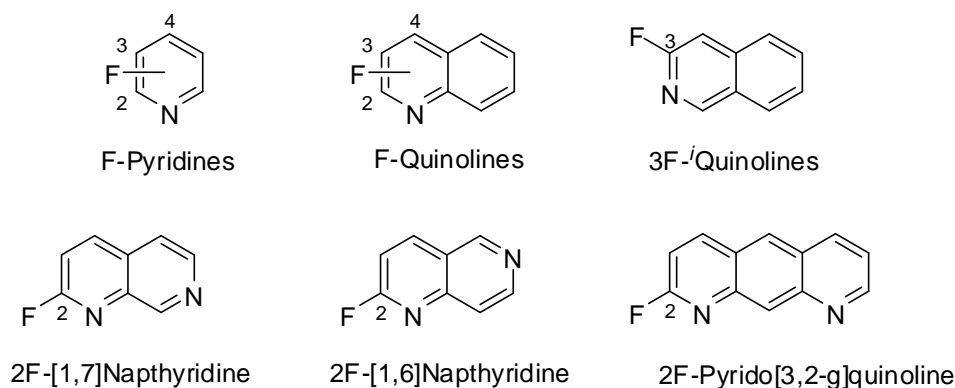
Figure 20: Fluoropyridines accessed using conventional fluorine-19 nucleophilic substitution chemistry.

Epibatidine is a natural pyridinyl containing compound which is isolated from the skin of *Epipedeobates Tricolour*, a poisonous frog. It is a potent nicotinic

acetylcholine receptor agonist.[83] The 2-[18F]fluoroepibatidine radiolabeled compound is prepared by nucleophilic aromatic substitution of the corresponding aryl bromide precursor **14** (Scheme 18).[84] There are currently no useful 4-[18F]fluoropyridine based imaging agents, even though the synthesis of this class of compounds proceeds with similar efficacy as their 2-[18F]fluoropyridine counterparts.[64]
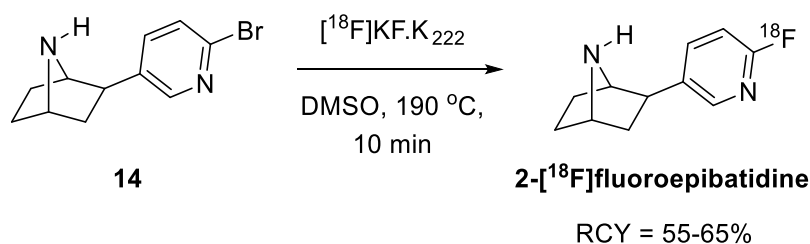
Scheme 18: One-step synthesis of 2-[18F]fluoroepibatidine.

The synthesis of 3-[18F]fluoropyridines requires an electron-withdrawing moiety, such as amido or cyano moieties, to be present para- to the desired fluorination site (Scheme 19).[85]. Bromo or chloro atoms may be successfully utilised as leaving groups in this case.
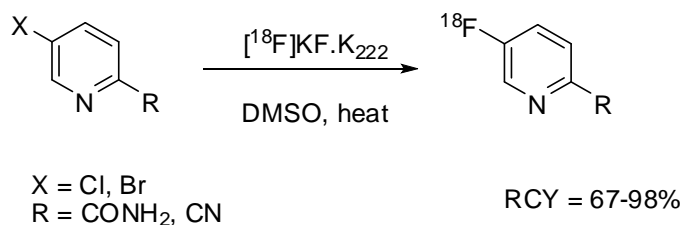
Scheme 19: A general one-step synthesis to 3-[18F]fluoropyridines.

1.8 Reactions with Nucleophilic Fluorine-18: Click Chemistry Approaches

The advantages that click chemistry possess are very relevant to the radiochemist, *i.e.* rapid, selective and relatively simple reactions which often only require mild conditions. The rapid formation of a triazole ring by a Huisgen cycloaddition (a 1,3-dipolar cycloaddition) of azide **15** with an alkyne,[86] has been described as "the cream of the crop" of click chemistry.[87] The cycloaddition reaction has been put to excellent use in the formation of a library of 2-[^{18}F]fluoroethyltriazoles (Scheme 20).[88]
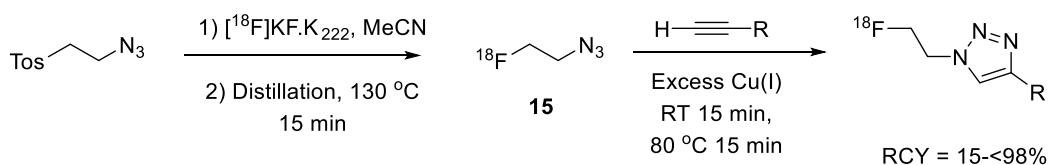
Scheme 20: Click-chemistry used to synthesise 2-[^{18}F]fluoroethylazides.

The Huisgen 1,3-dipolar cycloaddition requires the presence of a Cu(I) catalyst, else, the reaction would take many hours to complete.[86] Therefore an excess of Cu(I) and azide are employed in the radiosynthetic approach, meaning the conjugation step takes around 10 minutes at room temperature in a water/MeCN/DMF buffered solution (pH 6.0).[88] The terminal alkynes used in the reaction may include acidic functionality, ester, amide, amino and phenyl moieties, demonstrating that this reaction has an excellent functional group tolerance and therefore scope for future investigations regarding this type of chemistry.

1.9 Reactions with Nucleophilic Fluorine-18: Reactions with Diaryliodonium Salts

The major limitations that standard nucleophilic aromatic substitution of arenes with $^{18}F^-$ suffers are that they are poor at labelling electron-rich arenes, and poor at accessing all regioisomers of a particular fluoroarene, due to mechanistic considerations. Therefore, in many of the previous synthetic examples outlined above, only arenes possessing an electron-withdrawing moiety, and certain regioisomers of the arene, have been fluorinated. It may be desirable to incorporate the radiolabel into an electron-rich arene, in which case S_NAr with $^{18}F^-$ would prove troublesome. Also, during the evaluation of an imaging agent it may be found that a different regioisomer is required, which cannot be accessed by standard S_NAr methodologies. Diaryliodonium salts (Figure 21) provide a potential solution to this problem.
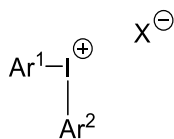
Figure 21: The general structure of a diaryliodonium salt.

Diaryliodonium salts were first reported in 1995 as precursors to radiofluorinated arenes,[89] and since then have received considerable attention for their utility both in radiochemistry and in cross-coupling reactions.[85] Both electron-deficient and electron-rich arenes can be fluorinated using diaryliodonium salts,[90] in addition, all regioisomers of a particular arene may be accessed, thus providing two distinct advantages over standard S_NAr chemistry. Additionally, diaryliodonium salts present the radiochemist with two useful selectivity features. Firstly, the selectivity of the fluorination of diaryliodonium salts tends to proceed according tothe so-called "*ortho*-effect", this effect results in preferential radiofluorination of the more sterically demanding arene.[91] A second mode of selectivity was determined by computational studies regarding the regioselectivity of nucleophilic attack by fluoride upon alkynyliodonium salts[92, 93] and heteroaromatic diaryliodonium salts.[94] These studies found that the electronic nature of substituents around the iodine atom

are the most important features in determining regioselectivity; if there is no *ortho* substituent present on either ring, the ring with the lowest electron density will be preferentially fluorinated. The study with heteroaromatic diaryliodonium salts also provided experimental evidence which supported this regioselectivity theory.[94]

It has been proposed that the mechanism of fluorination of a diaryliodonium proceeds in a "turnstile" fashion (Scheme 21).[85]

Scheme 21: The proposed "turnstile" mechanism for the radiofluorination of a diaryliodonium salt.[85]

This mechanism helps to account for the *ortho* selectivity discussed above, as the bulkier arene (Ar^2 in Scheme 21) lies in the more favoured equatorial position. $^{18}F^-$ attacks the positive iodine centre, forming a trivalent intermediate which then collapses forming the products.

Reactions of this type are typically carried out under milder conditions than their S_NAr counterparts, and may even be able to take place in the presence of large quantities of water.[95]

1.10   Chemistry of Diaryliodonium Salts

Diarylodonium salts are a class of compounds first synthesised in the late 19th century.[96] In these compounds iodine possesses a non-standard bonding number and therefore, according to IUPAC nomenclature, described by λ–notation. For instance, hydrogen iodide, HI, is classified as an iodane. However, due to the non-standard bonding present in H_3I, the iodane is described as a λ^3-iodane, H_5I as a λ^5-iodane and so on. The more common λ-iodanes are of the type Ar_2IL, and are termed diaryl-λ^3-iodanes. Therefore, it is more correct to describe diaryliodonium salts as diaryl-λ^3-iodanes, even though the former nomenclature is still the most common descriptor. It is important to note that the use of the term "salt" is not very accurate as two discreet ions are not always present. Single-crystal X-ray crystallographic methods have determined that the compounds adopt a trigonal bipyramidal structure, and the two axial ligands share a hypervalent bond (Figure 22).[97] As consequence of a node in the non-bonding orbital of the hypervalent bond being located on iodine, the iodine atom is highly electrophilic.
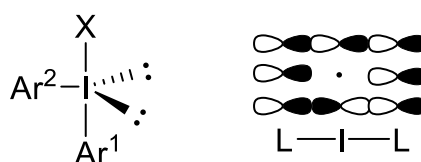
Figure 22: Diaryliodonium salt geometry, and a simplified molecular orbital diagram of the pseudo-axial hypervalent bond.

In solution, there is much debate about whether or not diaryliodonium salts retain the trigonal bipyramidal configuration which they adopt in the solid state; many speculate that the nature of the counter anion X, and the solvent, could affect the "T-shape" structure which was determined in the solid phase.[97]

It has been reported that the successful fluorination of diaryliodonium salts varies, especially where both arenes of the diaryliodonium salt are electron rich.[98, 99] Aromatic radicals may be generated from a hypervalent iodine compound, as a consequence of homolytic fission of an aryl iodine bond. As the process of homolytic

fission is spontaneous and random, particularly at elevated temperatures, the level of radicals present in the reaction vessel may differ between reactions, and may therefore cause a lack of reproducibility. Aromatic radical species may undergo further side reactions, leading to undesired products, leading to not only a lower yield but complicating the purification of the desired fluoroarene. Fortunately, it has been shown that the addition of radical scavengers, such as galvinoxyl and TEMPO (Figure 23), can improve the reproducibility and the material yield of the fluorination process, where both arenes of the diaryliodonium salt are electron-rich.[100]

Galvinoxyl   **TEMPO**
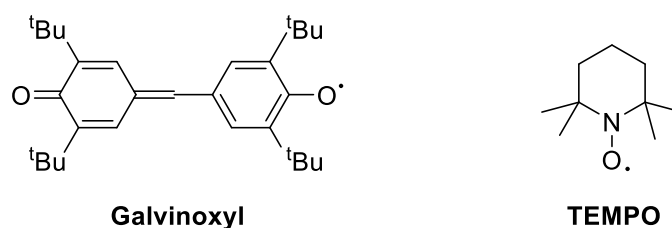
Figure 23: Radical scavengers used in the fluorination of diaryliodonium salts.

1.10.1   *Synthesis of Diaryliodonium Salts*

Diaryliodonium salts can be synthesised by several different means, often in two to three steps.[101] Oxidation of an iodoarene to an iodine(III) precursor, followed by reaction with an organometallic reagent is a popular choice. A typical approach to the initial oxidation of the iodoarene is to use sodium perborate mono or tetrahydrate as the oxidant, in acetic acid, furnishing a aryliodobisacetate (Scheme 22).[102]

where *x* = 1, 4
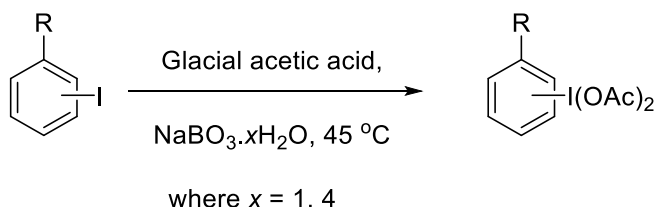
Scheme 22: Transformation of a substituted iodobenzene to a substituted diacetoxyiodobenzene.

The diacetoxyiodoarene can then be reacted with an organometallic reagent, such as an arylstannane in the presence of an acid, to prepare a diaryliodonium salt. As it is possible to generate a diacetoxyiodoarene and an organostannane at any given

position of an arene, it is possible to synthesise all regioisomers of a particular diaryliodonium salt. This means that upon reaction with a nucleophile, such as ^{18}F$^-$, all regioisomers of a radiolabeled arene can be accessed if careful choices are made about the arenes involved and the position of any substituents (Scheme 23).
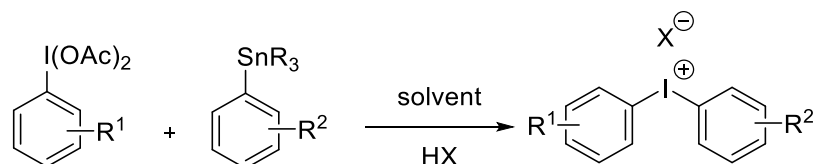
Scheme 23: Synthesis of a general diaryliodonium salt.

1.10.2   *Diaryliodonium Salt Chemistry Applied to Imaging Agents and Prosthetic Groups*

Many examples above have so far been concerned with the direct labelling of an imaging agent precursor, using either electrophilic or nucleophilic means. An excellent use of diaryliodonium salts is that they are compatible with both direct, and indirect radiolabeling approaches. For example, the synthesis of the imaging agent [^{18}F]DAA1106 was achieved by direct nucleophilic radiofluorination of diaryliodonium salt precursor **16** (Scheme 24).[103]
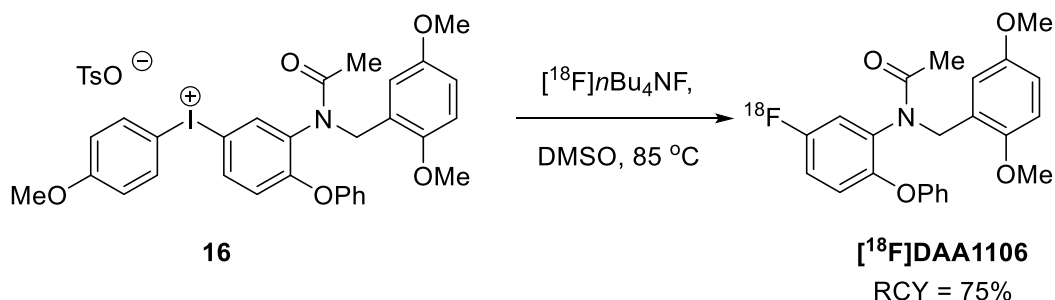
Scheme 24: Direct radiosynthesis of [^{18}F]DAA1106 from a diaryliodonium salt precursor.

By varying the position of the iodonium group on the target arene, further regioisomers of [^{18}F]DAA1106 could be obtained, as the electron-rich anisole moiety directs fluorination towards the target arene.

Many imaging agents have been studied as only their *ortho* or *para* regioisomers, as unsuccessful attempts have been made to synthesise *meta* regioisomers by nucleophilic means.[104] It is possible to access *meta* substituted fluorinated arenes with diaryliodonium salts,[105] for the reasons discussed above. A practical application of this approach has been demonstrated in the synthesis of *meta*-[18F]fluoropyridine, **[18F]18** from 3-pyridyliodonium salt **17** (Scheme 25).[91] If this chemistry were to be applied to the synthesis of other fluorine-18 labelled radiopharmaceuticals then optimisation of imaging agent structure could be achieved, akin to SAR in conventional drug discovery.
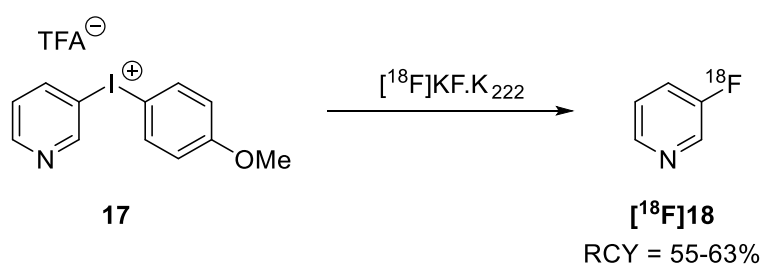
Scheme 25: Synthesis of *meta*-[18F]fluoropyridine, [18F]18.

1.11 Radiolabelling Biomacromolecules with Fluorine-18 Prosthetic Groups

The therapeutic use of biomacromolecules, a field termed biologics, are playing a progressively important role in medicine relative to small molecule therapeutics due to several key advantages.[106] For instance, due to the specific action of a protein, a desired pharmacological effect can be attained without impairment of normal biological processes. Furthermore, the complex nature of proteins means the requisite pharmacological effect often cannot be obtained by the use of a simple small molecule. The total US market for biologics was ~$48 billion in 2009,[107] ~$51.3 billion in 2010,[108] and ~$53.8 billion in 2011.[109] The biologics market has seen continued and sustained growth in sales since 2005, which then had sales of around $33 billion (Figure 24).[107]
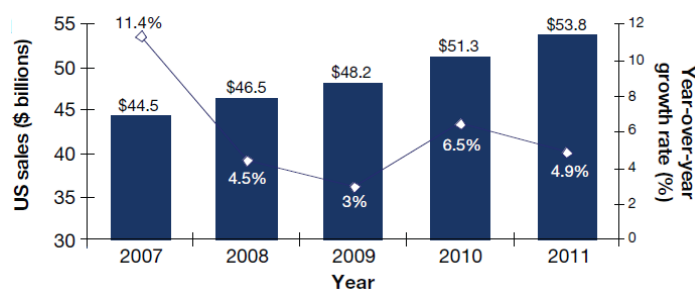
Figure 24: Continued growth in biologics sales in the US between 2007-2011.[109]

The biologics market is expected to continue to grow in future, as many more biologics are undergoing clinical trials for a range of disorders.[106] Additionally, the success rate of these therapeutics are now higher than that of small-molecule drugs, with a 32% and 13% approval rate respectively between 1993 and 2004.[107]

Additionally, the application of biologics as radiopharmaceuticals is also gaining interest in the field of nuclear medicine.[110-112] Unfortunately, direct radiolabelling of biomacromolecules with fluorine-18 is not always practical, save in certain circumstances, due to the harsh conditions which are often employed, for instance, in S_NAr radiolabeling processes. New methodologies have therefore been developed, whereby the radiolabel is introduced onto a small molecule (the prosthetic group) which bears the reactive functionality required to conjugate to a suitability

functionalised biomacromolecule precursor. A range of prosthetic groups are available which facilitate the indirect labelling of a range of biomacromolecules such as oligonucleotides (Scheme 26).
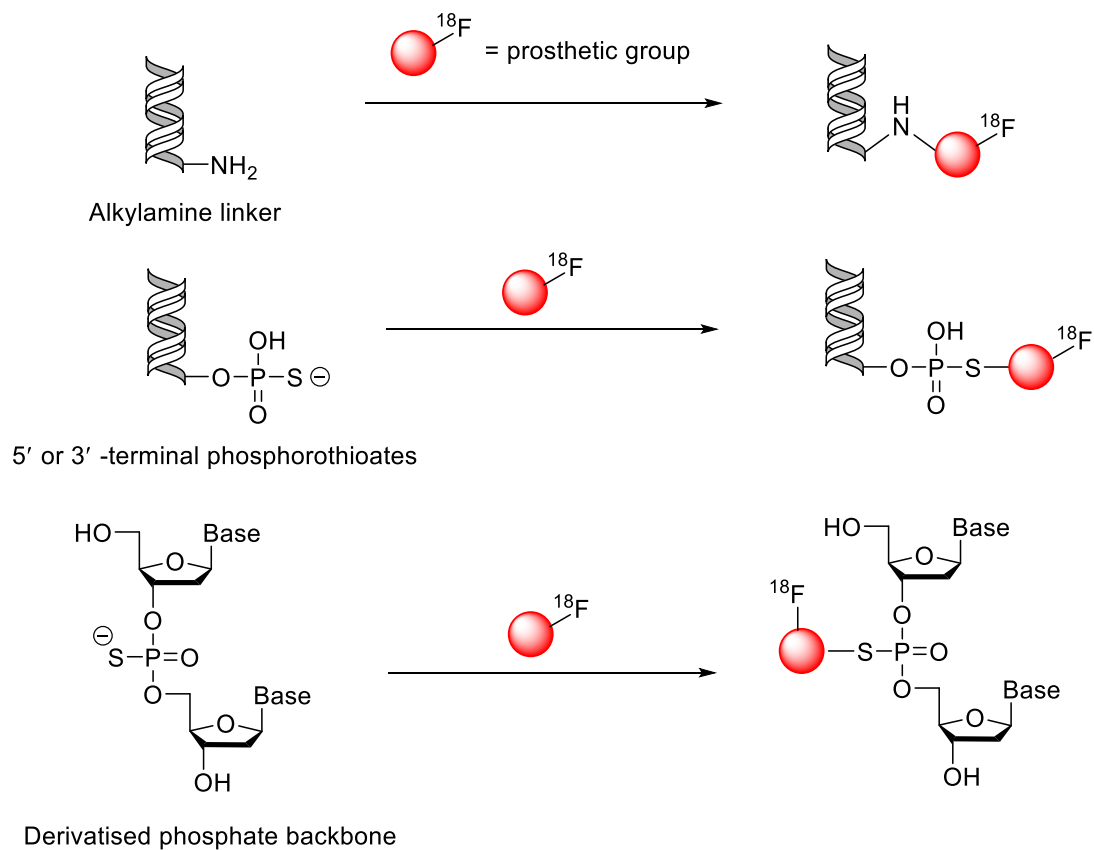
Scheme 26: Fluorine-18 radiolabelling of oligonucleotides with fluorine-18 radiolabeled prosthetic groups.

Furthermore, many prosthetic groups are available which facilitate the indirect labelling of a range peptides/proteins (Scheme 27).
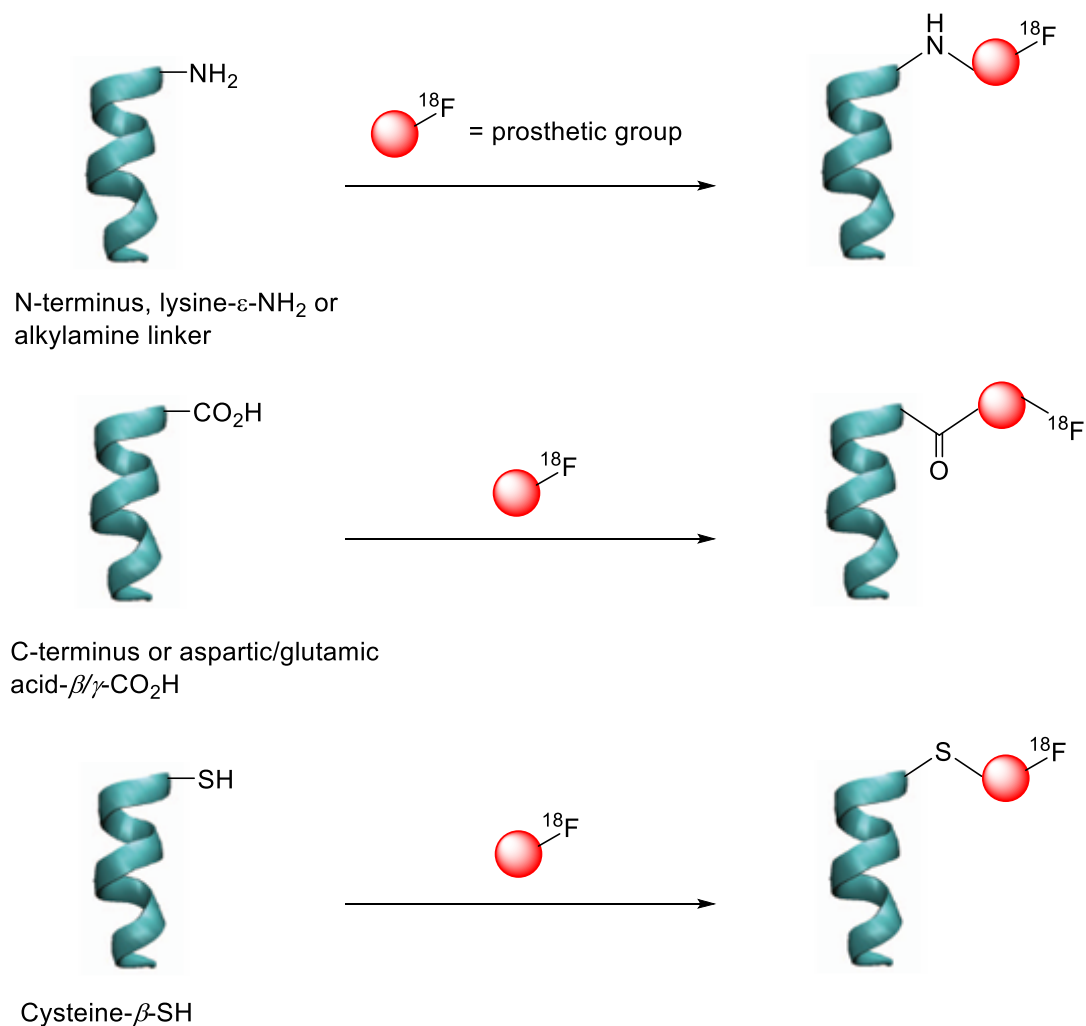
Scheme 27: Fluorine-18 radiolabelling of peptides/proteins with fluorine-18 radiolabeled prosthetic groups.

There is a great deal of interest in the indirect labelling approach using prosthetic groups, as not all biomacromolecules of interest tolerate direct radiolabelling conditions, for reasons highlighted above. Substrates such as peptides and proteins would not tolerate harsh S_NAr conditions. Utilisation of a prosthetic group provides a flexible choice of chemical routes to the desired radiolabeled biomacromolecule, as the conjugation step maybe performed under relatively mild conditions.

1.11.1 Amine-Reactive Prosthetic Groups

Many amine reactive prosthetic groups have been reported (Figure 25: Amine-reactive prosthetic groups: 4-[18F]FBA,[113] 4-[18F]SFB,[114, 115] [18F]19,[116] [18F]20,[117] [18F]21,[118] [18F]22,[119] [18F]23,[120] [18F]24,[121] [18F]25[110] and [18F]26.[110]).
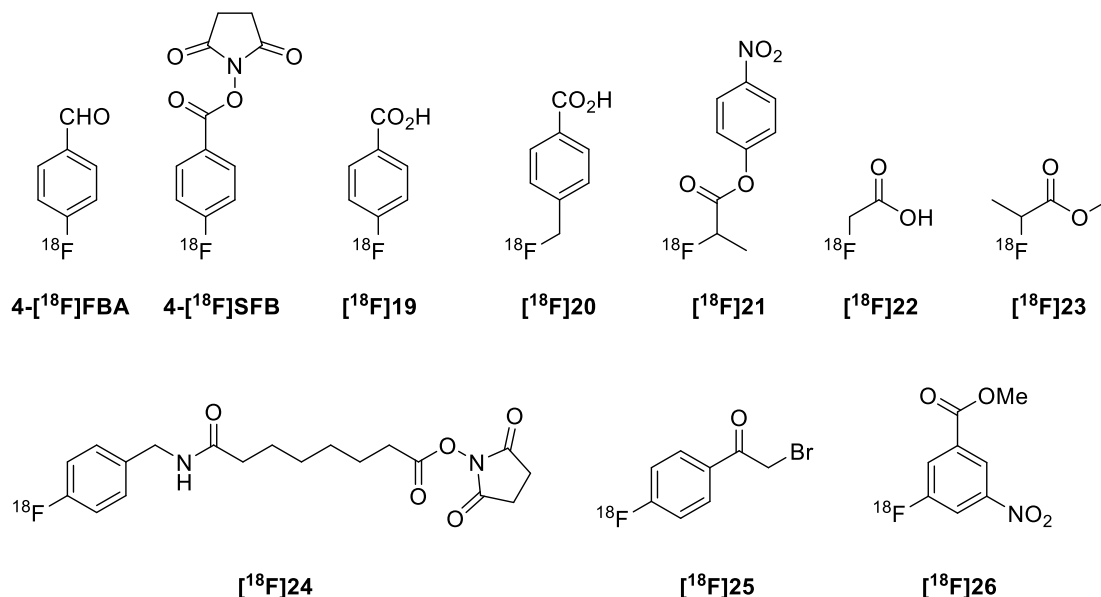
Figure 25: Amine-reactive prosthetic groups: 4-[18F]FBA,[113] 4-[18F]SFB,[114, 115] [18F]19,[116] [18F]20,[117] [18F]21,[118] [18F]22,[119] [18F]23,[120] [18F]24,[121] [18F]25[110] and [18F]26.[110]

4-[18F]Fluorobenzaldehyde (4-[18F]FBA) is an important prosthetic group used in PET and has been synthesised *via* several different routes. The traditional method of incorporating fluorine-18 onto an activated arene employs a nitro leaving group,[122] and this synthetic procedure was subsequently applied to the synthesis of 4-[18F]FBA using 4-nitrobenzaldeyde as the starting material. The 4-[18F]FBA was then used as an intermediate in the synthesis of radiolabeled 4-fluorobenzylhalides.[123] Aldehydes undergo many established reactions with many common functional groups, including amine bearing amino acid residues such as arginine and lysine. Hence a labelled fluorobenzoyl moiety can be delivered onto many diverse substrates, from a wide range of peptides[124] to large molecules such as the hormone leptin (Figure 26).[125]
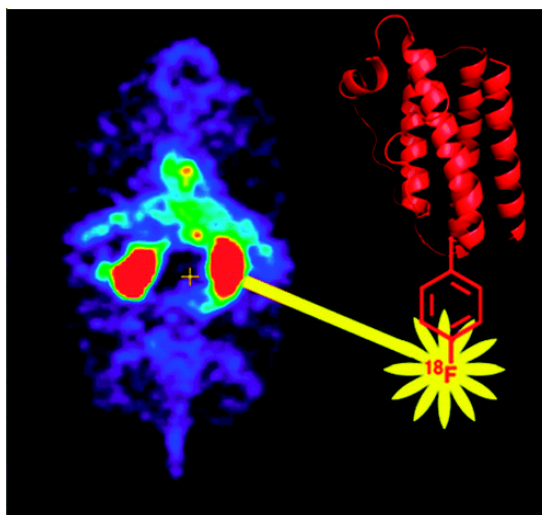
Figure 26: A schematic of leptin labelled with 4-[^{18}F]FBA (right), and PET scan image in *ob/ob* mice.[125]

Recent work has utilised [^{18}F]fluorobenzaldehydes in the convergent radiosynthesis of several imaging agents, by multi-component reactions, such as the Biginelli, Ugi, Passerini or Groebke reactions.[126] An optimised Groebke-Bienaymé-Blackburn reaction has been performed, using 4-[^{18}F]FBA, achieving a high RCY in accessing the complex target **19** (Scheme 28).[126]
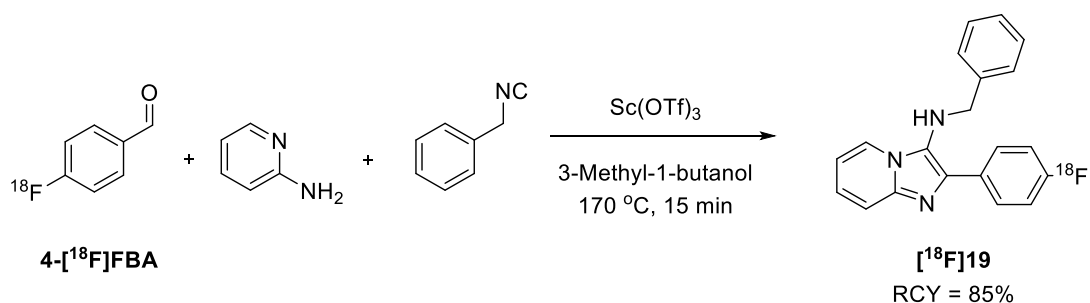
Scheme 28: Groebke-Bienaymé-Blackburn multi-component reaction affording [^{18}F]19.

1.11.2   Carboxylate-Reactive Prosthetic Groups

Amidation reactions, between carboxylate reactive synthons and carboxylic acid moieties present in biomacromolecules, have received considerably less attention than their amine counterparts. This is due to the imposition of certain requirements on the compound to be labelled, in particular, the compound should not possess free amine moieties, else inter- and intramolecular cross-linking may occur. Of course, the amine moiety could be protected, resulting in greater synthetic burden. An example of a carboxylic acid reactive prosthetic group is [^{18}F]FMBAA (Figure 27), which has been used to label a protected insulin.[127]
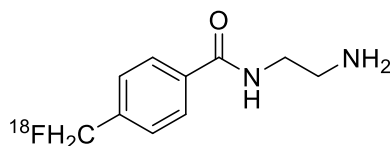
[^{18}F]FMBAA

Figure 27: [^{18}F]FMBAA – a carboxylic acid reactive prosthetic group.

1.11.3   Thiol-Reactive Prosthetic Groups

In nature, there is a marked lack of free sulfhydryl residues in biomacromolecules relative to amine and carboxylic acid residues.[128] This has advantages for the radiochemist, as biomacromolecules can be engineered to contain sulfhydryl residues, thus, thiol reactive prosthetic groups can be utilised to regioselectively synthesise imaging agents. Many thiol-reactive prosthetic groups are known (Figure 28).
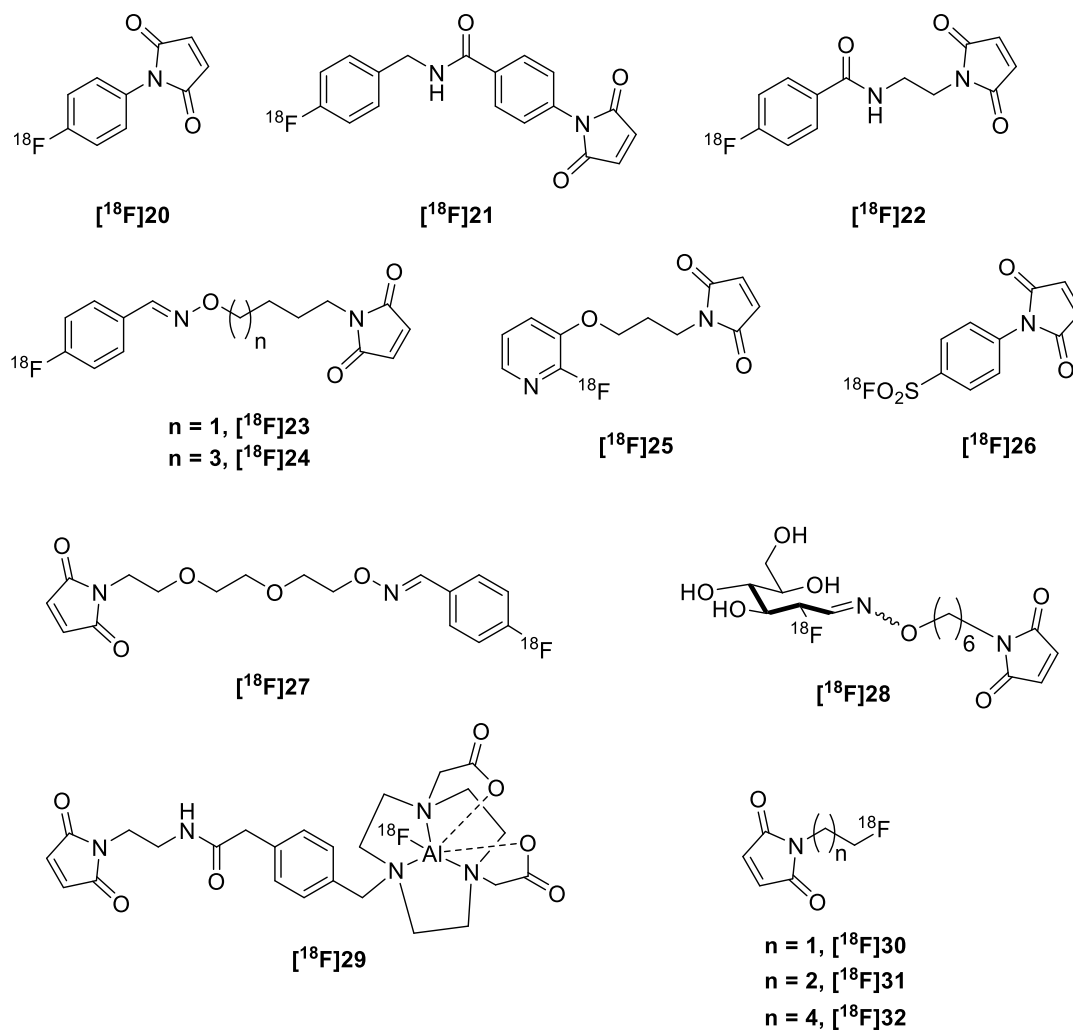
Figure 28: Thiol-reactive prosthetic groups: [18F]20,[129] [18F]21,[129] [18F]22,[130] [18F]23,[131] [18F]24[132], [18F]25,[133] [18F]26,[134] [18F]27,[135] [18F]28,[136] [18F]29,[137] [18F]30,[138] [18F]31[138] and [18F]32.[138]

Thiol-reactive prosthetic groups often possess a maleimide moiety. Maleimides are Michael acceptors and will therefore react with the soft sulfhydryl nucleophile in a conjugate fashion. This has been demonstrated by reaction of a maleimide, [18F]FBEM and a sulfhydryl containing RGD peptide for the imaging of vascular endothelial growth factor and vascular endothelial growth factor receptor, $\alpha_v\beta_3$ integrin (Scheme 29).[130]
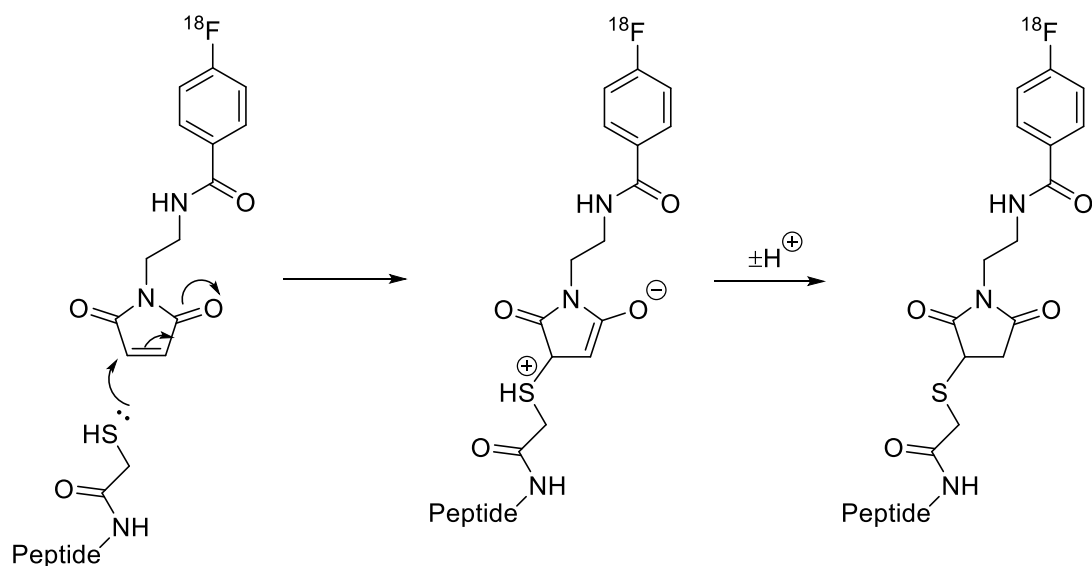
Scheme 29: A RGD peptide labelled *via* a Michael addition using [¹⁸F]FBEM.

A heteroaromatic fluorine-18 labelled prosthetic group used as a tumour imaging agent, [¹⁸F]FPyME, has also been synthesised, *via* a three step procedure (Scheme 30).[133] Due to the nature of nucleophilic heteroaromatic substitution, only the 2-regioisomer was synthesised.
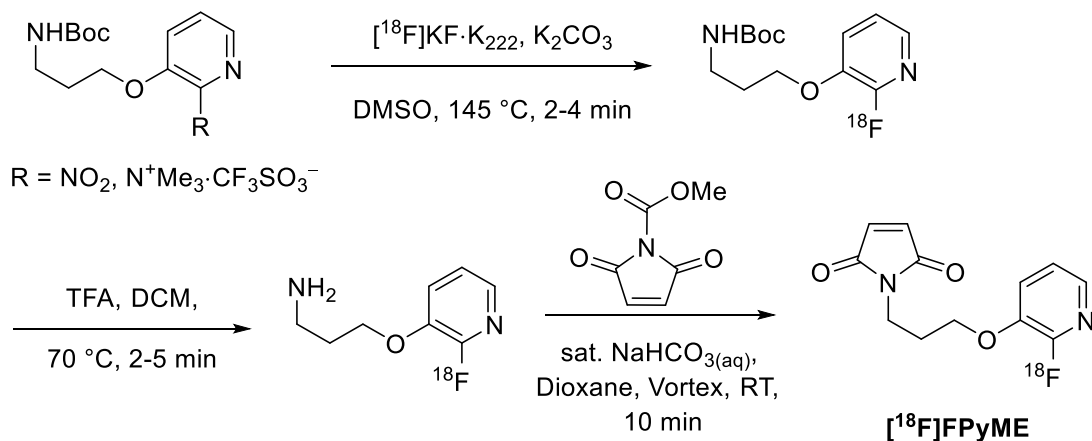
Scheme 30: Production of [¹⁸F]FPyME.

1.12 Radiolabeling Small Molecules with Fluorine-18 Prosthetic Groups

The use of prosthetic groups is not limited to the labelling of biomacromolecules; small molecules can also be labelled using this strategy. The labelling of small molecules is becoming increasingly important in the early stages of the drug discovery pipeline, enabling accurate selections of lead compounds for further evaluation.[4, 139]

For instance, [^{18}F]Lapatanib has recently been synthesised by labelling with the prosthetic group 3-[^{18}F]fluorobenzylbromide precursor. A prosthetic group approach is vital for the radiolabelling of Lapatinib, as the site of the radiolabel is a *meta*-substituted electron-rich aromatic. Lapatinib is approved for use in combination chemotherapy for the treatment of advanced metastatic breast cancer,[140] and is under investigation for use in the treatment of other forms of cancer.[141] Use of non-invasive preclinical imaging studies to facilitate rapid decision making regarding the efficacy of the treatment regimen can now be realised as a result of the use of a prosthetic group.

A further example of prosthetic group utility is in the form of the simple aliphatic compound such 2-[^{18}F]fluoroethyltosylate.[142] As a result many PET imaging agents have a pendant [^{18}F]fluoroalkyl group such as [^{18}F]FECwhich has been used an imaging agent in a wide range of imaging studies from human,[143] rodent[144] and within cells.[142]

1.13 Aims and Objectives

The aims and objectives of this research are:

- Develop a synthetic method to furnish the reference standard 2-[^{19}F]fluorothiophene
- Synthesis and subsequently investigate the use of diaryliodonium salts as precursors to radiolabelled prosthetic groups
- Develop an automated method for the synthesis of a range of radiolabelled prosthetic groups, taking steps to optimise the radiochemical yield and the reproducibility of the production of radiolabelled material

2 Chapter Two: 'Cold' Chemistry Results and Discussion

Chapter one highlights the need for strategies to radiolabel prosthetic group precursors in a procedurally straight forward and reproducible manner. Diaryliodonium salts have herein been described as useful prosthetic group precursors, and hence the first aim of this research is to synthesise a range of prosthetic group precursors for use in subsequent radiolabelling. Furthermore, use of the 2-thienyl moiety to direct nucleophilic attack of [18F]fluoride ion towards the diaryliodonium salts so-called 'target arene', i.e. the arene desired to bear the radiolabel, may potentiate the production of the 'off-target' 2-[18F]fluorothiophene. 2-[18F]Fluorothiophene is a material which is poorly characterised in the current literature and is to the best of the author's knowledge commercially unavailable (June 2015). Hence, a further aim is to develop a synthetic methodology to afford an authentic standard of this key material, where such a standard is able to be used in subsequent radiochemical syntheses where treating a diaryliodonium salt bearing a 2-thienyl moiety with [18F]fluoride ion.

2.1 Synthesis of Diacetoxyiodoarene

The synthesis of diacetoxyiodoarenes, as useful precursors to diaryliodonium salts, is well established and such compounds are used routinely in the synthesis of diaryliodonium salts.[101] Many oxidising agents have been used in the transformation of iodoarenes to diacetoxyiodoarenes, including: sodium periodate,[145] sodium percarbonate[146] hydrogen peroxide–urea,[147] Selectfluor™[148] and *m*-chloroperoxybenzoic acid.[149] The most general oxidation methodology makes use of sodium perborate tetrahydrate (referred to herein as SPB) as the oxidant, as a suspension in acetic acid.[102]

It is believed that mixing SPB and acetic acid results in the *in situ* formation of a peracetoxyborane species, which is attributed as the oxidising species in the reaction (Scheme 31).[150] The species reacting in step (C) may be the same as that formed in step (B), or there may be an intermediate solvolysis of the first of the B-O-O-B linkages. The scheme identifies species containing the B-OOAc unit as intermediates,

and it is possible that such species may act directly on organic substrates, either instead of, or in parallel with, their likely to be acid-catalysed hydrolysis to peracid.
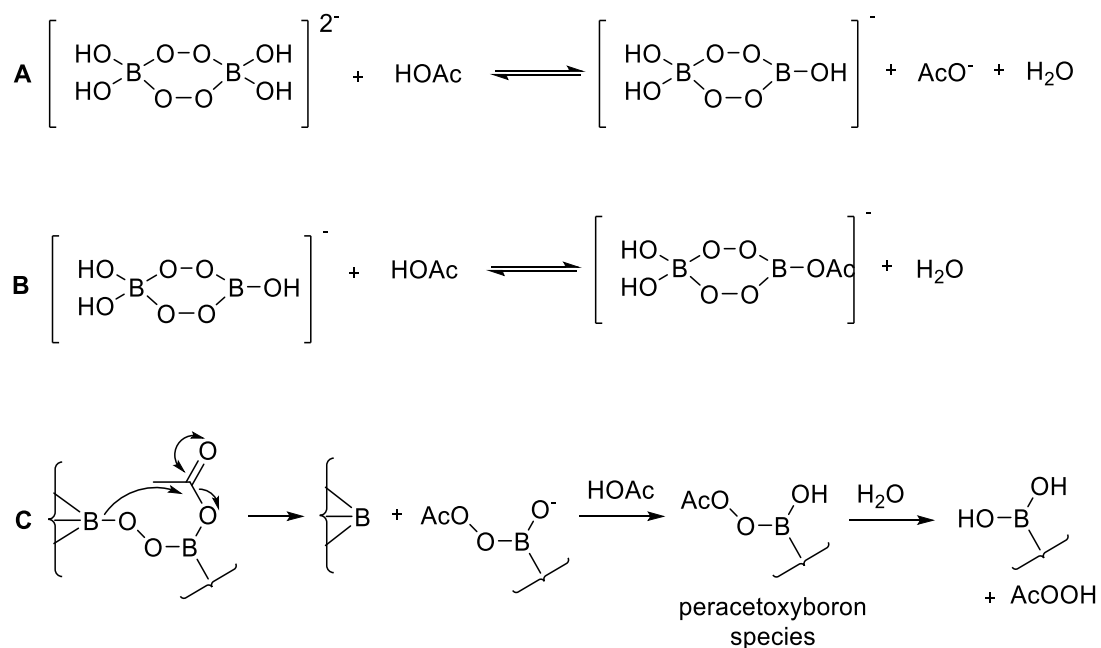
Scheme 31: Generation of the reactive peracetoxyboron species.

Diacetoxyiodoarenes **33** and **34** were synthesised in moderate yields of 13-49% following the widely utilised methodology developed by McKillop and co-workers.[102, 150] As McKillop *et al.* did not specify reaction times for the oxidation of 4-iodoanisole or 2-iodothiophene, several reactions have been carried out to investigate the most appropriate reaction time (Table 3).

$$\text{ArI} \xrightarrow[\text{Acetic acid, 45 °C}]{\text{NaBO}_3 \cdot 4\text{H}_2\text{O}} \text{ArI(OAc)}_2$$

Ar = **33** (with OMe), 20-45%

Ar = **34** (thienyl), 13-29%
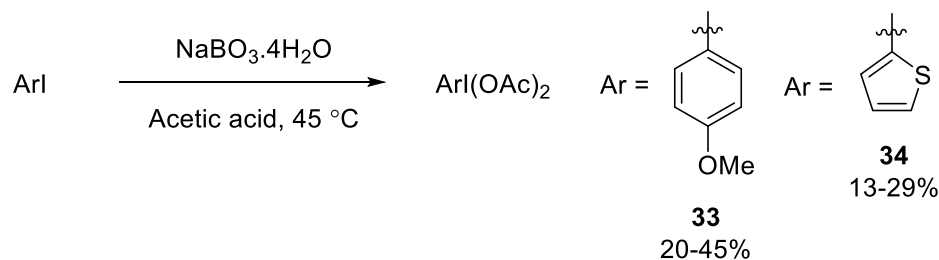
Entry	Ar	Time (h)	Yield (%)
1	4-iodoanisyl	3	29
2	"	4	44
3	"	5	41
4	"	4.5	45
5	2-iodothienyl	3	11
6	"	4	29
7	"	5	24
8	"	4.5	27
9	"	9	10

Table 3: Variation of reaction time to optimise the oxidation process outlined by McKillop *et al.*[102, 150]

The progress of the reaction could be followed by the formation of an off-white precipitate, which, with elongated reaction times (> 4 h), could also be seen to re-dissolve into the reaction mixture.

It has been reported that accelerated oxidation of electron-rich arenes is observed, particularly those which possess electron-donating *ortho-* or *para*-substituents, or electron-withdrawing *meta*-substituents.[102] The series of reactions performed above supports this hypothesis.

Silva *et al.* carried out an electrospray ionisation mass spectrometry study of the hydrolysis products of diacetoxyiodobenzene, **35**, encountered during its decomposition under atmospheric conditions.[151] ESI-MS studies were performed using a freshly prepared sample of **35**, as well as sample exposed for a 24 hours to atmospheric conditions. The resulting spectra were found to reveal a myriad of decomposition products, particularly for the sample exposed to air.[151] As may be anticipated by the study of Silva *et al.*, comparable decomposition products have

been identified in this work by ESI-MS, although the relative rates of decomposition were not considered in detail. Molecular ions were observed for **33** (374.9705) and **34** (350.9159) as sodium adducts, for high-resolution ESI-MS spectra, see appendix. Importantly, the main conclusions identified by Silva and co-workers are that spontaneous decomposition of **35** occurs in solution, and that the decomposition process is accelerated by an increase in temperature.[151] Accordingly, after work-up and crystallisation, **33** and **34** were dried under nitrogen and either used in subsequent reactions immediately or stored in a freezer to mitigate formation of decomposition adducts (Figure 29).
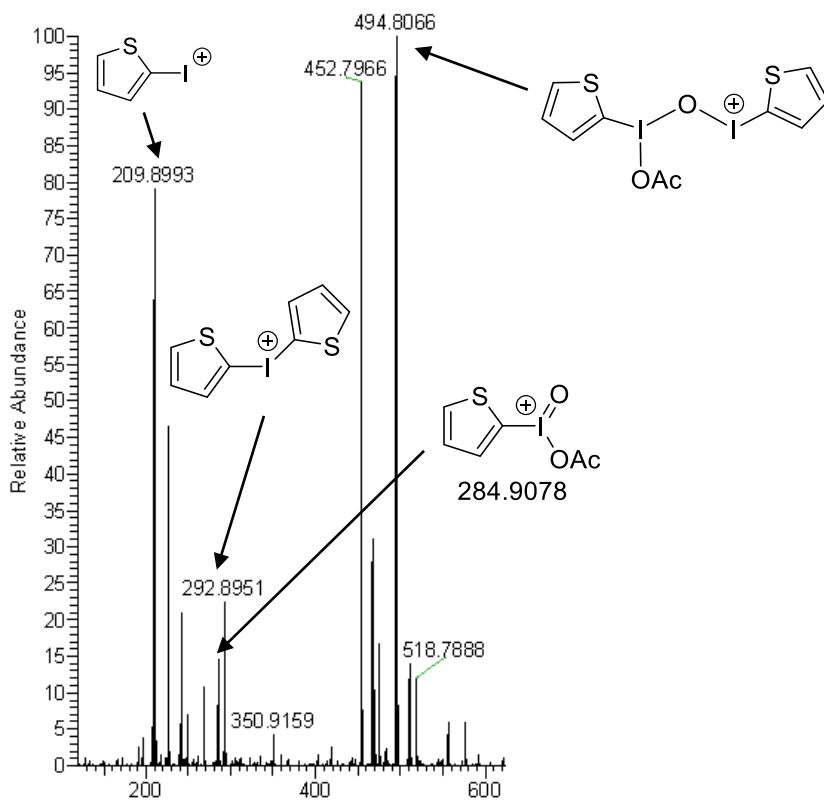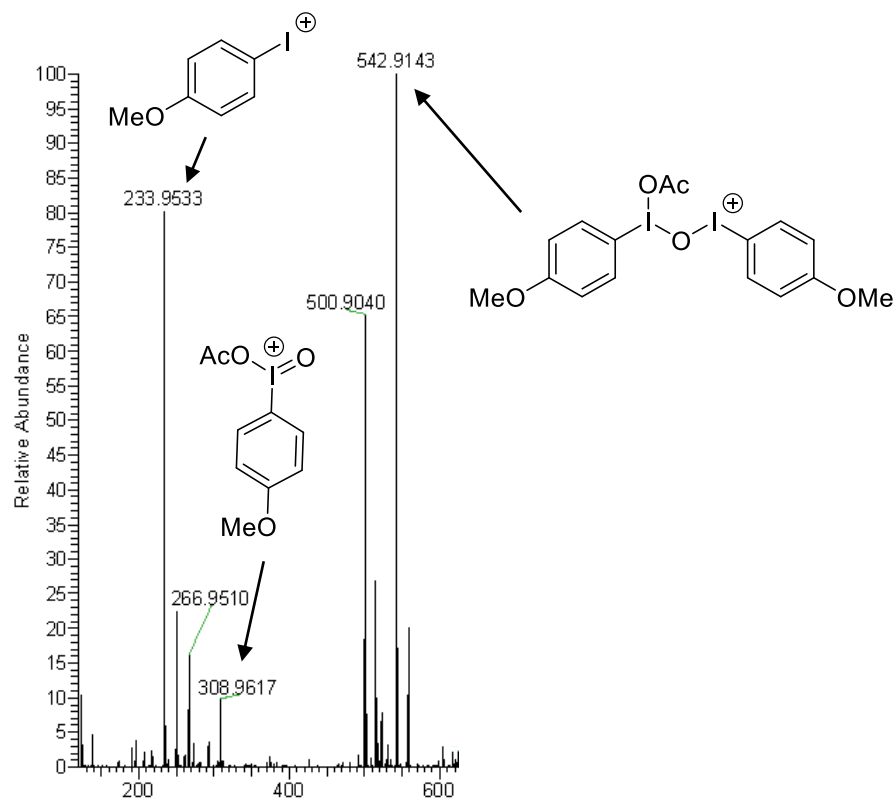
Figure 29: Decomposition products of 33 (top) and 34 (bottom). (ESI-MS in MeCN)

^{1}H and ^{13}C NMR were overall as expected in light of previously published examples,[100] demonstrating the expected downfield shift of protons –*ortho* to the iodane (8.0 ppm) relative to an iodide counterpart, e.g. 4-iodoanisole (7.5 ppm).

Although the process is moderate in yield, reasonable quantities of diacetoxyiodoarenes are required to be used in further studies, hence the reaction is still employed as it can be carried out on a large scale (50 mmol), is procedurally straight-forward; in addition to being viable (see section 2.8) across a number of iodoarenes.[102]

2.2   Synthesis of Substituted Arylstannanes

Substituted aryl stananes have been widely used in many synthetic procedures, from Stille couplings[152] to carbonylations.[153] The purpose of using an aryl stannane is to provide a nucleophilic coupling partner for subsequent reaction with a diacetoxyiodoarene, i.e. using a general approach to the synthesis of a diaryliodonium salt.

Diacetoxyiodoarenes are synthesised under oxidising conditions and therefore are often used to supply the so-called 'non-participating arene' of a diaryliodonium salt. It could be envisaged that the reactive functionality of certain substituted arenes (the 'target' arene) would not tolerate such oxidising conditions, and therefore such functionalities could be incorporated into the other aromatic ring (as the appropriate arylstannane) as this can be achieved under mild reaction conditions.

An example of a synthetic route to an arylstannane in the presence of reactive functionality is the synthesis of 4-tributylstannylbenzaldehyde **37**, from a bromobenzaldehyde **36**, where Pd(PPh3)4 was used as the catalyst, yielding **37** in 67% yield (Scheme 32).[154] The procedure requires an excess of 2 eq. hexa-*n*-butylditin to 1 eq. **36** in addition to 10 mol% of an expensive palladium catalyst. Furthermore, the excess of the stannane, as well as the high catalyst loading, lead to difficulties in purification of the resultant product. A further problem associated with the reported purification method, is that it has been shown that normal phase column chromatography may lead to destannylation of the desired product,[155, 156] which may be a factor to account for the yield of the reaction. Hence, a more efficient alternative was required.
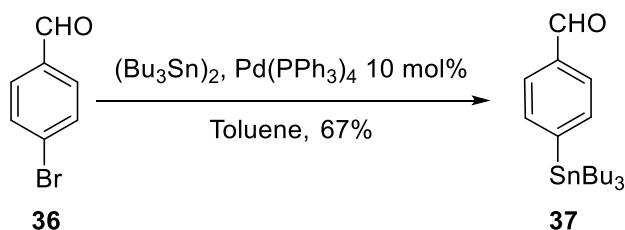
Scheme 32: Palladium catalysed synthesis of 4-tributylstannylbenzaldeyhde.

A method of introducing trialkylstannane functionality into a reactive arene using cobalt/zinc catalysis has been demonstrated by Gosmini et al.[157] Importantly, half the amount of tin starting material, in this case Bu_6Sn_2, is required.[157] The initiation point for the catalytic cycle is the reduction of cobalt dibromide using zinc dust which has been activated with trace acid. Oxidative insertion of cobalt bromide into the aryl-halide bond yields a trivalent complex, $ArCoBr_2$. The presence of excess zinc dust proceeds to reduce this complex, thus facilitating a transmetallation with zinc dibromide, furnishing the desired arylzinc compound and regenerating copper dibromide (Scheme 33).[158]
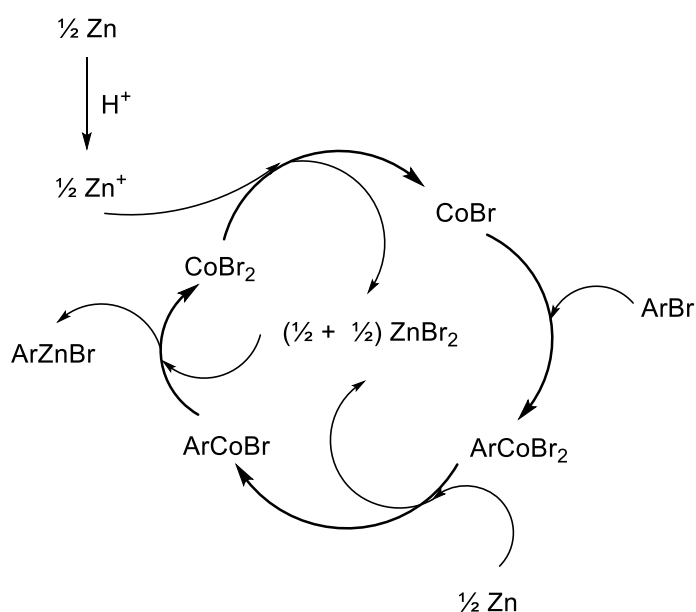
Scheme 33: The catalytic cycle which leads to the formation of an arylzinc species.

The conditions set forth by Gosmini and co-workers were therefore used to facilitate the stannylation of **36** (Scheme 34) in a 46-67% yield (n=4), which compares reasonably well with the palladium mediated stannylation reaction performed above, given the increased economy of the process.
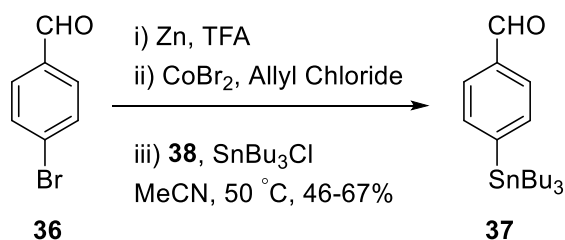
Scheme 34: Cobalt catalysed synthesis of 4-tributylstannylbenzaldeyhde, 37.

The reaction progress was monitored by TLC (95:5 petrol:ether) until it was found that all of the starting material **36** had been consumed. Of particular note is the problem which has been encountered with regards the purification of **37**. Some impurities, which have been attributed to oxidation of an organotin species (possibly Bu_3Sn-O-$SnBu_3$ and Bu_3SnO), have proven difficult to remove using normal phase chromatography, resulting in an inseparable mixture of the desired product and the undesired impurity. One method which aided the removal of the problematic impurity was reverse phase chromatography, which readily separated the proposed highly lipophilic tin oxide from less lipophilic **37**. It has been found that the appearance of this impurity was difficult to predict, as on occasion, normal phase column chromatography proved sufficient for purification. Overall, an advantage of reverse phase purification is that the destannylation problems attributed to the use of silica gel are avoided.

The 3- (**38**) and 2- (**39**) regioisomers of **37** were prepared utilising the same chemistry; varied yields (70% for **38**, 33% for **39**) were obtained for these regioisomers.

It should be noted that catalysis isn't an essential requirement to stannylate benzaldehydes. For instance, a Grignard reagent can be synthesised by reaction between a haloaryldioxolane and magnesium, followed by quenching with tri-*n*-butyltin chloride and acid catalysed removal of the protecting group (Scheme 35).[159]
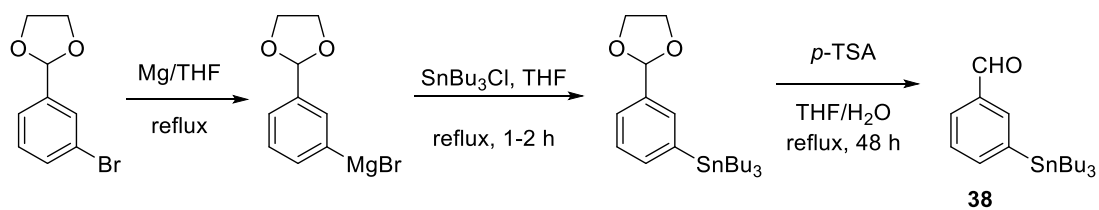
Scheme 35: Non-catalytic synthesis of 38 using a Grignard reagent. N.B. protection of the starting material is not shown.[159]

We did not attempt the Grignard strategy as it highly substrate dependent, *i.e.* synthesis of a Grignard reagent in the presence of many functional groups, such as the aldehyde, means additional protection and deprotection steps are required. Additionally, as we examine functionality which is more intricate than that of an aldehyde, the solubility of the starting material may not conform to the solvent requirements which are imposed upon Grignard reagents, *i.e.* only aprotic solvents are of use when synthesising the Grignard reagent.

2.3   Synthesis of Diaryliodonium Salts

As outlined in section 1.10.2, diaryliodonium salts are useful synthetic precursors to radiolabeled compounds, such as prosthetic groups. By using diaryliodonium salt chemistry, it is possible to avoid unwanted nucleophilic substitution reactions and to selectively introduce fluorine into any position desired arene precursor, thus, a generic synthetic route to all regioisomers of a particular prosthetic group becomes possible.

There are many synthetic strategies one could employ to synthesise a substituted diaryliodonium salt. The first reported regiospecific synthesis of a substituted diaryliodonium tosylate was carried out in 1980,[160] where Koser's reagent **40** is reacted with substituted arylsilanes **41a-d**. Exclusive substitution at the *ipso* position occurs, regardless of the other substituents present on **41a-d** (Scheme 36).[160]
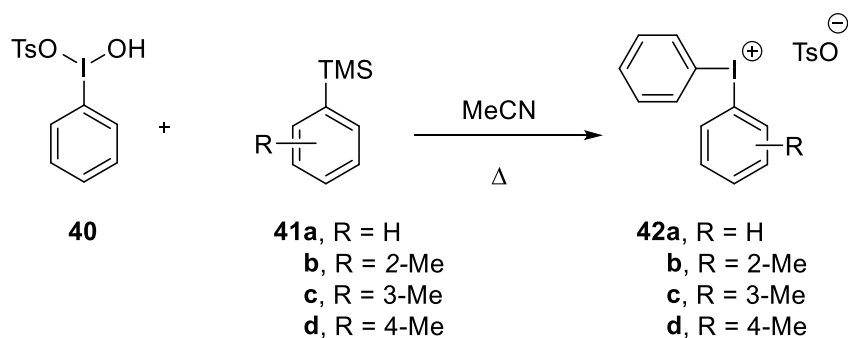
Scheme 36: Reaction of Koser's reagent with a substituted arylsilane.

One disadvantage of using Koser's reagent is that the counter anion generated is restricted to tosylate. Tosylate ion has been shown to be disadvantageous in radiolabelling studies of heteroaromatic iodonium salts, where it has been indicated that counter anions can compete as an alternative nucleophile to the fluoride ion during the radiolabeling process. The tosylate counter anion also performed poorest with respect to radiochemical yield (Scheme 37).[6]
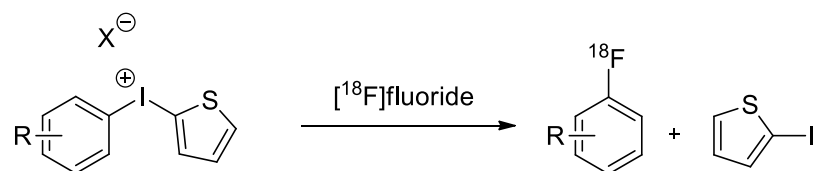
R = 2-OCH$_3$, 3-OCH$_3$, 4-OCH$_3$, 4-Me, 4-OBn, H, 4-I, 4-Br, 4-Cl
X = anion listed in graph below
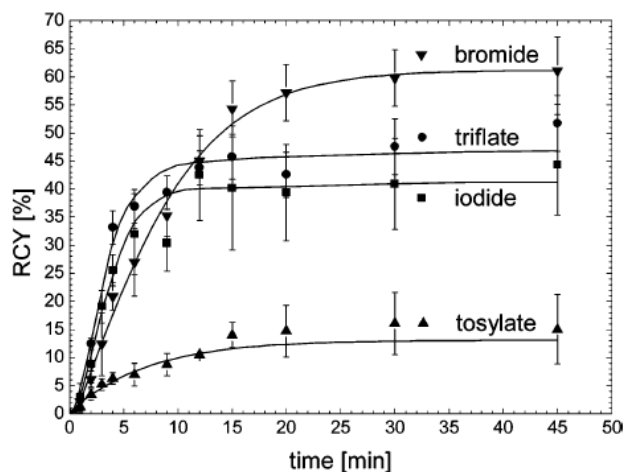
Scheme 37: Counter anion influence when radiolabeling heteroaromatic diaryliodonium salts.[6]

Noticeably, the common trifluoroacetate anion doesn't appear in the study outlined above. Work within our group has determined that the trifluoroacetate counter anion provides the best balance between ease of synthesis and overall radiochemical yield.[161]

We considered that a general approach (Scheme 38) would be most appropriate for the synthesis of the chosen diaryliodonium salts.[90] The synthetic methodology employs anhydrous conditions, whereby the diacetoxyiodoarene (1 eq.) is dissolved in dry DCM and the solution cooled to −30 °C (acetone/cardice), followed by dropwise addition of TFA (2 eq.). The resultant solution is stirred in the dark for 30 minutes, followed by 1 hour at room temperature. The solution is then re-cooled to −30 °C, when a substituted arylstannane (1 eq.) is added. The solution is warmed to room temperature for a second time and left to stir overnight. The reaction solvent is then removed *in vacuo*, leaving the addition of DCM/petrol to crystallise the diaryliodonium salt. This general approach was applied to the synthesis of the diaryliodonium salts discussed in this report, unless stated otherwise.
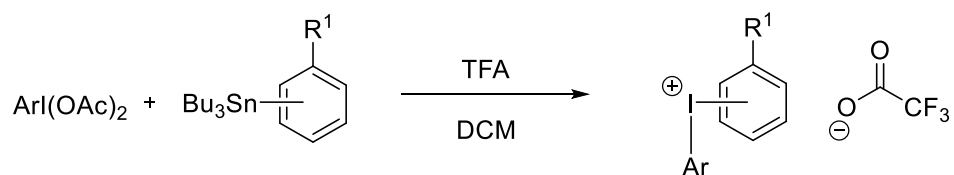
Scheme 38: General synthetic route to asymmetric diaryliodonium salts.

It has been proposed that diaryliodonium salts can react with nucleophiles either through an associative, or a dissociative pathway,[162] in a manner similar to that of an aryl-λ^3-iodane bearing two labile ligands (Scheme 39). To date, experimental results of the associative pathway have been reported, whereas no experimental results have been reported regarding the dissociative pathway.[97]

associative pathway
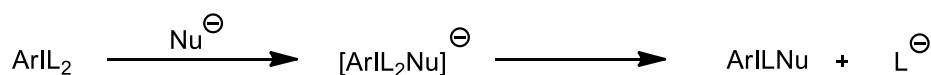
dissociative pathway
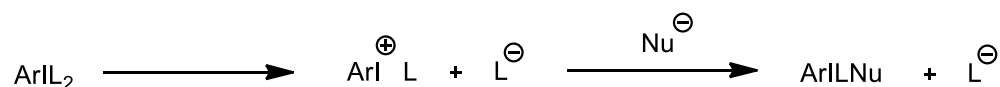
Scheme 39: Associative and dissociative nucleophilic reaction pathways of an aryl-λ^3-iodane.

Due to the electropositive nature of the tin atom in the arylstannane, the carbon atom bound to tin will be slightly δ^-. Consideration of the associative pathway mechanism reveals the bonding pair of the carbon-tin bond acts as a nucleophile, resulting in the arene becoming bonded to the iodine atom, which leads to an important feature of the mechanism by which an aryl-λ^3-iodane reacts. This feature is the ability for ligands to pseudo-rotate about the iodine centre. Consequently, many conformations may exist for a particular aryl-λ^3-iodane, which highlights the conformational instability this type of iodane. The formal terminology for the conformational flexibility is termed Berry pseudorotation (denoted as Ψ), after being first described in 1960 by R. S. Berry.[163] In the example below, Berry pseudorotation facilitates the elimination of a ligand from the equatorial position, a requirement imposed by both the proposed associative and dissociative mechanisms (Scheme 40), as well as a requirement of

the diaryl-λ^3-iodane itself, as the more electron-deficient and/or sterically demanding ligand will preferentially occupy an equatorial position.[94]
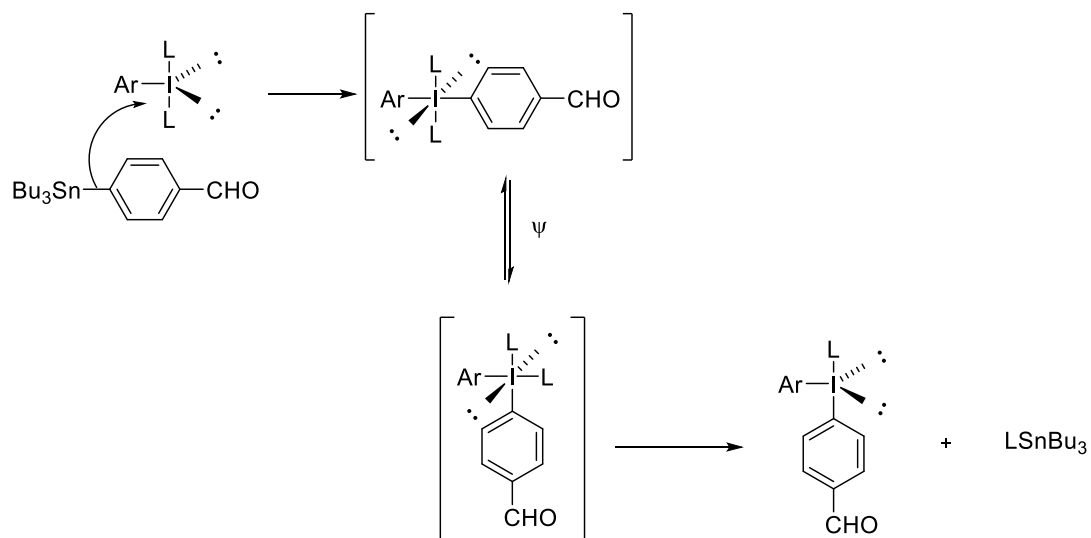
Scheme 40: The proposed mechanism of diaryliodonium salt synthesis by an associative pathway.

2.3.1 Synthesis of 4-Formylphenyl(aryl)iodonium Salts

Diaryliodonium salts **43, 44** and **45** were prepared in yields of 32-48% respectively (Scheme 41) from an aryliodobisacetate and an arylstannane.

i) -30 °C, TFA, 30 min
then 1 h at RT

ii) - 30 °C, **37**, then at RT
overnight

Ar—I(OAc)$_2$

33, Ar = phenyl
34, Ar = 4-anisyl
35, Ar = 2-thienyl

Bu$_3$Sn—⟨⟩—CHO
37

Ar—I$^{\oplus}$ $^{\ominus}$TFA

43, Ar = phenyl, 32%
44, Ar = 4-anisyl, 49%
45, Ar = 2-thienyl, 38%
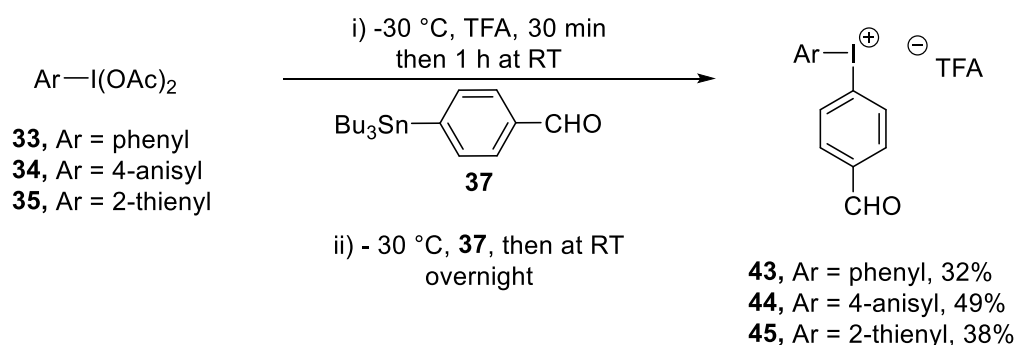
Scheme 41: Synthesis of diaryliodonium salts 43-45.

As previously reported the work-up procedure prior to crystallisation of the desired diaryliodonium salt is simply removal of the reaction solvent, in this instance DCM,

followed by the addition of a low polarity solvent, e.g. petrol, to effect crystallisation.[67] However, crystallisation of the diaryliodonium salts **43-45** proved challenging. On some occasions, amorphous white powders form, on other occasions colourless needles form. In some instances no crystalline material is observed, including over extended periods (4 weeks), even where ^{1}H-NMR of the crude product suggests successful diaryliodonium salt formation. A feature of the ^{1}H-NMR of the crude product revealed the presence of a significant quantity of butyl groups. The butyl groups are attributable to stannane impurities, which have proven difficult to remove as the stannane impurity appears to be remarkably soluble, being present in both DCM/MeCN and petrol/pentane extracts from the crude material. It is proposed that the presence of said impurity results in a lack of crystallisation of suitable quality.

In an attempt to evaluate the most appropriate conditions required to routinely yield crystals of good quality, a simple study of various solvent/anti-solvent combinations was undertaken using slow diffusion as well as an 'H-tube' (
Table 4). The general procedure comprised dissolution of crude material (25 mg) in the minimum amount of the system's polar solvent being pipetted into its respective section of the container. The corresponding ratio of pentane was added to the other section of the container. Containers were left in the dark in an undisturbed environment for a given time period.

Entry	System	Ratio	Result	Time
1	Pentane/MeCN	1:1	**43**: A	10 h
			44: X	4 weeks
			45: X	4 weeks
2	Pentane/MeCN	1:0.5	**43**: A	10 h
			44: A	10 h
			45: X	4 weeks
3	Pentane /MeCN	1:0.25	**43**: A	10 h
			44: C	3 days
			45: A	5 days
4	Pentane/DCM	1:1	**43**: X	4 weeks
			44: X	4 weeks
			45: X	4 weeks
5	Pentane/DCM	1:0.5	**43**: A	Immediately
			44: C	10 h
			45: C	4 weeks
6	Pentane/DCM	1:0.25	**43**: A	Immediately
			44: C	3 days week
			45: C	2 weeks
7	Pentane/Ether	1:1	**43**: A	Immediately
			44 C	10 h
			45: A	4 weeks
8	Pentane/Ether	1:0.5	**43**: A	Immediately
			44: C	1 week
			45: C	weeks
9	Pentane/Ether	1:0.25	**43**: A	Immediately
			44: C	1 week
			45: C	9 days
10	Pentane/TBME	1:1	**43-45**: X	4 weeks
11	Pentane/TBME	1:0.5	**43-45**: X	4 weeks
12	Pentane/TBME	1:0.25	**43-45**: X	4 weeks

Table 4: Solvent systems used to crystallise 43-45 (C = crystalline material, A = amorphous analytically pure material, X = crude material).

With respect to obtaining a sample of material, albeit crystalline or otherwise, for use in further reactions the most efficient system was pentane/ether (1:0.25). This system often produced crystals of suitable quality for single crystal x-ray crystallography studies, yielding previously unreported x-ray crystal structures for **44** and **45** (Figure 30). A bulk crystallisation using the same ratio also yields powders of all three compounds, within 10 h, which conform to the expected NMR, MS and CHN analyses, and is also tolerant of the use of petrol in place of pentane. Systems using DCM or MeCN were found to have no distinct advantages, and, in the case of or *tert*-butyl methyl ether (TBME), produced no solid material of any description.

Unfortunately, **43** was obtained as an amorphous white powder in all solvent systems tested. Powder diffraction measurements of the powder at the Diamond Light Source have not proven possible, as during the time required to acquire a powder diffracton of reasonable quality, the power of the beam destroyed the sample.
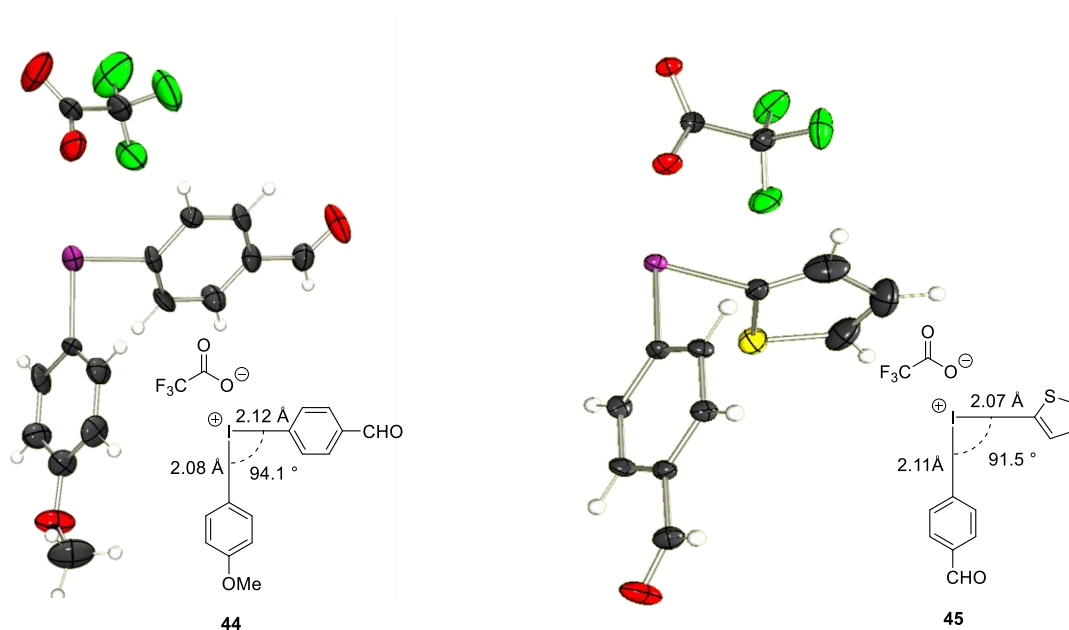
Figure 30: X-ray crystal structures of the monomers of 44 (left) and 45 (right) drawn using ORTEP-3,[164] plotted as thermal ellipsoids with a 50% probability, H atoms are presented as spheres with a constant radius, as are all further structures. Selected bond lengths and angles shown.

As discussed in the sections above, diaryliodonium salts can interact in an intra-molecular manner thus forming dimers, trimers and so on. The interactions in forming a dimer have been observed for compound **44** (Figure 31).
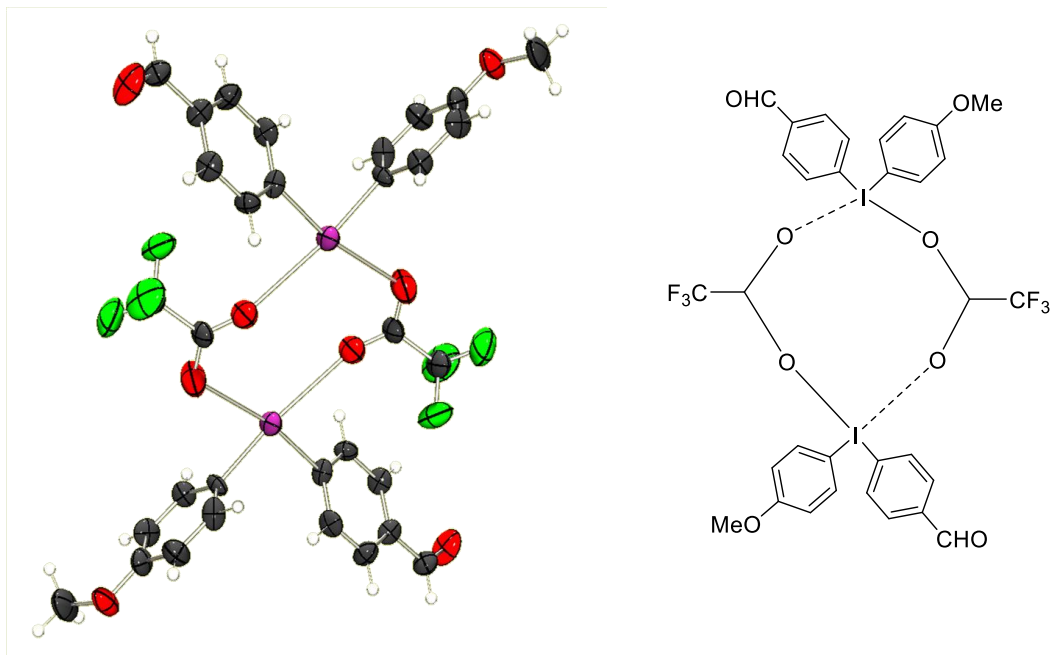
Figure 31: X-ray crystal structure of a dimer of 44.

Given that in their ground states, diaryliodonium salts, e.g. **44** above, can exist effectively in a polymeric state, judicious selection of part of the unit cell of a diaryliodonium salt from a structure determined in the ground state may be misleading and may also be different to that encountered in a transition state (

Figure 32). Selection of the blue groups places the aldehyde bearing moiety in the pseudo-equatorial position, whereas selection of the red groups places the aldehyde bearing moiety in the pseudo-axial position. Accordingly the part of the unit cell selected when conveying the monomer may not be representative of the actual conformation which is adopted during the course of a reaction with a nucleophile.
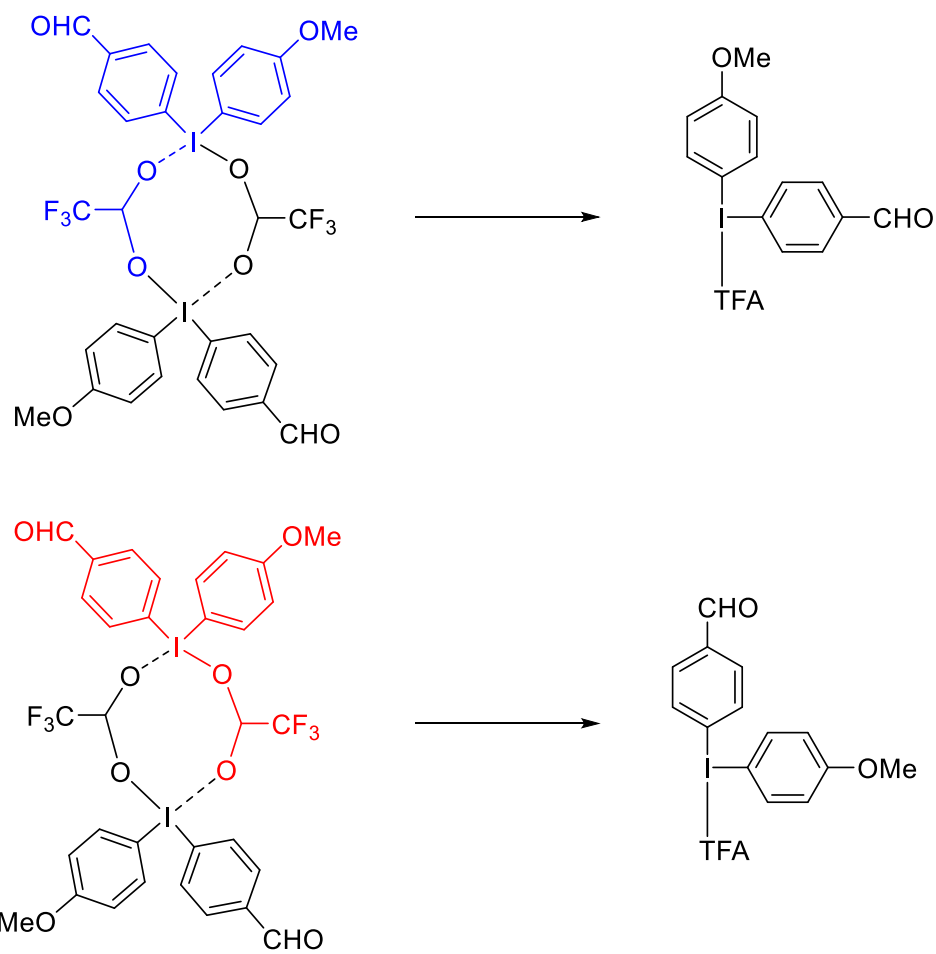
Figure 32: Polymeric unit selections yield different ground state structures.

2.4 [^{19}F]Fluorination of 4-Fluorobenzaldehyde Precursors

[^{19}F]Fluorination, so-called 'cold' fluorination, of 4-formylphenyl(aryl)iodonium salt precursors enables the determination, and the relative extent, of fluorination between the 4-formylphenyl and the other aryl moieties present per diaryliodonium salt. It is known that the most electron-deficient arene on the diaryliodonium salt will be preferentially fluorinated.[94] The 'target arene,' i.e. the arene bearing the aldehyde moiety, is clearly the more electron-deficient relative to the 'non-participating arene' counterparts, i.e. phenyl, 4-anisyl, and 2-thienyl arenes. Consequently, selective fluorination of the target arene should be observed. This data will be useful prior to any radiosynthetic chemistry with [^{18}F]fluoride being carried out, as the most appropriate diaryliodonium salt precursor can be determined.

The [^{19}F]fluorination of 4-fluorobenzaldehyde precursors **43-45** was determined by a variable temperature NMR (VT-NMR) experiment observing both ^{1}H and ^{19}F nuclei. The procedure used one equivalent of diaryliodonium salt **43-45**, two equivalents of caesium fluoride, and one equivalent of 3-methoxybenzotrifluoride as an internal standard, the study was conducted in deuterated dimethylformamide (d$_{7}$-DMF), which is a useful solvent for this experiment, as DMF is the solvent which is typically used for fluorine-18 radiolabeling (Scheme 42). Additionally, this solvent will enable the study to be conducted at temperatures up to 130 °C. Caesium fluoride was judiciously chosen on the basis of a report from Nairne *et al.* where several cold fluorinating reagents were examined and with respect to reaction yield: CsF > KF(18-crown-6) > KF(K$_{222}$) > KF = TBAF.[100]
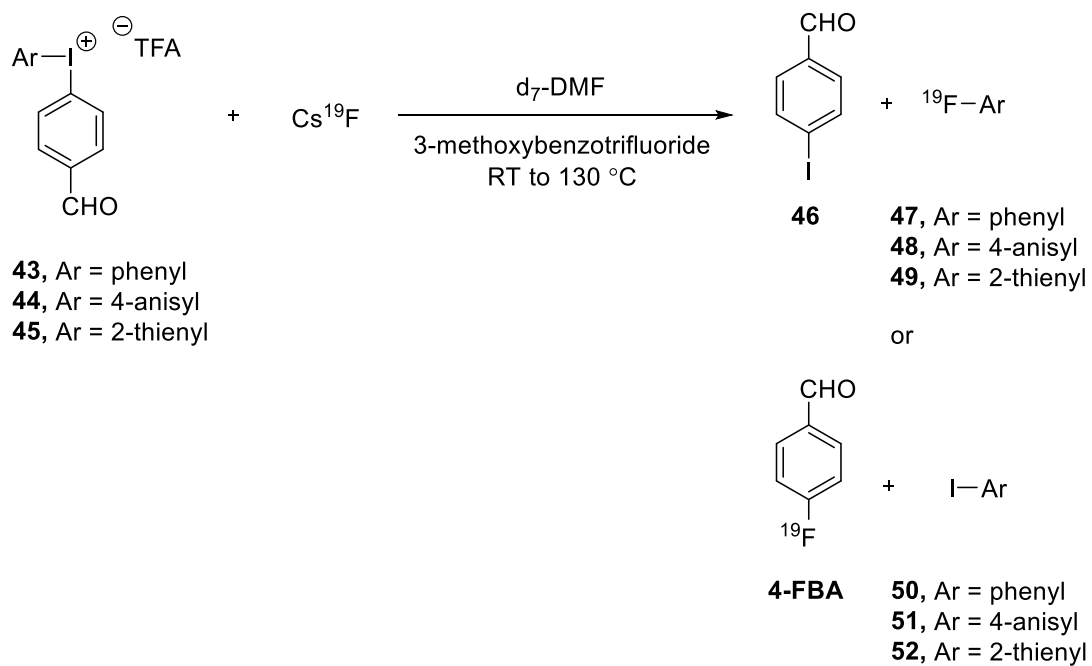
Scheme 42: [^{19}F]Fluorination of 4-fluorobenzaldehyde precursors 43-45.

The reaction was conducted over a two hour period, increasing the NMR probe temperature by roughly 20 °C every twenty minutes.

2.4.1 [¹⁹F]Fluorination of 4-formylphenyl(phenyl)iodonium TFA
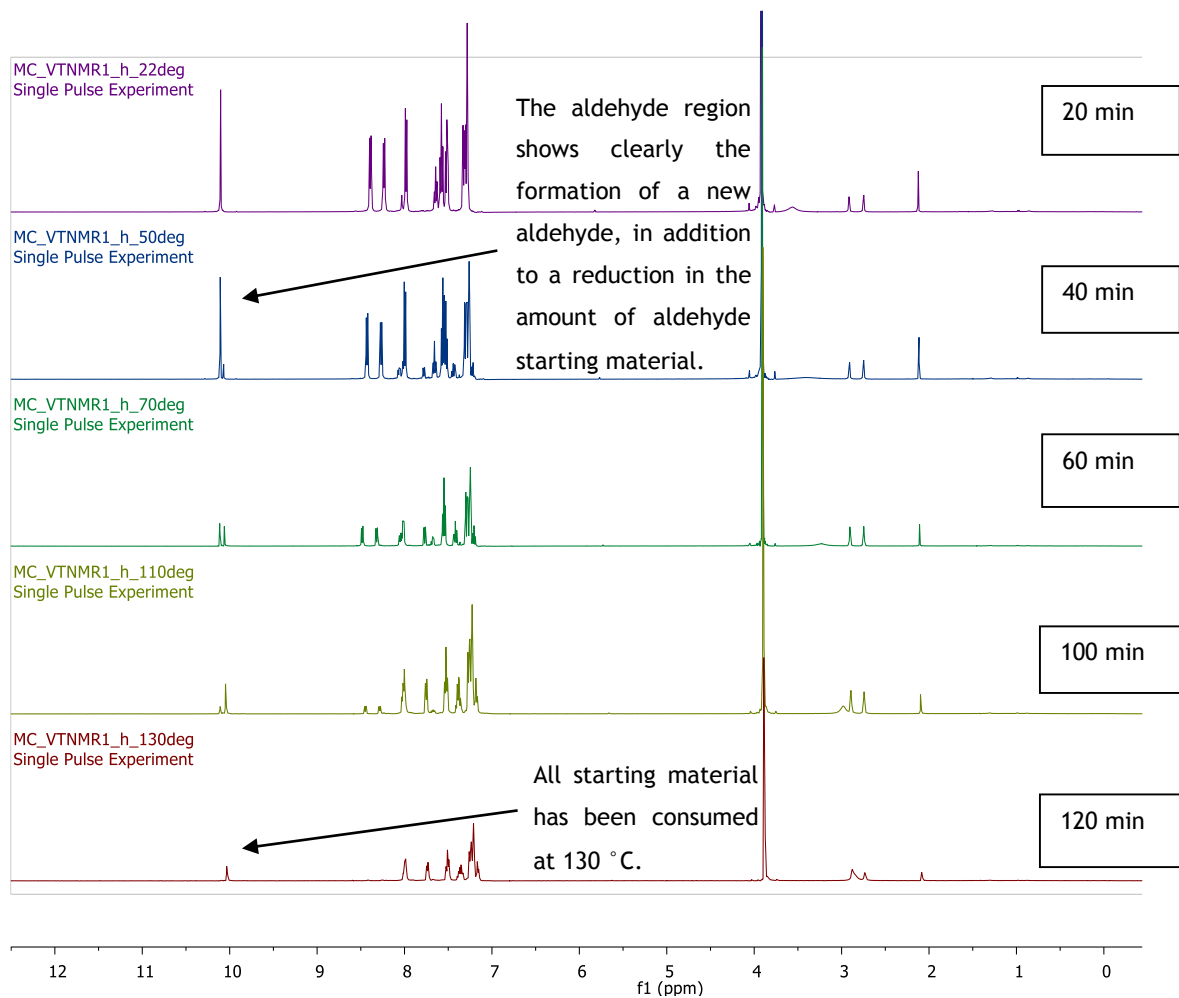
Figure 33: ¹H VT-NMR experiment following the fluorination of 4-formyl(phenyl)iodonium trifluoroacetate, 43.

2.4.2 [^{19}F]Fluorination of 4-formylphenyl(4-anisyl)iodonium TFA

The aldehyde region shows clearly the formation of a new aldehyde, in addition to a reduction in the amount of aldehyde starting material.

All of the starting material has been consumed at 90 °C.
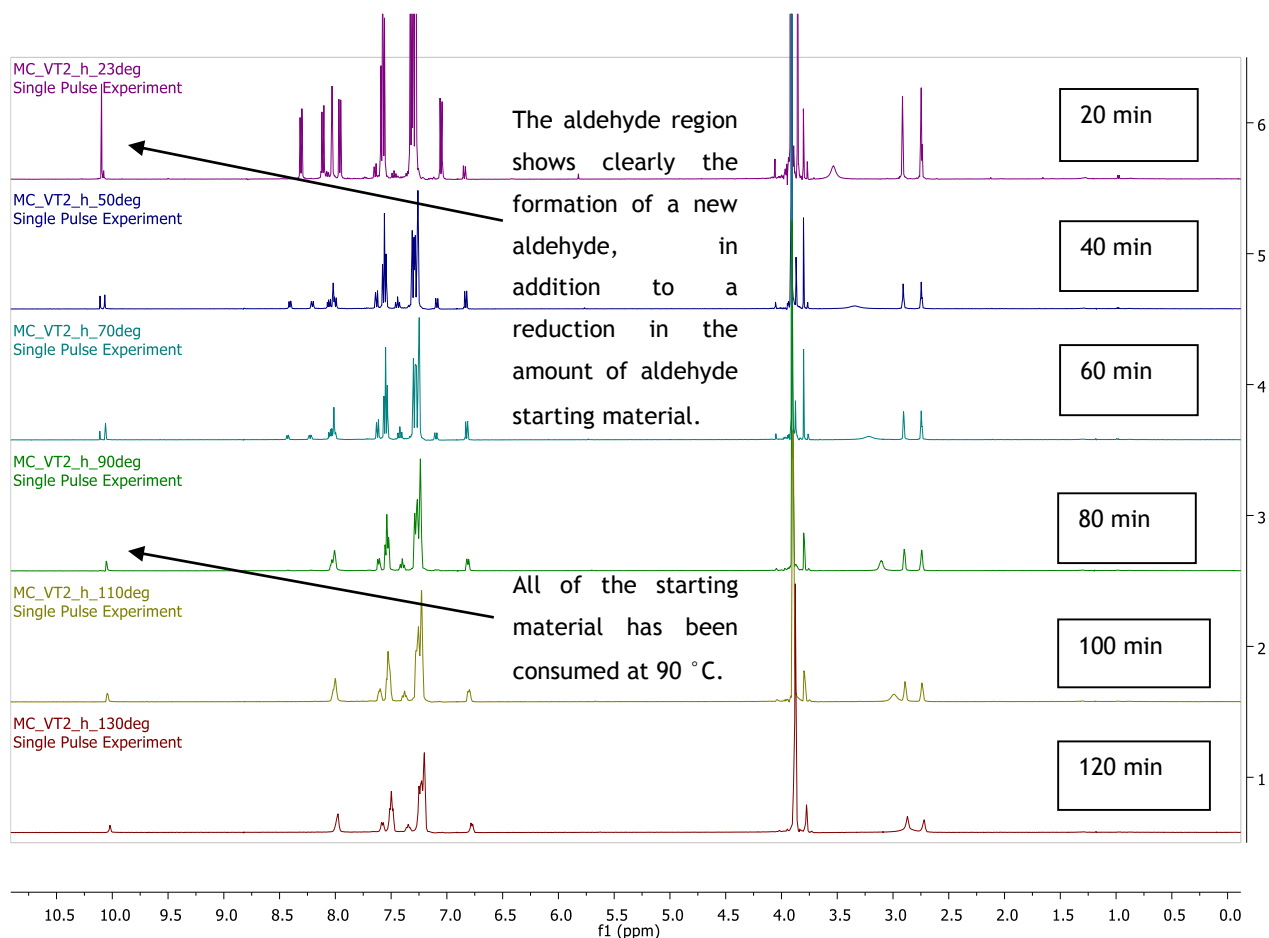
Figure 34: ^{1}H VT-NMR experiment following the fluorination of 4-formylphenyl(4-anisyl)iodonium trifluoroacetate, 44.

2.4.3 [^19^F]Fluorination of 4-formylphenyl(2-thienyl)iodonium TFA

The region between 6.2–10.4 is expanded for clarity. The starting material seems to be fully consumed at around 90 °C. Again, only one new aldehyde is observed.
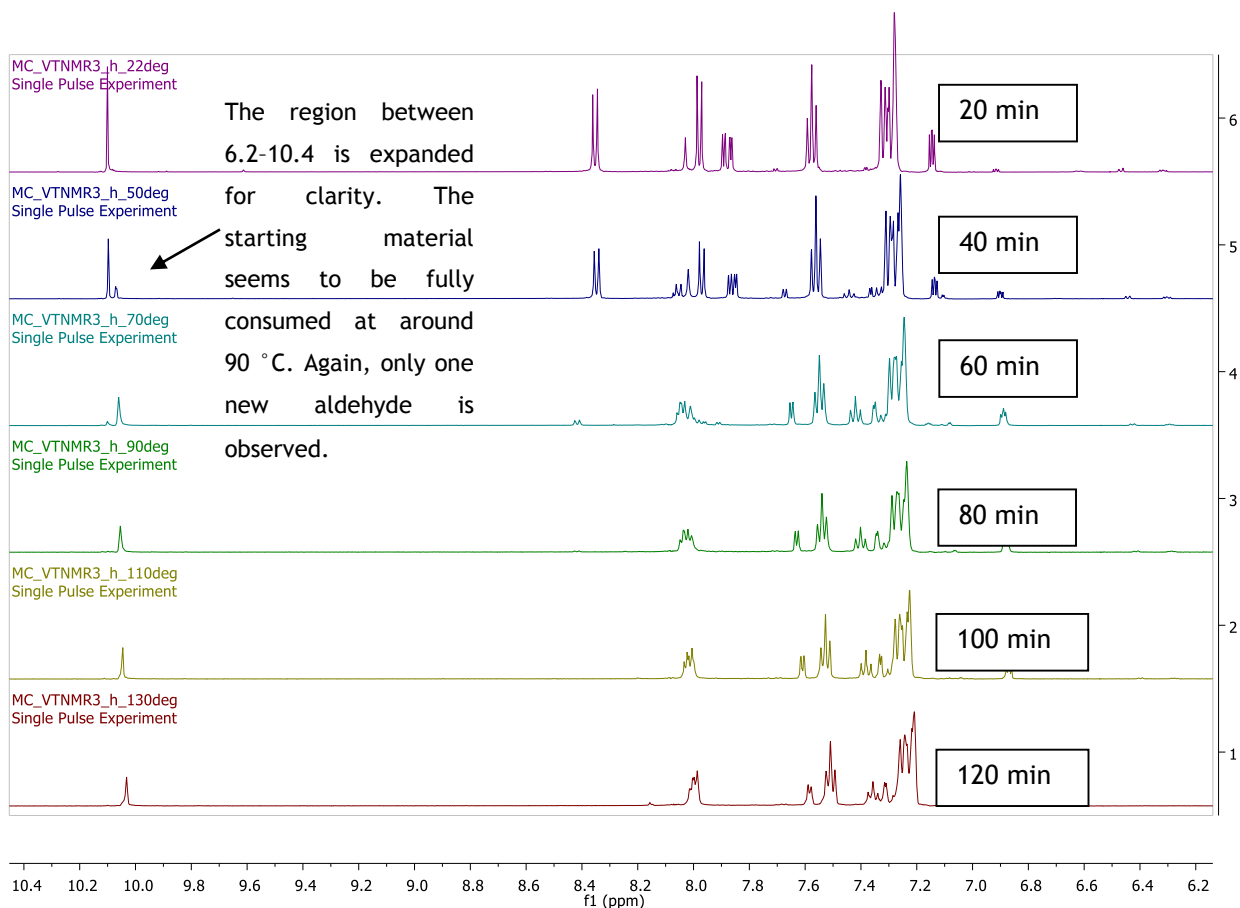
Figure 35: ^1^H VT-NMR experiment following the fluorination of 4-formylphenyl(2-thienyl)iodonium trifluoroacetate, 45.

There is an overall decrease in the amount of diaryliodonium salt as the reactions proceed (Figure 33, Figure 34 and Figure 35). It is also evident that new multiplets form in the aromatic region, which is consistent with what we expect regarding the fluorination of a diaryliodonium salt, i.e., the formation of an iodoarene and a fluoroarene. Note that multiplets form as a result of line broadening due to the higher temperatures of the NMR probe not being able to shim the sample as evenly as at room temperature. A ^{19}F VT-NMR experiment which was carried out simultaneously found that only one new fluorinated compound was synthesised, at around -105 ppm, corresponding to 4-fluorobenzaldeyhde, which was observed at -104 ppm at room temperature (the ^{1}H NMR spectrum does indicate the presence of an aldehyde other than the starting material. However, 4-iodobenzaldehyde **46** and 4-FBA appear in very similar regions). A problem arises at this point; this is because fluorobenzene, **47**, 4-fluoroanisole, **48** or 2-fluorothiophene, **49** were not detected. Consequently, upon initial examination, it would seem that selectivity towards the target arene is 100%. However, consideration of the boiling points of fluorinated arenes **47-49** reveals that in two instances their boiling points are lower than the highest temperature reached during the experiment. The boiling points of these fluoroarenes are; **47** 85 °C (1 atm),[165] **48** 150 °C (1 atm)[166] and **49** believed to be 82 °C (pressure at which boiling point determined not given).[167] The boiling point of **49** is higher than the 130 °C experiment limit, and **49** was not detected by ^{19}F NMR at any stage of the 2 hour experiment. To detect the volatile arenes, a specialist sealed NMR tube with a pressure regulation system would be required. This would ensure that any volatiles potentially generated over the course of the experiment remain inside the NMR tube, and therefore could be detected. A specialist NMR tube of this type was not available at the time of the experiment. A more traditional glass sealed and waxed NMR tube may not be able to cope with increased pressures as a result of the increased temperature, therefore the risk of damaging the expensive NMR probe is high if the NMR tube fails and as such was not attempted.

Three 4-formylphenyl(aryl)iodonium salts, **43-45**, have been synthesised and obtained as analytically pure material from the appropriate diacetoxyiodoarene and an arylstannane. X-ray crystal structures have been determined for **44** and **45**, and a 'cold' NMR study by reaction with [^{19}F]fluoride ion affirms that product selectivity cannot be ascertained by consideration of the ground state of a diaryliodonium salt.

2.5   Synthesis of 3-Formylphenyl(aryl)iodonium Salts

3-Formylphenyl(aryl)iodonium salts provide a means of synthesising 3-[^{18}F]FBA, a prosthetic group which cannot be synthesised *via* traditional nucleophilic means.[168] 3-Formylphenyltributyl stannane, **38**, was synthesised and purified in the manner described in section 2.2, affording the desired material in 46-70% yield (n=5) (Scheme 43). Interestingly, the purification of **38** was found to be more straightforward its 4-substituted counterpart **37**.
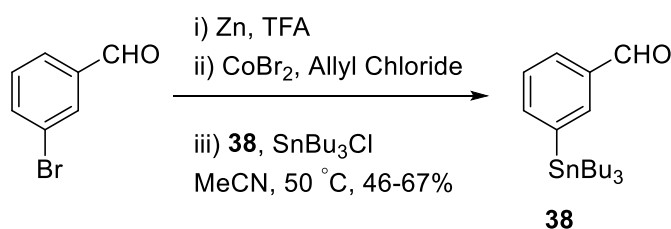
Scheme 43: Synthesis of 3-formylphenyltributyl stannane using the procedure of Gosmini *et al.*[157]

The 3-formyl(aryl)iodonium trifluoroacetates **50-52** were subsequently synthesised in a manner akin to their regioisomeric counterparts above, in 39-47% yield (Scheme 44).

35, Ar = phenyl
33, Ar = 4-anisyl
34, Ar = 2-thienyl

50, Ar = phenyl, 47%
51, Ar = 4-anisyl, 39%
52, Ar = 2-thienyl, 43%
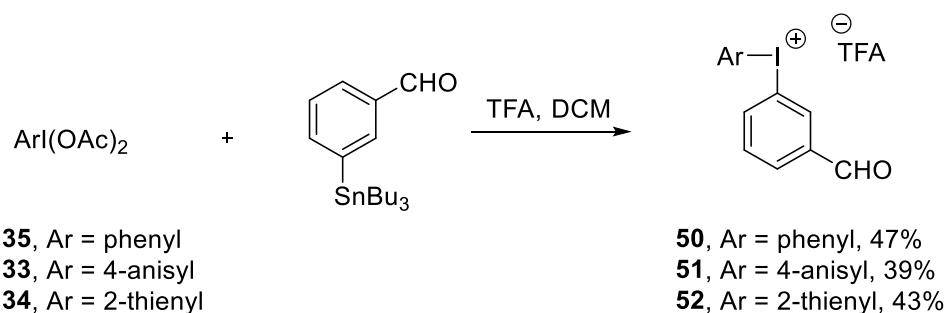
Scheme 44: Synthesis of 3-formylphenyl(aryl)iodonium salts 50-52.

A study was carried out in 2011 by Griffiths *et al.* to synthesise a range of diaryliodonium salts as precursors to the prosthetic group, 3-[^{18}F]FBA.[168] The reported synthetic approach followed previous work carried out by Olofsson *et al.*[169] whereby a non-isolated tetrafluoroborate salt is formed post oxidation of iodobenzene by *meta*-chloroperbenzoic acid (*m*CPBA), followed by various counter anion exchanges to yield a range of diaryliodonium salts (Scheme 45).
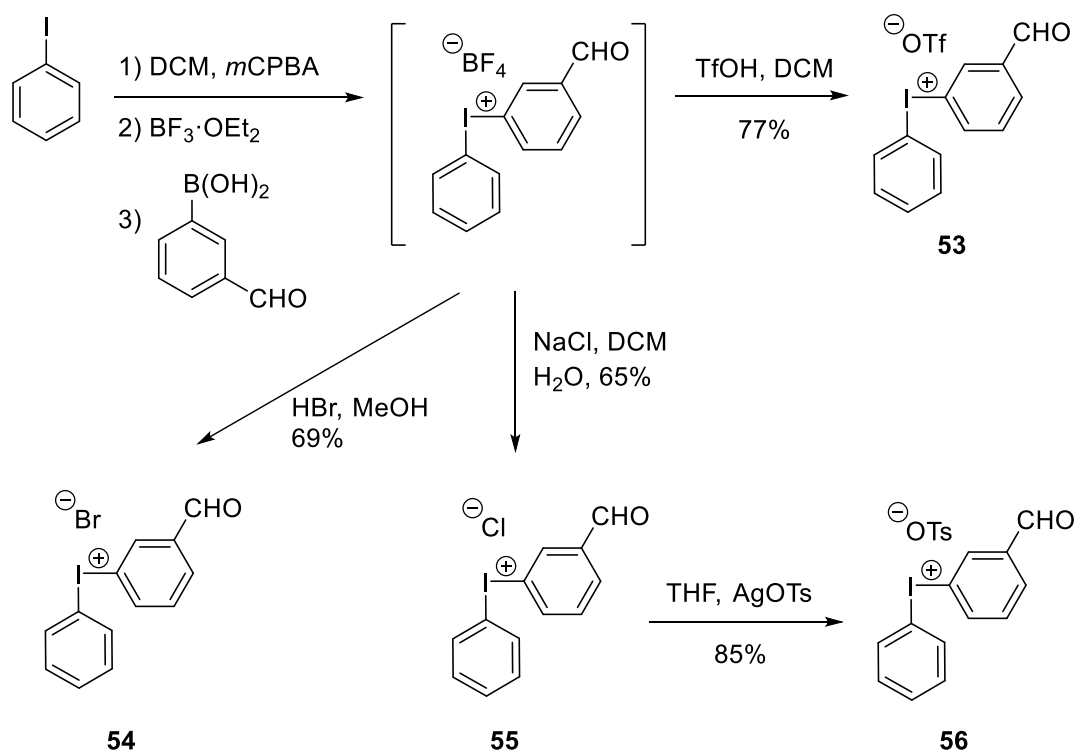
Scheme 45: Synthesis of diaryliodonium salts 53-56 via a non-isolated diaryliodonium tetrafluoroborate salt.[168]

It has been discussed in many previous publications that unavoidable dilution of [^{18}F]fluoride ion occurs when tetrafluoroborate salts are used and accordingly, use of tetrafluoroborate salts as precursors to high specific activity fluorine-18 labelled compounds is not appropriate.[72, 170, 171]

Griffiths and co-workers proceed with counter anion exchanges to avoid this problem, however, the experimental evidence provided does not attempt to quantify the extent of any undesired fluorine-19, and hence confirm the purity of the counter-ion, in the precipitated products. No ^{19}F-NMR analyses were provided for any of the reported diaryliodonium salts, even in instances where fluorine-19 is present as a constituent of a desired counter anion, such as **53**. Furthermore, identification of the bromide and chloride diaryliodonium salts was performed using ^{1}H, ^{13}C NMR and low resolution positive mode LC-MS only. These methods are not appropriate to identify, with any reasonable confidence, the presence of residual bromide or chloride. Elemental analysis is an analytical method which can be used to determine with a level of confidence the percentage of fluoride, bromide and chloride in the diaryliodonium

salt, such an analysis was not reported and therefore it is not possible to confirm the purity of the counter-ion component following these exchange reactions.

Diaryliodonium salts synthesised in this study benefit from additional characterisation, conforming with the expected results of ^{1}H, ^{13}C and ^{19}F-NMR, high resolution mass spectrometry, IR and elemental analysis (see appendix). Additionally, X-ray crystal structures of 50-52 have been determined (Figure 36).

In the case of the monomer of **51**, the electron-rich 4-anisyl moiety is sited in the equatorial position. Monomers of **50** and **52** can be seen to adopt the opposite structure. Analogous to their regiosiomeric counterparts reported above, selection of a portion of the refined unit cell determined in the ground state may result in an apparent 'flip' between arenes appearing as pseudo-equatorial or pseudo-axial. In the transition state, however, the relative position of the rings is likely to differ compared to the ground state (see section 2.3.1).
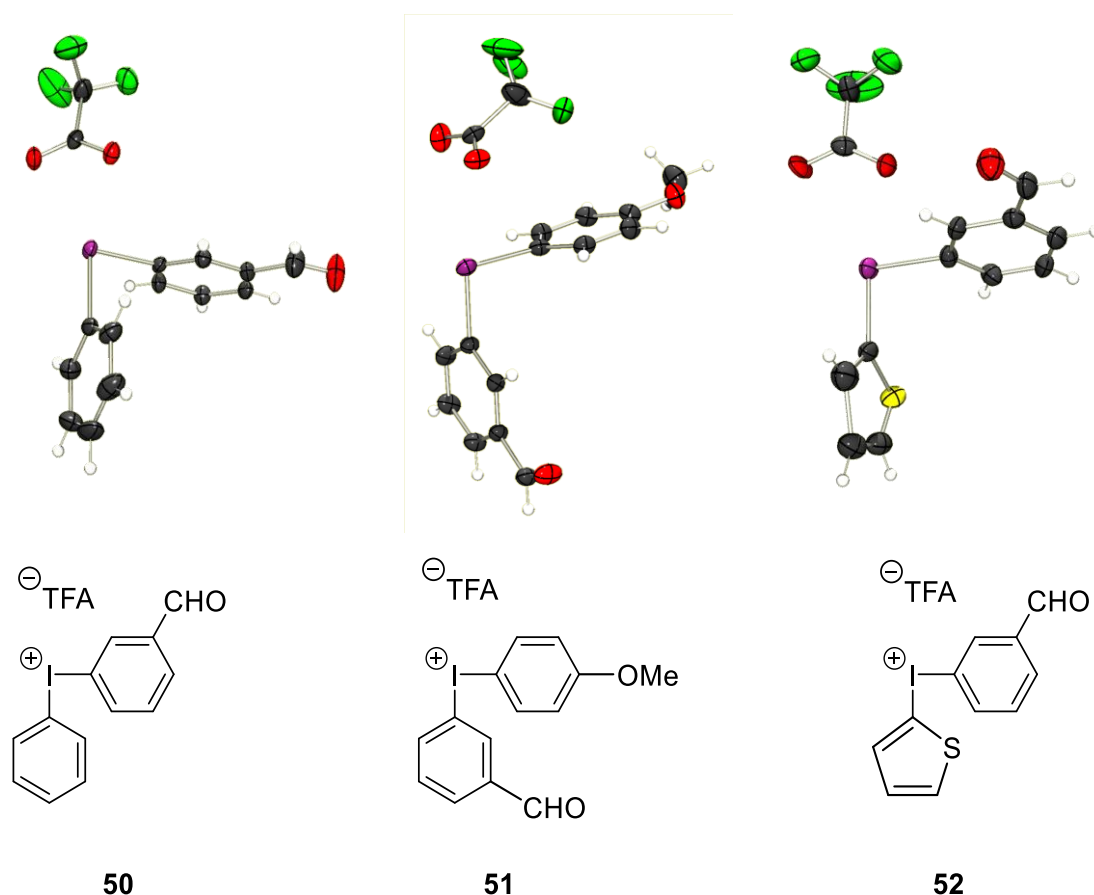
Figure 36: X–ray crystal structures of 3-formylphenyl(aryl)iodonium salts 50-52.

2.6   Synthesis of 2-Fluorothiophene: Current Methods

2-Fluorothiophene, **49**, is an important compound from the viewpoint of the radiosynthetic applications of diaryliodonium salts bearing the 2-thienyl moiety. This importance owes to the reaction mechanism arising where $Ar^1 \neq Ar^2$, thus potentiating the production of two product pairs (Scheme 46), where selectivity is dictated by steric and electronic controls, i.e., fluorination occurring preferentially on the more sterically encumbered and/or electron-deficient of the two.[92, 172] The products are often initially purified by HPLC, and upon further purification, e.g. solid-phase extraction (SPE), used as radiopharmaceuticals.
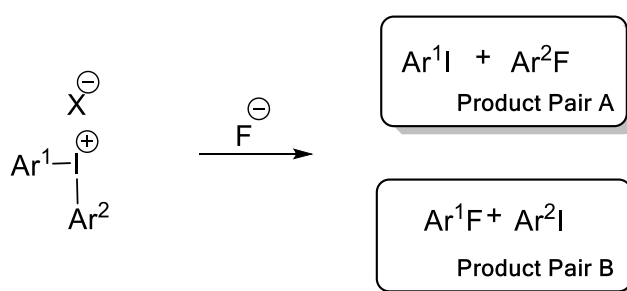
Scheme 46: Steric and electronic controls result in the generation of one or two pairs of products.

Due to its low steric encumbrance and relatively electron-rich nature, the 2-thienyl moiety is often used to promote fluorination of the desired arene in the diaryliodonium salt, especially where the target-arene, *i.e.* the arene intended to be radiofluorinated, is also electron-rich.[6] Unlike the fluorination products of other commonly used arenes, such as 4-fluoroanisole or fluorobenzene, 2-fluorothiophene is not commercially available. As such the λ_{max}, absorption coefficient and most importantly HPLC retention times, have never been reported, though unknown 'hot peaks' have been postulated as corresponding to the illusive 2-[^{18}F]fluorothiophene, **[^{18}F]49** (see Table 5 for selected literature examples).

Table 5: Selected literature examples of the use of the 2-thienyl moiety in the fluorination of diaryliodonium salts.

Compound	2-Fluorothiophene reported	Analytical method	λ_{max}	Ref
TsO⁻ Ph—I⁺—(2-thienyl)	0%	Computer calculation, references that typical radiochemical yields have been reported for the process, although the 2-thienyl moiety isn't used in the referenced studies.	No HPLC data provided	94
R—(aryl)—I⁺—(2-thienyl) TsO⁻, R= H, OMe	Detected, % not provided	HPLC	No HPLC data provided	173
R—(aryl)—I⁺—(2-thienyl) X⁻; X = Br, I, OTs, OTf; R = 2-OMe, 3-OMe, 4-OBn, 4-OMe, 4-Me, H, 4-I, 4-Br, 4-Cl	0%	Reversed-phase (RP) radio-HPLC using a Phenomenex Luna C18 column (3 mm × 250 mm) and MeCN/water (40/60) as eluent. Paper states that, 'It proved that the 2-thienyl group directs the n.c.a [18F]fluoride to a regiospecific attack of the *ipso*-carbon of the aryl group, and consequently only the desired [18F]fluoroarenes without any other radioactive side product were formed'.	No HPLC data provided	6, 174
(N-succinimidyl-oxycarbonyl-phenyl)—I⁺—(2-thienyl) TFA⁻	No details	HPLC	No HPLC data provided	105, 175
R—(aryl)—I⁺—(2-thienyl) TsO⁻; R= CN, NO₂, CF₃, OMe, Me	0–4% (d.c.)	HPLC (5.0 min Luna C18 column (250 × 4.6 mm i.d 10 μm, 280 nm) eluted at 1.75 mL/min with a gradient of MeCN/H2O with the percentage of MeCN increased linearly from 60 to 90% over 7 min. Fluorine-18 containing compounds were identified by their comobility with the respective reference fluoro compounds.	280 nm	176, 177
(2-thienyl)—I⁺—(2-thienyl) PF₆⁻	37% (plus 20% thiophene)	¹H-NMR	No HPLC data provided	178
(pyridinone-carboxamide-cycloheptyl / benzyl-phenyl)—I⁺—(2-thienyl) TFA⁻	No details	No details	No HPLC data provided	179
X—(aryl)—I⁺—(2-thienyl) A⁻; X = CH₂Cl, CH₂Br, CHO; A= OTs, Cl	No details	RP HPLC MeCN:H₂O (1:1, v/v)	No HPLC data provided	180
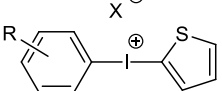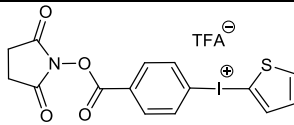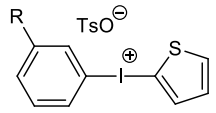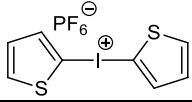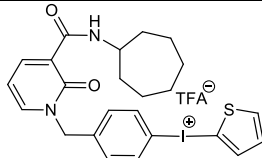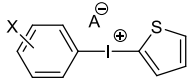
| | X = TFA, OTs, ClO$_4$, Br | No details | UPLC, Semi preparative HPLC. | No HPLC data provided | 181 |

It is therefore apparent that great importance is associated with the use of the 2-thienyl moiety as a non-participating arene both for simple and complex diaryliodonium salts. An authentic standard of the material was sought accordingly.

The earliest synthesis of **49**, reported in 1949 by VanVleck, employed the reaction of antimony trifluoride with 2-iodothiophene in refluxing nitromethane (Scheme 47), to produce moderate yields of the desired compound which was characterised only by sulfur and fluorine elemental analysis due to technological limitations of the time.[167]
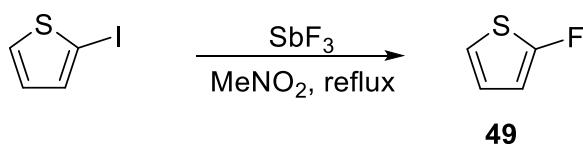
Scheme 47: The earliest reported preparation of 49.

A number of syntheses have since been reported for the production of **49**, the most successful of which being the reaction of perchloryl fluoride, an extremely toxic (TLV 3 ppm), potentially explosive and now unobtainable gaseous reagent,[182] with 2-thienyllithium (Scheme 48).[183, 184]
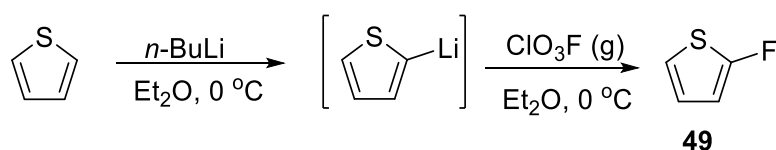
Scheme 48: Preparation of 49 using perchloryl fluoride.

Many of the attempted syntheses have resulted in mixtures of **49** and thiophene, with analytically pure samples being produced only by preparative gas chromatography.[183, 184] Other than some early work on the ^{1}H- and ^{19}F-NMR spectra[183] of **49** (as well as related compounds),[185-187] modern innovations are yet to

80

prompt a synthesis to produce large quantities of pure 2-fluorothiophene and thus, full characterisation remains to be reported.

Aryllithiums have previously been shown to be reactive towards NFSI, demonstrating the potential for fluorination of organometalics with NFSI[188] and thus forming the basis of our synthetic approach. The known volatility of **49**[167, 184] has forced careful solvent choice previously, to the extent that Schuetz *et. al.* found it necessary to synthesise their own *n*-butyllithium in diethylether to avoid the higher boiling commercially available solutions in, for example, hexanes. Following these precautionary measures an initial approach using high boiling solvents was postulated.

Although ionic liquids have been shown to be suitable for the synthesis of Grignard reagents,[189] these would be an expensive solvent for performing the reaction on larger scales, therefore a more common ethereal solvent was preferred.

2.7   Synthesis and Isolation of 2-[^{19}F]Fluorothiophene

Diglyme was initially selected as the reaction solvent during early attempts to synthesise 2-fluorothiophene, **49**, for the reasons that it is compatible with organolithium and Grignard reagents, it has a boiling point around 80 °C higher than that reported for **49**, and it could readily dissolve NFSI. Initial experiments showed *n*-butyllithium to be incompatible with anhydrous diglyme, immediately forming a cloudy suspension even before the introduction of any other reagents and thus was deemed unsuitable for this approach. The use of diethylether also had its problems, showing a triplet of triplets in the ^{19}F-NMR at -113.82 ppm in addition to the expected[183] double, double doublet for **49**. On the basis of its splitting and shift[*] the fluorinated impurity was assigned as the fluorinated hydrolysis product of directed 4-metalation, 4-fluorobenzenesulfonic acid, though no attempt was made to isolate this species (Figure 37).[190]
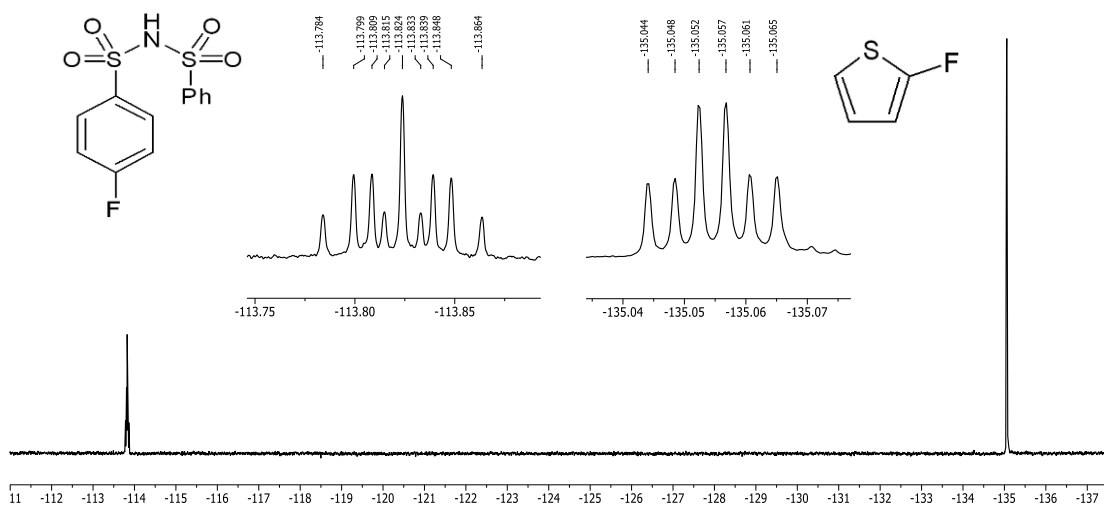
Figure 37: ^{19}F-NMR for the fluorinated impurity obtained via the organolithium reaction.

In light of the results observed with organolithium species, the analogous organomagnesium species were investigated (Scheme 49). It was found that 2-thienylmagnesium bromide could be synthesised more cleanly than its corresponding iodide. Despite quantitative formation of 2-thienylmagnesium bromide followed by

---

[*] Shift comparison made with *p*-fluorobenzene sulfonic acid (110.15 ppm)

its subsequent conversion to 2-fluorothiophene using NFSI, none of the distillation techniques attempted were able to separate the product from diglyme.
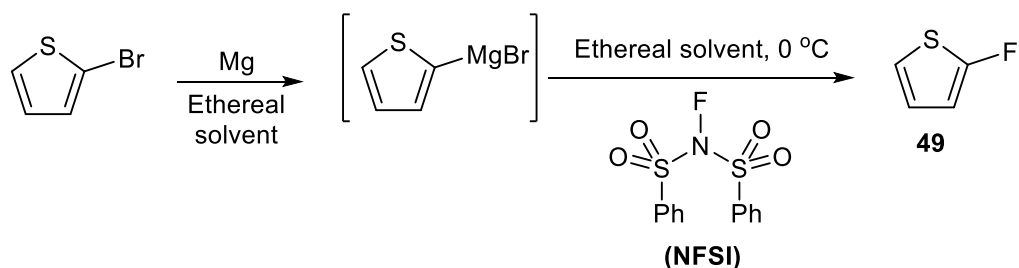
Scheme 49: Attempted synthesis of 49 using ethereal solvents diglyme and diethyl ether.

Accordingly, focus therefore returned to the use of diethylether as the reaction solvent due to its very low boiling point and, following successful small scale reactions using 2-thienylmagnesium bromide and NFSI as above, the reaction was repeated on a 750 mmol scale. After removal of the insoluble magnesium by-products by filtration, the product was isolated by careful distillation spanning several days.[†]

In spite of our best efforts to use only low boiling point solvents it was suggested that the commercial NFSI contained residual traces of ethyl acetate, which was found in the distilled product and having ruled out the other starting materials/reagents as potential sources. Residual diethylether levels could be reduced marginally using 5Å sieves providing 35.8 g of >95% purity 2-fluorothiophene, **49**, containing traces of ethyl acetate (<2.5%) and thiophene (<1%), as well as a separate fraction of 6.7 g of >70% purity material.[191, 192]

^{1}H- (Figure 38) and ^{19}F-NMR spectra (Figure 39, left) of >95 % pure **49** were in keeping with those reported previously as a component in a mixture; in addition, COSY, HMQC, HMBC and [1]H-decoupled-^{19}F spectra (Figure 39, middle and right) were also ran to provide further structural information.

[†] Distillation procedure performed both by Dr L. I. Dixon and the author.
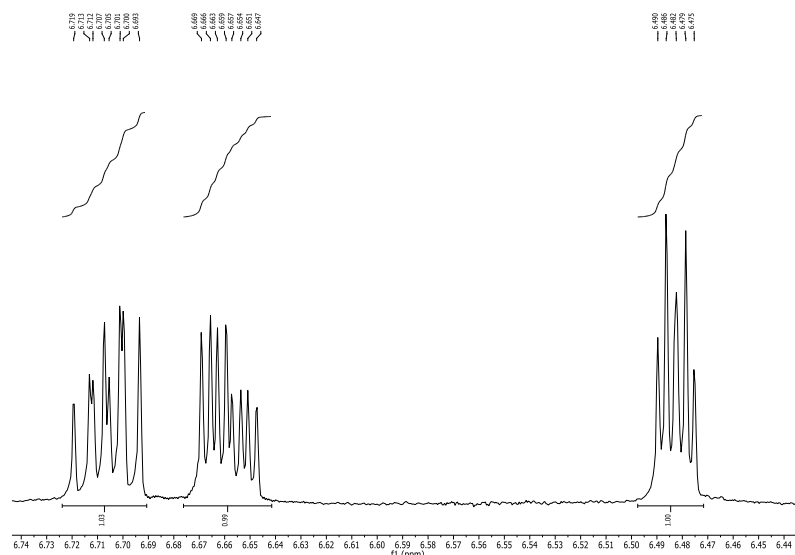
Figure 38: ^{1}H-NMR for 95+% pure 2-fluorothiophene, 49.
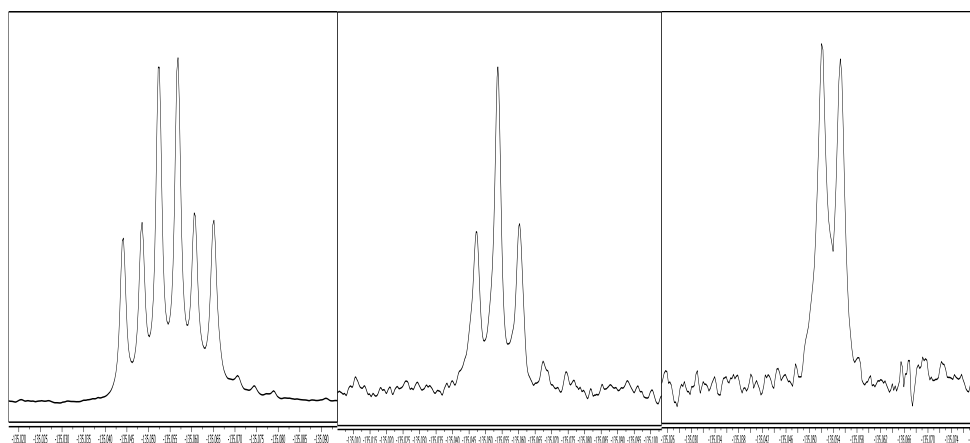
Figure 39: ^{19}F-NMR (376 MHz, d$_2$-DCM, CFCl$_3$) (left),[193] ^{19}F-NMR (471 MHz, d$_2$-DCM, CFCl$_3$) H3 (6.48ppm) irradiated (middle) and H4 and H5 (6.68ppm) irradiated (right).

Spectroscopic analysis of **49** by UV-Vis gave a molar absorption coefficient (ε) of 5150 M^{-1}cm^{-1} (λ_{max} (EtOH)/nm 226) (Figure 40) which is of similar magnitude to the parent molecule thiophene (λ_{max}(EtOH)/nm 231; ε=2232 M^{-1}cm^{-1}). The λ_{max} for **49** was also assessed for other common HPLC solvents to rule out solvatochromistic effects, i.e. the dependence between absorption (and emission) spectra as a consequence of a molecules various states of polarity in different solvents, showing almost no change in water or acetonitrile (λ_{max} = 225 and 226 nm respectively). It is interesting to note that upon fluorination of the 2-thienyl(aryl)iodonium salts reported in Table 5 the HPLC analyses were performed at 254 and 280 nm wavelengths for which there is minimal absorbance.
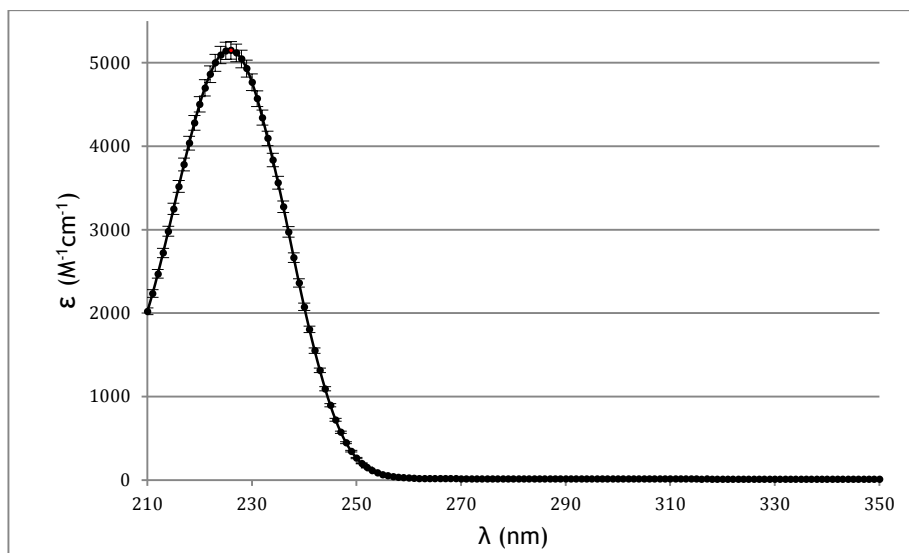
Figure 40: Absorption spectrum for 2-[^{19}F]fluorothiophene, 3.3×10^{-4} M in EtOH.

Using the HPLC analysis, the detection limits for 2-fluorothiophene have been established by generation of a series of calibration curves, where the minimum detection limit is 25 µM and maximum detection limit is ≤12 mM for 10 µL injection volumes of the respective concentration standards (Figure 41).[194] The linear portion of the calibration curve is taken when $R^2 = 1$ (3 d.p.). Greater concentrations results in a drop in R^2, revealing the detection limit.
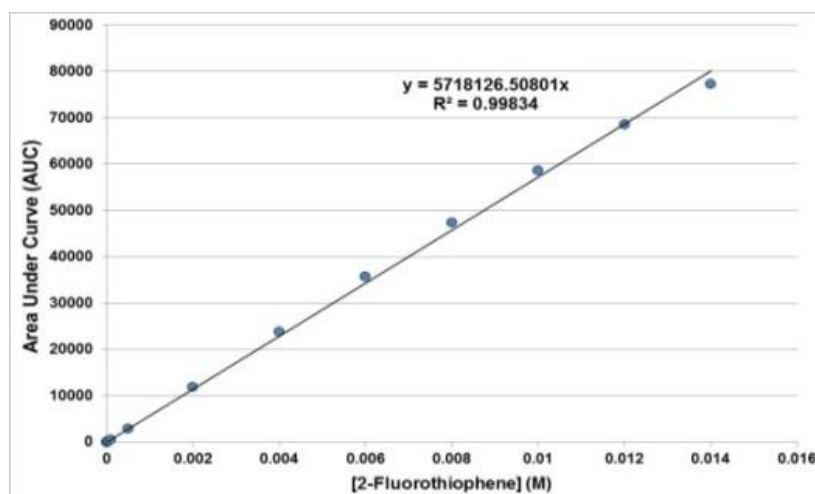
Figure 41: HPLC calibration curve demonstrates the detection limit for 2-[^{19}F]fluorothiophene.

2.8 Synthesis of 2-Thienyl(aryl)iodonium Salts

A radiosynthetic study was sought to determine if the corresponding 2-[^{18}F]fluorothiophene, **[^{18}F]49**, could be observed and quantified relative to a 2-fluorothiophene, **49**, standard. Following the procedures set forth above, a range of 2-thienyl(aryl)iodonium trifluoroacetates, **57-59**, were prepared (Scheme 50).

35, Ar = phenyl
33, Ar = 4-anisyl
34, Ar = 2-thienyl

57, Ar = phenyl, 28%
58, Ar = 4-anisyl, 39%
59, Ar = 2-thienyl, 19%
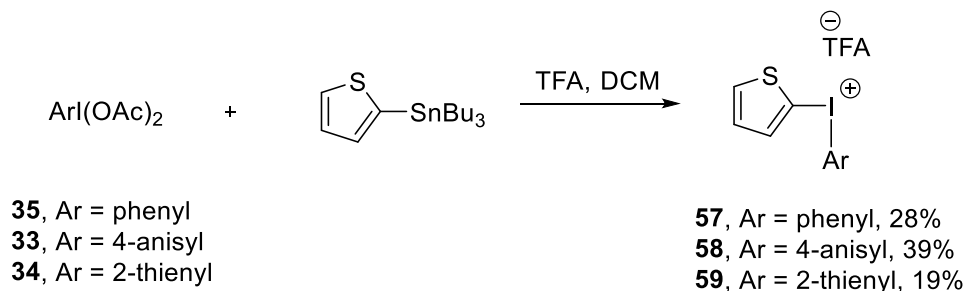
Scheme 50: Synthesis of 2-thienyl(aryl)iodonium salts 57-59.

No attempts were made to optimise the yields of the reaction, as sufficient quantities of the precursors could be obtained for the intended study. It is important to note that the more electron-rich diaryliodonium salt **59** was found to decompose to a brown/black tar-like substance within 48 hours, even when stored in a freezer (ca. -20 °C). The previously unreported X-ray crystal structures of **57-59** were obtained (Figure 42).
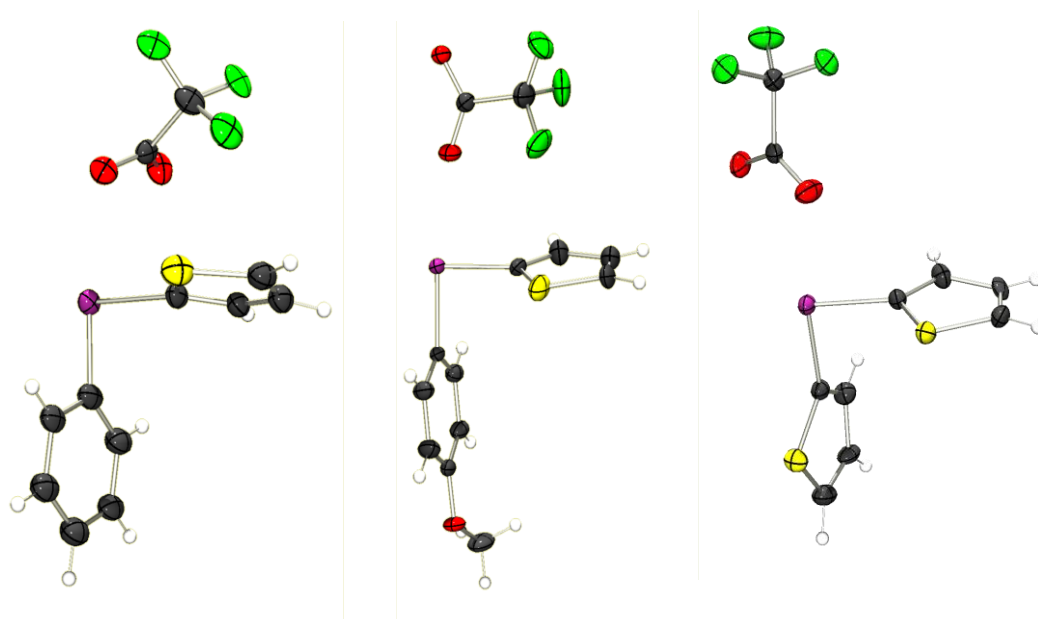
Figure 42: X-ray crystal structures of 57-59 (left to right).

In summary an authentic analytically pure sample of 2-fluorothiophene, **49**, has been prepared by a large scale synthesis from 2-thienylmagnesium bromide and NFSI and several key analytical parameters have been unambiguously determined. A range of simple diaryliodonium salts have also been synthesised and fully characterised, enabling a radiochemical study reported herein to determine if [^{18}F]**49** can be detected when using sealed microfluidic apparatus.

2.9 Synthesis of *N*-(4-fluorophenyl)maleimide and Related Compounds

As discussed in section 1.11.3, current approaches to thiol reactive prosthetic groups focus on the use of the maleimide moiety as a Michael acceptor for the conjugation of free sulfhydryl residue which may be readily incorporated into biomolecules. However, there is a marked lack of a simple and reproducible synthetic procedure to yield the simple [18F]radiolabeled maleimide, *N*-(4-[18F]fluorophenyl)maleimide, **[18F]60**, following the first report by Shiue *et al.* in 1989.[129] Multi-step synthetic procedures are the only known pathways to afford maleimide containing prosthetic groups. Several have postulated that the maleimide functionality does not tolerate the basic conditions required for the introduction of [18F]fluoride ion into the prosthetic group precursor.[129, 133] However, the aforementioned studies have not considered the use of diaryliodonium salts, nor the use of microfluidic apparatus during the radiosynthetic procedure.

Attempts were made to follow the general procedure given above for the synthesis of a diaryliodonium salt containing maleimide functionality, i.e. introduction of a stannane into the target-arene followed by reaction with preformed oxidised iodine species. Firstly, *N*-(4-halophenyl)maleimides were prepared[195] (Scheme 51) to investigate which species is most amenable to subsequent inclusion of stannane functionality. The synthesis of **61-63** proceeds via non-isolated *N*-halophenylmaleanic acid, which conveniently precipitates out of the reaction solvent. Once filtered, the acid is readily cyclised by using sodium acetate in acetic acid.

X = F, Br or I

X = F, **61,** 91%
X = Br, **62**, 98%
X = I, **63**, 61%
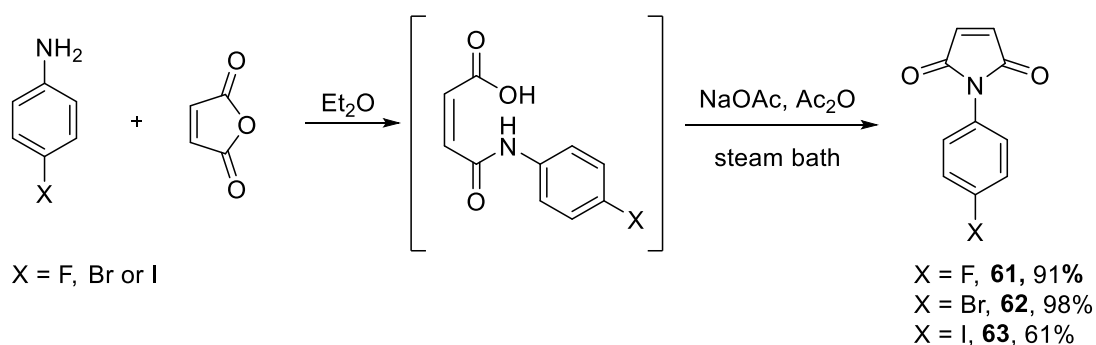
Scheme 51: Preparation of 4-*N*-halophenylmaleimides 61-63.

An x-ray crystal structure for **63** was obtained, demonstrating that the maleimide functionality lies at 90° relative to the arene (Figure 43) and is therefore not conjugated with the π-electrons of the benzene ring.
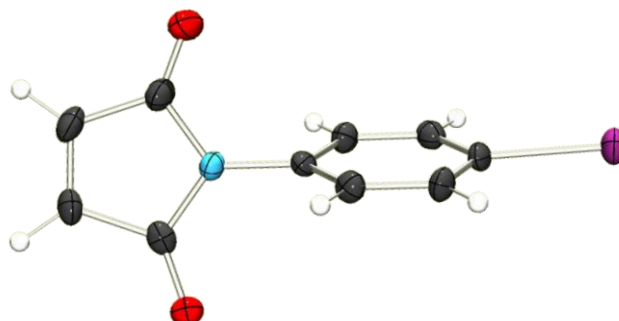
Figure 43: X-ray crystal structure of 63.

Catalytic incorporation of stannane functionality was attempted using a range of catalysts and reaction conditions for precursors **62** and **63**, where all reactions were performed under a positive pressure of nitrogen using MeCN freshly distilled over calcium hydride or toluene freshly distilled over sodium metal. Unfortunately, however, none of the attempted procedures furnished the desired arylstannane (Table 6). Consequently, the general procedure outlined above could not be applied to the synthesis of this diaryliodonium salt.

X = Br, **62**
X = I, **63**

64
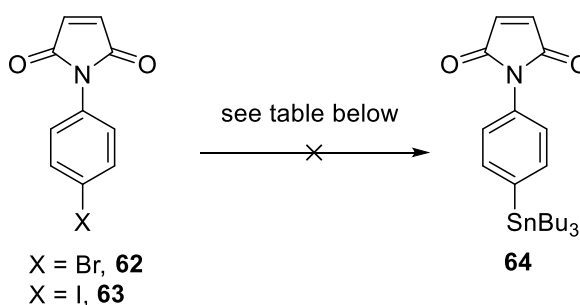
Entry	Catalytic System	Stannane	Solvent	Temperature	Time	Result
1	Co/Zn, allyl-chloride	Bu$_3$SnCl	MeCN	50 °C	8 h	Complex mixture of crude material
2	Pd(PPh$_3$)$_4$	(Bu$_3$Sn)$_2$	Toluene	Reflux	4 h	**62** and **63** decomp.
3	Pd(dba)$_2$	(Bu$_3$Sn)$_2$	Toluene	Reflux	12 h	Formation of an *N*-phenylmaleanic acid
4	Pd(OAc)$_2$	(Bu$_3$Sn)$_2$	Toluene	Reflux	8 h	**62** and **63** decomp.
5	Pd(dppf)Cl$_2$	(Bu$_3$Sn)$_2$	Toluene	Reflux	12 h	**62** and **63** decomp.

Table 6: Attempted synthesis of 64 from precursors 62 and 63 by examination of various catalysts and reaction conditions.

An early example of a diaryliodonium salt bearing maleimide functionality is reported in patent documentation, which describes a procedural enhancement which aims to improve the reproducibility of the preparation of diaryliodonium salt photoinitiatiors.[196] Crivello *et al.,* obtained 4,4'-bis-*N*-phenylmaleimidoiodonium bisulfate **66** by reaction of *N*-phenylmaleimide **65** with potassium iodate in the presence of acetic anhydride and sulfuric acid (Scheme 52). Conversion to the corresponding chloride salt was reported by addition of an excess of ammonium chloride, though limited analytical evidence was provided for either of the isolated species. Furthermore, limited experimental details were provided.
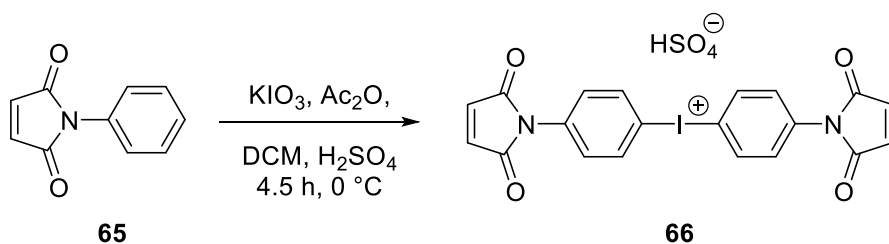
Scheme 52: Synthesis of 66 from *N*-phenylmaleimide.[196]

If the purpose of **66** was considered from the perspective of a prosthetic group, rather than a photoinitiator, the advantage of its symmetry becomes immediately apparent in that successful radiolabeling with [^{18}F]fluoride ion will lead to the formation of a single product pair. Accordingly, attempts were made to synthesise **66** using the method proposed by Crivello *et al.,* however, such endeavours were met with little success. Upon ^{1}H-NMR analysis of the crude product (n = 4), only starting material was observed in significant quantities, in addition to a myriad of crude species. A suggestion of the formation of a 4-substituted diaryliodonium salt was apparent upon examination of the precipitated reaction output by ^{1}H-NMR, as a diagnostic doublet at ~8.5 ppm was observed. However, the white powder obtained quickly decomposed to a black tar when attempts were made to dry the material under reduced in amber glass over a desiccant. An attempt to convert the potentially unstable bisulfate salt to the corresponding chloride species as a result of anion exchange by addition of an excess of ammonium chloride to the isolated precipitate was made. Unfortunately, however, attempts to dry the material also resulted in the formation of a crude tar-like product.

Due to the lack of reproducibility with the method outlined above, an alternative route to a maleimide bearing diaryliodonium salt was considered. Work by Olofsson *et al.* describes the use of *m*-chloroperbenzoic acid (*m*CPBA) as an oxidatant appropriate for the oxidation of a range of electron-rich and electron-poor iodoarenes, which when followed by treatment with an arene and trifluoromethanesulfonic acid, furnishes a range of symmetrical and unsymmetrical diaryliodonium triflates.[169, 197] Furthermore, molecular iodine could be used in place of an iodoarene, which greatly simplifies the synthesis of a symmetric salt. Accordingly, the aforementioned method was applied to the synthesis of a symmetric and asymmetric diaryliodonium salt bearing maleimide functionality.

The synthesis of **67** from molecular iodine and **65** proved unsuccessful. A range of conditions were examined as suggested by Olofsson and co-workers, from 10 minute reaction times to 22 hour reaction times, to the use of either 3 or 4 eq *m*CPBA, or varying the eq of TfOH to 4 or 6 relative to **65**. Care was taken using *m*CPBA, as the % of *m*CPBA present needs to be determined by iodometric titration prior to synthetic use.[198] Following the procedure of Olofsson *et al.*, in most instances, unreacted **65** was obtained, and following the course of the reaction by TLC (95:5, petrol:DCM) only **65** and *m*-chlorobenzoic acid were visualised (Scheme 53).
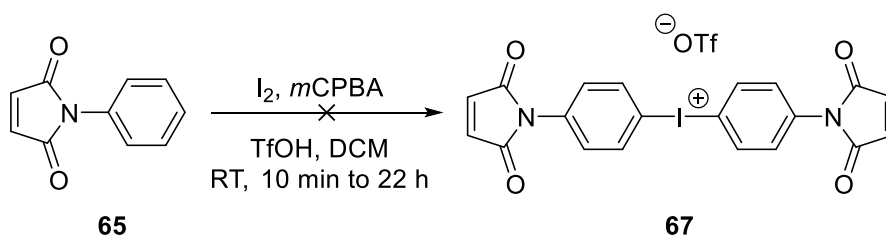
Scheme 53: Attempted synthesis of 67 following the methodology reported by Olofsson *et al.*[169, 197]

Following the methodology for the synthesis of an asymmetric diaryliodonium salt, **65** and **50** were mixed in the presence of *m*CPBA. Some slight modifications to the procedure, i.e. running the reaction at 0 °C, as well as using TFA in place of TfOH for both reaction temperatures, was also investigated (Scheme 54). No consumption of iodobenzene was observed when following the reaction by TLC (4:1, petrol:DCM) and the desired asymmetric diaryliodonium salt was not obtained.

Clearly, the use of the conditions above is not amenable to the production of a diaryliodonium salt containing maleimide functionality.
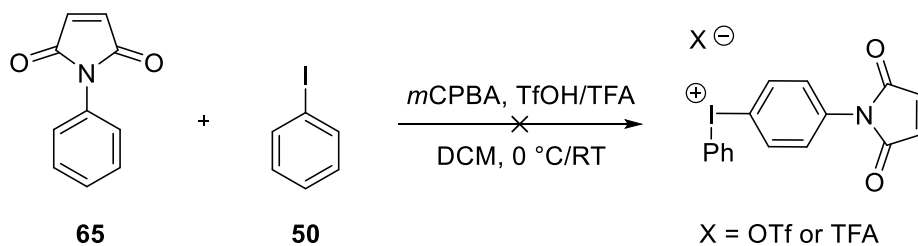
Scheme 54: Attempted synthesis of diaryliodonium salts following the methodology reported by Olofsson *et al.*[169, 197]

Additional synthetic methodologies were attempted, including:

- The preformed reactive Koser's reagent[199] was used instead as the source of the electrophilic iodine. However, no reaction was observed and starting material was recovered.

- Generation of an organolithium species at -78 °C by reaction of with 4-bromo and 4-iodo derivatives of *N*-phenylmaleimide, **62** and **63**, with *n*BuLi in ether. Upon quenching with Bu₃SnCl and work-up, ¹H NMR of the resultant red oil indicated various tin containing by-products were the only material extracted into the organic phase.

A further method was considered, which reverses the general diaryliodonium synthetic strategy given in section 1.10.1, i.e. oxidation of the target arene followed by reaction with the non-target arene bearing a stannane. Using the procedure outlined in section 2.1, synthesis of diacetoxyiodoarene **68** was attempted using sodium perborate tetrahydrate in acetic acid (Scheme 55). Upon filtration of the anticipated product, the off white powder began to darken. ¹H-NMR determined that the crude mixture consisted of roughly a 1:1 mix of starting material and **63**, and that the sample was found to decompose to a mixture of unidentified aromatic species after *ca.* 30 min. Purification of **68** is inherently difficult by chromatographic means given that the sample rapidly decomposes. Elongated reaction times (12 h) did not facilitate complete conversion of the starting material to the desired product. Additionally, recrystallisation techniques failed to separate the diacetoxyiodoarene from the iodoarene.
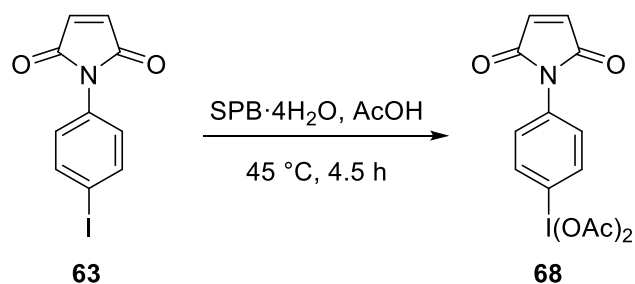
Scheme 55: Preparation of crude diacetoxyiodoarene 68.

The difficulty regarding the purification of **68**, coupled with the apparent instability of the compound, meant that a direct synthesis of a diaryliodonium salt from crude **68** was attempted (Scheme 56). Fortunately, diaryliodonium salt **69** was delivered in a 20% yield upon crystallisation as fine colourless needles. The material was found to be stable enough to perform a microanalysis several days post isolation, where **69** was found to conform to the expected percentages of C, H and N. Furthermore, an X-ray crystal structure of **69** was obtained (Figure 44).
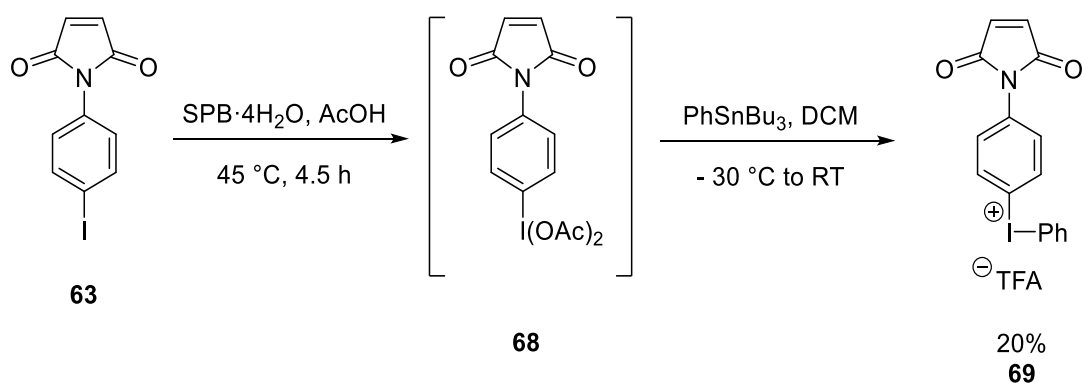
Scheme 56: Preparation of diaryliodonium salt 69 was achieved by use of impure 68.
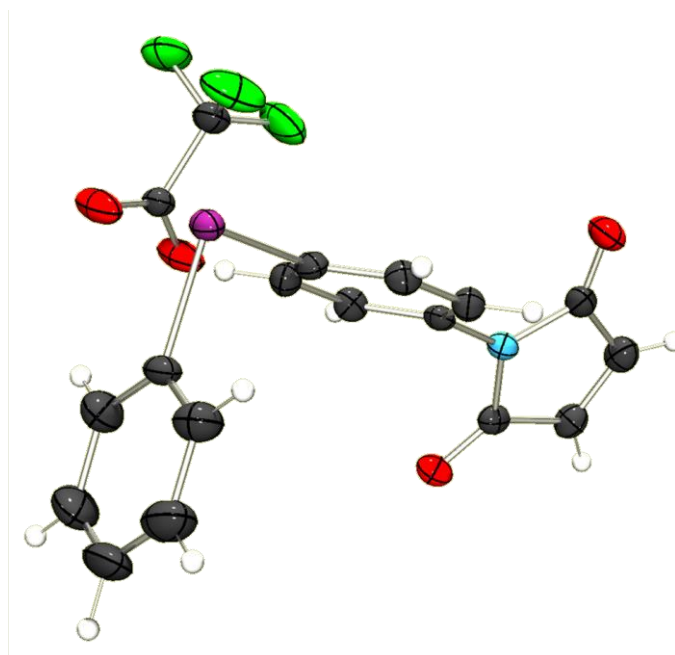
Figure 44: X-ray crystal structure of 69.

Accordingly, the synthesis of a maleimide bearing diaryliodonium salt has been successfully achieved after several attempted synthetic methodologies. Key to the synthesis, was the reversal of our general synthetic approach to diaryliodonium salts, which has furnished **69** as a material to be studied with respect to the first one-step synthesis of a maleimide bearing a fluorine-18 radiolabeled material.

2.10 Chapter Two: Overall Conclusions

- A range of diaryliodonium salts, precursors to prosthetic groups bearing aldehyde and maleimide functionaltiy, have been prepared and characterised.
- An authentic analytically pure sample of 2-[^{19}F]fluorothiophene, **49**, has been prepared by a large scale synthesis from 2-thienylmagnesium bromide and NFSI and several key analytical parameters have been unambiguously determined.
- A range of simple diaryliodonium salts bearing the 2-thienyl moiety have been synthesised and fully characterised, enabling a radiochemical study, reported herein, to determine if **[^{18}F]49** can be detected when using sealed microfluidic apparatus.

3 Chapter Three: Radiochemistry Results and Discussion

The aims of the radiosynthetic studies performed herein are to:

- Determine if it is possible to detect the presence of 2-[^{18}F]fluorothiophene using a sealed radiosynthetic system, by reference to the authentic standard 2-[^{19}F]fluorothiophene prepared above.

- Elucidate if diaryliodonium salts are suitable precursors to the key prosthetic groups, 4-[^{18}F]fluorobenzaldehyde and the counterpart 3-[^{18}F]fluorobenzaldehyde.

- Optimise the radiochemical yields of radiosyntheses by varying the parameters used as an input to automated microfluidic apparatus.

- Determine if a large scale radiosynthesis of 4-[^{18}F]fluorobenzaldehyde is feasible using diaryliodonium salts and microfluidic apparatus.

3.1 Introduction to Practical Microfluidic Apparatus used for Radiosyntheses

Microfluidic apparatus present many advantages for the production of radiolabeled compounds, *e.g.* the ability to use milligram quantities of precursor for multiple reactions. In a traditional radiosynthesis, greater quantities of the precursor are used, much of which may be wasted during the radiosynthetic process.[6] Microfluidics also provides an excellent degree of precision over several key reaction parameters, namely, temperature, stoichiometry and reaction time. Furthermore, microfluidic systems may operate at significantly elevated pressures (300 psi), enabling reactions to be carried out at temperatures above the boiling point of the reaction solvent.

Relative to batch radiosynthetic apparatus (discussed in section 1.5.1.2), one delivery of [^{18}F]fluoride ion can be sufficient for multiple reactions, up to 50 per delivery of a 3 GBq is feasible. Consequently, microfluidic apparatus is often used as a first-step in the development of new radiolabeled compounds, as many key reaction parameters can be conveniently and rapidly screened.

In light of the advantages discussed, the remotely controlled microfluidic Advion NanoTek[45] apparatus was used for all radiofluorination reactions performed as part this study (Figure 45).

Figure 45: Advion NanoTek (BM bottom left, RM middle and CM right), auto-injection valve (blue box) and Agilent Technologies 1200 series in-line HPLC.

The NanoTek system consists of a base module (BM), concentrator module (CM) and a reactor module (RM) with dedicated control software (Advion, LF software version 1.4.0) which is operable external to the hotcell housing the apparatus.

The BM comprises of two reagent syringes operated separately by high pressure syringe pumps (P1 and P2). The syringe pump is connected to an eight way distribution valve which is where so-called reagent loops are installed, prior to being dispensed towards to RM.

The CM comprises a low-pressure six-way valve, a reagent cartridge and an aluminium heating block. As the cyclotron produced (either delivered from Erigal[200] or prepared in-house using an ABT Biomarker Generator[201]) NCA [^{18}F]fluoride ion is delivered 'wet', i.e. in a solution of the target [^{18}O]water, a drying process is then

required to ensure 'naked' fluoride is used for radiolabelling.[3] A syringe line connected to the CM unit is inserted into the vessel bearing the wet [^{18}F]fluoride ion. The azeotropic drying procedure is then initiated. To summarise the procedure reported elsewhere,[67] the wet [^{18}F]fluoride ion solution is passed through a quaternary ammonium resin (QMA) cartridge, trapping the [^{18}F]fluoride ion and facilitating the elution of the [^{18}O]water. [^{18}F]Fluoride ion is then sequestered from the QMA cartridge using a phase transfer agent (PTA), tetraethylammonium hydrogen carbonate (TEA·HCO$_3$), followed by azeotropic drying with acetonitrile under a positive pressure of nitrogen in the CM heating block. Once the drying process is complete, a pre-set volume of DMF is dispensed and aspirated several times into the CM vial, the contents of the [^{18}F]fluoride ion/PTA complex are swept to the RM (Figure 46).
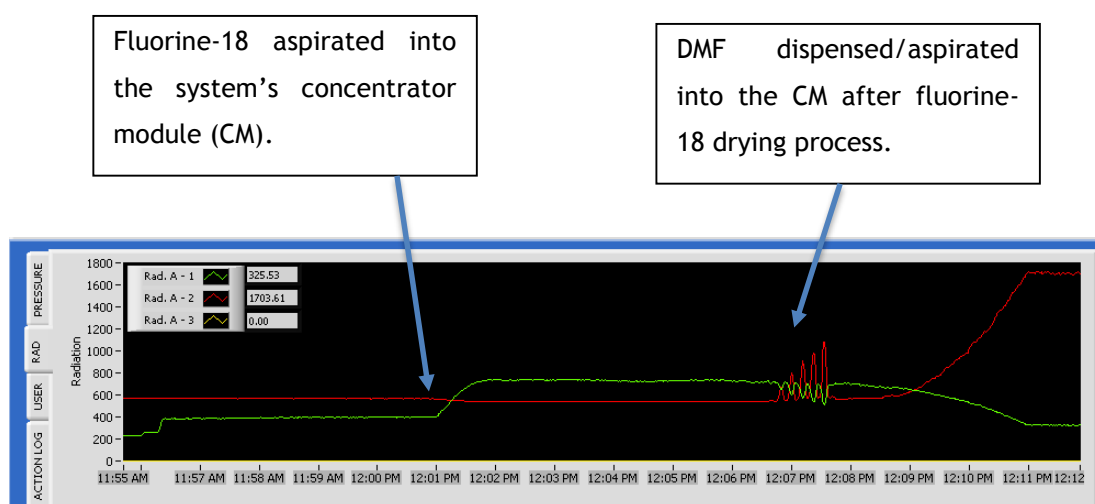
Figure 46: Decay counter attached to the P3 loop (red line) shows the repeated dispensing and aspiration of DMF into the concentrator vial (green line) followed by aspiration of the [^{18}F]fluoride ion/PTA complex into the P3 loop.

The RM houses a heating element and a microreactor, of which up to four can be installed per RM. Microreactors were made of fused silica tubing (internal diameter ($\varnothing_{INT}$) 0.1 μm; length 4.0 m) held in a brass ring, which is filled with a thermoresistant polymer to fix the fragile coiled tubing in place (Figure 47). An additional syringe pump (P3) and distribution valve, used to direct reaction boluses to intended ports, is housed at the RM. The dry radioisotope complex is stored at P3 prior to being dispensed towards the microreactor.
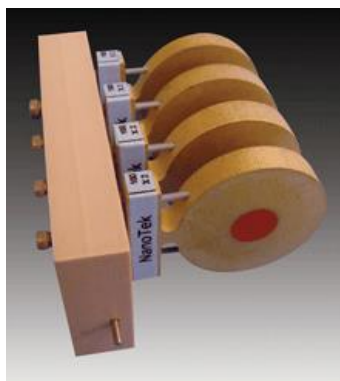
Figure 47: Four microreactors, each connected to the reactor board. The red thermoresistant polymer can be seen at the centre of the microreactor.

It is important to note that the PTA which has traditionally been used is a cryptand, *e.g.* K_{222}, or tetrabutylammonium hydrogen carbonate. Work discussed herein, however, makes use of the PTA discussed in section 1.7, as recent studies have indicated that tetraethylammonium hydrogen carbonate ($TEA.HCO_3$) is a suitable PTA replacement for cryptands, and does not cause blockages within microfluidic apparatus.[202]

Each precursor to be radiolabeled was stored in a loop (400 µL, P1) for use in subsequent reactions. Once both reagents are stored in their respective loop, they are swept into the reactor at pre-set flow rates. The reactants rapidly mix and reach the pre-set reaction temperature upon entering the chemically inert coiled silica glass capillary tube microreactor, which can be heated to 200 °C (Figure 47).[45] It is important to note that the microfluidic system is sealed and as such, any volatile material which may be lost in an open system can be detected during subsequent analysis.[173]

The crude reaction mixture is then swept out of the microreactor towards an auto-injection valve (Smartline Valve Drive: Knauer, Germany), where the crude reaction mixture is stored on a loop until all crude material is swept out of the microreactor, at which point, the valve is diverted to an in-line radio HPLC (Agilent Technologies 1200 HPLC system, LabLogic Flow Count) for analysis. The complete set up of the primary components used in this study can be seen below (Figure 48).

98
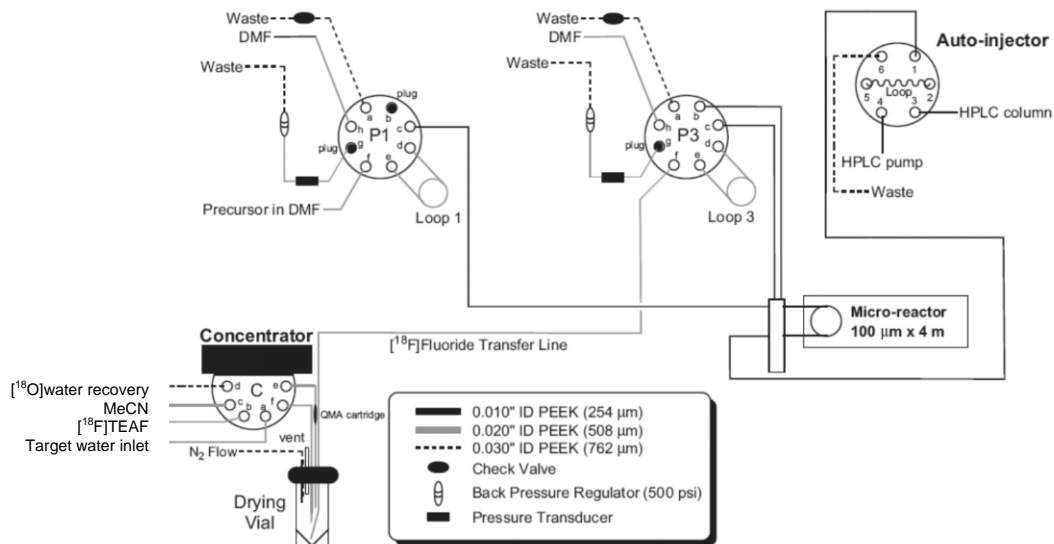
Figure 48: Radiosynthesis apparatus configuration (P2 not shown for clarity).[67]

3.2 Radiosynthesis of 2-[^{18}F]Fluorothiophene

Methods, both 'hot' and 'cold', to synthesise 2-[^{18}F/^{19}F]fluorothiophene have been described above. However, to the best of the authors' knowledge, no comparison to an authentic sample of 2-[^{19}F]fluorothiophene has been made when the 2-thienyl moiety is incorporated into a diaryliodonium salt. Accordingly, 2-[^{18}F]fluorothiophene precursors **53-55** were subjected to a radiofluorination study, whereby 10 mg/mL **53-55** in DMF was stored on P1 and reacted with [^{18}F]fluoride ion in an attempt to detect and characterise 2-[^{18}F]fluorothiophene (Scheme 57).

57, Ar = phenyl
58, Ar = 4-anisyl
59, Ar = 2-thienyl
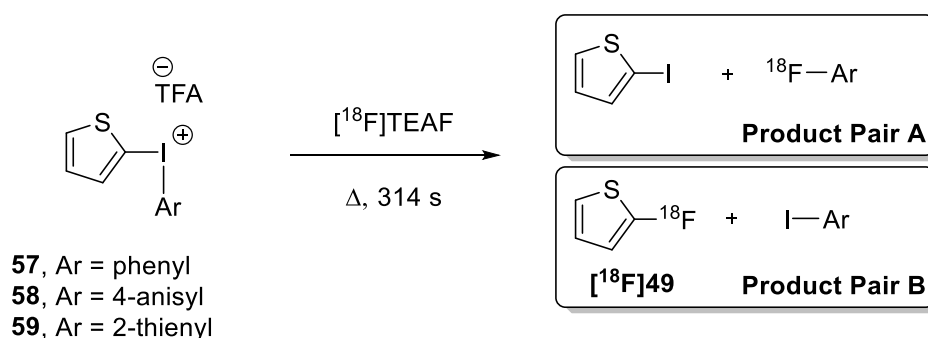
Scheme 57: Reaction of 53-55 with [^{18}F]fluoride ion to generate 2-[^{18}F]fluorothiophene, [^{18}F]49, as part of product pair B.

The first precursor to be examined was **57**, the least electron-rich precursor in the series. As may be expected of the directing nature of the 2-thienyl moiety, only one product pair, as well as decomposition products, was observed during the course of the fluorination reaction (n = 4, [^{18}F]fluorobenzene 31% RCY) (Figure 49). Less forcing reaction conditions, 170 °C (n = 3) and 110 °C (n = 1) were also screened, and still only one product pair was observed. A greater range of temperatures were not examined as part of the study, as the radio-HPLC method time needed to be extremely elongated, relative to typical radio-HPLC methodologies, in order to separate benzene (t_R 46.55 min) from 2-fluorothiophene (t_R 48.42 min).
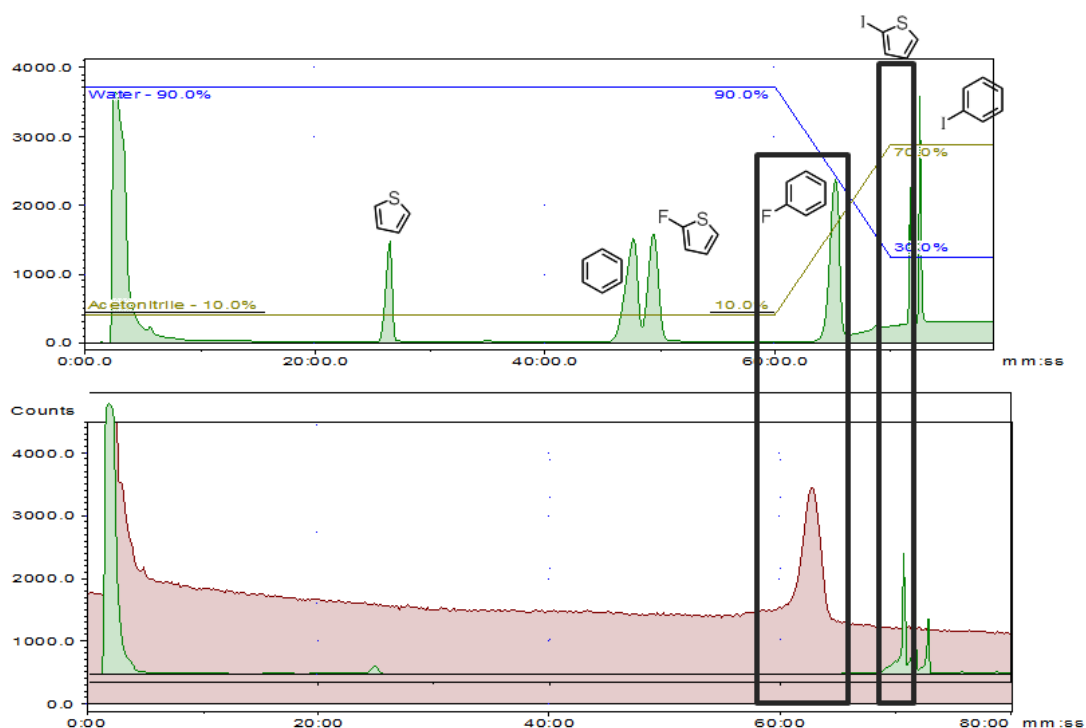
Figure 49: Top HPLC spectrum shows the 'cold' development method to separate the range of potential products of the reaction, bottom spectrum shows the results obtained during the radiolabeling of 57.

The next precursor to be examined, **58**, possesses two electron-rich arenes, 2-thienyl and 4-anisyl. Accordingly, the selectivity of the process may not be considered in advance to be as clear as in the above example. However, the selectivity for one product pair, i.e. 4-[^{18}F]fluoroanisole and 2-iodothiophene, amongst decomposition products, was apparent (Figure 50). It is therefore interesting to note that this study suggests the inclusion of the 2-thienyl moiety will direct [^{18}F]fluoride ion with 100% regioselectivity onto an electron-rich arene, which is in agreement with precedent set elsewhere.[6, 203] RCYs of 1% (n = 3, 150-190 °C) were obtained and no [^{18}F]labelled material was observed at temperatures <150 °C. No attempt was made to optimise the RCY for the process.
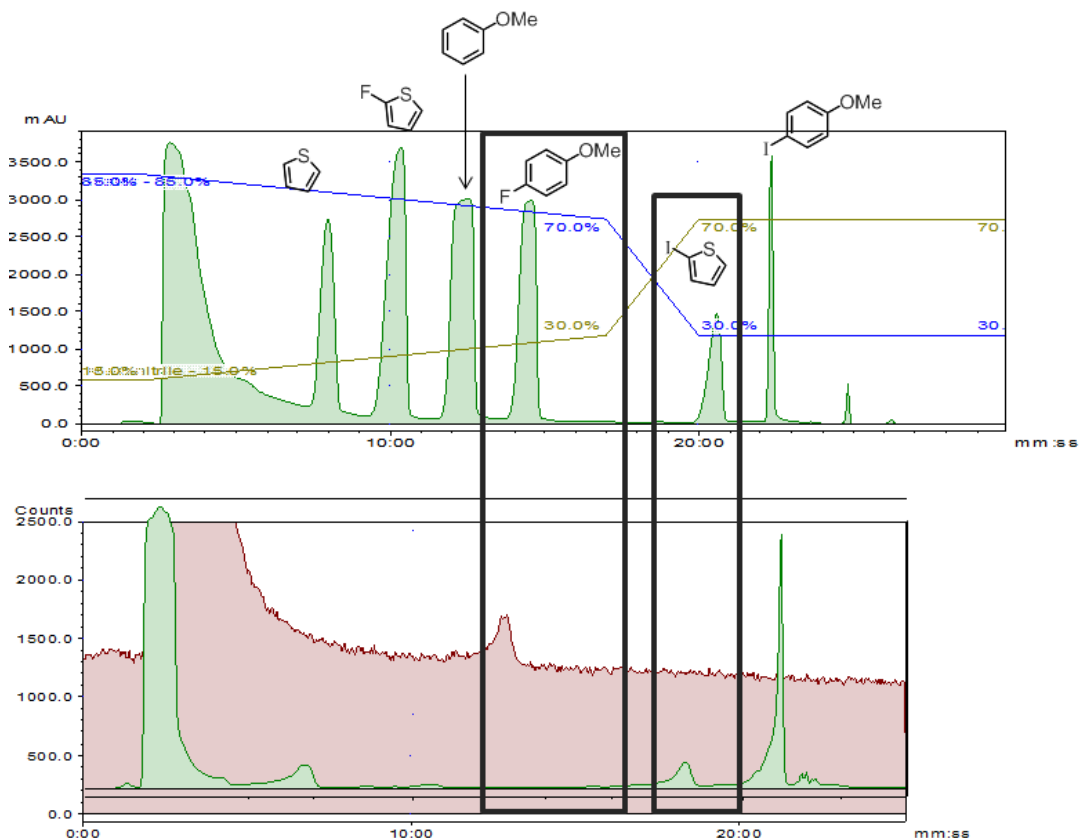
Figure 50: Top HPLC spectrum shows the 'cold' development method to separate the range of potential products of the reaction, bottom spectrum shows the results obtained during the radiolabeling of 58.

The final precursor to be tested bears two 2-thienyl moieties, hence successful incorporation of [^{18}F]fluoride ion will lead to the production of one product pair and therefore the detection of **[^{18}F]39**. Gratifyingly, the radiosynthetic process was successful, resulting in the formation of the desired product pair and thus the detection of **[^{18}F]39** (Figure 51). RCYs of 1% (n = 3, 170-190 °C) were obtained and minute quantities of **[^{18}F]39** were observed at temperatures <170 °C. No attempt was made to optimise the RCY for the process.
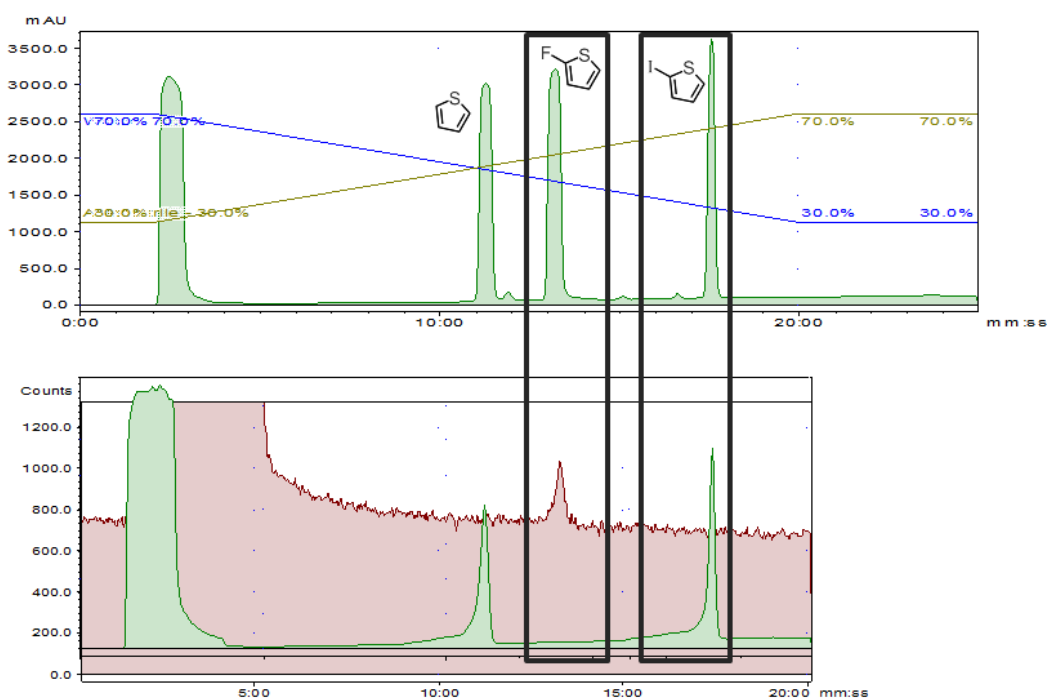
Figure 51: Top HPLC spectrum shows the 'cold' development method to separate the range of potential products of the reaction, bottom spectrum shows the results obtained during the radiolabeling of 59.

The quantification of previously unaccounted for 'hot peaks', i.e. not assigned to **[^{18}F]39**, may now be realised. Consequently, an accurate assessment of purity and RCY may now be reported by using **39** as a standard in HPLC method development for appropriate diaryliodonium salt precursors. These features will become of great importance should diaryliodonium salts bearing the 2-thienyl moiety enter routine pre-clinical/clinical use.

3.3 Radiosynthesis of [^{18}F]Fluorobenzaldehydes: Current Methods

Currently, 4-[^{18}F]FBA is synthesised *via* a S$_N$Ar reaction using [^{18}F]fluoride ion, which had been sequestered using Kryptofix® (K$_{222}$)/K$_2$CO$_3$, from a 4-substituted benzaldehyde. Typically, 4-nitro[204] **71** or 4-trimethylammonium triflate[205] **72** is the leaving group (Scheme 58). Radiochemical yields (RCYs) of 81%[204] and 90%[205] have been obtained for the 4-nitro and 4-trimethylammonium precursor respectively.
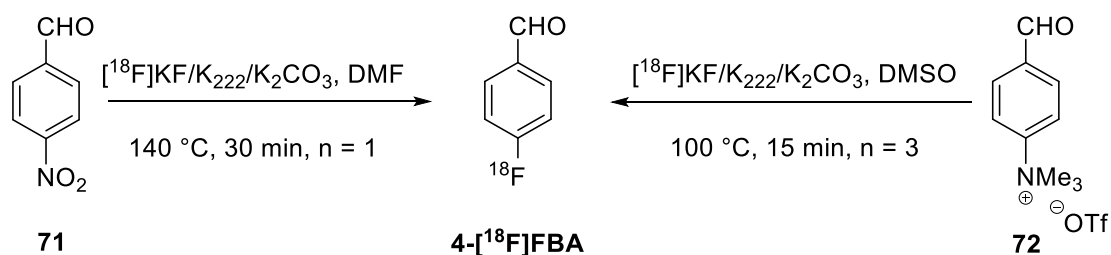
Scheme 58: Synthetic approaches to 4-[^{18}F]FBA.[204, 205]

Although both precursors generate 4-[^{18}F]FBA in high yield, there are limitations associated with the S$_N$Ar approach. Where the leaving group is trimethylammonium a competing fluorination reaction may occur resulting in two additional compounds in the reaction mixture, [^{18}F]methyl fluoride and 4-(*N,N*-dimethylamino)benzaldehyde, **73** (Scheme 59).[206]
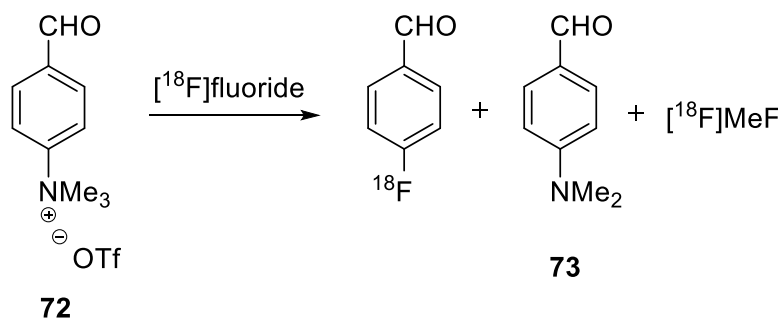
Scheme 59: Possible by-products obtained by reaction of 72 with [^{18}F]fluoride ion.

[^{18}F]Methyl fluoride is a flammable gaseous compound, which is generated by demethylation of the –NMe$_3$$^+$ moiety (*via* a reverse Menschutkin reaction) when -*ipso* substitution does not occur.[206] Gaseous radioactive compounds require

specialist facilities to handle safely; additionally, the quantity of radioactive gas generated will have to be determined and in each instance comply with local radiation regulations.

Åberg *et al.* performed the radiosynthesis of 4-[¹⁸F]FBA according to Scheme 58 as part of their investigation of chemokine receptor CXCR4 expression across a variety of cancers by radiolabelling a derivative of FC131,[207] a potent cyclic pentapeptide CXCR4 inhibitor first reported in 2003.[208] It was reported that the by-product **73** could not be separated from 4-[¹⁸F]FBA during their solid phase extraction (SPE) workup (Figure 52). Attempts to trap the by-product **73** (with an estimated pKa ~3.5, i.e. 2 pH units higher than the pH of the eluent on a strong cationic exchange cartridge (Phenomenex SCX) eluting with phosphate buffer solution adjusted to pH 1.5 in order to protonate the dimethylaniline moiety while keeping the solid phase bound sulfonic acid (estimated pKa <1) in its deprotonated state.[207] However, while the procedure reduced the amount of by-product **73**, 50% of the desired 4-[¹⁸F]FBA was trapped. Further attempts at purification using this approach were abandoned.
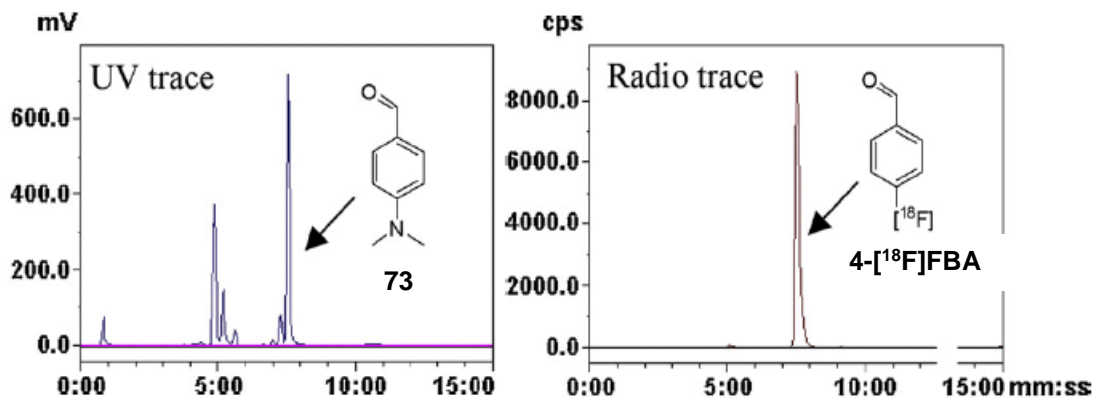
Figure 52: 73 and 4-[¹⁸F]FBA were inseparable after attempted purification.[207]

A critical consequence of the presence of by-product **73** was realised during the intended conjugation of 4-[¹⁸F]FBA to an aminooxy moiety present on the biomolecular substrate, that is, **73** competed in the same conjugation process.[207] The resultant conjugates **74** and **75** were inseparable, both being identified in the final formulation by LC-MS, thus affecting the specific activity of the formulation which varied from 2-60 GBq/µmol (Figure 53).[207]
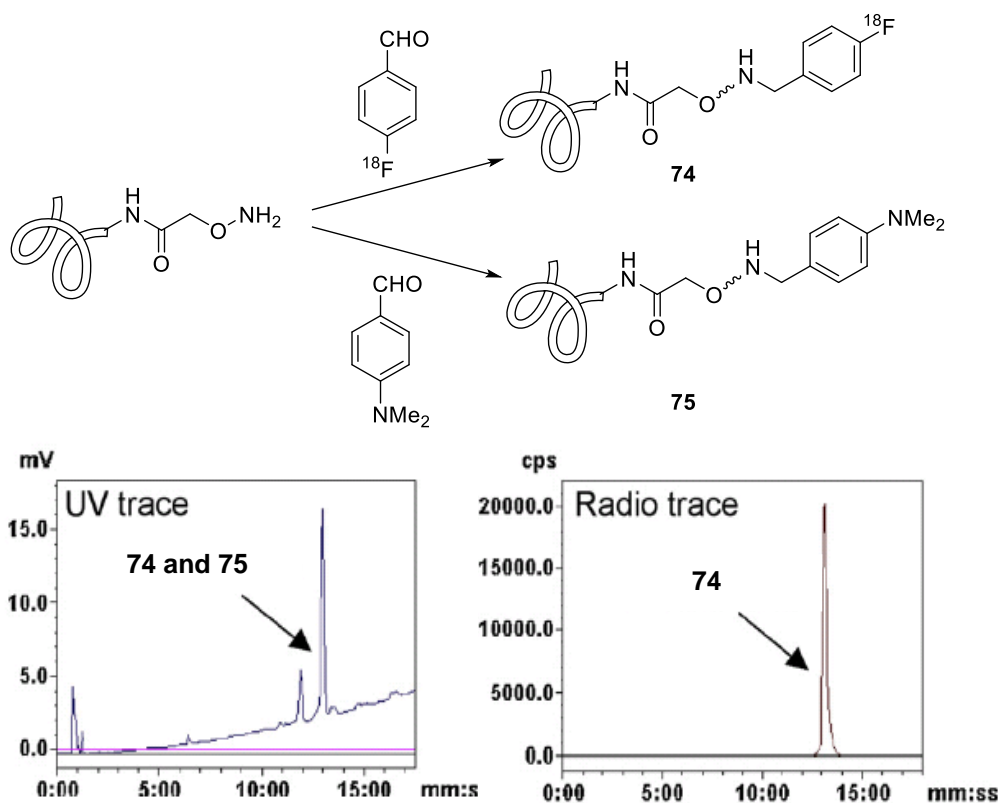
Figure 53: Formation of competing biomolecule 75 (top) reduces the specific activity of the formulated sample, as 74 and 75 could not be separated (bottom).[207]

An alternative route to 4-[¹⁸F]FBA, the use of its corresponding 4-nitro precursor, has been found to be unreliable;[209] therefore in the majority of cases, the 4-trimethylammonium precursor is used.

In addition to aforementioned problems, both nitro precursor **71** and dimethylamino precursors **72** are reliant upon S_NAr chemistry, thus limiting the introduction of [¹⁸F]fluoride ion to the 2- and 4- positions of the arene.[210] In some cases 3-substituted arenes have been shown to be more metabolically stable *in vivo* relative to their 4-substituted counterparts. This is especially important when performing an imaging study with PET, as any generated [¹⁸F]fluoride can accumulate in bone, compromising the quality of the PET image.[5] In addition, where a potential imaging agent is derived from a known fluorinated bioactive compound the fluorine atom may already be present in a position not compatible with traditional S_NAr methodology (e.g. the 3-position) and as such alternative approaches are needed. For example [¹⁸F]lapatanib[211] has been prepared using 3-[¹⁸F]fluorobenzaldehyde[168] as

the prosthetic group. Therefore we envisage that diaryliodonium salt precursors could address these limitations:

- All regioisomers of [^{18}F]FBA can potentially be obtained.
- Any competing reactions generate benign products which can be easily separated from [^{18}F]FBA.
- The same platform/kit maybe used for the synthesis of each regioisomer.

3.4 Synthesis of 4-[^{18}F]Fluorobenzaldehyde Using Diaryliodonium Salt Precursors

Fluorination of 4-formylphenyl(aryl)iodonium salts **43-45** (Figure 54: Diaryliodonium salts 43-45.) was performed using the microfluidic set up as described above.

Ar = phenyl, **43**
Ar = 4-anisyl, **44**
Ar = 2-thienyl, **45**
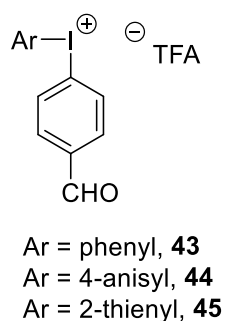
Figure 54: Diaryliodonium salts 43-45.

The plumbing diagram, i.e. the loop sizes, sweep path lengths, reactor sizes, etc., associated with all radiosyntheses performed in this section can be seen below (Figure 55).
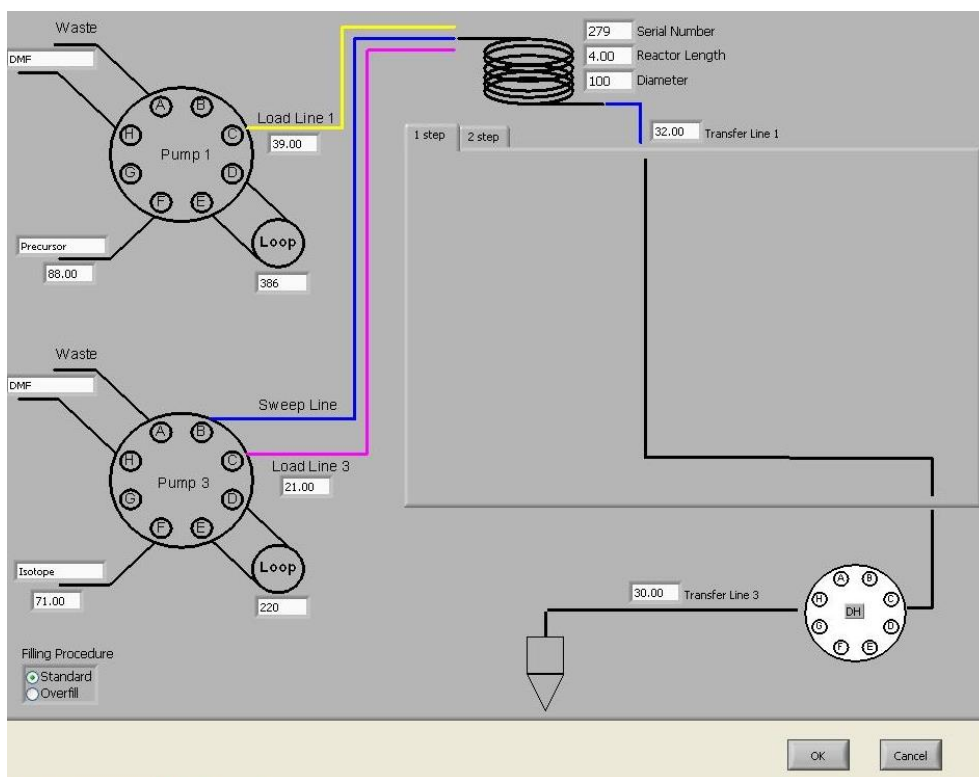
Figure 55: Plumbing diagram for the one-step radiofluorination process.

The following parameters were selected for the study based on optimisation of reaction conditions carried out elsewhere which determined that temperature has the greatest effect on reaction yield:[202]

- Varied temperature: from 50-190 °C (in 20 °C increments)
- Fixed diaryliodonium salt concentration – [10 mg/mL];
- Fixed reactor length - 4m (coiled silica glass, $\varnothing_{INT}$ 1.0 μm, 31.4 μL internal volume);
- Fixed P1:P3 volume ratio – 1:1;
- Fixed isotope complex volume - 10μL;
- Fixed flow rate - 10 μL/min;
- Fixed transfer rate – 60 μL/min.

Reactions were repeated in triplicate (unless stated otherwise) to ensure the robustness of the process at each given temperature, with the error bars representing the highest and lowest yields observed (Figure 56). Note that in this section of the study, no [^{18}F]fluoroarenes were isolated and the radiochemical yield (RCY) reported relates to the amount of radioactivity in the products relative to the total radioactivity detected by radio-HPLC upon analysis of the reaction mixture.
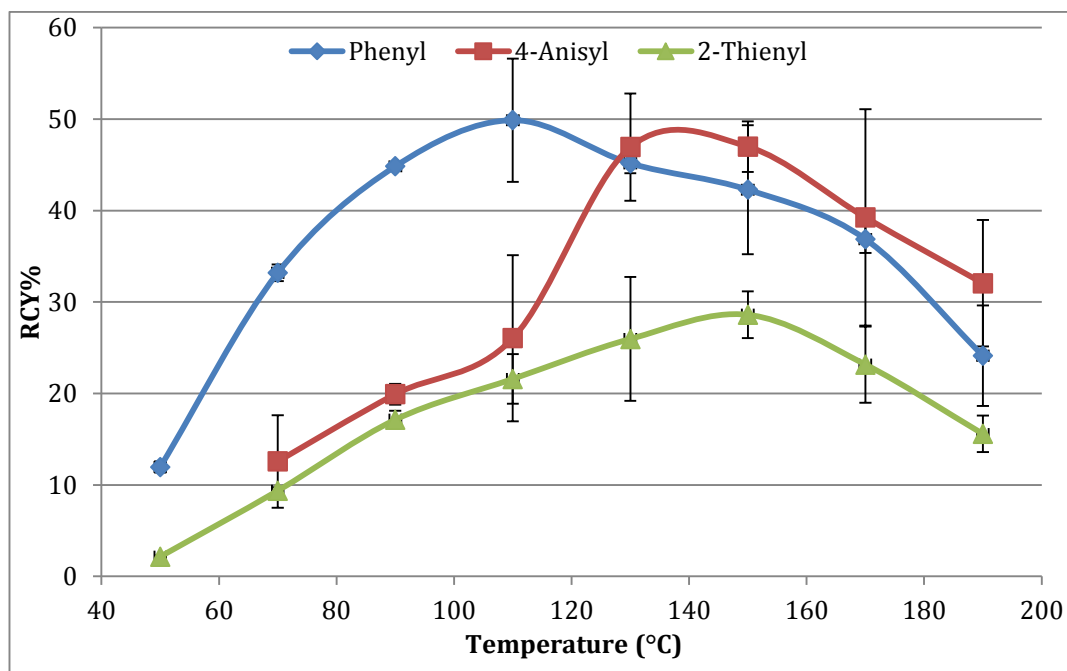
Figure 56: RCY vs Temperature during the radiolabelling (n = 3) of 43 (blue), 44 (red) and 45 (green), generating 4-[^{18}F]FBA. The legend indicates the 'non-participating arene'.

The selection of non-participating arene clearly affects the RCY, with phenyl>4-anisyl>2-thienyl. It is known that electron-rich non-participating arenes direct the incorporation of the radiolabel onto the electron-deficient arene.[90, 92, 94] Work performed herein supports this hypothesis, as the only undesired by-product formed was [^{18}F]fluorobenzene, **[^{18}F]47**, in < 1% RCY (Figure 57).
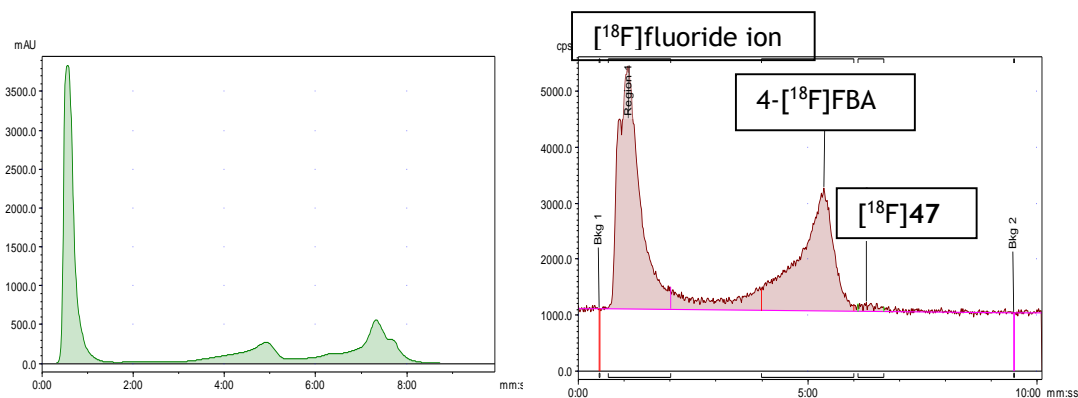
Figure 57: UV trace (left) and radio-HPLC (right) demonstrates the separation of 4-[^{18}F]FBA from [^{18}F]47.

Interestingly, during the [^{19}F]CsF 'cold' fluorination of **43** (section 2.4), no [^{19}F]fluorobenzene was detected. The reaction clearly initiated at 50 °C in both the case of the fluorine-18 and the cold study, however, the hot study is performed within a sealed system, therefore volatile by-products are not lost and can be detected. Although the [^{18}F]fluorination of **43** generates an undesired by-product, **49**, purification is quite straightforward (4-[^{18}F]FBA t_R = 325 s, [^{18}F]fluorobenzene t_R = 385 s).

All of the compounds studied demonstrate a reasonable degree of process reproducibility, the largest range of ±11.8% RCY being attributable to 4-formylphenyl(4-anisyl)iodonium trifluoroacetate **43**. Ranges of ±6% RCY are observed for formylphenyl(phenyl)iodonium trifluoroacetate **44** and ±7% RCY for formylphenyl(2-thienyl)iodonium trifluoroacetate **45**.

Of particular note, RCY is sometimes not considered in great detail during radiochemical syntheses. The reason is that if one commences the process with a high level of radioactivity, e.g. 50 GBq, a decay corrected radiochemical yield of

10% affords 5 GBq of desired radiolabeled product, a more than sufficient quantity for a number of PET imaging studies. Consequently, there is no need to optimise the radiosynthetic process. However, to realise such a level of starting radioactivity, a powerful (i.e. large) cyclotron is required (see section 1.2). The nature of a cyclotron of this type is that a specialist facility is almost certainly required, e.g. a concrete bunker with appropriate shielding.[212] As the demand for radiolabelling studies of promising bioactive compounds is increasing, more low power cyclotrons, which are more affordable and do not require such extensive infrastructure, are now being deployed. Concomitant with a low power unit, the starting levels of radioactivity achievable decrease. For instance, the ABT Biomarker Generator installed in the Sir Bobby Robson Foundation PET Tracer Product Unit at Newcastle University can generate a maximum of 2 GBq [^{18}F]fluoride ion per run (~ 60 min). Accordingly, taking the example above, a decay corrected radiochemical yield of 10% would afford 200 MBq of radiolabeled product when commencing with 2 GBq [^{18}F]fluoride ion, barely enough for one clinical PET scan.

It is interesting to note that the ground state single-crystal structures obtained for **44** and **45** (section 2.3.1) would suggest that the product of the reaction with fluoride ion would be 4-FBA and 2-fluorothiophene, **49**, respectively, as these moieties are located in the pseudo-equatorial position. The work reported above supports that carried out elsewhere, i.e. it is the relative position of the arenes about the iodine atom in the transition state, which dictates the major product of the reaction.[92, 93]

Initial findings are positive, as the RCY associated with the diaryliodonium radiolabeling process certainly affords 4-[^{18}F]FBA in yields useful for subsequent transformations. RCYs may appear moderate relative to current synthetic procedures, though those procedures start with significantly greater activities of fluorine-18.

As discussed in section 1.10, radical scavengers have been reported to improve the reproducibility of some radiosynthetic processes.[100] Aromatic radicals may be generated *in situ* from a parent hypervalent iodine compound, as a consequence of homolytic fission of an aryl iodine bond. To mitigate the risk of such radicals undergoing further, undesired reactions – potentially decreasing the realised RCY, a

radical trap (10 mol% TEMPO), was added to the diaryliodonium salt solution prior to being loaded into P1.

The results encouragingly demonstrate the principle that use of a radical trap when radiolabeling sensitive diaryliodonium salts with [^{18}F]fluoride ion improves the associated reproducibility (Figure 58).
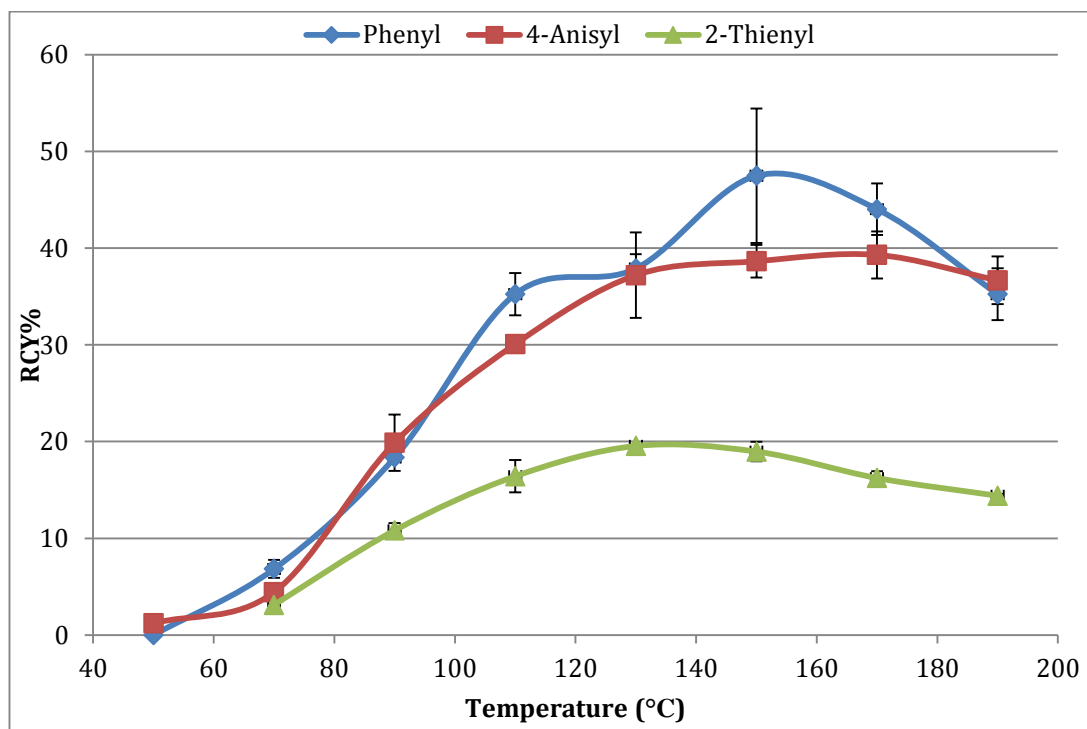
Figure 58: RCY vs Temperature during the synthesis of 4-[^{18}F]FBA with the addition of 10 mol% TEMPO to the starting solutions of 43-45 improves reproducibility. N.B. n =2 for 44 at 70, 130 and 170 °C. The legend indicates the 'non-participating arene'.

The hypervalent character of the iodine atom in a diaryliodonium salt, apparent due to the 3c-4e bond, is in the most stable relative to the equivalent λ^3-bromanes and λ^3-chloranes, as the most electropositive atom increases the stability of the hypervalent bond to better effect.[213, 214] By increasing electron density around the iodine atom, e.g. **44** and **45**, the stability afforded by the electropositive nature of the centre is decreased. Accordingly, the propensity for homolytic fission of the aryl-iodine bond increases.

Indicative of the aforementioned theory, it is clear that in practice there is an increase in reproducibility during the radiolabeling of the more electron-rich diaryliodonium salts, **44** and **45**, upon inclusion of a radical trap relative to the exclusion of a radical

112

trap (Figure 56). The greatest range in RCY associated with the diaryliodonium salts bearing 4-anisyl and 2-thienyl non-participating arenes, **44** and **45**, is reduced to ±4.5% and ±1.0% RCY, relative to the exclusion of TEMPO respectively. The range associated for **43**, i.e. where phenyl is the 'non-participating arene', is the highest, ±7.0%, which is slightly higher relative to the exclusion of a radical trap. Nonetheless, an overall improvement in the reproducibility profile across the range of screened temperatures is apparent.

Although the reproducibility of the process is markedly improved upon inclusion of TEMPO, there is a slight determent to the RCY observed across the temperature profile. Accordingly, a method was sought which aimed to increase the RCY of the radiolabeling process.

It has been reported elsewhere, that the addition of water, during nucleophilic fluorinations, can influence the associated RCY. Early studies in the 1980s determined that in a solid-liquid biphasic system, the presence of a limited amount of water was found to increase the rate of fluorination.[215, 216] The reported affect has been described as a consequence of the solid-liquid system favouring extraction of fluoride ion into the organic phase in response to the addition of water, thus increasing the rate of fluorination accordingly.[217] However, in a liquid-liquid system, the rate of fluorination has been shown to decrease the rate of fluorination due to the hydration of fluoride ion.[218]

The first known of example of the addition of water to a radiofluorination process was reported in a patent document by Wandsworth *et al.*[95] The document describes how the addition of certain ratios of water, preferably 10-30% in a mixture with a water miscible solvent, improves the yield of the radiofluorination of a diaryliodonium salt. In fact, the inventors report that radiolabeled material was obtained, even where the solvent system was 100% water – a feat yet, to the best of the authors' knowledge, to be reproduced elsewhere.

There are further reports of water being added to the radiofluorination process. Chun *et al.* reported in 2010 the addition of 0.25% water during the fluorination of several diaryliodonium salts.[219] However, a limited comparison of one diaryliodonium salt

fluorination in the presence (1.5%) and absence of water was provided, where 2-methylphenyl(phenyl)iodonium tosylate was used as a precursor to 2-[^{18}F]fluorotoluene, obtained in RCYs of 34% and 9% respectively, and [^{18}F]fluorobenzene, in RCYs of 16% and 3% respectively. A further study within their report using several diaryliodonium chlorides in the presence of 0.25% water was provided, with no discussion of the results where water was absent from the reaction process.

In 2012, we reported some of our initial findings of the work which follows in this section, regarding the inclusion of known quantities of water during the radiolabeling with fluorine-18 of a range of diaryliodonium salts.[220, 221]

A further study reported by Chun *et al.* in 2013 regarded the fluorination of a range of diaryliodonium tosylates in where [^{18}F]fluoride ion was derived directly from the cyclotron and therefore in a solution of target [^{18}O] water (maximum of 28%).[222] The reported methodology is advantageous as firstly time is saved as no drying of the [^{18}F]fluoride ion is required to achieve moderate yields of radiolabeled product,[222] secondly as no removal of a phase transfer agent is required – a necessary procedure during the formulation of a radiolabeled material for a PET imaging study with human subjects.[223] As in the previous 2010 study, there was limited discussion of the effect of the addition of water upon the RCY, as no studies were carried out on the same compounds in the absence of water.

Of the diaryliodonium salts examined herein, 4-formylphenyl(phenyl)iodonium trifluoroacetate **43** has afforded 4-[^{18}F]FBA in the highest RCY. Accordingly, **43** was subjected to a range of conditions whereby the percentage of water present in the starting solution, stored at P1 of the microfluidic apparatus, was examined (Figure 59).

Figure 59: RCY vs Temperature during the synthesis of 4-[¹⁸F]FBA with addition of known quantities of water to a starting solution of 43 (n =2 for 20% water).

An excellent trend was observed, whereby the addition of any of the known quantities of water to the starting solution outperformed the RCY obtained relative to the water-free counterpart; the order of RCY improvement 5% > 10% > 20%. A maximum RCY of 83% (n = 3, 110 °C) has been achieved, a remarkable increase of 33% relative to water-free conditions. The errors associated with the process remain unchanged relative to the water-free process, showing an outstanding tolerance in observed RCY across all temperature ranges. However, there is a slight increase in off-target fluorination, i.e. the generation of [¹⁸F]fluorobenzene, in RCYs of 3%, 2% and 2% across 20%, 10% and 5% additions of water respectively.

Whilst it is gratifying, and even in light of some known precedence, it is certainly surprising to observe such behaviour upon the addition of water. A practical study has demonstrated that the intrinsic reactivity of fluoride ion in a quaternary ammonium complex shows a dependence upon the degree of solvation of the fluoride ion, such that an increase in hydration results in a decrease in nucleophilicity.[218] Experimental evidence reports a decrease of almost three orders of

Figure 59: RCY vs Temperature during the synthesis of 4-[^{18}F]FBA with addition of known quantities of water to a starting solution of 43 (n =2 for 20% water).

An excellent trend was observed, whereby the addition of any of the known quantities of water to the starting solution outperformed the RCY obtained relative to the water-free counterpart; the order of RCY improvement 5% > 10% > 20%. A maximum RCY of 83% (n = 3, 110 °C) has been achieved, a remarkable increase of 33% relative to water-free conditions. The errors associated with the process remain unchanged relative to the water-free process, showing an outstanding tolerance in observed RCY across all temperature ranges. However, there is a slight increase in off-target fluorination, i.e. the generation of [^{18}F]fluorobenzene, in RCYs of 3%, 2% and 2% across 20%, 10% and 5% additions of water respectively.

Whilst it is gratifying, and even in light of some known precedence, it is certainly surprising to observe such behaviour upon the addition of water. A practical study has demonstrated that the intrinsic reactivity of fluoride ion in a quaternary ammonium complex shows a dependence upon the degree of solvation of the fluoride ion, such that an increase in hydration results in a decrease in nucleophilicity.[218] Experimental evidence reports a decrease of almost three orders of

magnitude as the number of water molecules involved in hydration is increased from 0 to 6.[218] Several theoretical studies indicate that a single fluoride ion in an aqueous medium may be hydrated by up to 16 water molecules, and that the hydration energy is exceptionally high at 367 kcal mol^{-1}.[224-226] Theoretically, the nucleophilicity of fluoride ion has an inverse relationship with the number of water molecules associated with its hydration.[227]

Separate studies have been concerned with the fact that so-called 'naked' fluoride ion, i.e. fluoride determined to possess and extremely low degree of hydration, and therefore a high nucleophilicity, can go on to perform undesired sided reactions.[228-230] Control of the degree of hydration of fluoride ion mitigated the effect of unwanted side reactions.[217] It may be considered that the effect of the degree of hydration is being observed in the work reported herein, i.e., a balance of the hydration of [^{18}F]fluoride ion is necessary to realise the optimum RCY.

As the addition of 5% water to the starting diaryliodonium salt solution appears to be the most beneficial to the RCY obtained, the same amount of water was added to **44** and **45** to determine if a similar advantage could be realised (Figure 60).
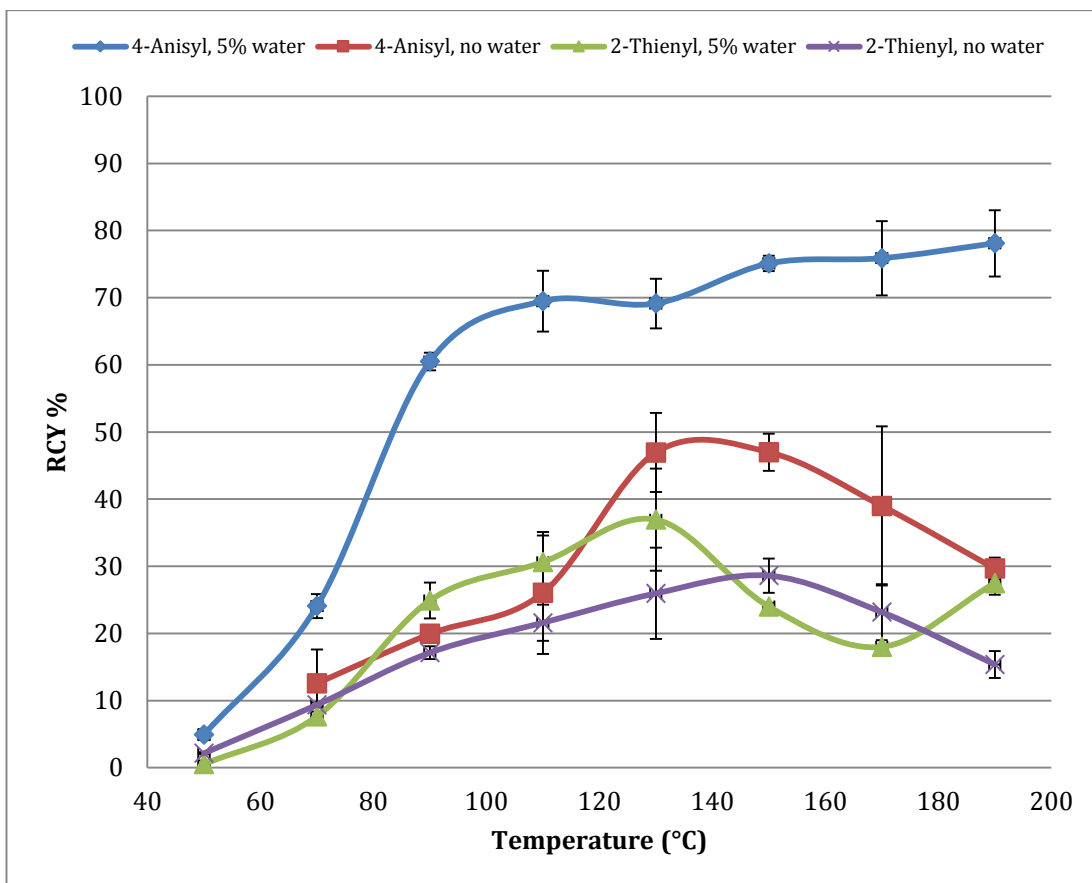
Figure 60: RCY vs Temperature during the synthesis of 4-[^{18}F]FBA is impacted by the addition of 5% water to starting solutions of 44 and 45.

A significant 31% increase in RCY relative to water-free conditions was observed for **44**, with a maximum RCY of 78% (n = 3, 190 °C). The RCYs obtained under these conditions appear to plateau in the 150-190 °C range and that the errors are reduced relative to water-free conditions. It would be interesting to ascertain the effects of temperatures beyond 190 °C, however, the microfluidic apparatus limited such as study as the thermoresistant polymer holding the silica glass coil in place within the reactor can degrade at temperature exceeding 190 °C.

Although the reproducibility profile of **45** was reduced, a significant increase in RCY relative to water-free conditions was not apparent, with an increase in RCY of 8% (n = 3, 130 °C). As with the water-free and radical scavenger conditions reported above, no off-target fluorination products were detected during the process.

The optimum quantity of water along with 10 mol% TEMPO was added to a starting solution of **43**, the best performing diaryliodonium salt studied thus far with respect

to the RCY of 4-[^{18}F]FBA obtained, to determine if a synergistic effect, i.e. a significant increase in RCY whilst maintaining a tight reproducibility profile, could be realised (Figure 61).
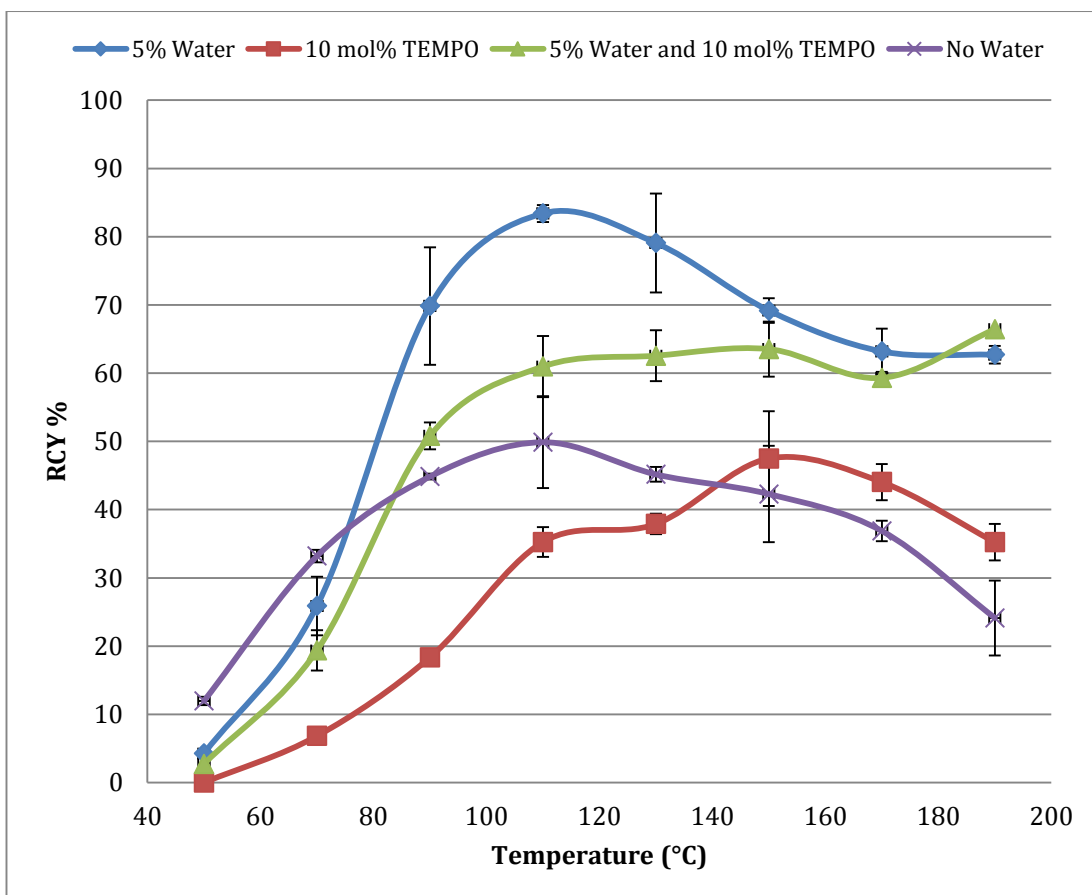
Figure 61: RCY vs Temperature during in the presence of simultaneous addition of 5% water and 10 mol% TEMPO to a solution of 43 generates 4-[^{18}F]FBA.

It is apparent that although the results are positive relative to water-free and 10 mol% TEMPO conditions, the addition of 10 mol% TEMPO to the system is detrimental to the RCY observed when 5% water is the sole additive in the process. The combined additives do appear to stabilise the reaction such that the RCY profile remains somewhat consistent between 110-190 °C.

3.5　Synthesis of 3-[18F]Fluorobenzaldehyde Using Diaryliodonium Salt Precursors

As determined above, the optimum conditions with respect to RCY for diaryliodonium salts **43-45** is the addition of 5% water to the starting solution and a reaction temperature of between 90-190 °C. Accordingly, the same conditions were applied to the 3-[18F]FBA precursors **50-52** (Figure 62).
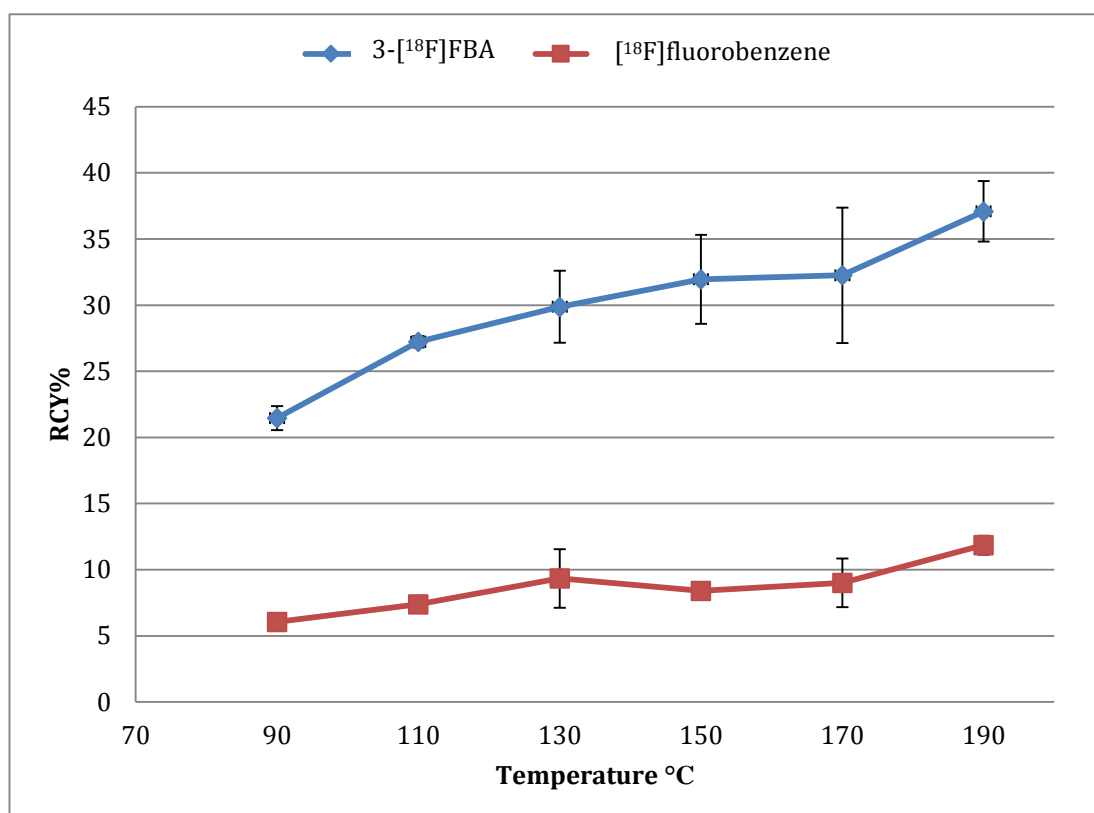
Figure 62: Synthesis of 3-[18F]FBA from 50 in the presence of 5% water.

The RCY of the 3-[18F]FBA precursor **50** appears to follow a different reaction profile to it 4-[18F]FBA counterpart **43**, as higher temperatures appear to favour an increase in RCY. It would be interesting to examine temperature beyond 190 °C to determine where the plateau with respect to RCY lies, however, as discussed above, the microfluidic apparatus places a restriction on reaching such temperatures. An impact upon the RCY of 3-[18F]FBA relative to 4-[18F]FBA could be attributed to the *ipso* position of **43** is markedly more δ- than counterpart **50** due to 3-substitution of the aldehyde moiety. Hence, when the turnstile mechanism (section 1.10) approaches

the elimination step, [18F]fluoride ion is less likely to favour *ipso* incorporation onto the target arene, thus impacting the RCY obtained.

A significantly increased quantity of [18F]fluorobenzene, **[18F]47**, was obtained across the reaction series, where an increased RCY of 3-[18F]FBA is concomitant with an increased RCY of [18F]fluorobenzene. In addition to the reason highlighted above, the 3-position of the aldehyde moiety on the target arene results in a lack of delocalisation of electron density out of the arene (the opposite of its 4-substituted counterpart **43**). Accordingly, the selectivity associated with electronic directing effect of unsymmetrical diaryliodonium salts is less pronounced, resulting in an increase in off-target fluorination. [18F]Fluorobenzene has been obtained in yields of up to 12%, compared with RCY of <1% for the 4-substituted counterpart. As in the example above, it is procedurally straight forward to separate 3-[18F]FBA from the non-target product in addition to adducts arising from decomposition/side reactions, as can be seen, a mixture of 3-iodobenzaldehyde, iodobenzene and decomposition products are readily separated from the desired compound (Figure 63).
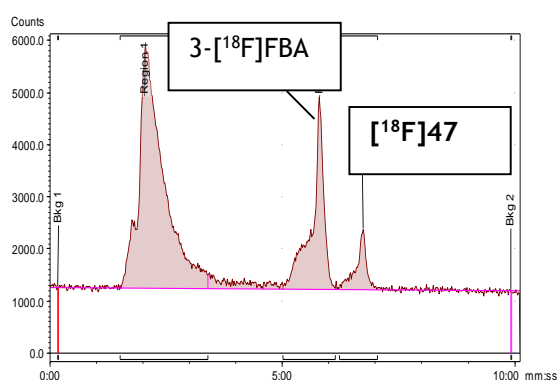
Figure 63: Generation of off-target [18F]47.

In the case of **51**, the diarylidodonium salt bearing the 4-anisyl non-participating arene, useful RCYs of 3-[18F]FBA have been obtained (Figure 64). Higher reaction temperatures result in an increase in RCY, and RCYs of up to 48% have been achieved where the reactor is set to 190 °C. The range of RCYs observed across the temperature profile remain pleasingly consistent, apart from the reactions performed at 150 °C, although the range of RCY is only ± 12%. Importantly, and as may be expected, no 3-[18F]fluoroanisole was detected at any of the temperatures examined throughout the study.

120
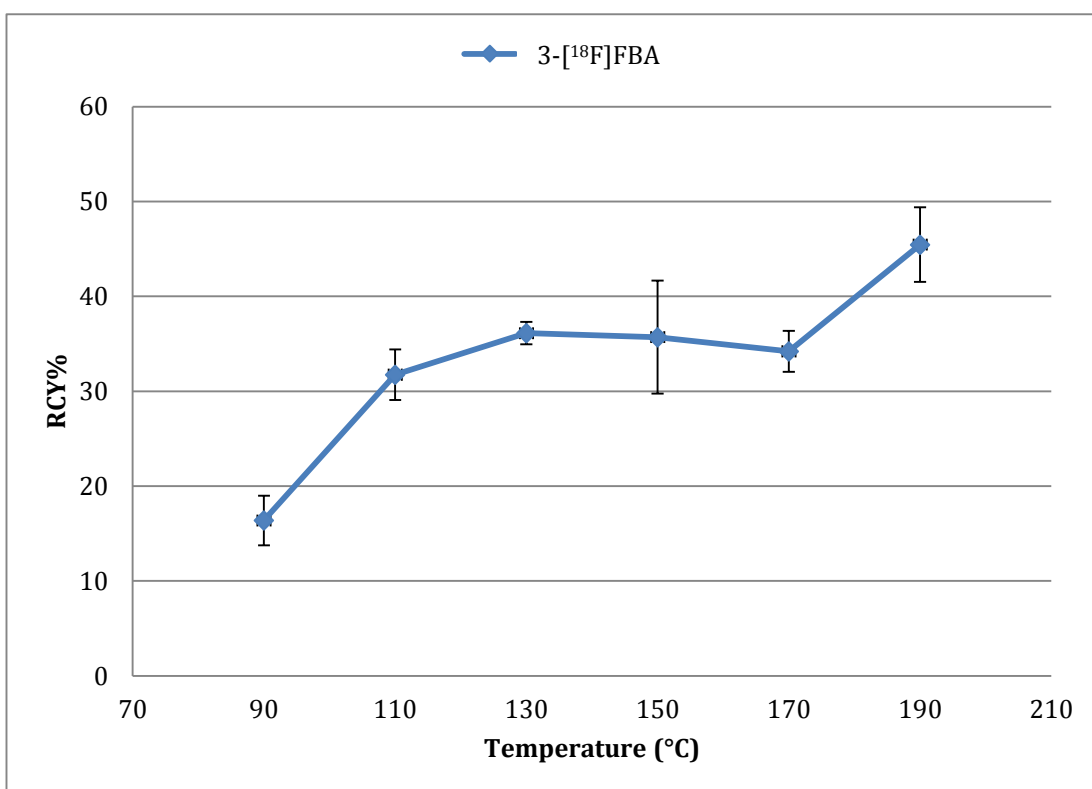
Figure 64: An increase in the temperature during the radiolabeling of 51 generates 3-[18F]FBA in greater RCYs.

In the case of **52**, the diarylidodonium salt bearing the 2-thienyl non-participating arene, the results of the radiolabeling study were somewhat disappointing (Figure 65). The range of RCY associated with the radiolabeling procedure is markedly increased across the temperature profile relative to the regioisomer 4-formylphenyl(2-thienyl)iodonium trifluoroacetate, **45**, although the range of ±7% RCY is in keeping with expectations based upon the study above. An important advantage associated with **52** is that no off-target fluorination, i.e. 2-[18F]fluorothiophene, **[18F]39**, was observed, a point which may now be accurately ascertained by comparison to the authentic sample of 2-[19F]fluorothiophene, **39**, prepared as described above (section 2.6).
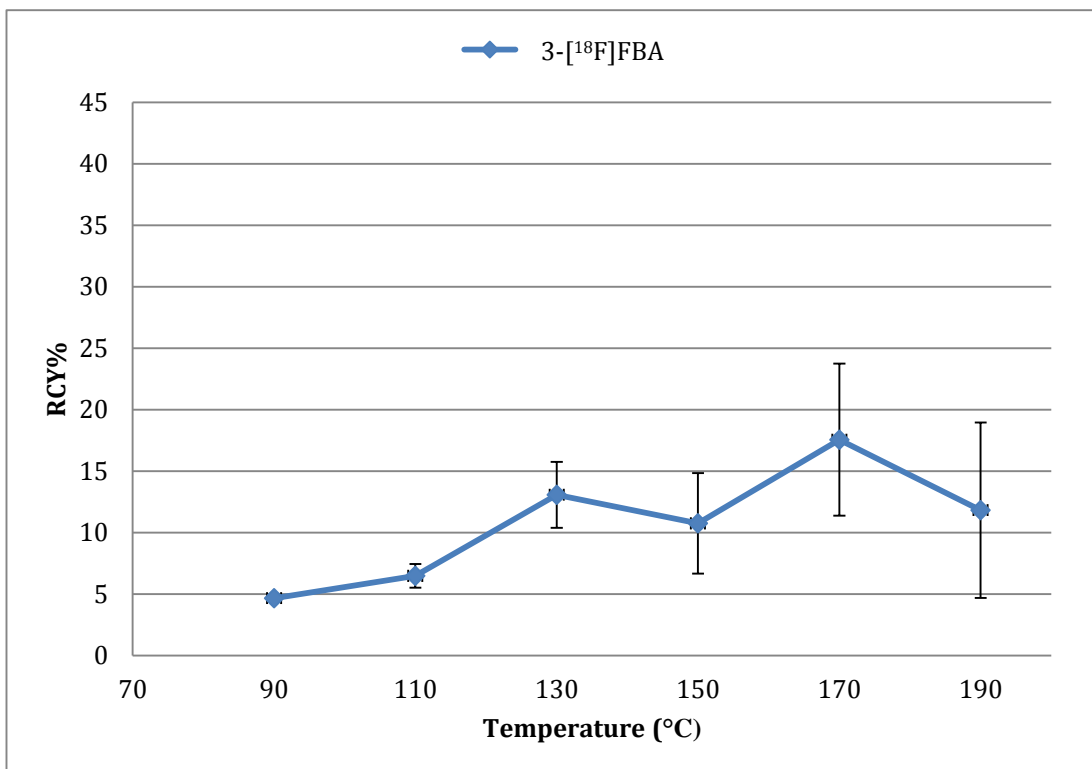
Figure 65: Radiolabeling of 52 affords a varied range of RCY for 3-[^{18}F]FBA.

In summary, the greatest average RCY of 17% (n = 3, 170 °C) is achieved with **51**, but is less than that obtained for its regioisomer **44** without the addition of water, 29% (n = 3, 150 °C) or with the addition of water, 37% (n = 3, 130 °C). Taking into account the RCY obtained by use of **52** as a precursor to 3-[^{18}F]FBA, it is difficult to consider using **52** as a precursor relative to **50** and **51**.

3.6   Batch Synthesis of 4-[^{18}F]FBA Using Microfluidic Apparatus

The optimisation of the radiolabeling procedure has determined that the addition of 5% water to the starting diaryliodonium salts solution is greatly beneficial to the resulting RCY, a production of 4-[^{18}F]FBA, on a scale suitable for routine production, was attempted using the optimal conditions.

The diaryliodonium salt used in the study was chosen as 4-formylphenyl(4-anisyl)iodonium trifluoroacetate, **44**. Even though in the optimisation study above the phenyl bearing counterpart **43** slightly outperformed with respect to RCY, however **44** did not facilitate the production of a non-target radiolabeled product.

Accordingly, whilst maintaining the aforementioned reaction conditions a slight modification was made to the microfluidic apparatus, as both loops are dispensed entirely through the microreactor during the large scale process; the resultant bolus being collected at a large (1000 µL) loop connected to the auto-injector. Radio-HPLC was scaled up to semi-preparative scale to accommodate the increased volume of material to be analysed. Over the course of two runs, 4-[^{18}F]FBA was obtained in an RCY of 96% determined by radio-HPLC, from starting activities 1.3-1.5 GBq fluorine-18 (Figure 66), clearly indicating the extend increased starting activities has upon the RCY.
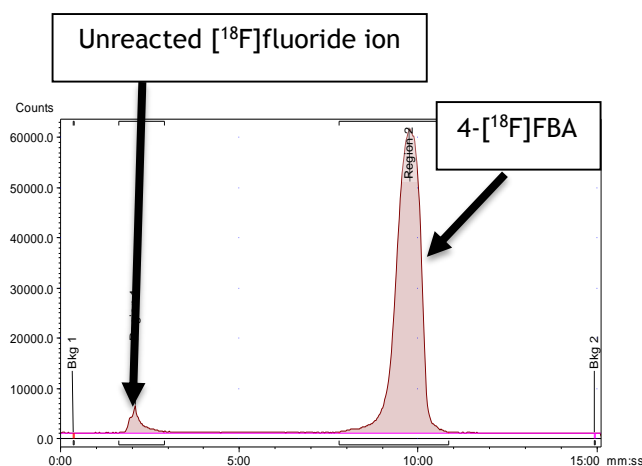
Figure 66: A radio-HPLC obtained during batch production of 4-[^{18}F]FBA from 43 in 96% RCY (n = 2, 190 °C).

3.7 Chapter Three: Overall Conclusions

A summary of the conclusions arising from chapter three are given below:

- It is possible to detect 2-[^{18}F]fluorothiophene generated in a sealed system upon reaction of a diaryliodonium salt bearing the 2-thienyl moiety with [^{18}F]fluoride ion, by reference to an authentic standard of 2-[^{19}F]fluorothiophene.

- In general, increasing temperatures increase the RCY associated with the production of 4-[^{18}F]FBA and 3-[^{18}F]FBA from a range of diaryliodonium salt precursors.

- Inclusion of 5% water into a starting solution of a diaryliodonium salt has a positive effect upon the RCY achieved, whereas the additive TEMPO has a positive effect upon the reproducibility of the process.

- 4-[^{18}F]FBA can be synthesised in batch in excellent RCY using microfluidic apparatus.

4 Final Conclusions and Future Work

There have been several key conclusions from the work reported herein, namely:

- Successful preparation of substituted diacetoxyiodoarenes and substituted aryl stannanes.
- Preparation of a range of diaryliodonium salts bearing aldehyde and maleimide functionality, as well as simple electron-rich species such as the dithienyliodonium trifluoroacetate. X-ray crystal structures have been determined for many diaryliodonium salts following a robust investigation into the conditions requisite for single crystal growth.
- A cold fluorine-19 study of selected diaryliodonium salts has been performed as a prologue to a fluorine-18 study to ascertain in advance a selectivity profile.
- 2-[^{18}F/^{19}F]Fluorothiophene have been prepared and unambiguously characterised for the first time.
- The effect of water upon the radiolabeling process has been investigated using the 4-[^{18}F]FBA precursors diaryliodonium salts **43-45**, resulting in an observation that the presence of water is both well tolerated and beneficial to the RCYs which are obtained.
- The effect of TEMPO has been investigated, which confirms that the range of RCYs observed decreases upon its inclusion although no benefit to the overall RCY obtained.
- Simultaneous use of water and TEMPO as additives to the radiolabeling process is not as beneficial as the sole addition of water.
- 4-[^{18}F]FBA and 3-[^{18}F]FBA have been obtained in RCYs which are suitable for routine clinical production.

Future work should be directed to consider the conjugation of the prosthetic groups synthesised herein to a range of biomacromolecules, such as peptides/antibodies, using the optimised prosthetic group production conditions reported here.

Batch production of 3-[^{18}F]FBA should be examined to determine if, as is the case for its regioisomer, the starting activity can profoundly affect the RCY.

Radiolabeling of the maleimide containing diaryliodonium salt **69** should be examined, and the optimised conditions reported herein applied to determine the tolerance of a separate species of diaryliodonium salt to the presence of water.

5   Notes Added in Proof

Articles related to work reported herein have recently been published by others since cessation of this project in 2013.

Recent synthesis of 3-[^{18}F]FBA, has been achieved by the manual, i.e. by hand rather than using automated apparatus, radiolabeling of mesityl(3-formylphenyl)iodonium tetrafluoroborate by Scott and co-workers, via a copper catalysed process (Scheme 60).[231]
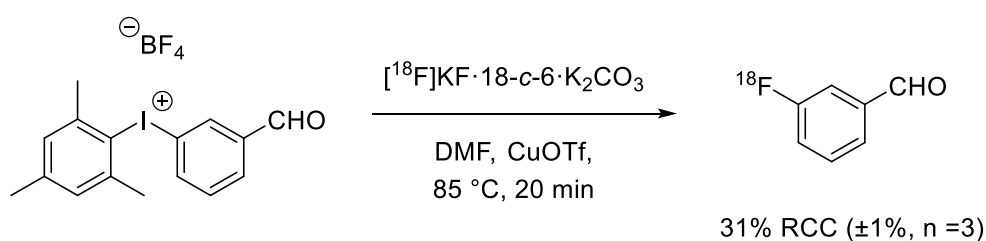
Scheme 60: Synthesis of 3-[^{18}F]FBA via a catalytic procedure.[231]

Recent synthesis of 3-[^{18}F]FBA and 4-[^{18}F]FBA have been reported by Gouverneur and co-workers, by a copper catalysed manual radiofluorination of arylboronic acids (Scheme 61).[232]
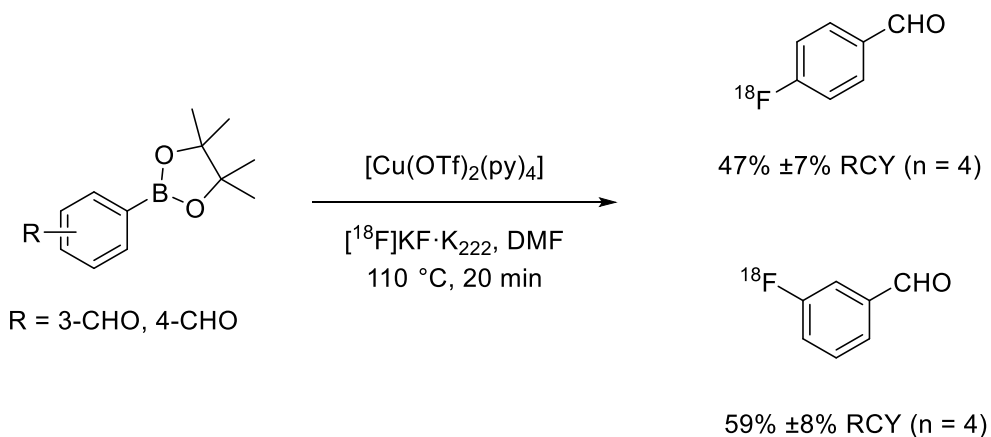
Scheme 61: Synthesis of 4-[^{18}F]FBA and 3-[^{18}F]FBA via a catalytic procedure.[232]

127

6   Experimental

All manipulations involving air-sensitive materials were carried out using standard Schlenk line techniques under a nitrogen atmosphere, using oven dried glassware.[233] Anhydrous DCM and MeCN were prepared by refluxing over CaH_2. ^1H and ^{13}C NMR spectra were recorded on a Bruker 300 MHz, JEOL 400 MHz, or a JEOL 500 MHz spectrometer at room temperature. ^1H and ^{13}C shifts were relative to tetramethylsilane. ^{19}F spectra were recorded on either a JEOL 400 MHz, or a JEOL 500 MHz spectrometer at room temperature. ^{19}F shifts were relative to $CFCl_3$. Thin-layer chromatography was carried out on aluminum sheets pre-coated with silica gel 60F 254, and performed using Merck Kieselgel 60. Melting points were determined with a Gallenkamp MF-370 and are uncorrected. Automated flash chromatography was performed using a Varian IntelliFlash 971-FP discovery scale flash purification system. Mass spectrometry data was obtained from the EPSRC National Mass Spectrometry Service Centre, Swansea. Microanalysis data was obtained from the London Metropolitan University Elemental Analysis Serivce and Medac Ltd.

Practical considerations: Hypervalent iodine compounds are potentially explosive and should be handled taking appropriate precautions.[234, 235]

6.1   4-Anisyliodobisacetate (33)[100, 236]
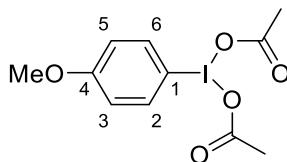
4-Iodoanisole (12.15 g, 50 mmol) was added to glacial acetic acid (500 mL), and the solution stirred at 45 °C. Sodium perborate tetrahydrate (76.93 g, 500 mmol) was carefully added to the reaction mixture over 30 minutes, followed by 4.5 hours stirring. The crude mixture was left to cool to room temperature. Water (500 mL) was added, followed by extraction with DCM (3 × 150 mL). The combined organic layers were washed with water (3 × 500 mL). The washed organic layer was then concentrated *in vacuo* to afford a pale yellow oil. **33** was obtained as colourless crystals by crystallisation from DCM/Petrol (8.23 g, 45%). Mp 89-93 °C (from DCM/Petrol) (lit:[236] mp 92.4-96 °C); IR ν_{MAX}/cm^{-1} (neat) 1648, 1576,1487, 1354, 1290, 1250, 1189; ^{1}H NMR (400 MHz, CDCl$_3$) δ 7.96 (2H, d, H2/H6 J = 9.1 Hz), 6.92 (2H, d, H3/H5 J = 9.1 Hz), 3.81 (3H, s, OCH_3), 1.94 (6H, s, Me); ^{13}C NMR (101 MHz, CDCl$_3$) δ 176.49 (CO), 137.22 (C4), 135.50, 116.74, 116.47 (C1), 55.65 (OMe), 20.49 (OAc); HRMS (NSI positive) found: M+Na$^+$, 374.9696. C$_{11}$H$_{13}$IO$_5$Na$^+$ requires 374.9705; Anal. Calcd. for C$_{11}$H$_{13}$IO$_5$: C, 37.52; H, 3.72. Found: C, 37.35; H, 3.73.

6.2   2-Thienyliodobisacetate (34)[237]
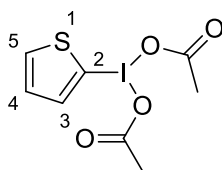
2-iodothiophene (12.15 g, 50 mmol) was added to glacial acetic acid (500 mL), and the solution stirred at 45 °C. Sodium perborate tetrahydrate (76.93 g, 500 mmol) was carefully added to the reaction mixture over 30 minutes, followed by 4 hours stirring. The crude mixture was left to cool to room temperature, and the product was extracted with DCM (3 × 500 mL). The combined organic layers were washed with water (3 × 500 mL). The washed organic layer was then concentrated *in vacuo* to afford a pale oil. **34** was crystallised as off-white crystals from DCM/Petrol obtained by filtration (4.74 g, 29%). Mp 123-127 °C (decomp. from DCM/petrol/ether) (lit:[237] 119-125 °C); IR v_{MAX}/cm^{-1} (neat) 1646, 1389, 1349, 1262, 1219, 1037, 1014; ^{1}H NMR (400 MHz, CDCl$_3$) δ 7.76 (1H, dd, J = 3.9, 1.2 Hz), 7.62 (1H, dd, J = 5.4, 1.2 Hz), 7.11 (1H, dd, J = 5.4, 3.9 Hz), 1.99 (6H, s); ^{13}C NMR (101 MHz, CDCl$_3$) δ 177.10 (CO), 139.17, 134.96, 128.72, 106.31 (C2), 20.45 (OAc); HRMS (NSI positive) found: M+Na$^+$, 350.9159. C$_8$H$_9$IO$_4$SNa$^+$ requires 350.9158; Anal. Calcd. for C$_8$H$_9$IO$_4$S: C, 29.28; H, 2.76. Found: C, 29.32; H, 2.69.

6.3   4-Tributylstannylbenzaldehyde (37)[157]
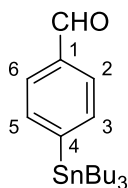
A flask was charged with zinc dust (6.14 g, 93.8 mmol), MeCN (70 mL) was added. Trifluoroacetic acid (0.13 g, 1.15 mmol) was carefully added, and the solution stirred for 5 minutes. Cobalt dibromide (1.38 g, 6.25 mmol) was added, the resultant blue solution was stirred for a further 5 minutes. Addition of allyl chloride (1.44 g, 18.8 mmol) turned the solution red upon 10 minutes stirring. 4-Bromobenzaldeyhde (9.25 g, 50.0 mmol) was added, followed immediately by tri-*n*-butylstannyl chloride (22.3 g, 68.5 mmol). The reaction was heated to 50 °C and monitored by TLC (95:5 petrol:ether) until all of the starting material had been consumed. Once cooled to RT, aqueous saturated ammonium chloride (50 mL) was added and the mixture extracted with ether (3 × 50 mL). The organic fractions were combined and dried over $MgSO_4$, filtered and concentrated *in vacuo*. The crude orange oil was purified by column chromatography on SiO_2 (petrol, then 90:10 petrol:ether) or using automated flash reverse phase chromatography (neat MeCN) obtaining **37** as a clear oil (10.86 g, 55%). R_f 0.46 (95:5 petrol:ether); IR ν_{MAX}/cm^{-1} (neat) 2957, 2925, 1704, 1587, 1379, 1174; ^{1}H NMR (300 MHz, CDCl$_3$) δ 9.86 (1H, s, CHO), 7.67 (2H, d, H2/H6 J = 8 Hz), 7.53 (2H, d, H3/H5 J = 8 Hz), 1.49 − 1.34 (6H, m), 1.20 (6H, m), 1.03 − 0.93 (m, 6H), 0.76 (9H, t, CH$_2$C*H*$_3$ J = 7 Hz); ^{13}C NMR (75 MHz, CDCl$_3$) δ 190.89 (CHO), 150.86 (C1), 135.37, 134.60, 126.84 (C4), 27.45 (Sn*C*H$_2$), 25.67 (SnCH$_2$*C*H$_2$), 11.93 (CH$_2$CH$_2$*C*H$_2$), 8.27 (CH$_2$*C*H$_3$); HRMS (ESI positive) found: M+H$^+$, 395.1549. $C_{19}H_{33}O^{117}Sn^+$ requires 395.1551; Anal. Calcd. for $C_{19}H_{32}SnO$: C, 57.75; H, 8.16. Found: C, 57.93; H, 8.07.

6.4 3-Tributylstannylbenzaldehyde (38)[159]
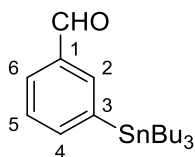
$$\text{CHO}$$

A flask was charged with zinc dust (6.14 g, 93.8 mmol), MeCN (70 mL) was added. Trifluoroacetic acid (0.13 g, 1.15 mmol) was added carefully, and the solution stirred for 5 minutes. Cobalt dibromide (1.38 g, 6.25 mmol) was added, the resultant blue solution was stirred for a further 5 minutes. Addition of allyl chloride (1.44 g, 18.8 mmol) turned the solution red upon 10 minutes stirring. 3-Bromobenzaldeyhde (9.25 g, 50.0 mmol) was added, followed immediately by tributylstannyl chloride (22.3 g, 68.5 mmol). The reaction was heated to 50 °C and monitored by TLC (95:5 petrol:ether) until all of the starting material had been consumed. Once cooled to RT, aqueous saturated ammonium chloride (50 mL) was added and the mixture extracted with ether (3 × 50 mL). The organic fractions were combined and dried over $MgSO_4$, filtered and concentrated *in vacuo*. The crude orange oil was purified by column chromatography on SiO_2 (petrol, then 90:10 petrol:ether) or using automated flash reverse phase chromatography (neat MeCN) obtaining **38** as a clear oil (13.8g, 70%). R_f 0.44 (95:5 petrol:ether); IR ν_{MAX}/cm^{-1} (neat) 2956, 2923, 2361, 1701, 1580, 1377, 1203; ^{1}H NMR (300 MHz, $CDCl_3$) δ 10.00 − 9.89 (1H, s, CHO), 7.97 − 7.81 (1H, s, H2), 7.75 − 7.68 (1H, dt, J = 8, 2 Hz), 7.68 − 7.62 (1H, dt, J = 7, 1 Hz), 7.46 − 7.34 (1H, m), 1.58 − 1.38 (6H, m), 1.31 − 1.23 (6H, m), 1.19 − 0.88 (6H, m), 0.85 − 0.71 (9H, m); ^{13}C NMR (75 MHz, $CDCl_3$) δ 193.01 (CHO), 143.94, 142.72, 137.89, 136.21, 129.62, 128.64, 29.34 (SnCH_2), 27.53 (SnCH$_2$$CH_2$), 13.78 (CH$_2CH_2$$CH_2$), 10.17 (CH$_2$$CH_3$); Anal. Calcd. for $C_{19}H_{32}SnO$: C, 57.75; H, 8.16. Found: C, 57.88; H, 8.00.

6.5 4-Formylphenyl(phenyl)iodonium trifluoroacetate (43)
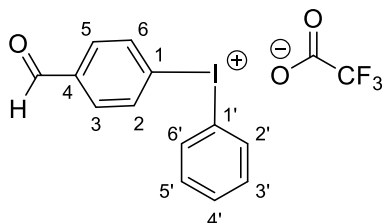
Diacetoxyiodobenzene (3.34 g, 10.4 mmol) was dissolved in DCM (40 mL). The solution was cooled to −30 °C. TFA (2.37 g, 20.8 mmol) was added dropwise, the yellow solution was stirred at −30 °C for 30 minutes, followed by 1 hour stirring at room temperature. The reaction mixture was recooled to −30 °C, 4-tributylstannylbenzaldehyde (4.11 g, 10.4 mmol) was added, and stirred for 30 minutes. The reaction was warmed to room temperature and stirred overnight. The solvent was removed *in vacuo*, affording a yellow oil, which was triturated with DCM/petrol/ether to given the crude product as an off-white powder. **43** was obtained by recrystallisation (DCM/Petrol) as a white powder (1.36 g, 32%). Mp 159–163 °C (from DCM/Petrol); IR ν_{MAX}/cm^{-1} (neat) 1707, 1648, 1581, 1175, 1181; ^{1}H NMR (300 MHz, CD$_3$CN) δ 10.01 (1H, s, CHO), 8.25 (2H, d, H2/H6 *J* = 8.4 Hz), 8.13 (2H, d, H2′/H6′ *J* = 7.4 Hz), 7.94 (2H, d, H3/H5 *J* = 8.6 Hz), 7.68 (1H, t, H4′ *J* = 7.5 Hz), 7.52 (2H, t, H3′/H5′ *J* = 7.7 Hz); ^{13}C NMR (75 MHz, CD$_3$CN) δ 191.31 (CHO), 138.33 (C4), 135.47 (C2/C6), 135.24 (C2′/C6′), 132.15 (C4′), 131.75 (C3/C5), 131.59 (C3′/C5′), 122.05 (C1), 116.50 (C1′); ^{19}F NMR (376 MHz, CD$_3$CN) δ −75.51 (s); HRMS (ESI) found: M$^+$, 308.9766. C$_{13}$H$_{10}$IO$^+$ requires 308.9771; Anal. Calcd. for C$_{15}$H$_1$F$_3$IO$_3$: C, 42.68; H, 2.39. Found: C, 42.56; H, 2.45.

6.6 4-Formylphenyl(4-anisyl)iodonium trifluoroacetate (44)
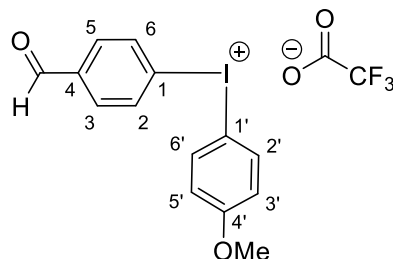
4-Anisyliodobisacetate (5.61 g, 15.9 mmol) was dissolved in dry DCM (50 mL). The solution was cooled to -30 °C in a dry ice/acetone bath. TFA (3.63 g, 31.8 mmol) was added dropwise, the yellow solution was stirred at -30 °C for 30 minutes, followed by 1 hour stirring at room temperature. The reaction mixture was recooled to -30 °C, 4-tributylstannylbenzaldehyde (6.28 g, 15.9 mmol) was added, and stirred for 30 minutes. The reaction was warmed to room temperature and stirred overnight. The solvent was removed *in vacuo*, affording an orange oil, which was triturated with DCM/petrol/ether and placed in the freezer. **44** was obtained by filtration as a white powder (3.43 g, 49%). Mp 149-151 °C (from DCM/Petrol); IR ν_{MAX}/cm^{-1} (neat) 1701, 1660, 1582, 1487, 1262, 1174; ^{1}H NMR (300 MHz, CD$_3$CN) δ 10.01 (1H, s, CHO), 8.21 (2H, d, H2/H6 J = 8.4 Hz), 8.04 (2H, d, H2′/H6′ J = 9.2 Hz), 7.93 (2H, d, H3/H5 J = 8.6 Hz, 2H), 7.04 (2H d, H3′/H5′ J = 9.2 Hz), 3.84 (3H, s, Me); ^{13}C NMR (101 MHz, CD$_2$Cl$_2$) δ 190.72 (*C*HO), 162.78 (C4′), 137.99 (C4), 137.31 (C2′/C6′), 134.67 (C2/C6), 131.78 (C3/C5), 123.31 (C1), 117.70 (C3′/C5′), 105.27 (C1′), 55.79 (OMe); ^{19}F NMR (376 MHz, CD$_2$Cl$_2$) δ -75.44 (s); HRMS (ESI positive) found: M$^+$, 338.9877. C$_{14}$H$_{12}$IO$_2^+$ requires 338.9876; Anal. Calcd. for C$_{16}$H$_{12}$F$_3$IO$_4$: C, 42.5; H, 2.67. Found: C, 42.35; H, 2.60. For X-ray crystal structure data, see appendix.

6.7 4-Formylphenyl(2-theinyl)iodonium trifluoroacetate (45)
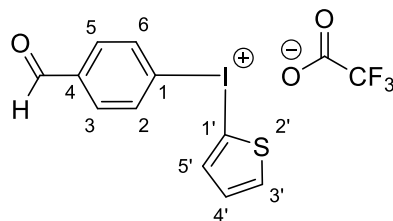
2-Thienyliodobisacetate (2.96 g, 7.49 mmol) was dissolved in dry DCM (30 mL). The solution was cooled to -30 °C in a dry ice/acetone bath. TFA (1.71 g, 15.0 mmol) was added dropwise, the resultant yellow solution was stirred at -30 °C for 30 minutes, followed by 1 hour stirring at room temperature. The reaction mixture was recooled to -30 °C, 4-tributylstannylbenzaldehyde (2.96 g, 7.49 mmol) was added, and stirred for 30 minutes. The reaction was warmed to room temperature and stirred overnight. The solvent was removed *in vacuo*, affording a yellow oil, which was triturated with DCM/petrol/ether and placed in the freezer. Pure **45** was obtained by filtration as an off-white powder (1.21 g, 38%). Mp 155-159 °C (from DCM/Petrol); IR ν_{MAX}/cm^{-1} (neat) 2981, 1702, 1645, 1381, 1190, 1141; ^{1}H NMR (400 MHz, CD$_3$CN) δ 9.95 (1H, s, CHO), 8.23 (2H, d, H2/H6 *J* = 8.5 Hz), 7.92 – 7.83 (3H, m), 7.74 (1H, dd, H5′ *J* = 5.3, 1.2 Hz), 7.10 (1H, dd, H4′ *J* = 5.2, 3.8 Hz). ^{13}C NMR (101 MHz, CD$_3$CN) δ 191.60 (CHO), 140.87 (C4), 138.26, 137.27, 134.80, 131.83, 129.83, 125.50 (C1), 101.97 (C1′). ^{19}F NMR (376 MHz, CD$_3$CN) δ -75.62 (s); HRMS (ESI positive) found: M$^+$, 314.9333. C$_8$H$_{11}$IOS$^+$ requires 314.9335; Anal. Calcd. for C$_{13}$H$_8$F$_3$IO$_3$S: C, 36.47; H, 1.88. Found: C, 36.36; H, 1.73. For X-ray crystal structure data, see appendix.

6.8   3-Formylphenyl(phenyl)iodonium trifluoroacetate (50)
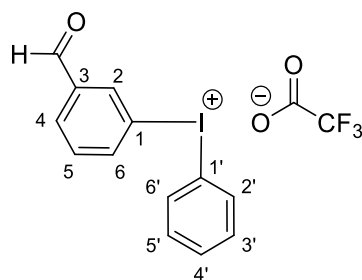
Diacetoxyiodobenzene (1.30 g, 4.05 mmol) was dissolved in dry DCM (15 mL). The solution was cooled to -30 °C in a dry ice/acetone bath. TFA (2.37 g, 20.8 mmol) was added dropwise, and the yellow solution was stirred at -30 °C for 30 minutes, followed by 1 hours stirring at room temperature. The reaction mixture was then recooled to -30 °C, 3-tributylstannylbenzaldehyde (1.60 g, 4.05 mmol) was added, and stirred for 30 minutes. The reaction was warmed to room temperature, and stirred overnight. The solvent was removed *in vacuo*, affording a pale yellow oil, which was triturated with DCM/petrol/ether and placed in the freezer. Pure **50** was obtained by filtration as a white powder (804 mg, 47%). Mp 150-153 °C (decomp.)(from DCM/Petrol); IR ν_{MAX}/cm^{-1} (neat) 1707, 1648, 1581, 1175, 1128; ^{1}H NMR (500 MHz, d_6- DMSO) δ 10.00 (1H, s, CHO), 8.74 (1H, s, H2), 8.53 (1H, d, H6 J = 8.0 Hz), 8.30 (2H, d, H2′/H6′ J = 8.4 Hz), 8.17 (1H, d, H4 J = 7.7 Hz), 7.76 (1H, t, H5 J = 7.8 Hz), 7.67 (1H, t, H4′ J = 7.5 Hz), 7.54 (2H, t, H3′/H5′ J = 7.8 Hz); ^{13}C NMR (101 MHz, d_2-DCM) δ 189.90 (CHO), 139.91 (C3), 135.19, 135.11, 132.48, 132.19, 132.06, 131.84, 117.70 (C1), 116.86 (C1′); ^{19}F NMR (376 MHz, d_2-DCM) δ -75.47; HRMS (ESI) found: M$^+$, 308.9768. $C_{13}H_{10}IO^+$ requires 308.9771; Anal. Calcd. for $C_{15}H_1F_3IO_3$: C, 42.68; H, 2.39. Found: C, 42.81; H, 2.29. For X-ray crystal structure data, see appendix.

6.9 3-Formylphenyl(4-anisyl)iodonium trifluoroacetate (51)
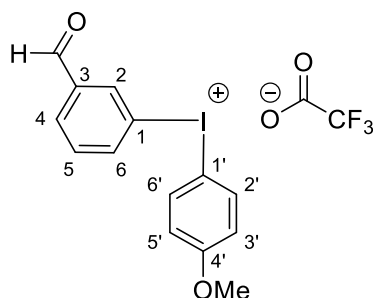
4-Diacetoxyiodoanisole (1.60 g, 4.56 mmol) was dissolved in dry DCM (15 mL). The solution was cooled to -30 °C in a dry ice/acetone bath. TFA (1.04 g, 9.12 mmol) was added dropwise, the yellow solution was stirred at -30 °C for 30 minutes, followed by 1 hour stirring at room temperature. The reaction mixture was recooled to -30 °C, and 3-tributylstannylbenzaldehyde (1.80 g, 4.56 mmol) was added, and stirred for 30 minutes. The reaction was warmed to room temperature and stirred overnight. The solvent was removed *in vacuo*, affording a pale yellow oil, which was triturated with DCM/petrol/ether and placed in the freezer. Pure **51** was obtained by filtration as a white powder (803 mg, 39%). Mp 148-158 °C (decomp.)(from DCM/Petrol). IR v_{MAX}/cm^{-1} (neat) 1703, 1650, 1571, 1489, 1254, 1176, 1130; ^{1}H NMR (500 MHz, DMSO-d6) δ 9.99 (1H, s, CHO), 8.69 (1H, s, H2), 8.47 (1H, d, H6 *J* = 8.1 Hz), 8.22 (2H, d, H2′/H6′ *J* = 9.0 Hz), 8.16 (1H, d, H4 *J* = 7.6 Hz), 7.75 (t, H5 *J* = 7.8 Hz), 7.09 (2H, d, H3′/H5′ *J* = 9.0 Hz), 3.79 (3H, s, OMe); ^{13}C NMR (75 MHz, DMSO) δ 191.34 (CHO), 162.11 (C4), 139.80 (C6), 138.38 (C3), 137.36 (C2′/C6′), 134.56 (C2), 132.75 (C4), 132.19 (C5), 117.71 (C1), 117.52 (C3′/C5′), 105.55 (C1′), 55.70 (OMe); ^{19}F NMR (471 MHz, DMSO-D6) δ -73.27; HRMS (ESI positive) found: M$^+$, 338.9875. $C_{14}H_{12}IO_2^+$ requires 338.9876; Anal. Calcd. for $C_{16}H_{12}F_3IO_4$: C, 44.06; H, 2.77. Found: C, 43.93; H, 2.69. For X-ray crystal structure data, see appendix.

6.10 3-Formylphenyl(2-thienyl)iodonium trifluoroacetate (52)
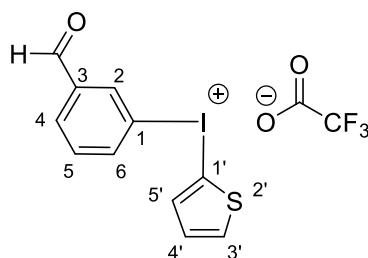
2-Diacetoxyiodothiophene (1.33 g, 4.05 mmol) was dissolved in dry DCM (15 mL). The solution was cooled to -30 °C in a dry ice/acetone bath. TFA (924 mg, 8.10 mmol) was added dropwise, the yellow solution was stirred at -30 °C for 30 minutes, followed by 1 hour stirring at room temperature. The reaction mixture was recooled to -30 °C, and 3-tributylstannylbenzaldehyde (1.60 g, 4.05 mmol) was added, and stirred for 30 minutes. The reaction was warmed to room temperature and stirred overnight. The solvent was removed *in vacuo*, affording a yellow oil, which was triturated with DCM/petrol/ether and placed in the freezer. **52** was obtained by filtration as a white powder (744 mg, 43%). Mp 134-141 °C (decomp.)(from DCM/petrol/ether); IR v_{MAX}/cm^{-1} (neat) 1705, 1644, 1588, 1423, 1384, 1185, 1132; ^{1}H NMR (400 MHz, DMSO-d$_6$) δ 9.95 (1H, s, CHO), 8.69 (1H, s, H2), 8.49 (1H, d, H6 J = 8.5 Hz), 8.11 (1H, d, H4 J = 8.6 Hz), 8.07 (1H, d, J = 3.7 Hz), 7.92 (1H, d, J = 5.4 Hz), 7.70 (1H, t, J = 7.9 Hz), 7.16 − 7.09 (1H, m); ^{13}C NMR (101 MHz, DMSO-D6) δ 192.12 (*C*HO), 158.65 (q, CF3(O)*C*O J_{C-F} = 30.7 Hz), 141.06, 140.26, 138.76, 137.84, 134.83, 133.59, 132.78, 130.13, 121.04 (C1), 102.28 (C1′); HRMS (ESI positive) found: M$^+$, 314.9331. C$_8$H$_{11}$IOS$^+$ requires 314.9335; Anal. Calcd. for C$_{13}$H$_8$F$_3$IO$_3$S: C, 36.47; H, 1.88. Found: C, 36.34; H, 1.81; For X-ray crystal structure data, see appendix.

6.11   2-Fluorothiophene (49)
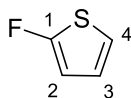
Magnesium turnings (18.45 g, 759 mmol) were stirred for 24 h using a glass[‡] stirrer bar under argon in a dry 3-necked 3 L round bottomed flask fitted with a double walled water condenser and a dropping funnel. Freshly distilled, dry diethylether (1.5 L) was then transferred to the reaction vessel by cannula. 2-Bromothiophene (72.6 mL, 750 mmol) was loaded into the dropping funnel then around 100 drops were added to the reaction vessel without stirring and left for 1 h. Stirring was then started and the remainder of the 2-bromothiophene added to the vessel at a rate which maintained a steady reflux (*ca.* 3 h); following addition, residual 2-bromothiophene was washed into the reaction mixture with dry diethylether (20 mL). An increase in the lustre of the magnesium turnings could be observed upon initiation accompanied by their gradual consumption. The reaction mixture was left overnight, after which the mixture was pale brown and slightly cloudy in appearance with a few small flakes of magnesium remaining. In a separate dry, single-necked 3 L round bottomed flask fitted with a water condenser, NFSI (237.72 g, 754 mmol) was dissolved in dry diethylether (750 mL, transferred to the flask as before) and the suspension cooled to 0 ˚C. The Grignard solution was then transferred by cannula (12 gauge) to the NFSI suspension with vigorous stirring. Consumption of the NFSI was accompanied by the formation of a large amount of white precipitate and a slight exotherm. The suspension was stirred at 0 ˚C for 5 h then at room temperature for a further 3 h. A 1 mL sample was taken from the reaction mixture, quenched with a few drops of methanol then mixed with D_6-DMSO and analysed by ^{1}H- and ^{19}F-NMR showing all the NFSI to be consumed but around 10% thiophene to be present relative to 2-fluorothiophene. The condenser was quickly removed, more NFSI added (11.70 g, 37.1 mmol) and the condenser replaced. The reaction was left for 48 h then analysed as before showing only one fluorinated product, 2-fluorothiophene. The reaction mixture was filtered through a pad of Celite (3 cm depth, 10 cm diameter) and silica (7 cm depth, 10 cm diameter) and the white residue washed with diethylether (2 x 200 mL). The solvent was carefully removed from the reaction mixture by

---

[‡] Previous activation of magnesium turnings using a PTFE stirrer bar resulted in reaction with the PTFE coating, visible by the formation of 'soot'

distillation over several days, analysing the fractions by ^{19}F- and ^{1}H-NMR. Fractions of similar purity were combined to give 2-fluorothiophene as a clear colourless liquid (35.8 g, 47%). bp 82-84 °C (lit: 82 ˚C); λ_{max} (EtOH)/nm 226 (ε/dm^3 mol^{-1} cm^{-1} 5150; IR ν_{max}/cm^{-1} (neat) 1556, 1451, 1229, 1187, 1085, 1027, 843, 807, 705, 673; ^{1}H NMR (500 MHz, D$_2$-DCM) δ 6.71 (1H, ddd, H4 $^{3}J_{4,5}$ 6.0, $^{3}J_{4,3}$, 3.9, $^{4}J_{4,F}$ 3.1), 6.66 (1H, ddd, H5 $^{3}J_{5,4}$ 6.0, $^{4}J_{5,3}$ 1.8, $^{4}J_{5,F}$ 3.1), 6.48 (1H, dt, H3 $^{3/4}J_{3,4/5}$ 2.0, $^{3}J_{3,F}$ 1.8); ^{13}C NMR (125 MHz, D$_2$-DCM) δ 168.06 (d, C2 $^{1}J_{2,F}$ 286.4) 125.69 (d, C4 $^{3}J_{4,F}$ 286.4), 115.70 (d, C5 $^{3}J_{5,F}$ 1.5), 109.03 (d, C3 $^{2}J_{3,F}$ 11.1); ^{19}F NMR (376 MHz, D$_2$-DCM) δ 135.05 (1F, dt, $^{4}J_{F,4/5}$ 3.2, $^{3}J_{F,3}$ 1.6); Mass spec. (HRMS) Found: M$^+$, 101.9933. C$_4$H$_3$FS requires 101.9934. Anal. Calcd. for C$_5$H$_3$FS: C, 47.04; H, 2.96, found C, 47.43; H, 2.95.

6.12 2-Thienyl(phenyl)iodonium trifluoroacetate (57)[238]
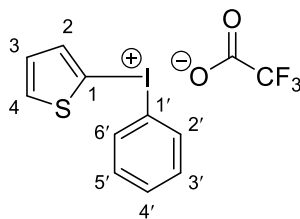
Phenyliodobisacetate (1.28 g, 5 mmol) was dissolved in dry DCM (25 mL), and the solution was cooled to -30 °C in a dry ice/acetone bath. TFA (0.57 g, 10 mmol) was added dropwise, the yellow solution was stirred at -30 °C for 30 minutes, followed by 1 hour at room temperature. The reaction mixture was recooled to -30 °C, 2-thienyltributylstannane (1.87 g, 5 mmol) was added and stirred for 30 minutes. The reaction was then warmed to room temperature and stirred overnight. The solvent was removed *in vacuo*, affording a pale yellow oil, which was triturated with DCM/petrol/ether and placed in a freezer. Pure **57** was obtained by filtration as a white crystalline solid (434 mg, 28%). Mp 147-153 °C (decomp.)(from DCM/petrol/ether); IR v_{max}/cm^{-1} 1651, 1577, 1488, 1259, 1173, 1137; ^{1}H NMR (400 MHz, CDCl$_3$) δ 7.95 (2H, dd, J = 8.5, 0.9 Hz), 7.71 (1H, dd, J = 3.7, 1.1 Hz), 7.58 (1H, dd, J = 5.3, 1.1 Hz), 7.50 (1H, t, J = 7.4 Hz), 7.41 – 7.34 (2H, m), 7.04 (1H, dd, J = 5.3, 3.8 Hz); ^{13}C NMR (101 MHz, DMSO-d_6) δ 158.50 (q, $J_{C\text{-}F}$ = 30.8 Hz) 140.72, 137.62, 135.10, 132.44, 132.11, 130.09, 122.19, 120.19, 119.20, 116.21, 101.95; ^{19}F NMR (376 MHz, CDCl$_3$) δ -75.33; HRMS (ESI positive) found: M$^+$, 286.9378. C$_{10}$H$_8$IS$^+$ requires 286.9366. Anal. Calcd. for C$_{12}$H$_8$F$_3$IO$_2$S: C, 36.30; H, 2.34. Found: C, 36.49; H, 2.25. For X-ray crystal structure data, see appendix.

6.13 2-Thienyl(4-anisyl)iodonium trifluoroacetate (58)[239]
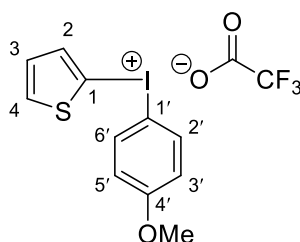
4-Anisyliodobisacetate (1.76 g, 5 mmol) was dissolved in dry DCM (25 mL), and the solution was cooled to -30 °C in a dry ice/acetone bath. TFA (0.57 g, 10 mmol) was added dropwise, the yellow solution was stirred at -30 °C for 30 minutes, followed by 1 hour at room temperature. The reaction mixture was recooled to -30 °C, 2-Thienyltributylstannane (1.87 g, 5 mmol) was added and stirred for 30 minutes. The reaction was then warmed to room temperature and stirred overnight. The solvent was removed *in vacuo*, affording a pale yellow oil, which was triturated with DCM/petrol/ether and placed in a freezer. **58** was obtained by filtration as a white crystalline solid (839 mg, 39%). Mp 147-153 °C (decomp.)(from DCM/petrol/ether); IR ν_{max}/cm^{-1} 1650, 1572, 1488, 1259, 1174, 1137, 1016; ^{1}H NMR (400 MHz, DMSO-d6) δ 8.14 (2H, d, H2′/H6′ J = 9.0 Hz), 8.00 – 7.95 (1H, m), 7.90 (1H, dd, J = 5.3, 1.0 Hz), 7.13 – 7.10 (1H, m), 7.02 (2H, d, H3′/H5′ J = 9.0 Hz). ^{13}C NMR (101 MHz, DMSO-d6) δ 162.39, 140.26, 137.35, 137.27, 130.01, 117.82, 109.03, 102.30, 56.23; ^{19}F NMR (376 MHz, CDCl$_3$) δ -75.25; HRMS (ESI positive) found: M$^+$, 316.9485. C$_{10}$H$_{11}$IOS$^+$ requires 316.9492. Anal. Calcd. for C$_{13}$H$_{10}$F$_3$IO$_3$S: C, 36.30; H, 2.34. Found: C, 36.22; H, 1.92. For X-ray crystal structure data, see appendix.

6.14　2-Thienyl(2-thienyl) trifluoroacetate (59)[178, 238]
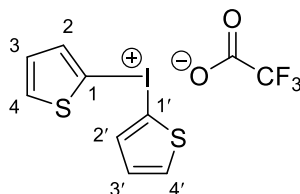
2-Thienyliodobisacetate (1.64 g, 5 mmol) was dissolved in dry DCM (25 mL), and the solution was cooled to -30 °C in a dry ice/acetone bath. TFA (0.57 g, 10 mmol) was added dropwise, the yellow solution was stirred at -30 °C for 30 minutes, followed by 1 hour at room temperature. The reaction mixture was recooled to -30 °C, 2-Thienyltributylstannane (1.87 g, 5 mmol) was added and stirred for 30 minutes. The reaction was then warmed to room temperature and stirred overnight. The solvent was removed *in vacuo*, affording a pale yellow oil, which was triturated with MeCN/ether and placed in a freezer. Pure **59** was obtained by filtration as a white crystalline solid (103 mg, 19%). Mp 123-125 °C (decomp.)(from MeCN/ether). IR ν_{max}/cm^{-1} 1645, 1420, 1386, 1180, 1137, 947, 831, 797, 699; δ_H (400 MHz, D$_3$-MeCN, Me$_4$Si) 7.80 (2 H, d, H-3 $^3J_{3/4}$ 3.20), 7.69 (2 H, d, H-5 $^3J_{5,4}$ 5.20), 7.04 (2 H, t$_{app}$, H-4 $^3J_{3,5/4}$ 4.80); δ_C (100 MHz, D$_3$-MeCN, Me$_4$Si) 139.50 (C3), 136.26 (C5), 129.27 (C4), 104.57 (C2); δ_F (376 MHz, CDCl$_3$, CFCl$_3$) -75.36; Mass spec. (High Res. LCMS) *m/z* (ESI) 292 (M-TFA)$^+$, 100%), 239 (12), 210 (27), 166 (15). Found: (M-TFA)$^+$ 292.8950. C$_8$H$_6$IS$_2$ requires 292.8950. Anal. calcd. for C$_{10}$H$_6$F$_3$IO$_2$S$_2$: C, 29.57; H, 1.49. Found: C, 29.61; H, 1.45. For X-ray crystal structure data, see appendix.

6.15 *N*-4-(Fluoro)phenylmaleimide (61)[195]
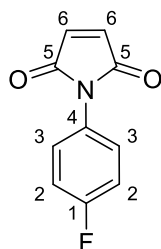
Maleic anhydride (19.62 g, 200 mmol) was added to a dry flask equipped with a dropping funnel, and dissolved in dry ether (240 mL). 4-Fluoroaniline (22.22 g, 200 mmol) was placed in the dropping funnel and dissolved in dry ether (40 mL), the resultant solution was added dropwise to the reaction flask, forming a thick green/yellow solution, which was stirred at room temperature for 1.25 hr. Upon filtration and drying a yellow/green solid was obtained, the solid was placed in a dry flask, equipped with a condenser, containing NaOAc (6.56 g, 80 mmol). Upon dissolution with acetic anhydride (70 mL), and heating at 100 °C a clear yellow/brown solution formed after 0.5 hr stirring. The reaction mixture was cooled to room temperature; the resultant yellow/brown precipitate was collected by filtration. Washing with ice cold water (2×50 mL) followed by recrystallisation (from EtOH/water) and drying afforded **61** as a fluffy orange/yellow crystalline powder (34.61 g, 91%). Mp 136-143 °C (from EtOH/water) (lit:[195] 146-148 °C); IR ν_{MAX}/cm^{-1} (neat) 3104, 1708, 1514, 1390, 1230, 1148; ^{1}H NMR (400 MHz, CDCl$_3$) δ 7.29 (2H, m), 7.18 – 7.10 (2H, m), 6.84 (2H, s, H6). ^{13}C NMR (101 MHz, CDCl$_3$) δ 169.51 (C5), 161.89 (C1, d, J_{C-F} = 247.8 Hz), 134.32 (C6), 128.00 (C2, d, J_{C-F} = 8.7 Hz), 127.17 (C4, d, J_{C-F} = 3.0 Hz), 116.26 (C3, d, J_{C-F} = 23.0 Hz). ^{19}F NMR (471 MHz, Chloroform-d) δ -113.01. HRMS (ESI positive) found: [M+H]$^+$, 192.0455. C$_{10}$H$_7$FNO$_2^+$ requires 192.0453; Anal. calcd. for C$_{10}$H$_6$FNO$_2$: C, 47.65; H, 2.40; N, 5.56. Found: C, 47.48; H, 2.23; N, 5.56.

6.16 *N*-4-(Bromo)phenylmaleimide (62)
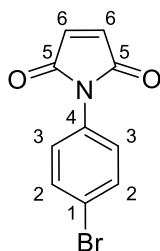
Maleic anhydride (19.62 g, 200 mmol) was added to a dry flask equipped with a dropping funnel, and dissolved in dry ether (240 mL). 4-Bromoaniline (34.40 g, 200 mmol) was placed in the dropping funnel and dissolved in dry ether (50 mL) forming a dark purple solution, which upon addition to the reaction flask generated a thick yellow/green mixture. The mixture was stirred at room temperature for one hour. Upon filtration a yellow/green solid was obtained, dried, and placed in a dry flask, equipped with a condenser, containing NaOAc (6.56 g, 80 mmol). Upon dissolution with acetic anhydride (70 mL), and heating at 100 °C a clear yellow/brown solution formed after 30 minutes stirring. The reaction mixture was cooled to room temperature, and poured onto a water/ice mixture (200 mL), the resultant yellow/brown precipitate was collected by filtration. Washing with ice cold water (3 × 100 mL) followed by recrystallisation (from EtOH/water) and drying afforded **62** as a yellow powder (33.78 g, 98%). Mp 130-134 °C (from EtOH/water) (lit:[195] 128-130 °C); IR ν_{MAX}/cm^{-1} (neat) 3090, 2981, 1716, 1490, 1383, 1146; ^{1}H NMR (400 MHz, CDCl$_3$) δ 7.62 – 7.47 (2H, d, *J* = 8.7 Hz), 7.29 – 7.15 (2H, d, *J* = 8.7 Hz), 6.88 – 6.69 (2H, s, H6). ^{13}C NMR (101 MHz, CDCl$_3$) δ 169.16 (CO), 134.39, 132.39, 130.37, 127.45, 121.69. HRMS (ESI positive) found: [M+H]$^+$, 283.9919. C$_{10}$H$_7$BrNO$_2$$^+$ requires 283.9917. Anal. calcd. for C$_{10}$H$_6$BrNO$_2$: C, 47.65; H, 2.40; N, 5.56. Found: C, 47.48; H, 2.23; N, 5.56.

6.17　*N*-4-(Iodo)phenylmaleimide (63)[195]

Maleic anhydride (9.81 g, 100 mmol) was added to a dry flask equipped with a dropping funnel, and dissolved in dry ether (40 mL). 4-Iodoaniline (21.90 g, 100 mmol) was placed in the dropping funnel and dissolved in dry ether (40 mL), the resultant solution was added dropwise to the reaction flask, forming a thick green/yellow solution, which was stirred at room temperature for 1.25 hr. Upon filtration and drying a yellow/green solid was obtained, the solid was placed in a dry flask, equipped with a condenser, containing NaOAc (3.28 g, 40 mmol). Upon dissolution with acetic anhydride (34 mL), and heating at 100 °C a clear yellow/brown solution formed after 0.5 hr stirring. The reaction mixture was cooled to room temperature, and poured onto a water/ice mixture (200 mL), the resultant yellow/brown precipitate was collected by filtration. Washing with ice cold water (2 × 50 mL) followed by recrystallisation (from EtOH/water) and drying afforded **63** as a yellow crystalline powder (18.06 g, 61%). Mp 139-144 °C (from EtOH/water) (lit:[195] 145-147 °C); IR ν_{MAX}/cm^{-1} (neat) 2981, 1703, 1485, 1388, 1152; ^{1}H NMR (300 MHz, CDCl$_3$) δ 7.80 (2H, d *J* = 8.6 Hz), 7.14 (2H, d *J* = 8.6 Hz), 6.87 (2H, s, H6); ^{13}C NMR (75 MHz, CDCl$_3$) δ 168.82 (CO), 138.22, 134.23, 131.27, 127.51, 92.77 (C1); HRMS (ESI positive) found: [M+H]$^+$, 299.9522. C$_{10}$H$_7$INO$_2$$^+$ requires 299.9516. Anal. calcd. for C$_{10}$H$_6$INO$_2$: C, 40.16; H, 2.02; N, 4.68. Found: C, 40.05; H, 2.07; N, 4.74. For X-ray crystal structure data, see appendix.

6.18 4-*N*-phenylmaleimide(phenyl)iodonium trifluoroacetate (69)
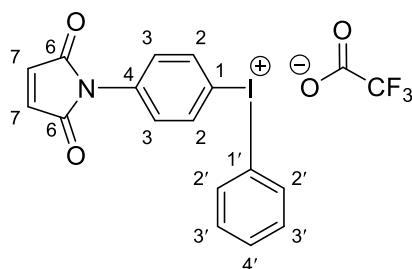
4-*N*-phenylmaleimideiodobisacetate (1.8 g, 4.31 mmol as a 50% mixture determined by ^{1}H-NMR with 4-iodo-*N*-phenylmaleimide, **63**) was dissolved in dry DCM (25 mL). The solution was cooled to -30 °C in a dry ice/acetone bath. TFA (0.98 g, 8.61 mmol) was added dropwise, the yellow solution was stirred at -30 °C for 30 minutes, followed by 1 hour stirring at room temperature. The reaction mixture was recooled to -30 °C, and phenyltributylstannane (1.58 g, 4.31 mmol) was added, and stirred for 30 minutes. The reaction was warmed to room temperature and stirred overnight. The solvent was removed in *vacuo*, affording a pale yellow oil, which was triturated with DCM/petrol/ether and placed in the freezer. **69** was obtained by filtration as colourless needles (422 mg, 20%). Mp 123-134 °C (decomp.)(from DCM/petrol/ether); ^{1}H NMR (400 MHz, DMSO-d_6) δ 8.31 (2H, d, *J* = 8.7 Hz, 1H), 8.24 (d, *J* = 8.1 Hz, 1H), 7.64 (t, *J* = 7.3 Hz, 1H), 7.56 − 7.44 (m, 4H), 7.19 (s, 1H). ^{13}C NMR (101 MHz, DMSO-D_6) δ 169.87 (CO), 136.39 (C7), 135.72, 135.48, 135.23, 132.55, 132.25, 129.68, 117.64, 115.29. ^{19}F NMR (376 MHz, DMSO-D6) δ -68.36; HRMS (ESI positive) found: [M]$^+$, 375.9827. $C_{16}H_{11}NIO_2^+$ requires 375.9829; Anal. Calcd. for $C_{16}H_{11}F_3IO_3S$: C, 44.20; H, 2.27 N, 2.86. Found: C, 44.08; H, 2.34 N, 2.98. For X-ray crystal structure data, see appendix.

References

1. J. Czernin and M. E. Phelps, *Annu. Rev. Med.*, 2002, **53**, 89-112.
2. K. A. Wood, P. J. Hoskin and M. I. Saunders, *Clinical Oncology*, 2007, **19**, 237-255.
3. P. W. Miller, N. J. Long, R. Vilar and A. D. Gee, *Angew. Chem., Int. Ed.*, 2008, **47**, 8998-9033.
4. S. M. Ametamey, M. Honer and P. A. Schubiger, *Chem. Rev.*, 2008, **108**, 1501-1516.
5. V. W. Pike, *Trends Pharmacol. Sci.*, 2009, **30**, 431-440.
6. T. L. Ross, J. Ermert, C. Hocke and H. H. Coenen, *J. Am. Chem. Soc.*, 2007, **129**, 8018-8025.
7. C. C. Watson, *IEEE Trans. Nucl. Sci.*, 2004, **51**, 2670-2680.
8. A. H. Compton, *Physical Review*, 1923, **21**, 483-502.
9. M. Gerd and S. K. Joel, *Physics in Medicine and Biology*, 2006, **51**, R117.
10. J. M. Ollinger and J. A. Fessler, *IEEE Signal Proc. Mag.*, 1997, **14**, 43-55.
11. W. H. Sweet, *N. Engl. J. Med.*, 1951, **245**, 875-878.
12. F. R. Wrenn, M. L. Good and P. Handler, *Science*, 1951, **113**, 525-527.
13. M. E. Phelps, E. J. Hoffman, N. A. Mullani, C. S. Higgins and M. M. T. Pogossian, *IEEE Trans. Nucl. Sci.*, 1976, **23**, 516-522.
14. E. J. Hoffman, M. E. Phelps, N. A. Mullani, C. S. Higgins and M. M. Ter-Pogossian, *Journal of Nuclear Medicine*, 1976, **17**, 493-502.
15. T. Beyer, D. W. Townsend, T. Brun, P. E. Kinahan, M. Charron, R. Roddy, J. Jerin, J. Young, L. Byars and R. Nutt, *Journal of Nuclear Medicine*, 2000, **41**, 1369-1379.
16. L. S. Cai, R. B. Innis and V. W. Pike, *Curr. Med. Chem.*, 2007, **14**, 19-52.
17. M. Schwaiger, S. Ziegler and S. G. Nekolla, *Journal of Nuclear Medicine*, 2005, **46**, 1664-1678.
18. W. Cai, J. Rao, S. S. Gambhir and X. Chen, *Mol. Cancer Ther.*, 2006, **5**, 2624-2633.
19. Z. Li and P. S. Conti, *Adv. Drug Delivery Rev.*, 2010, **62**, 1031-1051.
20. M. E. Phelps, *PET: Molecular Imaging and its Biological Applications*, Springer-Verlag, New York, 2004.
21. E. O. Lawrence and M. S. Livingston, *Physical Review*, 1932, **40**, 19-35.
22. H. N. Wagner Jr, *Seminars in Nuclear Medicine*, 1998, **28**, 213-220.
23. K. Müller, C. Faeh and F. Diederich, *Science*, 2007, **317**, 1881-1886.
24. K. L. Kirk, *J. Fluorine Chem.*, 2006, **127**, 1013-1029.
25. D. O'Hagan, *J. Fluorine Chem.*, 2010, **131**, 1071-1081.
26. J. Wang, M. Sánchez-Roselló, J. L. Aceña, C. del Pozo, A. E. Sorochinsky, S. Fustero, V. A. Soloshonok and H. Liu, *Chem. Rev.*, 2013, **114**, 2432-2506.
27. W. K. Hagmann, *J. Med. Chem.*, 2008, **51**, 4359-4369.
28. D. O'Hagan, *Beilstein J. Org. Chem.*, 2013, **9**, 2180-2181.
29. B. K. Park, N. R. Kitteringham and P. M. O'Neill, *Annu. Rev. Pharmacol. Toxicol.*, 2001, **41**, 443-470.
30. H.-J. Böhm, D. Banner, S. Bendels, M. Kansy, B. Kuhn, K. Müller, U. Obst-Sander and M. Stahl, *ChemBioChem*, 2004, **5**, 637-643.
31. J. W. Clader, *J. Med. Chem.*, 2003, **47**, 1-9.

32. J. M. Domagala, L. D. Hanna, C. L. Heifetz, M. P. Hutt, T. F. Mich, J. P. Sanchez and M. Solomon, *J. Med. Chem.*, 1986, **29**, 394-404.
33. M. Kah and C. D. Brown, *Chemosphere*, 2008, **72**, 1401-1408.
34. H. J. Bohm, D. Banner, S. Bendels, M. Kansy, B. Kuhn, K. Muller, U. Obst-Sander and M. Stahl, *ChemBioChem*, 2004, **5**, 637-643.
35. E. Schweizer, A. Hoffmann-Roder, K. Scharer, J. A. Olsen, C. Fah, P. Seiler, U. Obst-Sander, B. Wagner, M. Kansy and F. Diederich, *ChemMedChem*, 2006, **1**, 611-621.
36. M. Morgenthaler, E. Schweizer, A. Hoffmann-Roder, F. Benini, R. E. Martin, G. Jaeschke, B. Wagner, H. Fischer, S. Bendels, D. Zimmerli, J. Schneider, F. Diederich, M. Kansy and K. Mueller, *ChemMedChem*, 2007, **2**, 1100-1115.
37. M. B. van Niel, I. Collins, M. S. Beer, H. B. Broughton, S. K. F. Cheng, S. C. Goodacre, A. Heald, K. L. Locker, A. M. MacLeod, D. Morrison, C. R. Moyes, A. Pike, M. Rowley, D. O'Connor, M. Rowley, M. G. N. Russell, B. Sohal, J. A. Stanton, S. Thomas, H. Verrier, A. P. Watt and J. L. Castro, *J. Med. Chem.*, 1999, **42**, 2087-2104.
38. R. G. Zimmermann, *Nucl. Med. Biol.*, 2013, **40**, 155-166.
39. T. Ido, C. N. Wan, V. Casella, J. S. Fowler, A. P. Wolf, M. Reivich and D. E. Kuhl, *J. Labelled Compd. Radiopharm.*, 1978, **14**, 175-183.
40. C. C. Rowe, S. Pejoska, R. S. Mulligan, G. Jones, J. G. Chan, S. Svensson, Z. Cselényi, C. L. Masters and V. L. Villemagne, *Journal of Nuclear Medicine*, 2013, **54**, 880-886.
41. D. W. Wooten, J. D. Moraino, A. T. Hillmer, J. W. Engle, O. J. DeJesus, D. Murali, T. E. Barnhart, R. J. Nickles, R. J. Davidson, M. L. Schneider, J. Mukherjee and B. T. Christian, *Synapse*, 2011, **65**, 592-600.
42. K. Ishiwata, M. Monma, R. Iwata and T. Ido, *J. Labelled Compd. Radiopharm.*, 1982, **19**, 1347-1349.
43. G. Pascali, P. Watts and P. A. Salvadori, *Nucl. Med. Biol.*, 2013, **40**, 776-787.
44. C. Rensch, A. Jackson, S. Lindner, R. Salvamoser, V. Samper, S. Riese, P. Bartenstein, C. Wängler and B. Wängler, *Molecules*, 2013, **18**, 7930-7956.
45. http://www.advion.com/products/nanotek/, Accessed 26/01, 2012.
46. A. M. Elizarov, R. M. van Dam, Y. S. Shin, H. C. Kolb, H. C. Padgett, D. Stout, J. Shu, J. Huang, A. Daridon and J. R. Heath, *Journal of Nuclear Medicine*, 2010, **51**, 282-287.
47. P. Y. Keng, S. Chen, H. Ding, S. Sadeghi, G. J. Shah, A. Dooraghi, M. E. Phelps, N. Satyamurthy, A. F. Chatziioannou, C.-J. C. Kim and R. M. van Dam, *Proceedings of the National Academy of Sciences*, 2012, **109**, 690-695.
48. R. B. Fair, *Microfluidics and Nanofluidics*, 2007, **3**, 245-281.
49. S. K. Cho, H. Moon and K. Chang-Jin, *Journal of Microelectromechanical Systems*, 2003, **12**, 70-80.
50. J. Gong and C.-J. C. Kim, *Lab Chip*, 2008, **8**, 898-906.
51. M. J. Schertzer, R. Ben-Mrad and P. E. Sullivan, *Sensors and Actuators B: Chemical*, 2010, **145**, 340-347.
52. W. C. Nelson, I. Peng, G.-A. Lee, J. A. Loo, R. L. Garrell and C.-J. "Cj" Kim, *Anal. Chem.*, 2010, **82**, 9932-9937.
53. J. N. Lee, C. Park and G. M. Whitesides, *Anal. Chem.*, 2003, **75**, 6544-6554.
54. J. Mukherjee, Z.-Y. Yang, M. K. Das and T. Brown, *Nucl. Med. Biol.*, 1995, **22**, 283-296.
55. A. Lebedev, R. Miraghaie, K. Kotta, C. E. Ball, J. Zhang, M. S. Buchsbaum, H. C. Kolb and A. Elizarov, *Lab Chip*, 2013, **13**, 136-145.

56.   A. Salskov, V. S. Tammisetti, J. Grierson and H. Vesselle, *Seminars in Nuclear Medicine*, 2007, **37**, 429-439.

57.   J. Loon, M. M. Janssen, M. Öllers, H. W. L. Aerts, L. Dubois, M. Hochstenbag, A.-M. Dingemans, R. Lalisang, B. Brans, B. Windhorst, G. Dongen, H. Kolb, J. Zhang, D. Ruysscher and P. Lambin, *European Journal of Nuclear Medicine and Molecular Imaging*, 2010, **37**, 1663-1668.

58.   http://sofiebio.com/products/chemistry/, Accessed 28/07/14.

59.   J. Bergman and O. Solin, *Nucl. Med. Biol.*, 1997, **24**, 677-683.

60.   R. E. Ehrenkaufer, J. F. Potocki and D. M. Jewett, *Journal of Nuclear Medicine*, 1984, **25**, 333-337.

61.   H. Teare, E. G. Robins, A. Kirjavainen, S. Forsback, G. Sandford, O. Solin, S. K. Luthra and V. Gouverneur, *Angew. Chem., Int. Ed.*, 2010, **49**, 6821-6824.

62.   H. Teare, E. G. Robins, E. Arstad, K. L. Sajinder and V. Gouverneur, *Chem. Commun. (Cambridge, U. K.)*, 2007, 2330-2332.

63.   H. H. Coenen, in *Ernst Schering Foundation Symposium Proceedings*, eds. P. A. Schubiger, L. Lehmann and M. Friebe, Springer-Verlag, Berlin, 2007, pp. 15-50.

64.   L. Cai, S. Lu and V. W. Pike, *Eur. J. Org. Chem.*, 2008, 2843-2843.

65.   K. Hamacher and H. H. Coenen, *Appl. Radiat. Isot.*, 2002, **57**, 853-856.

66.   H. Sun and S. G. DiMagno, *Chem. Commun. (Cambridge, U. K.)*, 2007, 528-529.

67.   C. D. Reed, G. G. Launay and M. A. Carroll, *J. Fluorine Chem.*, 2012, **143**, 231-237.

68.   E. Benedetto, M. Tredwell, C. Hollingworth, T. Khotavivattana, J. M. Brown and V. Gouverneur, *Chem. Sci.*, 2013, **4**, 89-96.

69.   J. H. Chun and V. W. Pike, *Organic and Biomolecular Chemistry*, 2013, **11**, 6300-6306.

70.   S. H. Liang, T. L. Collier, B. H. Rotstein, R. Lewis, M. Steck and N. Vasdev, *Chem. Commun. (Cambridge, U. K.)*, 2013, **49**, 8755-8757.

71.   G. S. Balz, G., *Ber. Dtsch. Chem. Ges.*, 1927, **60**, 1186-1190.

72.   A. Knochel and O. Zwernemann, *Appl. Radiat. Isot.*, 1991, **42**, 1077-1080.

73.   O. Wallach, *Justus Liebigs Annalen der Chemie*, 1886, **235**, 233-255.

74.   T. Pages and B. R. Langlois, *J. Fluorine Chem.*, 2001, **107**, 321-327.

75.   N. N. Ryzhikov, N. Seneca, R. N. Krasikova, N. A. Gomzina, E. Shchukin, O. S. Fedorova, D. A. Vassiliev, B. Gulyás, H. Hall, I. Savic and C. Halldin, *Nucl. Med. Biol.*, 2005, **32**, 109-116.

76.   K. Hamacher, H. H. Coenen and G. Stocklin, *Journal of Nuclear Medicine*, 1986, **27**, 235-238.

77.   F. Dollé, J. Helfenbein, F. Hinnen, S. Mavel, Z. Mincheva, W. Saba, M.-A. Schöllhorn-Peyronneau, H. Valette, L. Garreau, S. Chalon, C. Halldin, J.-C. Madelmont, J.-B. Deloye, M. Bottlaender, J. Le Gailliard, D. Guilloteau and P. Emond, *J. Labelled Compd. Radiopharm.*, 2007, **50**, 716-723.

78.   H. J. Machulla, A. Blocher, M. Kuntzsch, M. Piert, R. Wei and J. R. Grierson, *J. Radioanal. Nucl. Chem.*, 2000, **243**, 843-846.

79.   L. B. Been, A. J. H. Suurmeijer, D. C. P. Cobben, P. L. Jager, H. J. Hoekstra and P. H. Elsinga, *European Journal of Nuclear Medicine and Molecular Imaging*, 2004, **31**, 1659-1672.

80.   D. R. Hwang, C. S. Dence, T. A. Bonasera and M. J. Welch, *Appl. Radiat. Isot.*, 1989, **40**, 117-126.

81.   P. Ayotte, M. Hbert and P. Marchand, *J. Chem. Phys.*, 2005, **123**, 1-8.

82.   F. Dollé, *Curr. Pharm. Des.*, 2005, **11**, 3211-3235.
83.   F. Dollé, in *Ernst Schering Foundation Symposium Proceedings*, eds. P. A. Schubiger, L. Lehmann and M. Friebe, Springer-Verlag, Berlin, 2007, pp. 113-157.
84.   Y. S. Ding, F. Liang, J. S. Fowler, M. J. Kuhar and F. I. Carroll, *J. Labelled Compd. Radiopharm.*, 1997, **39**, 827-832.
85.   V. V. Grushin, *Acc. Chem. Res.*, 1992, **25**, 529-536.
86.   R. Huisgen, *Proceedings of the Chemical Society*, 1961, 357-396.
87.   H. C. Kolb, M. G. Finn and K. B. Sharpless, *Angew. Chem., Int. Ed.*, 2001, **40**, 2004-2021.
88.   M. Glaser and E. Årstad, *Bioconjugate Chem.*, 2007, **18**, 989-993.
89.   V. W. Pike and F. I. Aigbirhio, *J. Chem. Soc., Chem. Commun.*, 1995, 2215-2216.
90.   A. Shah, V. W. Pike and D. A. Widdowson, *J. Chem. Soc. Perkin Trans. 1*, 1998, 2043-2046.
91.   M. A. Carroll, J. Nairne and J. L. Woodcraft, *J. Labelled Compd. Radiopharm.*, 2007, **50**, 452-454.
92.   M. A. Carroll, S. Martin-Santamaria, V. W. Pike, H. S. Rzepa and D. A. Widdowson, *J. Chem. Soc. Perkin Trans. 2*, 1999, 2707-2714.
93.   S. Martin-Santamaria, M. A. Carroll, V. W. Pike, H. S. Rzepa and D. A. Widdowson, *J. Chem. Soc. Perkin Trans. 2*, 2000, 2158-2161.
94.   S. Martin-Santamaria, M. A. Carroll, C. M. Carroll, C. D. Carter, V. W. Pike, H. S. Rzepa and D. A. Widdowson, *Chem. Commun. (Cambridge, U. K.)*, 2000, 649-650.
95.   H. J. Wadsworth and T. Devenish, WO2005/097713, 2005.
96.   R. W. Weber, S. O'Day, M. Rose, R. Deck, P. Ames, J. Good, J. Meyer, R. Allen, S. Trautvetter, M. Timmerman, S. Cruickshank, M. Cook, R. Gonzalez and L. E. Spitler, *Journal of Clinical Oncology*, 2005, **23**, 8992-9000.
97.   M. Ochiai, *Top. Curr. Chem.*, 2003, **224**, 5-68.
98.   F. R. Wüst and T. Kniess, *J. Labelled Compd. Radiopharm.*, 2003, **46**, 699-713.
99.   J. Ermert, C. Hocke, T. Ludwig, R. Gail and H. H. Coenen, *J. Labelled Compd. Radiopharm.*, 2004, **47**, 429-441.
100.   M. A. Carroll, J. Nairne, G. Smith and D. A. Widdowson, *J. Fluorine Chem.*, 2007, **128**, 127-132.
101.   E. A. Merritt and B. Olofsson, *Angew. Chem., Int. Ed.*, 2009, **48**, 9052-9070.
102.   A. McKillop and D. Kemp, *Tetrahedron*, 1989, **45**, 3299-3306.
103.   M.-R. Zhang, K. Kumata and K. Suzuki, *Tetrahedron Lett.*, 2007, **48**, 8632-8635.
104.   C. Lemaire, P. Damhaut, A. Plenevaux, R. Cantineau, L. Christiaens and M. Guillaume, *International Journal of Radiation Applications and Instrumentation. Part A. Applied Radiation and Isotopes*, 1992, **43**, 485-494.
105.   R. Yan, L. Brichard, D. Soloviev, F. I. Aigbirhio and M. A. Carroll, *J. Labelled Compd. Radiopharm.*, 2009, **52**, 216.
106.   B. Leader, Q. J. Baca and D. E. Golan, *Nat Rev Drug Discov*, 2008, **7**, 21-39.
107.   S. Aggarwal, *Nat Biotech*, 2010, **28**, 1165-1171.
108.   S. Aggarwal, *Nat Biotech*, 2011, **29**, 1083-1089.
109.   S. Aggarwal, *Nat Biotech*, 2012, **30**, 1191-1197.
110.   M. R. Kilbourn, C. S. Dence, M. J. Welch and C. J. Mathias, *Journal of Nuclear Medicine*, 1987, **28**, 462-470.

111. Okarvi, *European Journal of Nuclear Medicine and Molecular Imaging*, 2001, **28**, 929-938.
112. B. Tavitian, in *Ernst Springer Research Foundation, Molecular Imaging*, Springer-Verlag, Berlin - Heidelberg - New York, 2004, pp. 1-34.
113. C. Lemaire, M. Guillaume, L. Christiaens, A. J. Palmer and R. Cantineau, *International Journal of Radiation Applications and Instrumentation. Part A. Applied Radiation and Isotopes*, 1987, **38**, 1033-1038.
114. G. Vaidyanathan and M. R. Zalutsky, *International Journal of Radiation Applications and Instrumentation. Part B. Nuclear Medicine and Biology*, 1992, **19**, 275-281.
115. G. Vaidyanathan and M. R. Zalutsky, *Nat. Protocols*, 2006, **1**, 1655-1661.
116. E. Hostetler, W. Edwards, C. Anderson and M. Welch, *J. Labelled Compd. Radiopharm.*, 1999, **42**, S720-S722.
117. L. Lang and W. C. Eckelman, *Appl. Radiat. Isot.*, 1994, **45**, 1155-1163.
118. S. Guhlke, H. H. Coenen and G. Stöcklin, *Appl. Radiat. Isot.*, 1994, **45**, 715-727.
119. C. M. Müller-Platz, G. Kloster, G. Legler and G. Stöcklin, *J. Labelled Compd. Radiopharm.*, 1982, **19**, 1645-1646.
120. D. Block, H. H. Coenen and G. Stöcklin, *J. Labelled Compd. Radiopharm.*, 1988, **25**, 185-200.
121. P. K. Garg, S. Garg and M. R. Zalutsky, *Bioconjugate Chem.*, 1991, **2**, 44-49.
122. M. Attina, F. Cacace and A. P. Wolf, *J. Chem. Soc., Chem. Commun.*, 1983, 108-109.
123. K. Hatano, T. Ido and R. Iwata, *J. Labelled Compd. Radiopharm.*, 1991, **29**, 373-380.
124. C. P. R. Hackenberger and D. Schwarzer, *Angew. Chem., Int. Ed.*, 2008, **47**, 10030-10074.
125. R. R. Flavell, P. Kothari, M. Bar-Dagan, M. Synan, S. Vallabhajosula, J. M. Friedman, T. W. Muir and G. Ceccarini, *J. Am. Chem. Soc.*, 2008, **130**, 9106-9112.
126. L. Li, M. N. Hopkinson, R. L. Yona, R. Bejot, A. D. Gee and V. Gouverneur, *Chem. Sci.*, 2011, **2**, 123-131.
127. Y. Shai, K. L. Kirk, M. A. Channing, B. B. Dunn, M. A. Lesniak, R. C. Eastman, R. D. Finn, J. Roth and K. A. Jacobson, *Biochemistry*, 1989, **28**, 4801-4806.
128. H. J. Wester and M. Schottelius, in *Ernst Schering Foundation Symposium Proceedings*, eds. P. A. Schubiger, L. Lehmann and M. Friebe, Springer-Verlag, Berlin, 2007, pp. 79-111.
129. C. Y. Shiue, A. P. Wolf and J. F. Hainfeld, *J. Labelled Compd. Radiopharm.*, 1989, **26**, 287-289.
130. W. Cai, X. Zhang, Y. Wu and X. Chen, *J Nucl Med*, 2006, **47**, 1172-1180.
131. T. Toyokuni, J. C. Walsh, A. Dominguez, M. E. Phelps, J. R. Barrio, S. S. Gambhir and N. Satyamurthy, *Bioconjugate Chem.*, 2003, **14**, 1253-1259.
132. M. Berndt, J. Pietzsch and F. Wuest, *Nucl. Med. Biol.*, 2007, **34**, 5-15.
133. B. de Bruin, B. Kuhnast, F. Hinnen, L. Yaouancq, M. Amessou, L. Johannes, A. Samson, R. Boisgard, B. Tavitian and F. Dollé, *Bioconjugate Chem.*, 2005, **16**, 406-420.
134. J. A. H. Inkster, K. Liu, S. Ait-Mohand, P. Schaffer, B. Guérin, T. J. Ruth and T. Storr, *Chemistry – A European Journal*, 2012, **18**, 11079-11087.

135. F. Wuest, L. Köhler, M. Berndt and J. Pietzsch, *Amino Acids*, 2009, **36**, 283-295.
136. F. Wuest, M. Berndt, R. Bergmann, J. van den Hoff and J. Pietzsch, *Bioconjugate Chem.*, 2008, **19**, 1202-1210.
137. W. J. McBride, C. A. D'Souza, R. M. Sharkey and D. M. Goldenberg, *Appl. Radiat. Isot.*, 2012, **70**, 200-204.
138. X. Yue, D. O. Kiesewetter, J. Guo, Z. Sun, X. Zhang, L. Zhu, G. Niu, Y. Ma, L. Lang and X. Chen, *Bioconjugate Chem.*, 2013, **24**, 1191-1200.
139. J. K. Willmann, N. van Bruggen, L. M. Dinkelborg and S. S. Gambhir, *Nat Rev Drug Discov*, 2008, **7**, 591-607.
140. K. G. Petrov, Y.-M. Zhang, M. Carter, G. S. Cockerill, S. Dickerson, C. A. Gauthier, Y. Guo, R. A. Mook Jr, D. W. Rusnak, A. L. Walker, E. R. Wood and K. E. Lackey, *Bioorg. Med. Chem. Lett.*, 2006, **16**, 4686-4691.
141. K. J. Kimball, T. M. Numnum, T. O. Kirby, W. C. Zamboni, J. M. Estes, M. N. Barnes, D. E. Matei, K. M. Koch and R. D. Alvarez, *Gynecologic Oncology*, 2008, **111**, 95-101.
142. T. Hara, N. Kosaka and H. Kishi, *Journal of Nuclear Medicine*, 2002, **43**, 187-199.
143. T. Steuber, T. Schlomm, H. Heinzer, M. Zacharias, S. Ahyai, K. F. Chun, A. Haese, S. Klutmann, J. Köllermann, G. Sauter, J. Mester, P. Mikecz, M. Fisch, H. Huland, M. Graefen and G. Salomon, *European Journal of Cancer*, 2010, **46**, 449-455.
144. J. Kolthammer, D. Corn, N. Tenley, C. Wu, H. Tian, Y. Wang and Z. Lee, *European Journal of Nuclear Medicine and Molecular Imaging*, 2011, **38**, 1248-1256.
145. P. Kazmierczak, L. Skulski and L. Kraszkiewicz, *Molecules*, 2001, **6**, 881-891.
146. A. Zielinska and L. Skulski, *Molecules*, 2002, **7**, 806-809.
147. T. K. Page and T. Wirth, *Synthesis*, 2006, 3153-3155.
148. C. Ye, B. Twamley and J. n. M. Shreeve, *Org. Lett.*, 2005, **7**, 3961-3964.
149. H. Tohma, A. Maruyama, A. Maeda, T. Maegawa, T. Dohi, M. Shiro, T. Morita and Y. Kita, *Angew. Chem., Int. Ed.*, 2004, **43**, 3595-3598.
150. A. McKillop and W. R. Sanderson, *Tetrahedron*, 1995, **51**, 6145-6166.
151. L. F. Silva Jr, R. S. Vasconcelos and N. P. Lopes, *Int. J. Mass Spectrom.*, 2008, **276**, 24-30.
152. J. K. Stille, *Angew. Chem., Int. Ed.,*, 1986, **25**, 508-524.
153. X.-F. Wu, H. Neumann and M. Beller, *Chem. Rev. (Washington, DC, U. S.)*, 2012, **113**, 1-35.
154. J. L. Sessler, B. Wang and A. Harriman, *J. Am. Chem. Soc.*, 1995, **117**, 704-714.
155. V. Farina, B. Krishnan, D. R. Marshall and G. P. Roth, *J. Org. Chem.*, 1993, **58**, 5434-5444.
156. L. Torun, B. K. Madras and P. C. Meltzer, *Bioorg. Med. Chem.*, 2012, **20**, 2762-2772.
157. C. Gosmini and J. Perichon, *Org. Biomol. Chem.*, 2005, **3**, 216-217.
158. H. Fillon, C. Gosmini and J. Périchon, *J. Am. Chem. Soc.*, 2003, **125**, 3867-3870.
159. S. S. Al-Deyab and M. H. El-Newehy, *Molecules*, 2010, **15**, 1425-1432.
160. G. F. Koser, R. H. Wettach and C. S. Smith, *J. Org. Chem.*, 1980, **45**, 1543-1544.

161. *Private communication.* M. A. Carroll.
162. R. M. Moriarty and O. Prakash, *Acc. Chem. Res.*, 1986, **19**, 244-250.
163. R. S. Berry, *The Journal of Chemical Physics*, 1960, **32**, 933-938.
164. L. Farrugia, *J. Appl. Crystallogr.*, 1997, **30**, 565.
165. G. A. Olah, J. T. Welch, Y. D. Vankar, M. Nojima, I. Kerekes and J. A. Olah, *J. Org. Chem.*, 1979, **44**, 3872-3881.
166. R. G. Clewley, F. Fischer and G. N. Henderson, *Can. J. Chem.*, 1989, **67**, 1472-1479.
167. R. T. VanVleck, *J. Am. Chem. Soc.*, 1949, **71**, 3256-3257.
168. F. Basuli, H. Wu and G. L. Griffiths, *J. Labelled Compd. Radiopharm.*, 2011, **54**, 224-228.
169. M. Bielawski, M. Zhu and B. Olofsson, *Adv. Synth. Catal.*, 2007, **349**, 2610-2618.
170. A. J. Palmer, J. C. Clark and R. W. Goulding, *Radiopharmaceuticals and Other Compounds Labelled with Short-lived Radionuclides*, Pergamon, New York, 1977.
171. M. A. Carroll, V. W. Pike and D. A. Widdowson, *Tetrahedron Lett.*, 2000, **41**, 5393-5396.
172. K. M. Lancer and G. H. Wiegand, *J. Org. Chem.*, 1976, **41**, 3360-3364.
173. M. A. Carroll, C. Jones and S.-L. Tang, *J. Labelled Compd. Radiopharm.*, 2007, **50**, 450-451.
174. T. Ross, J. Ermert and H. H. Coenen, *J. Labelled Compd. Radiopharm.*, 2005, **48**, S153.
175. M. Carroll, R. Yan, F. Aigbirhio, D. Soloviev and L. Brichard, *Journal of Nuclear Medicine*, 2008, **49S**, 298P.
176. J.-H. Chun, S. Lu and V. W. Pike, *Eur. J. Org. Chem.*, 2011, **2011**, 4439-4447.
177. J. Chun, S. Lu and V. W. Pike, *J. Labelled Compd. Radiopharm.*, 2009, **52**, S2.
178. P. P. Onys'ko, T. V. Kim, O. I. Kiseleva, Y. V. Rassukana and A. A. Gakh, *J. Fluorine Chem.*, 2009, **130**, 501-504.
179. G. Pascali, S. Pitzianti, G. Saccomanni, S. Del Carlo, C. Manera, M. Macchia and P. A. Salvadori, *J. Labelled Compd. Radiopharm.*, 2011, **54**, S502.
180. J.-H. Chun and V. W. Pike, *J. Labelled Compd. Radiopharm.*, 2011, **54**, S482.
181. S. Selivanova, A. P. Schubiger, S. M. Ametamey, T. Stellfeld, T. K. Heinrich, J. Meding, M. Bauser and J. Hütter, *J. Labelled Compd. Radiopharm.*, 2011, **54**, O005.
182. W. Adcock and T. C. Khor, *J. Organomet. Chem.*, 1975, **91**, C20.
183. S. Rodmar, B. Rodmar and M. K. Sharma, *Acta Chem. Scand.*, 1968, **22**, 907-920.
184. R. D. Schuetz, D. D. Taft, J. P. O'Brien, J. L. Shea and H. M. Mork, *J. Org. Chem.*, 1963, **28**, 1420-1422.
185. S. Rodmar, L. Moraga, S. Gronowitz and U. Rosen, *Acta Chem. Scand.*, 1971, **25**, 3309-3323.
186. S. Rodmar, S. Gronowitz and U. Rosen, *Acta Chem. Scand.*, 1971, **25**, 3841-3854.
187. S. Gronowitz, I. Johnson and S. Rodmar, *Acta Chem. Scand.*, 1972, **26**, 1726-1727.
188. S. D. Taylor, C. C. Kotoris and G. Hum, *Tetrahedron*, 1999, **55**, 12431-12477.

189. M. C. Law, K.-Y. Wong and T. H. Chan, *Chem. Commun.*, 2006, 2457-2459.
190. H. Dungan and R. Van Wazer, *Compilation of Reported 19F-NMR Chemical Shifts* John Wiley & Sons, Inc., 1970.
191. P. V. Roberts and R. York, *Ind. Eng. Chem. Process Des. Dev.*, 1967, **6**, 516-525.
192. S. D. Manjare and A. K. Ghoshal, *The Canadian Journal of Chemical Engineering*, 2005, **83**, 232-241.
193. H. J. Lee, J. M. Jeong, G. Rai, Y. S. Lee, Y. S. Chang, Y. J. Kim, H. W. Kim, D. S. Lee, J. K. Chung, I. Mook-Jung and M. C. Lee, *Nucl. Med. Biol.*, 2009, **36**, 107-116.
194. V. R. Meyer, *Pitfalls and Errors of HPLC in Pictures*, Huthig, 1997.
195. N. Matuszak, G. G. Muccioli, G. Labar and D. M. Lambert, *J. Med. Chem.*, 2009, **52**, 7410-7420.
196. J. V. Crivello and J. H. W. Lam, 1979.
197. M. Bielawski and B. Olofsson, *Chem. Commun. (Cambridge, U. K.)*, 2007, 2521-2523.
198. A. I. Vogel, B. S. Furniss, A. J. Hannaford, V. Rogers, P. W. G. Smith and A. R. Tatchell, *Vogel's Textbook of Practical Organic Chemistry*, 1978.
199. G. F. Koser and R. H. Wettach, *J. Org. Chem.*, 1980, **45**, 1542-1543.
200. http://www.alliancemedical.co.uk/erigal, Accessed 10/8/14.
201. http://abt-mi.com/en/our-solutions/overview, Accessed 12/12/13.
202. M. A. Carroll, G. G. Launay, C. D. Reed and S. J. Hobson, *J. Labelled Compd. Radiopharm.*, 2011, **54**, S554.
203. B. S. Moon, H. S. Kil, J. H. Park, J. S. Kim, J. Park, D. Y. Chi, B. C. Lee and S. E. Kim, *Org. Biomol. Chem.*, 2011, **9**, 8346-8355.
204. B. Shen, D. Löffler, K.-P. Zeller, M. Übele, G. Reischl and H.-J. Machulla, *J. Fluorine Chem.*, 2007, **128**, 1461-1468.
205. X. Li, J. M. Link, S. Stekhova, K. J. Yagle, C. Smith, K. A. Krohn and J. F. Tait, *Bioconjugate Chem.*, 2008, **19**, 1684-1688.
206. H. Sun and S. G. DiMagno, *J. Fluorine Chem.*, 2007, **128**, 806-812.
207. O. Åberg, F. Pisaneschi, G. Smith, Q.-D. Nguyen, E. Stevens and E. O. Aboagye, *J. Fluorine Chem.*, 2012, **135**, 200-206.
208. N. Fujii, S. Oishi, K. Hiramatsu, T. Araki, S. Ueda, H. Tamamura, A. Otaka, S. Kusano, S. Terakubo, H. Nakashima, J. A. Broach, J. O. Trent, Z.-x. Wang and S. C. Peiper, *Angew. Chem., Int. Ed.*, 2003, **42**, 3251-3253.
209. T. J. McCarthy, A. U. Sheriff, M. J. Graneto, J. J. Talley and M. J. Welch, *Journal of Nuclear Medicine*, 2002, **43**, 117-124.
210. C. Lemaire, L. Libert, A. Plenevaux, J. Aerts, X. Franci and A. Luxen, *J. Fluorine Chem.*, 2012, **138**, 48-55.
211. F. Basuli, H. Wu, C. Li, Z.-D. Shi, A. Sulima and G. L. Griffiths, *J. Labelled Compd. Radiopharm.*, 2011, **54**, 633-636.
212. https://www.comecer.com/nuclear-medicine/radiochemistry-pet-cyclotron-conventional-nuclear-medicine/shielded-door-for-bunker/shielded-doors-for-cyclotron-bunker-model-pmc/, Accessed 10/01/2013.
213. T. T. Nguyen and J. C. Martin, in *Comprehensive Heterocyclic Chemistry*, eds. A. R. Katritzky and C. W. Rees, Pergamon, Oxford, 1984, pp. 563-572.
214. G. F. Koser, in *PATAI'S Chemistry of Functional Groups*, John Wiley & Sons, Ltd, 2009.
215. M. Tordeux and C. Wakselman, *Synth. Commun.*, 1982, **12**, 513-520.

216. J. H. Clark, A. J. Hyde and D. K. Smith, *J. Chem. Soc., Chem. Commun.*, 1986, 791-793.
217. S. Dermeik and Y. Sasson, *J. Org. Chem.*, 1985, **50**, 879-882.
218. D. Landini, A. Maia and A. Rampoldi, *J. Org. Chem.*, 1989, **54**, 328-332.
219. J.-H. Chun, S. Lu, Y.-S. Lee and V. W. Pike, *J. Org. Chem.*, 2010, **75**, 3332-3338.
220. M. Charlton and M. A. Carroll, *J. Labelled Compd. Radiopharm.*, 2012, **56**, 57-58.
221. M. Charlton and M. A. Carroll, *J. Labelled Compd. Radiopharm.*, 2012, **56**, S152.
222. J. H. Chun, S. Telu, S. Lu and V. W. Pike, *Organic and Biomolecular Chemistry*, 2013, **11**, 5094-5099.
223. M. Kuntzsch, D. Lamparter, N. Brüggener, M. Müller, G. Kienzle and G. Reischl, *Pharmaceuticals*, 2014, **7**, 621-633.
224. C.-G. Zhan and D. A. Dixon, *The Journal of Physical Chemistry A*, 2004, **108**, 2020-2029.
225. D. D. Kemp and M. S. Gordon, *The Journal of Physical Chemistry A*, 2005, **109**, 7688-7699.
226. M. Trumm, Y. O. G. Martínez, F. Réal, M. Masella, V. Vallet and B. Schimmelpfennig, *The Journal of Chemical Physics*, 2012, **136**, -.
227. J. J. R. Pliego and D. Pilo-Veloso, *Phys. Chem. Chem. Phys.*, 2008, **10**, 1118-1124.
228. A. E. Feiring, *J. Org. Chem.*, 1980, **45**, 1958-1961.
229. J. H. Clark, *Chem. Rev. (Washington, DC, U. S.)*, 1980, **80**, 429-452.
230. R. K. Sharma and J. L. Fry, *J. Org. Chem.*, 1983, **48**, 2112-2114.
231. N. Ichiishi, A. F. Brooks, J. J. Topczewski, M. E. Rodnick, M. S. Sanford and P. J. H. Scott, *Org. Lett.*, 2014, **16**, 3224-3227.
232. M. Tredwell, S. M. Preshlock, N. J. Taylor, S. Gruber, M. Huiban, J. Passchier, J. Mercier, C. Génicot and V. Gouverneur, *Angew. Chem., Int. Ed.*, 2014, **53**, 7751-7755.
233. R. J. Errington, *Advanced Practical Inorganic and Metalorganic Chemistry*, Blackie Academic and Professional, London, 1997.
234. D. B. Dess and J. C. Martin, *J. Am. Chem. Soc.*, 1991, **113**, 7277-7287.
235. H. Tohma, S. Takizawa, T. Maegawa and Y. Kita, *Angew. Chem., Int. Ed.*, 2000, **39**, 1306-1308.
236. J. E. Leffler and L. J. Story, *J. Am. Chem. Soc.*, 1967, **89**, 2333-2338.
237. H. Togo, T. Nabana and K. Yamaguchi, *J. Org. Chem.*, 2000, **65**, 8391-8394.
238. F. M. Beringer, H. E. Bachofner, R. A. Falk and M. Leff, *J. Am. Chem. Soc.*, 1958, **80**, 4279-4281.
239. M. A. Carroll and R. A. Wood, *Tetrahedron*, 2007, **63**, 11349-11354.

7 Appendix

Note that further appendices may be found on the accompanying CD.

7.1 Crystal data and structure refinement for 4-formylphenyl(4-anisyl)iodonium trifluoroacetate (44)

Chemical formula (moiety)	$C_{16}H_{12}F_3IO_4$
Chemical formula (total)	$C_{16}H_{12}F_3IO_4$
Formula weight	452.16
Temperature	150(2) K
Radiation, wavelength	MoKα, 0.71073 Å
Crystal system, space group	monoclinic, P12$_1$/c1
Unit cell parameters	a = 5.7022(4) Å $\qquad$ $\alpha = 90°$
	b = 17.4185(13) Å $\qquad$ $\beta = 97.454(7)°$
	c = 16.6821(11) Å $\qquad$ $\gamma = 90°$
Cell volume	1642.9(2) Å^3
Z	4
Calculated density	1.828 g/cm^3
Absorption coefficient μ	1.998 mm^{-1}
F(000)	880
Reflections for cell refinement	2037 (θ range 3.4 to 28.6°)
Data collection method	Xcalibur, Atlas, Gemini ultra thick-slice ω scans
θ range for data collection	3.4 to 25.0°
Index ranges	h −6 to 6, k −17 to 20, l −16 to 19
Completeness to $\theta = 25.0°$	99.8 %
Reflections collected	7100
Independent reflections	2887 (R$_{int}$ = 0.0646)
Reflections with $F^2 > 2\sigma$	1957
Absorption correction	semi-empirical from equivalents
Min. and max. transmission	0.63325 and 1.00000
Structure solution	direct methods
Refinement method	Full-matrix least-squares on F^2
Weighting parameters a, b	0.0646, 0.0000
Data / restraints / parameters	2887 / 0 / 218
Final R indices [$F^2 > 2\sigma$]	R1 = 0.0625, wR2 = 0.1277
R indices (all data)	R1 = 0.1019, wR2 = 0.1492
Goodness-of-fit on F^2	1.034
Largest and mean shift/su	0.000 and 0.000
Largest diff. peak and hole	1.39 and −1.97 e Å^{-3}

7.2 Crystal data and structure refinement for 4-formylphenyl(2-thienyl)iodonium trifluoroacetate (45)

Chemical formula (moiety)	$C_{13}H_8F_3IO_3S$
Chemical formula (total)	$C_{13}H_8F_3IO_3S$
Formula weight	428.15
Temperature	150(2) K
Radiation, wavelength	MoKα, 0.71073 Å
Crystal system, space group	monoclinic, C2/c
Unit cell parameters	a = 23.0590(13) Å $\quad$ α = 90°
	b = 8.0398(3) Å $\quad$ β = 110.324(6)°
	c = 16.4429(8) Å $\quad$ γ = 90°
Cell volume	2858.6(2) Å^3
Z	8
Calculated density	1.990 g/cm^3
Absorption coefficient μ	2.426 mm^{-1}
F(000)	1648
Reflections for cell refinement	9027 (θ range 2.9 to 28.6°)
Data collection method	Xcalibur, Atlas, Gemini ultra
	thick-slice ω scans
θ range for data collection	2.9 to 28.6°
Index ranges	h −30 to 29, k −10 to 10, l −17 to 20
Completeness to θ = 25.0°	99.8 %
Reflections collected	15278
Independent reflections	3274 (R_{int} = 0.0381)
Reflections with $F^2 > 2\sigma$	2852
Absorption correction	semi-empirical from equivalents
Min. and max. transmission	0.72172 and 1.00000
Structure solution	direct methods
Refinement method	Full-matrix least-squares on F^2
Weighting parameters a, b	0.0205, 5.1722
Data / restraints / parameters	3274 / 0 / 209
Final R indices [$F^2 > 2\sigma$]	R1 = 0.0248, wR2 = 0.0503
R indices (all data)	R1 = 0.0335, wR2 = 0.0539
Goodness-of-fit on F^2	1.066
Largest and mean shift/su	0.001 and 0.000
Largest diff. peak and hole	1.12 and −0.72 e Å^{-3}

7.3 Crystal data and structure refinement for 3-formylphenyl(phenyl)iodonium trifluoroacetate (50)

Chemical formula (moiety)	$C_{15}H_{10}F_3IO_3$
Chemical formula (total)	$C_{15}H_{10}F_3IO_3$
Formula weight	422.13
Temperature	150(2) K
Radiation, wavelength	MoKα, 0.71073 Å
Crystal system, space group	triclinic, P$\bar{1}$
Unit cell parameters	a = 8.1943(4) Å α= 98.177(4)°
	b = 8.2924(5) Å β = 103.038(4)°
	c = 11.7005(6) Å γ = 101.490(4)°
Cell volume	744.30(7) Å^3
Z	2
Calculated density	1.884 g/cm^3
Absorption coefficient μ	2.193 mm^{-1}
F(000)	408
Crystal colour and size	colourless, 0.20 × 0.20 × 0.15 mm^3
Reflections for cell refinement	4414 (θ range 2.8 to 28.6°)
Data collection method	Xcalibur, Atlas, Gemini ultra
	thick-slice ω scans
θ range for data collection	2.8 to 28.6°
Index ranges	h −10 to 10, k −10 to 9, l −15 to 15
Completeness to θ = 26.0°	97.3 %
Reflections collected	6132
Independent reflections	3093 (R$_{int}$ = 0.0271)
Reflections with F^2>2σ	2900
Absorption correction	semi-empirical from equivalents
Min. and max. transmission	0.6682 and 0.7345
Structure solution	direct methods
Refinement method	Full-matrix least-squares on F^2
Weighting parameters a, b	0.0306, 1.5647
Data / restraints / parameters	3093 / 0 / 200
Final R indices [F^2>2σ]	R1 = 0.0289, wR2 = 0.0727
R indices (all data)	R1 = 0.0314, wR2 = 0.0744
Goodness-of-fit on F^2	1.101
Extinction coefficient	0.0016(7)
Largest and mean shift/su	0.000 and 0.000
Largest diff. peak and hole	1.42 and −0.56 e Å^{-3}

7.4 Crystal data and structure refinement for 3-formylphenyl(4-anisyl)iodonium trifluoroacetate (51)

Chemical formula (moiety)	$C_{14}H_{12}IO_2^+ \cdot C_2F_3O_2^- \cdot CH_2Cl_2$
Chemical formula (total)	$C_{17}H_{14}Cl_2F_3IO_4$
Formula weight	537.08
Temperature	150(2) K
Radiation, wavelength	MoKα, 0.71073 Å
Crystal system, space group	triclinic, P$\overline{1}$
Unit cell parameters	a = 5.9676(3) α = 91.507(4)°
	b = 12.4791(5) Å β = 93.060(4)°
	c = 13.5288(7) Å γ = 95.936(4)°
Cell volume	1000.15(8) Å^3
Z	2
Calculated density	1.783 g/cm^3
Absorption coefficient μ	1.915 mm^{-1}
F(000)	524
Crystal colour and size	colourless, $0.34 \times 0.30 \times 0.10$ mm^3
Reflections for cell refinement	4163 (θ range 3.0 to 29.6°)
Data collection method	Xcalibur, Atlas, Gemini ultra
	thick-slice ω scans
θ range for data collection	3.0 to 29.7°
Index ranges	h −6 to 8, k −15 to 17, l −17 to 17
Completeness to θ = 26.0°	99.9 %
Reflections collected	9247
Independent reflections	4734 (R$_{int}$ = 0.0323)
Reflections with F^2>2σ	4188
Absorption correction	semi-empirical from equivalents
Min. and max. transmission	0.5621 and 0.8316
Structure solution	direct methods
Refinement method	Full-matrix least-squares on F^2
Weighting parameters a, b	0.0326, 1.3833
Data / restraints / parameters	4734 / 6 / 273
Final R indices [F^2>2σ]	R1 = 0.0347, wR2 = 0.0783
R indices (all data)	R1 = 0.0430, wR2 = 0.0840
Goodness-of-fit on F^2	1.047
Largest and mean shift/su	0.003 and 0.000
Largest diff. peak and hole	1.54 and −0.80 e Å^{-3}

7.5 Crystal data and structure refinement for 3-formylphenyl(2-thienyl)iodonium trifluoroacetate (52)

Chemical formula (moiety)	$C_{13}H_8F_3IO_3S$
Chemical formula (total)	$C_{13}H_8F_3IO_3S$
Formula weight	428.15
Temperature	150(2) K
Radiation, wavelength	MoKα, 0.71073 Å
Crystal system, space group	monoclinic, C2/c
Unit cell parameters	a = 23.0590(13) Å α = 90°
	b = 8.0398(3) Å β = 110.324(6)°
	c = 16.4429(8) Å γ = 90°
Cell volume	2858.6(2) Å^3
Z	8
Calculated density	1.990 g/cm^3
Absorption coefficient μ	2.426 mm^{-1}
F(000)	1648
Reflections for cell refinement	9027 (θ range 2.9 to 28.6°)
Data collection method	Xcalibur, Atlas, Gemini ultra thick-slice ω scans
θ range for data collection	2.9 to 28.6°
Index ranges	h −30 to 29, k −10 to 10, l −17 to 20
Completeness to θ = 25.0°	99.8 %
Reflections collected	15278
Independent reflections	3274 (R$_{int}$ = 0.0381)
Reflections with F^2>2σ	2852
Absorption correction	semi-empirical from equivalents
Min. and max. transmission	0.72172 and 1.00000
Structure solution	direct methods
Refinement method	Full-matrix least-squares on F^2
Weighting parameters a, b	0.0205, 5.1722
Data / restraints / parameters	3274 / 0 / 209
Final R indices [F^2>2σ]	R1 = 0.0248, wR2 = 0.0503
R indices (all data)	R1 = 0.0335, wR2 = 0.0539
Goodness-of-fit on F^2	1.066
Largest and mean shift/su	0.001 and 0.000
Largest diff. peak and hole	1.12 and −0.72 e Å^{-3}

7.6 Crystal data and structure refinement for 2-thienyl(phenyl)iodonium trifluoroacetate (57)

Empirical formula	$C_{12}H_8O_2F_3SI$
Formula weight	400.14
Temperature/K	0.0
Crystal system	monoclinic
Space group	$P2_1/n$
a/Å	9.9078(7)
b/Å	22.2153(13)
c/Å	12.2494(7)
α/°	90
β/°	90.845(2)
γ/°	90
Volume/Å^3	2695.9(3)
Z	8
ρ_{calc}g/cm^3	1.972
μ/mm^{-1}	2.559
F(000)	1536.0
Crystal size/mm^3	$0.336 \times 0.146 \times 0.145$
Radiation	MoKα ($\lambda = 0.71073$)
2Θ range for data collection/°	4.502 to 50.694
Index ranges	$-11 \leq h \leq 11, 0 \leq k \leq 26, 0 \leq l \leq 14$
Reflections collected	4944
Independent reflections	4944 [R_{int} = ?, R_{sigma} = 0.0503]
Data/restraints/parameters	4944/1149/516
Goodness-of-fit on F^2	1.133
Final R indexes [I>=2σ (I)]	$R_1 = 0.0624$, $wR_2 = 0.1568$
Final R indexes [all data]	$R_1 = 0.0672$, $wR_2 = 0.1621$
Largest diff. peak/hole / e Å^{-3}	5.63/-1.55

7.7 Crystal data and structure refinement for 2-thienyl(4-anisyl)iodonium trifluoroacetate (58)

Empirical formula	$C_{13}H_{10}O_3F_3SI$
Formula weight	430.17
Temperature/K	120.0(2)
Crystal system	triclinic
Space group	P-1
a/Å	8.2626(5)
b/Å	9.2855(5)
c/Å	11.5270(6)
α/°	67.2341(15)
β/°	80.1262(15)
γ/°	65.0867(14)
Volume/Å^3	739.56(7)
Z	2
ρ_{calc}g/cm^3	1.932
μ/mm^{-1}	2.345
F(000)	416.0
Crystal size/mm^3	$0.23 \times 0.11 \times 0.09$
Radiation	MoKα (λ = 0.71073)
2Θ range for data collection/°	5.168 to 50.698
Index ranges	-9 ≤ h ≤ 9, -11 ≤ k ≤ 11, -13 ≤ l ≤ 13
Reflections collected	9049
Independent reflections	2706 [R$_{int}$ = 0.0218, R$_{sigma}$ = 0.0211]
Data/restraints/parameters	2706/289/225
Goodness-of-fit on F^2	1.100
Final R indexes [I>=2σ (I)]	R$_1$ = 0.0183, wR$_2$ = 0.0447
Final R indexes [all data]	R$_1$ = 0.0196, wR$_2$ = 0.0454
Largest diff. peak/hole / e Å^{-3}	0.49/-0.49

7.8 Crystal data and structure refinement for 2-thienyl(2-thienyl)iodonium trifluoroacetate (59)

Empirical formula	$C_{10}H_6O_2F_3IS_2$
Formula weight	406.17
Temperature/K	150.0(2)
Crystal system	triclinic
Space group	P-1
a/Å	7.1291(4)
b/Å	8.3112(5)
c/Å	11.9268(7)
α/°	103.2231(16)
β/°	104.6033(15)
γ/°	105.3008(17)
Volume/Å^3	625.73(6)
Z	2
ρ_{calc}g/cm^3	2.156
μ/mm^{-1}	2.919
F(000)	388.0
Crystal size/mm^3	$0.27 \times 0.19 \times 0.07$
Radiation	MoKα ($\lambda = 0.71073$)
2Θ range for data collection/°	5.356 to 55.146
Index ranges	$-9 \leq h \leq 9$, $-10 \leq k \leq 10$, $-15 \leq l \leq 15$
Reflections collected	8948
Independent reflections	2893 [$R_{int} = 0.0200$, $R_{sigma} = 0.0183$]
Data/restraints/parameters	2893/210/189
Goodness-of-fit on F^2	1.065
Final R indexes [I>=2σ (I)]	$R_1 = 0.0175$, $wR_2 = 0.0446$
Final R indexes [all data]	$R_1 = 0.0182$, $wR_2 = 0.0449$
Largest diff. peak/hole / e Å^{-3}	1.06/-0.48

7.9 Crystal data and structure refinement for 4-iodo-*N*-phenylmaleimide (63)

Chemical formula (moiety)	$C_{10}H_6INO_2$
Chemical formula (total)	$C_{10}H_6INO_2$
Formula weight	299.06
Temperature	150(2) K
Radiation, wavelength	MoKα, 0.71073 Å
Crystal system, space group	orthorhombic, $P2_12_12_1$
Unit cell parameters	a = 6.6205(5) Å $\quad\quad$ $\alpha = 90°$
	b = 7.4850(6) Å $\quad\quad$ $\beta = 90°$
	c = 19.7683(13) Å $\quad$ $\gamma = 90°$
Cell volume	979.61(13) Å^3
Z	4
Calculated density	2.028 g/cm^3
Absorption coefficient μ	3.239 mm^{-1}
F(000)	568
Crystal colour and size	, 0.30 × 0.04 × 0.04 mm^3
Reflections for cell refinement	1547 (θ range 4.1 to 27.6°)
Data collection method	Xcalibur, Atlas, Gemini ultra thick-slice ω scans
θ range for data collection	2.9 to 28.7°
Index ranges	h −8 to 6, k −10 to 9, l −25 to 20
Completeness to $\theta = 25.0°$	99.9 %
Reflections collected	4151
Independent reflections	2064 ($R_{int} = 0.0283$)
Reflections with $F^2 > 2\sigma$	1878
Absorption correction	semi-empirical from equivalents
Min. and max. transmission	0.4432 and 0.8813
Structure solution	direct methods
Refinement method	Full-matrix least-squares on F^2
Weighting parameters a, b	0.0099, 0.0000
Data / restraints / parameters	2064 / 0 / 128
Final R indices [$F^2 > 2\sigma$]	R1 = 0.0275, wR2 = 0.0440
R indices (all data)	R1 = 0.0354, wR2 = 0.0485
Goodness-of-fit on F^2	1.067
Absolute structure parameter	−0.03(3)
Extinction coefficient	0.0013(3)
Largest and mean shift/su	0.001 and 0.000
Largest diff. peak and hole	0.59 and −0.63 e Å^{-3}

7.10 Crystal data and structure refinement for 4-*N*-phenylmaleimide(phenyl)iodonium trifluoroacetate (69)

Empirical formula	$C_{18}H_{13}NO_3F_3I$
Formula weight	508.09
Temperature/K	150.00(10)
Crystal system	monoclinic
Space group	$P2_1/n$
a/Å	11.7417(4)
b/Å	6.62347(19)
c/Å	27.4536(9)
α/°	90
β/°	93.635(3)
γ/°	90
Volume/Å^3	2130.80(12)
Z	4
ρ_{calc}mg/mm^3	1.584
m/mm^{-1}	1.778
F(000)	992.0
Crystal size/mm^3	$0.8315 \times 0.1191 \times 0.04$
2Θ range for data collection	7.066 to 58.14°
Index ranges	$-15 \leq h \leq 15$, $-8 \leq k \leq 8$, $-36 \leq l \leq 36$
Reflections collected	29746
Independent reflections	4513[R(int) = 0.0471]
Data/restraints/parameters	4513/0/281
Goodness-of-fit on F^2	1.165
Final R indexes [I>=2σ (I)]	$R_1 = 0.0418$, $wR_2 = 0.0837$
Final R indexes [all data]	$R_1 = 0.0514$, $wR_2 = 0.0873$
Largest diff. peak/hole / e Å^{-3}	0.88/-0.74

7.11 Macros

The following bespoke macros were used to control various stages of the microfluidic preparation of radiolabeled compounds using the Advion NanoTek LF software.

7.11.1   Fluorine-18 Drying Macro

0   Wait Drying macro. Ensure needle is fully inserted into target water vial. Ensure QMA cartridge is loaded. Ensure all solutions are prepared and installed. Ensure all plumbing is correct.

1000
     L37020000800054   ──────────────────────────L3602000300004E
     ─────────────────────────   Set Conc 1 to 80oC
2000 /5o1V1200A6000M3000o5V1200A0M2000R Load target water
15000 /5o6V1200A6000M2000o3V1200A0R Remove target water
15000
     L3702000100004D   ──────────────────────────L3602000300004E
     ─────────────────────────   Set Conc 1 to 100oC
2000 /7U2M5000U1M5000u2R   Turn on the Nitrogen
10000 /5o2V1000P5000M2000go5V400D750M15000G4o2V2000A0R   Add   400 uL of PTA
105000   /5M90000R   Wait 100s for conc vial to dry PTA solution

100000
     /5o4V1000P6000M2000o5V75D3600M2000o6V75D1200M2000o2V2000A0R
     Add 400 uL of MeCN (1) and flush back PTA line
75000 /5M30000R   Wait 20s for conc vial to dry MeCN (1)
20000 /5o4V1000P6000M2000o6V75D3600M2000o2V2000A0R   Add   400 uL of MeCN (2) and flush back PTA line
45000 /5M30000R   Wait 20s for conc vial to dry MeCN (2)
20000 /7u1R Turn off the Nitrogen
2000 /3o1V2000A0M2000o8V2000A15600M2000o6V800A0R   Add 325 uL of DMF
40000 /3go4V1600A19200M2000V3200A0M2000G6o8V3200A3600M2000o4V3200A0R
     Mix the solvent with the fluoride. Add 75 uL of DMF to flush line F

140000

L37020000250053 ——————————————————L3602000300004E

Set Conc 1 to 25oC

2000 Wait End of drying macro. Pump 3 can now be prepared.

7.11.2   Autodiscovery Mode Cleaning

2000 Wait P1,2,3 reagent lines will be back-flushed. Place Reactor
outlet into waste

1000
/1o1V3200A0o8A48000M1000o1A0o8A48000M1000o4V1600A0o8V3200A48000M1000
o3V100A0R   P1, Clean reagent line, loop and load line

5000
/2o1V3200A0o8A48000M1000o1A0o8A48000M1000o4V1600A0o8V3200A48000M1000
o3V100A0R   P2, Clean reagent line, loop and load line

2000 /7o1R Hub to Waste (A)

5000
/3o1V3200A0o8A48000M1000o1A0o8A48000M1000o4V1600A0o8V3200A24000o3V10
0A0R P3, Clean reagent line, loop and load line Sweep

1000 /6go4V600P3600M10006o2V60D3600G2R   Flush APT line x2

160000   /6go4V600P3600M10006o5V60D3600G2R   Flush QMA x2

160000   /6go4V600P3600M10006o6V60D3600G2R   Flush line F x2

230000   /3o8V3200A24000M1000o2V100A0R P3,   Sweeps   reactor
contents to waste